

School of Molecular and Life Sciences

# Synthesis of Novel Ethylene Antagonists

Jan Maria Sożyński

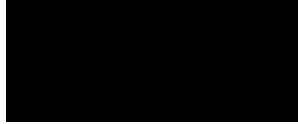
This thesis is presented for the degree  
of  
Doctor of philosophy  
Curtin University

October 2022

## Declaration

To the best of my knowledge and belief this thesis contains no material previously published by any other person except where due acknowledgement has been made. This thesis contains no material which has been accepted for the award of any other degree or diploma in any university.

Signature:



Date: 14/10/2022

## **Dedication**

To Sarah, my Highschool Sweetheart.

## Acknowledgements

The topic, direction and focus on ethylene antagonists for this thesis came from Dr. Alan Payne and Prof. Zora Singh, and their achievement and award of the Overall Winner of the Mitsubishi Corporation Western Australian Innovator of the Year Award for the research on the development of 'Ethylene Antagonists' in year 2017. This award carried a cash prize which funded the first year of these studies and allowed me to pursue my interest in chemistry.

The chapter on Degradation of DMSO was sponsored by 2020 Curtin HDR Internship Scholarship and lead under guidance of Prof. Mark Ogden and Dr. Alan Payne.

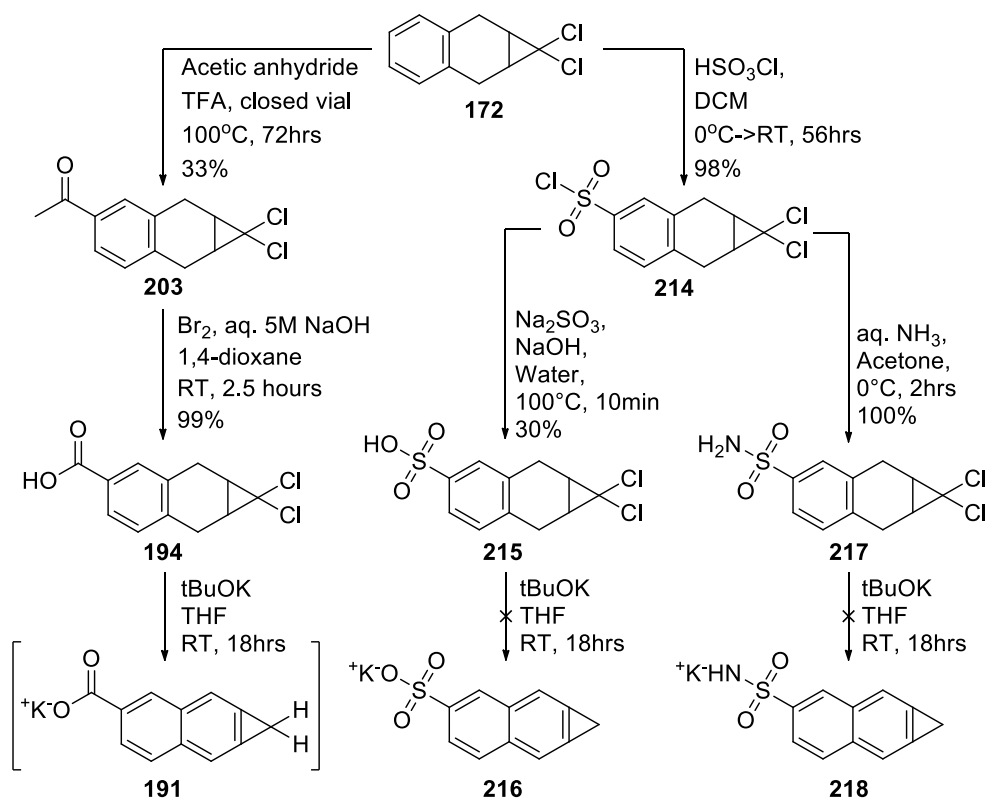
I would like to sincerely thank my supervisor Dr. Alan Payne for his endless wisdom, breadth of ideas and always being available for a quick chat.

I extend my thanks to friends and colleagues of the OMG Group and other departments that exchanged tips and tricks of the lab world, shared lunch time to eat and laugh as well as to discuss fantasy novels.

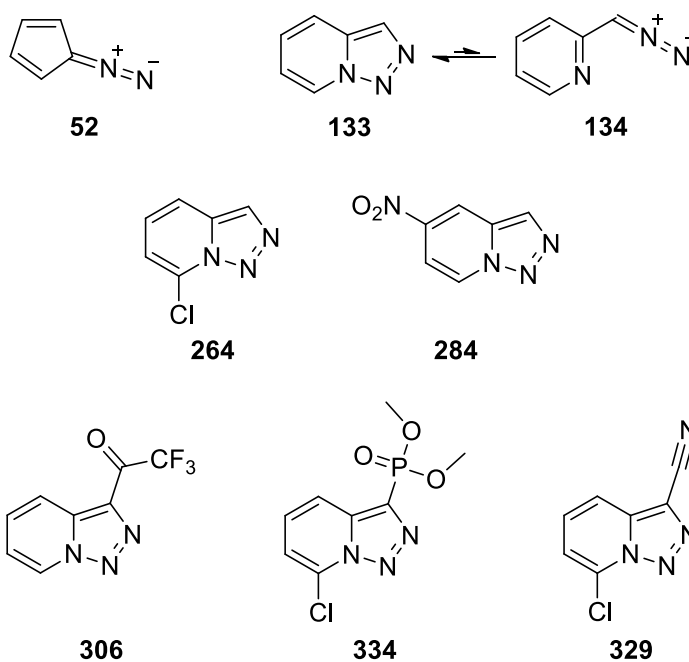
I thank my family for being a pillar of strength and support in this endeavour and being an essential part of my life.

## Abstract

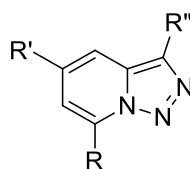
Fresh fruit and vegetables are essential to a healthy diet and almost 2 billion metric tonnes are consumed globally each year. In Australia, this accounts to ~\$1.5 trillion of revenue. However, nearly a third of all horticultural produce leaving the farm does not make it to the customers and is wasted. Up to 50% of these losses are due to premature ripening and spoilage of the produce caused by presence of ethylene **1** throughout the food supply chain. Ethylene antagonists are, in theory, the most effective way to delay ripening, however few examples are known, and a practical product has yet to be developed. The only product used to date is 1-methylcyclopropene **53** (1-MCP), a pungent, volatile and water insoluble compound. Recently, the mode of action of 1-MCP **53** based on its reactivity with the copper(I) cofactor in the ethylene receptor was proposed by Pirrung et al. which allowed for a mechanistic approach to discovery of novel ethylene antagonists. In earlier studies, cycloproprenes reacted with Cu(I) in a similar manner and were as effective as 1-MCP **53** in preventing the action of ethylene on fruit and flowers. This study builds on these initial results to prepare more user-friendly treatments. Synthesis of naphthalene-based cycloproparene salts were attempted by dehydrochlorination of 1,1-dichlorocarbene adducts using a Billups synthesis. Although tentative evidence was observed for the cycloproparene **191**, all three cycloproparenes could not be isolated, producing ring-opened products.



Building on the known ethylene antagonistic properties of diazocyclopentadiene **52**, alternative diazo compounds were investigated for potential as ethylene antagonists. [1,2,3]Triazolo[1,5-*a*]pyridine **133** is known for forming an equilibrium with a ring open diazomethyl pyridine structure **134**, while possessing significantly less hazardous properties. While the parent compound was unreactive, some derivatives displayed greater reactivity with transition metals, and therefore may antagonise the effect of ethylene. A range of novel triazolopyridines were synthesised using diazo transfer reactions and the reaction of tosyl hydrazones with a base. Using these two methods, [1,2,3]triazolo[1,5-*a*]pyridines with various electron withdrawing groups were made.



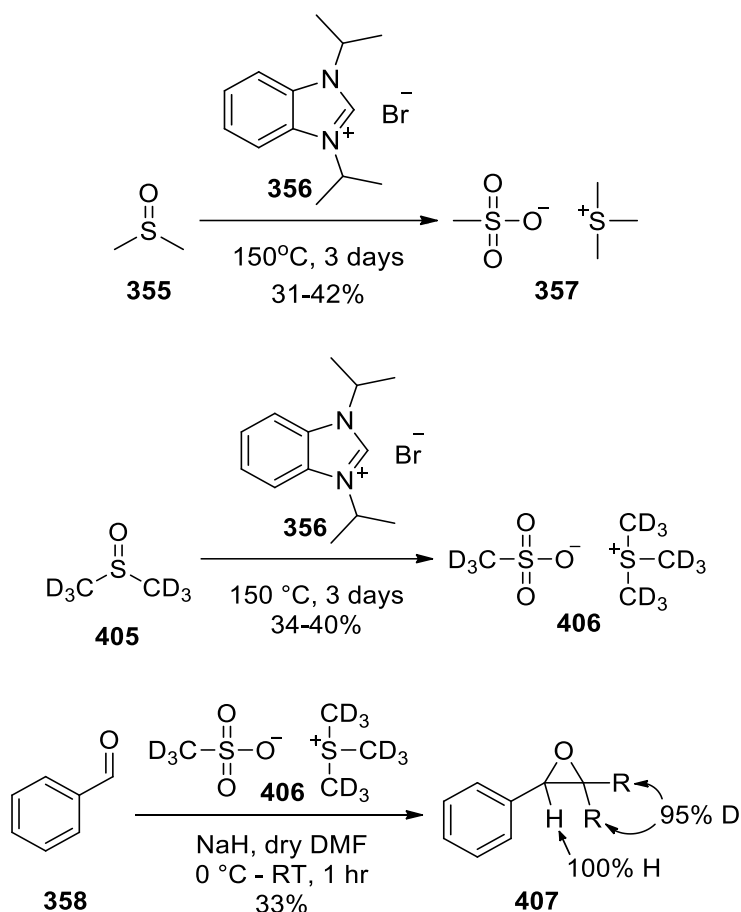
The inherent chemical reactivity of a library of triazolopyridines with a copper(I) complex was tested. The triazolopyridines were either unreactive or gave a complex mixture of products, generally depending on the substituent at position 7 on the triazolopyridine ring. The chemical reactivity was compared against a simple, in-house *in vivo* assay using Geraldton wax. Geraldton wax is native to Western Australia that exhibits flower abscission when exposed to ethylene. The triazolopyridines did not cause senescence or abscission of flowers on their own. When these treated flowers were exposed to ethylene, some compounds had a protective effect. There was correlation between the observed protective effect in Geraldton wax (ethylene antagonism) and the reactivity of the compounds towards copper(I) complexes. This validated the mechanistic approach to the discovery of ethylene antagonists based on the mechanism proposed by Pirrung in 2008.



| No. | R<br>Position 7 | R'<br>Position 5 | R''<br>Position 3                  | Cu(I)<br>complex<br>reactivity | Ethylene action<br>Inhibition<br>minimum<br>concentration<br>(mmol/L) |
|-----|-----------------|------------------|------------------------------------|--------------------------------|---|
| 233 | H               | H                | H                                  | ✗                              | ✗   |
| 278 | H               | H                | Me                                 | ✗                              | ✗   |
| 309 | H               | H                | COOMe                              | ✗                              | ✗   |
| 306 | H               | H                | COCF <sub>3</sub>                  | ✗                              | ✗   |
| 284 | H               | NO <sub>2</sub>  | H                                  | ✗                              | ✗   |
| 354 | N*              | H                | H                                  | ✗                              | ✗   |
| 263 | Br              | H                | H                                  | ✓                              | ✗   |
| 264 | Cl              | H                | H                                  | ✓                              | ✗   |
| 332 | Cl              | H                | COO <sup>-</sup> Li <sup>+</sup>   | ✓                              | ✗   |
| 334 | Cl              | H                | PO(OCH <sub>3</sub> ) <sub>2</sub> | ✓                              | 1   |
| 251 | Cl              | H                | COOMe                              | ✓                              | 0.1   |
| 329 | Cl              | H                | CN                                 | ✓                              | 0.1   |

\*Refers to [1,2,3]Triazolo[1,5-*a*]pyridazine

In a separate study, the degradation of dimethyl sulfoxide **355** (DMSO) in presence of catalytic amounts of ionic liquids was investigated. The reaction produced an interesting ionic product, namely trimethylsulfonium methanesulfonate **357** (TMSMS), in a good yield. This product is similar to trimethylsulfonium iodide and was shown to convert ketones and aldehydes to epoxides. Through a series of reactions to probe the mechanism of the reaction, the mechanism for this reaction is promoted by HBr produced by degradation of the ionic liquids. The degradation was also shown effective for  $d_6$ -DMSO **405**, yielding a unique  $d_{12}$ - trimethylsulfonium methanesulfonate **406** and creating a simple reagent to produce deuterated epoxides (e.g. **407**), particularly useful for the pharmaceutical industry.



# Contents

|  |             |
|--|-------------|
| <b>Declaration</b>   | <b>i</b>    |
| <b>Dedication</b>  | <b>ii</b>   |
| <b>Acknowledgements</b>                                    | <b>iii</b>  |
| <b>Abstract</b>  | <b>iv</b>   |
| <b>Contents</b>  | <b>viii</b> |
| <b>List of figures</b>                                     | <b>xi</b>   |
| <b>List of schemes</b>                                     | <b>xv</b>   |
| <b>List of tables</b>                                      | <b>xxi</b>  |
| <b>List of symbols and abbreviations</b>                   | <b>xxii</b> |
| <b>Chapter 1 – Introduction</b>                            | <b>1</b>    |
| 1.1 Horticultural produce industry and food wastage        | 1           |
| 1.2 Climacteric produce and spoilage by ripening           | 4           |
| 1.3 Ethylene as one of the 5 major plant hormones          | 5           |
| 1.3.1 Ethylene history and storage of climacteric products | 6           |
| 1.3.2 Ethylene biosynthesis                                | 8           |
| 1.3.3 The ethylene receptor                                | 10          |
| 1.4 Agonists of the ETR-1                                  | 11          |
| 1.5 Preventing ethylene action                             | 12          |
| 1.5.1 Substitution of the copper ion in ETR-1              | 12          |
| 1.6 Inhibitors of ethylene action                          | 13          |
| 1.6.1 Olefins  | 13          |
| 1.6.2 Diazocyclopentadiene (DACP)                          | 16          |
| 1.7 1-Methylcyclopropene (1-MCP)                           | 18          |
| 1.7.1 History of 1-MCP                                     | 18          |
| 1.7.2 Application of 1-MCP                                 | 21          |

|   |           |
|---|-----------|
| 1.7.3 Synthesis of 1-MCP  | 22        |
| 1.7.4 Pirrung's mode of action  | 23        |
| 1.8 Cycloproparenes   | 24        |
| 1.8.1 Discovery of antagonistic effects of cycloproparenes  | 24        |
| 1.8.2 Synthesis   | 25        |
| 1.8.3 Reactions   | 30        |
| 1.9 Cycloproparenes as ethylene antagonists   | 33        |
| 1.9.1 Effectiveness of cycloproparenes as ethylene antagonists  | 33        |
| 1.9.2 Proposed Mode of action of cycloproparenes  | 34        |
| 1.9.3 Attempts to prepare water-soluble cycloproparenes   | 35        |
| 1.10 Project aims   | 39        |
| 1.10.1 Optimal properties of an ethylene antagonist   | 39        |
| 1.10.2 Synthesis of water soluble cycloproparenes   | 40        |
| 1.10.3 Synthesis of diazo-active triazolopyridines  | 40        |
| <b>Chapter 2 – Water soluble cycloproparenes</b>  | <b>41</b> |
| 2.1 Carboxylate analogues   | 43        |
| 2.2 Sulfonate analogues   | 51        |
| 2.2.1 Hydrolysis approach   | 52        |
| 2.2.2 Aminolysis approach   | 54        |
| <b>Chapter 3 – Development of an <i>in vivo</i> assay as a preliminary assessment of ethylene antagonism in water soluble compounds</b> | <b>55</b> |
| 3.1 Preface   | 55        |
| 3.1.1 Pea seedlings   | 56        |
| 3.1.2 Birch leaves  | 57        |
| 3.1.3 Geraldton wax   | 57        |
| 3.2 Development of a simple in-house assay  | 59        |
| 3.2.1 Containers for sealed ethylene exposure   | 60        |

|   |            |
|---|------------|
| 3.2.2 Optimisation of ethylene exposure amount                            | 61         |
| 3.2.3 Validation of ethylene controls used across all assays              | 63         |
| 3.2.4 Finalised model assay   | 64         |
| 3.2.5 Preliminary attempts of the in-house assay                          | 65         |
| 3.2.6 Differences between fumigation, spray, dipping and watering         | 66         |
| <b>Chapter 4 – Diazo-active [1,2,3]Triazolo[1,5-<i>a</i>]pyridines</b>    | <b>67</b>  |
| 4.1 Background  | 67         |
| 4.1.1 Diazocyclopentadiene (DACP)   | 67         |
| 4.1.2 Ethyl diazoacetate  | 68         |
| 4.1.3 [1,2,3]Triazolo[1,5- <i>a</i> ]pyridine                             | 70         |
| 4.1.4 Synthesis pathways to [1,2,3]triazolo[1,5- <i>a</i> ]pyridines      | 76         |
| 4.2 Synthesis of [1,2,3]triazolo[1,5- <i>a</i> ]pyridine derivatives      | 78         |
| 4.2.1 [1,2,3]Triazolo[1,5- <i>a</i> ]pyridine                             | 78         |
| 4.3 5-EWG-[1,2,3]triazolo[1,5- <i>a</i> ]pyridines                        | 81         |
| 4.4 7-Halo-[1,2,3]triazolo[1,5- <i>a</i> ]pyridines                       | 84         |
| 4.5 7-Chloro-3-EWG-[1,2,3]triazolo[1,5- <i>a</i> ]pyridines               | 91         |
| 4.5.1 3-EWG-[1,2,3]triazolo[1,5- <i>a</i> ]pyridines                      | 92         |
| 4.5.2 Halogenation of EWG substituted triazolopyridines                   | 95         |
| 4.5.3 EWG substitution of halogenated triazolopyridines                   | 96         |
| 4.6 [1,2,3]Triazolo[1,5]azines  | 109        |
| 4.6.1 [1,2,3]Triazolo[1,5- <i>b</i> ]pyridazine                           | 110        |
| 4.7 Summary of Cu(I) reactivity and <i>in vivo</i> results                | 112        |
| <b>Chapter 5 – Degradation of DMSO catalysed by benzimidazolium salts</b> | <b>114</b> |
| 5.1 Preface   | 114        |
| 5.2 Stability of DMSO   | 115        |
| 5.3 Catalytic degradation   | 116        |
| 5.3.1 Preparation of benzimidazolium salts                                | 121        |

|   |            |
|---|------------|
| 5.3.2 Catalysed degradation of DMSO                               | 122        |
| 5.3.3 Deuterated DMSO   | 127        |
| 5.3.4 Epoxidation reactions with TMSMS and d <sub>12</sub> -TMSMS | 128        |
| <b>Chapter 6 – General conclusions</b>                            | <b>131</b> |
| 6.1 Cycloproparenes   | 131        |
| 6.2 Triazolopyridines   | 133        |
| 6.3 DMSO Degradation  | 135        |
| <b>Chapter 7 – Experimental</b>                                   | <b>136</b> |
| 7.1 Cycloproparenes   | 137        |
| 7.2 Triazolopyridines   | 151        |
| 7.3 DMSO  | 193        |
| <b>References</b>   | <b>201</b> |
| <b>Appendix A Permission Statements</b>                           | <b>221</b> |
| <b>Appendix B NMR Spectra of selected compounds</b>               | <b>228</b> |

## List of figures

|  |    |
|--|----|
| Figure 1 Distribution of horticultural produce wastage between global areas and sectors of food industry <sup>6</sup> .....  | 1  |
| Figure 2 Approximate produce losses between the farm and a customer <sup>8</sup> .....   | 2  |
| Figure 3 Examples of climacteric and non-climacteric fruits <sup>20</sup> .....  | 4  |
| Figure 4 5 Major plant hormones.....   | 5  |
| Figure 5 Involvement of the five major plant hormones life stages of a plant based on summary by B. Cornell <sup>26</sup> .....  | 5  |
| Figure 6 Inhibition of ethylene action by cyclopropene analogues in banana fruit peels. <sup>128</sup> The properties of each compound is noted below each structure (Solubility in water, Minimum apparent vapour concentration nL/L gas and Time of protection (days)) ..... | 20 |
| Figure 7 $\beta$ -Cyclodextrin <sup>136</sup> .....  | 21 |

|   |    |
|---|----|
| Figure 8 Synthesis methods of 1-methylcyclopropene <b>53</b> a) from methallyl chloride <b>80</b> and sodamide <sup>137</sup> b) reductive debromination of the tribromocyclopropane <b>81</b> <sup>141-144</sup> c) by lithiation-borylation release <sup>132, 145</sup> ..... | 22 |
| Figure 9 Proposed mechanism of 1-MCP action by Pirrung et al. <sup>144</sup> .....  | 23 |
| Figure 10 benzocyclopropene <b>8</b> , 1H-naphtho[b]cyclopropene <b>9</b> and 1H-cyclopropa[b]anthracene <b>10</b> .....  | 24 |
| Figure 11 Molecular structure of 2-chloro-1,1-dimethyl-1H-cycloprop-[e]azulene , by permission of John Wiley and Sons publisher <sup>162</sup> .....  | 24 |
| Figure 12 Pathways to cycloproparenes <sup>152</sup> .....  | 25 |
| Figure 13 Chemistry of cycloproparenes <sup>172</sup> a) with electrophiles and nucleophiles, b) with transition metal complexes, c) in cycloadditions, d) upon flash vacuum pyrolysis .....  | 30 |
| Figure 14 In-vivo test of 1H-naphtho[b]cyclopropene (left) in comparison to 1-MCP (middle), effect on Geraldton wax vs an ethylene control (right), experiment performed by Abdalghani <sup>204</sup> .....   | 34 |
| Figure 15 Potential salt analogues of 1H-naphtho[b]cyclopropane <b>93</b> .....   | 40 |
| Figure 16 Potential analogues of [1,2,3]Triazolo[1,5-a]pyridine.....  | 40 |
| Figure 17 Acid/Base equilibria of 2-naphthoic acid <b>190</b> as well as 1H-cyclopropa[b]naphthalene-4-carboxylic acid <b>192</b> .....   | 43 |
| Figure 18 Salt mixture of the potassium 1H-cyclopropa[b]naphthalene-4-carboxylate <b>191</b> buffer workup.....   | 49 |
| Figure 19 Preliminary samples of ethylene action on green peas, “Controls” are procedural blanks, “Tests” are ethylene exposed.....   | 56 |
| Figure 20 Preliminary assay of a silver birch cutting.....  | 57 |
| Figure 21 Effect of ethylene <b>1</b> (2 µL/L) and 1-MCP <b>53</b> (200 nL/L) on bud and flower abscission (%) from freshly harvested Geraldton waxflower, by Serek <sup>194</sup> .....  | 58 |
| Figure 22 Sistema 2.35L containers used for Geraldton wax testing of potential ethylene antagonists.....  | 60 |
| Figure 23 Variability of control (ethylene <b>1</b> alone) abscission of Geraldton wax on repeated container use .....  | 61 |
| Figure 24 Effect of ethylene <b>1</b> concentration on abscission of Geraldton wax.....   | 62 |
| Figure 25 Distribution of results for ethylene gassed control samples of Geraldton wax .....  | 63 |
| Figure 26 Geraldton wax assay model .....   | 64 |

|   |    |
|---|----|
| Figure 27 Geraldton wax flower abscission on treatment with 1H-naphtho[b]cyclopropene <b>93</b> .....   | 65 |
| Figure 28 Geraldton wax flower abscission on treatment with limonene .....  | 65 |
| Figure 29 Loss of colour and senescence in Geraldton wax after fumigation: ethyl diazoacetate <b>227</b> + ethylene <b>1</b> (left), ethylene <b>1</b> (middle) and a procedural blank (right) .....    | 69 |
| Figure 30 Equilibrium of [1,2,3]triazolo[1,5-a]pyridine <b>233</b> with 2-(diazomethyl)pyridine <b>234</b> .....  | 71 |
| Figure 31 Equilibrium of tert-butyl 7-fluoro-[1,2,3]triazolo[1,5-a]pyridine-3-carboxylate <b>235</b> with tert-butyl 2-diazo-2-(6-fluoropyridin-2-yl)acetate <b>236</b> <sup>255</sup> .....            | 71 |
| Figure 32 Substituted triazolopyridines IC50 Inhibition of D1 proteins belonging to photosystem II of plants <sup>256</sup> .....   | 71 |
| Figure 33 Three key components of shifting equilibrium of the triazolopyridines .....   | 72 |
| Figure 34 Halogen variations of tert-butyl 7-halo-[1,2,3]triazolo[1,5-a]pyridine-3-carboxylate <sup>255</sup> .....   | 74 |
| Figure 35 Ring-chain isomerism of [1,2,3]triazolo[1,5-a]pyridine <b>233</b> <sup>262</sup> .....  | 74 |
| Figure 36 <sup>1</sup> H NMR expanded spectrum of [1,2,3]triazolo[1,5-a]pyridine <b>233</b> .....   | 78 |
| Figure 37 Geraldton wax flower abscission on treatment with [1,2,3]triazolo[1,5-a]pyridine <b>233</b> and 3-methyl-[1,2,3]triazolo[1,5-a]pyridine <b>278</b> at 1M solution concentration.....          | 80 |
| Figure 38 <sup>1</sup> H NMR spectrum of 5-nitro-[1,2,3]triazolo[1,5-a]pyridine <b>284</b> .....  | 82 |
| Figure 39 Geraldton wax flower abscission on treatment with 5-nitro-[1,2,3]triazolo[1,5-a]pyridine <b>284</b> at 1M solution concentration.....   | 83 |
| Figure 40 <sup>1</sup> H NMR splitting of 7-chloro-[1,2,3]triazolo[1,5-a]pyridine <b>264</b> .....  | 85 |
| Figure 41 <sup>1</sup> H NMR spectrum of 7-chloro-[1,2,3]triazolo[1,5-a]pyridine <b>264</b> .....   | 86 |
| Figure 42 Geraldton wax flower abscission on treatment with 7-chloro-[1,2,3]triazolo[1,5-a]pyridine <b>264</b> and 7-bromo-[1,2,3]triazolo[1,5-a]pyridine <b>263</b> at 1M solution concentration ..... | 91 |
| Figure 43 Proposed synthesis pathways of 3-Substituted-[1,2,3]triazolo[1,5-a]pyridine analogues <b>299</b> and <b>302</b> .....   | 92 |
| Figure 44 <sup>1</sup> H NMR spectrum of 1,1,1-Trifluoro-2-([1,2,3]triazolo[1,5-a]pyridin-3-yl)ethanone <b>306</b> .....  | 93 |

|  |     |
|--|-----|
| Figure 45 Geraldton wax flower abscission on treatment with 3-COCF <sub>3</sub> -[1,2,3]triazolo[1,5-a]pyridine <b>306</b> and 3-COOMe-[1,2,3]triazolo[1,5-a]pyridine <b>309</b> at 1M solution concentration.....   | 95  |
| Figure 46 <sup>1</sup> H NMR expanded spectrum of trimer <b>321</b> .....  | 98  |
| Figure 47 NMR analysis of proposed 3,4,5-tris(6-chloropyridin-2-yl)-4-nitroisoxazolidin-2-olate <b>321</b> .....   | 99  |
| Figure 48 <sup>1</sup> H NMR expanded spectrum of 7-chloro-[1,2,3]triazolo[1,5-a]pyridine-3-carboxylate <b>251</b> .....   | 102 |
| Figure 49 <sup>1</sup> H NMR expanded spectrum of dimethyl (7-chloro-[1,2,3]triazolo[1,5-a]pyridin-3-yl)phosphonate <b>334</b> .....   | 105 |
| Figure 50 Geraldton wax flower abscission on treatment with 7-chloro-3-EWG-[1,2,3]triazolo[1,5-a]pyridines <b>251</b> , <b>329</b> , <b>332</b> and <b>334</b> at 1M solution concentration  | 108 |
| Figure 51 Geraldton wax flower abscission on treatment with 7-chloro-3-EWG-[1,2,3]triazolo[1,5-a]pyridines <b>251</b> and <b>329</b> at 0.1M solution concentration .....  | 108 |
| Figure 52 pKa values of various nitrogen containing heterocycles <b>341-346</b> .....  | 109 |
| Figure 53 Proposed equilibrium of the [1,2,3]triazolo[1,5-a]azines <b>347</b> .....  | 109 |
| Figure 54 <sup>1</sup> H NMR expanded spectrum of [1,2,3]triazolo[1,5-b]pyridazine <b>354</b> .....  | 111 |
| Figure 55 Geraldton wax flower abscission on treatment with [1,2,3]triazolo[1,5-b]pyridazine <b>354</b> at 1M solution concentration.....  | 111 |
| Figure 56 [1,2,3]Triazolo[1,5-a]pyridine derivatives.....  | 113 |
| Figure 57 Comparison between spectra <sup>2</sup> H NMR of d <sub>12</sub> -TMSMS <b>406</b> (top), <sup>1</sup> H NMR of d <sub>12</sub> -TMSMS <b>406</b> (middle) and <sup>1</sup> H NMR of TMSMS <b>357</b> .....                                      | 128 |
| Figure 58 Comparison between <sup>13</sup> C NMR spectra of d <sub>12</sub> -TMSMS <b>406</b> (top) and TMSMS <b>357</b> (bottom) in D <sub>2</sub> O.....   | 128 |
| Figure 59 Comparison between spectra <sup>2</sup> H NMR of phenyloxirane-3,3-d <sub>2</sub> <b>407</b> (top), <sup>1</sup> H NMR of phenyloxirane-3,3-d <sub>2</sub> <b>407</b> (middle) and <sup>1</sup> H NMR of phenyloxirane <b>359</b> (bottom) ..... | 130 |
| Figure 60 <sup>13</sup> C NMR Spectrum of phenyloxirane-3,3-d <sub>2</sub> <b>407</b> .....  | 130 |

## List of schemes

|  |    |
|--|----|
| Scheme 1 Ethylene biosynthesis through the Methionine (Yang) cycle <sup>63</sup> .....   | 8  |
| Scheme 2 Biosynthesis of ethylene from SAM and antagonists of ethylene biosynthesis <sup>63, 71</sup> .....  | 9  |
| Scheme 3 Examples of Cu(I)-ethylene complexes <sup>85, 87</sup> .....  | 10 |
| Scheme 4 Preparation of silver thiosulphate <sup>96</sup> .....  | 12 |
| Scheme 5 Synthesis of diazocyclopentadiene by Doering and DePuy <sup>110</sup> .....   | 16 |
| Scheme 6 Dimerization of 1-hexylcyclopropene and reaction between 1-hexylcyclopropene and methanol, in presence of copper(I) complex <sup>147</sup> .....  | 23 |
| Scheme 7 First synthesis of a cycloproparene <sup>149</sup> .....  | 26 |
| Scheme 8 Equilibrium of 3-monosubstituted indazoles <sup>129</sup> .....   | 26 |
| Scheme 9 Synthesis of 2-chloro-1,1-dimethyl-1H-cycloprop- [e]azulene <b>109</b> by photolysis <sup>168</sup> .....   | 26 |
| Scheme 10 Synthesis of benzocyclopropene <b>92</b> by double dehydrohalogenation of 7,7-dichloro-bicyclo[4.1.0]heptane <b>111</b> <sup>172</sup> .....   | 27 |
| Scheme 11 Cycloproparene structures synthesised by double dehydrochlorination of a 7,7-dihalo precursor <sup>172</sup> and an ineffective synthesis target – 1H-cyclopropa[b]anthracene <sup>173, 174</sup> .....                  | 27 |
| Scheme 12 Synthesis of 1H-cyclopropa[b]naphthalene <b>93</b> derived from the 1a-bromo-7a-chlorocyclopropene <b>127</b> <sup>172, 175, 177</sup> .....   | 28 |
| Scheme 13 Comparison between double dehydrohalogenation of 7,7-dihalo and 1,6-dihalo precursors <sup>176, 178</sup> .....  | 28 |
| Scheme 14 Pyridyl derivatives of cycloproparenes and their methods of synthesis <sup>181-183</sup> .....   | 29 |
| Scheme 15 Nitration of bicyclo[4.1.0]hepta-1,3,5-triene-7,7-diylbis(triisopropylsilane) <b>49</b> .....  | 30 |
| Scheme 16 Trifluoroacetylation of 2-chloro-1,1-dimethylcycloprop[e]azulene <b>109</b> <sup>162</sup> .....   | 31 |
| Scheme 17 General benzylation reaction of the 1H-cyclopropa[b]naphthalene <b>93</b> <sup>153, 188</sup> and formation of norcaradiene-cycloheptatriene equilibrium from benzocyclopropene <b>92</b> <sup>186, 187, 189</sup> ..... | 31 |

|           |  |    |
|-----------|--|----|
| Scheme 18 | Reaction between 3-chlorobicyclo[4.1.0]hepta-1,3,5-triene <b>144</b> and methanol in presence of silver(I) complex <sup>190</sup> .....    | 32 |
| Scheme 19 | Proposed mechanism of dimerization of benzocyclopropene <b>92</b> in presence of silver(I) complex, by Billups et al. <sup>192</sup> ..... | 32 |
| Scheme 20 | Dimerization of rocketene <b>150</b> in presence of silver(I) complex <sup>192</sup> .....   | 32 |
| Scheme 21 | Proposed mode of action of benzocyclopropene <b>16</b> on ETR-1 receptor ...   | 34 |
| Scheme 22 | Synthesis pathway of bicyclo[4.1.0]hepta-1,3,5-triene-3,4-diyl dimethanol <b>163</b> <sup>193</sup> .....                                  | 35 |
| Scheme 23 | Attempted synthesis pathway of 4-(2-(2-(2-methoxyethoxy)ethoxy)ethoxy)-1H-cyclopropa[b]naphthalene <b>171</b> <sup>193</sup> .....         | 36 |
| Scheme 24 | Attempted synthesis pathway of 4,5-bis((2-(2-methoxyethoxy)ethoxy)methyl)-1H-cyclopropa[b]naphthalene <b>177</b> .....                     | 37 |
| Scheme 25 | Attempted synthesis pathway of 4,5-bis(3-(2-(2-methoxyethoxy)ethoxy)propyl)-1H-cyclopropa[b]naphthalene <b>182</b> <sup>206</sup> .....    | 38 |
| Scheme 26 | Potential synthesis of substituted 1H-cyclopropa[b]naphthalenes via electrophilic aromatic substitution <sup>152, 176</sup> .....          | 41 |
| Scheme 27 | Comparison of products of the Billups synthesis between organic and water soluble analogues of the 1H-cyclopropa[b]naphthalene .....       | 42 |
| Scheme 28 | Proposed synthesis pathway of potassium naphtha[b]cyclopropenoate through EAS .....  | 44 |
| Scheme 29 | Reductions of naphthalene <sup>207, 209</sup> .....  | 44 |
| Scheme 30 | Synthesis pathway of 1,1-Dichloro-1a,2,7,7a-tetrahydro-1H-cyclopropa[b]naphthalene .....   | 45 |
| Scheme 31 | Synthesis of 1H-naphtho[b]cyclopropane .....   | 45 |
| Scheme 32 | Dibromomethylation of tetralin <b>199</b> by Matt et al. <sup>211</sup> .....  | 46 |
| Scheme 33 | Attempted synthesis of 4-(bromomethyl)-1,1-dichloro-1a,2,7,7a-tetrahydro-1H-cyclopropa[b]naphthalene <b>202</b> .....                      | 46 |
| Scheme 34 | Proposed synthesis pathway of potassium naphtha[b]cyclopropenoate <b>191</b> through acetylation .....                                     | 46 |
| Scheme 35 | Acylation of tetralin <b>199</b> .....   | 47 |
| Scheme 36 | Synthesis of 1-(1,1-dichloro-1a,2,7,7a-tetrahydro-1H-cyclopropa[b]naphthalen-4-yl)ethanone <b>203</b> .....                                | 47 |
| Scheme 37 | Synthesis of 1,1-dichloro-1a,2,7,7a-tetrahydro-1H-cyclopropa[b]naphthalene-4-carboxylic acid <b>194</b> .....                              | 48 |

|  |    |
|--|----|
| Scheme 38 Attempted synthesis of potassium 1H-naphtho[b]cyclopropen-4-oate <b>191</b>  | 49 |
| Scheme 39 Attempts at isolation of potassium 1H-cyclopropa[b]naphthalene-4-carboxylate <b>191</b>  | 50 |
| Scheme 40 Attempted synthesis of methyl 1H-cyclopropa[b]naphthalene-4-carboxylate <b>208</b>   | 51 |
| Scheme 41 Hydrolysis and aminolysis of sulfonyl chloride <b>211</b>  | 51 |
| Scheme 42 Attempted synthesis of 1,1-dichloro-1a,2,7,7a-tetrahydro-1H-cyclopropa[b]naphthalene-4-sulfonyl chloride <b>214</b>  | 52 |
| Scheme 43 Synthesis of 1,1-dichloro-1a,2,7,7a-tetrahydro-1H-cyclopropa[b]naphthalene-4-sulfonyl chloride <b>214</b>  | 52 |
| Scheme 44 Synthesis of 1,1-dichloro-1a,2,7,7a-tetrahydro-1H-cyclopropa[b]naphthalene-4-sulfonic acid <b>215</b> and attempted synthesis of potassium 1H-cyclopropa[b]naphthalene-4-sulfonate <b>216</b>        | 53 |
| Scheme 45 Synthesis of 1,1-dichloro-1a,2,7,7a-tetrahydro-1H-cyclopropa[b]naphthalene-4-sulfonamide <b>217</b> and attempted synthesis of potassium ((1H-cyclopropa[b]naphthalen-4-yl)sulfonyl)amide <b>218</b> | 54 |
| Scheme 46 Decomposition of ethephon <b>219</b> to ethylene <b>1</b> under basic conditions   | 61 |
| Scheme 47 Resonance structures of diazocyclopentadiene <b>2</b> <sup>251</sup>   | 67 |
| Scheme 48 Reactivity of diazocyclopentadiene <b>52</b> in presence of a rhodium catalyst <sup>251</sup>  | 68 |
| Scheme 49 Proposed mode of action of diazocyclopentadiene <b>52</b> as an ethylene antagonist  | 68 |
| Scheme 50 Dimerisation of ethyl diazoacetate <b>227</b> catalysed by copper(I) triflate by Reck et al. <sup>253</sup>  | 68 |
| Scheme 51 Synthesis of ethyl diazoacetate <b>227</b> <sup>254</sup>  | 69 |
| Scheme 52 Proposed mode of action of ethyl diazoacetate <b>227</b> as an ethylene antagonist   | 70 |
| Scheme 53 Proposed mode of action of [1,2,3]Triazolo[1,5-a]pyridines as ethylene antagonists   | 72 |
| Scheme 54 Reaction of 7-chloro-[1,2,3]triazolo[1,5-a]pyridylacetate <b>251</b> catalysed by rhodium(II) complex <sup>257</sup>   | 73 |

|   |    |
|---|----|
| Scheme 55 Synthesis of [1,2,3]triazolo[1,5-a]pyridine by: a) oxidation of a hydrazone, <sup>263-273</sup> b) elimination of a sulfonylhydrazone, <sup>268, 274-276</sup> c) diazo transfer reaction <sup>275, 277-281</sup> and d) diazotation by tBuONO <sup>282</sup> ..... | 77 |
| Scheme 56 Synthesis of [1,2,3]triazolo[1,5-a]pyridines by Tamura et al. <sup>283</sup> .....  | 77 |
| Scheme 57 Synthesis of [1,2,3]triazolo[1,5-a]pyridine <b>233</b> .....  | 78 |
| Scheme 58 Synthesis of 3-methyl-[1,2,3]triazolo[1,5-a]pyridine <b>278</b> .....   | 79 |
| Scheme 59 Degradation of [1,2,3]triazolo[1,5-a]pyridines <b>233</b> and <b>278</b> in presence of copper(I) complex .....   | 79 |
| Scheme 60 Synthesis pathway of 5-nitro[1,2,3]triazolo[1,5-a]pyridine <b>284</b> .....   | 82 |
| Scheme 61 Degradation of 5-nitro-[1,2,3]triazolo[1,5-a]pyridine <b>284</b> catalysed by copper(I) complex in ethanol .....  | 83 |
| Scheme 62 Halogen variations of triazolopyridine esters .....   | 84 |
| Scheme 63 Bromination of [1,2,3]triazolo[1,5-a]pyridines by Abarca et al. <sup>290</sup> .....  | 84 |
| Scheme 64 Synthesis of 7-halo-[1,2,3]triazolo[1,5-a]pyridine analogues <b>263</b> and <b>264</b> .....  | 85 |
| Scheme 65 Synthesis of 7-chloro-[1,2,3]triazolo[1,5-a]pyridine <b>264</b> .....   | 86 |
| Scheme 66 Synthesis of diazo compounds by Liu et al. <sup>292</sup> .....   | 87 |
| Scheme 67 Effect of solvents on elimination of sulfonylhydrazones by Liu et al. <sup>292</sup> ..   | 88 |
| Scheme 68 Effect of bases on elimination of sulfonylhydrazones by Liu et al. <sup>292</sup> .....   | 88 |
| Scheme 69 Synthesis of 7-chloro-[1,2,3]triazolo[1,5-a]pyridine <b>264</b> .....   | 89 |
| Scheme 70 Degradation of 7-bromo-[1,2,3]triazolo[1,5-a]pyridine <b>263</b> catalysed by copper(I) complex .....   | 90 |
| Scheme 71 Degradation of 7-chloro-[1,2,3]triazolo[1,5-a]pyridine <b>264</b> catalysed by copper(I) complex .....  | 90 |
| Scheme 72 Proposed synthesis pathway of 7-chloro-3-substituted-[1,2,3]triazolo[1,5-a]pyridine analogues <b>302</b> .....  | 92 |
| Scheme 73 Synthesis pathway of 1,1,1-Trifluoro-2-([1,2,3]triazolo[1,5-a]pyridin-3-yl)ethanone <b>306</b> .....  | 93 |
| Scheme 74 Attempted synthesis pathway of methyl 3-([1,2,3]triazolo[1,5-a]pyridine)acetate <b>309</b> .....  | 94 |
| Scheme 75 Attempted degradation of [1,2,3]triazolo[1,5-a]pyridine acetyl derivatives <b>306</b> and <b>309</b> in presence of copper(I) complex in ethanol .....  | 94 |
| Scheme 76 Attempted synthesis pathway of 7-chloro-3-COCF <sub>3</sub> -[1,2,3]triazolo[1,5-a]pyridine derivative <b>312</b> .....   | 96 |

|   |     |
|---|-----|
| Scheme 77 Proposed synthesis pathway of disubstituted [1,2,3]triazolo[1,5-a]pyridine analogues <b>315</b> .....   | 96  |
| Scheme 78 Synthesis of 2-(bromomethyl)-6-chloropyridine <b>313</b> .....  | 97  |
| Scheme 79 Synthesis of 1-chloro-3-(nitromethyl)benzene <b>319</b> <sup>316</sup> and 2-chloro-6-(nitromethyl)pyridine <b>320</b> .....                                    | 97  |
| Scheme 80 Attempted synthesis of 7-chloro-3-nitro-[1,2,3]triazolo[1,5-a]pyridine <b>323</b> .....   | 98  |
| Scheme 81 Proposed mechanism of trimerization of 2-chloro-6-(nitromethyl)pyridine <b>320</b> .....  | 100 |
| Scheme 82 Synthesis of (6-chloropyridin-2-yl)acetonitrile <b>328</b> and 7-chloro-[1,2,3]triazolo[1,5-a]pyridine-3-carbonitrile <b>329</b> .....                          | 101 |
| Scheme 83 Degradation of 7-chloro-[1,2,3]triazolo[1,5-a]pyridine-3-carbonitrile <b>329</b> in presence of copper(I) complex in ethanol.....                               | 101 |
| Scheme 84 Synthesis of methyl 2-(6-chloropyridin-2-yl)acetate <b>330</b> and methyl 7-chloro-[1,2,3]triazolo[1,5-a]pyridine-3-carboxylate <b>251</b> .....                | 102 |
| Scheme 85 Degradation of methyl 7-chloro-[1,2,3]triazolo[1,5-a]pyridine-3-carboxylate <b>251</b> in presence of copper(I) complex in ethanol.....                         | 102 |
| Scheme 86 Synthesis of lithium 7-chloro-[1,2,3]triazolo[1,5-a]pyridine-3-carboxylate <b>332</b> .....   | 103 |
| Scheme 87 Degradation of lithium 7-chloro-[1,2,3]triazolo[1,5-a]pyridine-3-carboxylate <b>332</b> in presence of copper(I) complex in ethanol.....                        | 103 |
| Scheme 88 Synthesis of dimethyl (6-chloropyridin-2-yl)phosphonate <b>333</b> .....  | 104 |
| Scheme 89 Synthesis of dimethyl (7-chloro-[1,2,3]triazolo[1,5-a]pyridin-3-yl)phosphonate <b>334</b> .....   | 104 |
| Scheme 90 Degradation of dimethyl (7-chloro-[1,2,3]triazolo[1,5-a]pyridin-3-yl)phosphonate <b>334</b> .....   | 105 |
| Scheme 91 Synthesis of 2-chloro-6-((methylsulfonyl)methyl)pyridine <b>335</b> .....   | 106 |
| Scheme 92 Attempted synthesis of 7-chloro-3-(methylsulfonyl)-[1,2,3]triazolo[1,5-a]pyridine <b>336</b> and mechanism of 6-chloropicolinonitrile <b>337</b> formation..... | 106 |
| Scheme 93 Transformation of $\alpha$ -azido sulfones <b>338</b> into nitriles <b>340</b> under basic conditions <sup>325, 326</sup> .....                                 | 107 |
| Scheme 94 Synthesis pathway of [1,2,3]triazolo[1,5-b]pyridazine <b>354</b> .....  | 110 |
| Scheme 95 Degradation of [1,2,3]triazolo[1,5-b]pyridazine <b>354</b> .....  | 111 |
| Scheme 96 Epoxidation of benzaldehyde <b>358</b> with TMSMS <b>357</b> .....  | 114 |

|  |     |
|--|-----|
| Scheme 97 Various products of the autocatalysed degradation of pure DMSO <b>355</b> , by Deguchi <sup>333, 334</sup> .....                 | 115 |
| Scheme 98 Attempted synthesis of alkylated pincer compound <b>374</b> , by Sealy and Brown <sup>340</sup> .....                            | 116 |
| Scheme 99 Degradation of DMSO <b>355</b> catalysed by 1,3-diisopropylbenzimidazolium bromide <b>356</b> , by Travers <sup>339</sup> .....  | 117 |
| Scheme 100 Degradation of DMSO <b>355</b> catalysed by 1,3-Diisopropylbenzimidazolium bromide <b>356</b> , by Travers <sup>339</sup> ..... | 117 |
| Scheme 101 Proposed balanced equation for degradation of DMSO <b>355</b> to TMSMS <b>357</b> , by Travers <sup>339</sup> .....             | 118 |
| Scheme 102 Degradation of DMSO <b>355</b> catalysed by 2-(bromomethyl)-5-nitrofurane <b>374</b> , by Banci <sup>341</sup> .....            | 118 |
| Scheme 103 Degradation of DMSO <b>355</b> catalysed by calix[4]resorcinarene <b>375</b> , by Fronczek <sup>342</sup> .....                 | 118 |
| Scheme 104 Epoxidation with trimethylsulfonium cation <sup>339, 341, 348-355, 358</sup> .....  | 119 |
| Scheme 105 Scope of epoxidation reaction with TMSMS <b>357</b> , by Travers <sup>339</sup> .....   | 119 |
| Scheme 106 Proposed mechanism of degradation of DMSO <b>355</b> , by Travers <sup>339</sup> .....  | 120 |
| Scheme 107 Synthesis of 1,3-diisopropyl-1H-benzo[d]imidazol-3-ium bromide <b>356</b> .....   | 121 |
| Scheme 108 Synthesis of 1,3-dipropyl-1H-benzo[d]imidazol-3-ium bromide <b>390</b> .....  | 122 |
| Scheme 109 Degradation of DMSO <b>355</b> catalysed by 1,3-diisopropylbenzimidazolium bromide <b>356</b> .....                             | 123 |
| Scheme 110 Degradation of DMSO <b>355</b> catalysed by bromic ionic liquids .....  | 124 |
| Scheme 111 Attempted degradation of DMSO <b>355</b> catalysed by non-bromic ionic liquids .....  | 125 |
| Scheme 112 Degradation of DMSO <b>355</b> catalysed by hydrobromic acid .....  | 125 |
| Scheme 113 Proposed mechanism of formation of hydrobromic acid by degradation of 1,3-diisopropylbenzimidazolium bromide <b>356</b> .....   | 125 |
| Scheme 114 Proposed mechanism of degradation of DMSO <b>355</b> by hydrobromic acid <b>397</b> .....                                       | 126 |
| Scheme 115 Degradation of DMSO <b>355</b> catalysed by nitric acid, <sup>371</sup> phosgene or hydrochloric acid <sup>370</sup> .....      | 126 |
| Scheme 116 Degradation of d <sub>6</sub> -DMSO <b>405</b> catalysed by 1,3-diisopropylbenzimidazolium bromide <b>406</b> .....             | 127 |

|  |     |
|--|-----|
| Scheme 117 Epoxidation of benzaldehyde <b>358</b> with TMSMS <b>357</b> .....                                  | 129 |
| Scheme 118 Epoxidation of benzaldehyde <b>358</b> with d <sub>12</sub> -TMSMS <b>407</b> .....                 | 129 |
| Scheme 119 Alternative epoxidation of benzaldehyde <b>358</b> with d <sub>12</sub> -TMSMS <b>406</b> ...       | 130 |
| Scheme 120 Epoxidation of benzaldehyde <b>358</b> with d <sub>12</sub> -TMSMS <b>406</b> .....                 | 131 |
| Scheme 121 Summary of attempts on synthesis of water soluble cycloproprenes..                                  | 132 |
| Scheme 122 Proposed synthesis of precursors to analogues of 1H-naphtho[b]cyclopropene.....                     | 132 |
| Scheme 123 Synthesis pathway of [1,2,3]triazolo[1,5-a]pyridine analogues.....                                  | 133 |
| Scheme 124 Assessment of inhibition of ethylene action with analogues of [1,2,3]triazolo[1,5-a]pyridine.....   | 134 |
| Scheme 125 Degradation of DMSO <b>355</b> catalysed by bromic ionic liquids .....                              | 135 |
| Scheme 126 Epoxidation of benzaldehyde <b>358</b> with d <sub>12</sub> -TMSMS <b>406</b> .....                 | 135 |
| Scheme 127 Proposed structure of 3,4,5-tris(6-chloropyridin-2-yl)-4-nitroisoxazolidin-2-olate <b>321</b> ..... | 177 |

## List of tables

|   |    |
|---|----|
| Table 1 Optimal storage conditions for selected fruits and vegetables <sup>17</sup> .....   | 3  |
| Table 2 Biological Activity of Ethylene <b>1</b> and other unsaturated compounds as determined by the pea straight growth test by Burg and Burg in 1967 <sup>90</sup> ..... | 11 |
| Table 3 Effect of ethylene and 1-alkenes on etiolated pea growth by Sisler in 2008 <sup>102</sup> .....   | 13 |
| Table 4 The inhibition of ethylene action by various compounds by Sisler and Yang in 1984 <sup>103</sup> .....  | 14 |
| Table 5 Competition of cyclooctenes and cyclooctadienes with ethylene <b>1</b> for binding in tobacco leaves by Sisler, Blankenship and Guest in 1990 <sup>107</sup> .....  | 15 |
| Table 6 Concentration of compound needed to protect plants against ethylene by Sisler and Serek in 1999 <sup>122</sup> .....  | 18 |
| Table 7 Minimal concentration of selected cyclopropenes and time of imposed insensitivity on banana fruits <sup>127</sup> .....   | 19 |
| Table 8 Ring opening of <b>93</b> in presence of various metal(I) complexes, by Musa <sup>193</sup> .   | 33 |
| Table 9 Effectiveness of ethyl diazoacetate <b>227</b> as ethylene antagonist in Geraldton wax .....  | 70 |

|  |     |
|--|-----|
| Table 10 Calculated relative energies (kJ mol <sup>-1</sup> ) of the [1,2,3]triazolo[1,5- <i>a</i> ]pyridine structures <sup>262</sup> ..... | 75  |
| Table 11 Summary of the copper reactivity model tests and Geraldton wax in-house assays on triazolopyridine analogues .....                  | 113 |
| Table 12 NMR spectra analysis of the compound <b>321</b> .....   | 177 |

## List of symbols and abbreviations

|                |  |
|----------------|--|
| <i>p</i> -ABSA | 4-Acetamidobenzenesulfonyl azide                   |
| ACC            | 1-Aminocyclopropane-carboxylate                    |
| ACS            | 1-Aminocyclopropane-carboxylate synthase           |
| MeCN           | Acetonitrile                                       |
| ATP            | Adenosine triphosphate                             |
| AVG            | 2-aminoethoxyvinylglycine                          |
| BHT            | Butylated hydroxytoluene                           |
| DACP           | Diazocyclopentadiene                               |
| DBU            | 1,8-Diazabicyclo[5.4.0]undec-7-ene                 |
| DCM            | Dichloromethane                                    |
| DMSO           | Dimethyl sulfoxide                                 |
| EAS            | Electrophilic aromatic substitution                |
| EDG            | Electron donating group                            |
| EWG            | Electron withdrawing group                         |
| EtOAc          | Ethyl acetate                                      |
| ETR            | Ethylene Receptor                                  |
| KMTB           | $\alpha$ -Keto- $\gamma$ -methylthio-butyrlic acid |
| 1-MCP          | 1-Methylcyclopropene                               |
| MTA            | 5'-Methylthioadenosine                             |
| MTR            | 5'-Methylthioribose                                |
| MTR-P          | 5'-Methylthio-ribose-1-phosphate                   |
| NMR            | Nuclear magnetic resonance                         |
| SAMe           | <i>S</i> -Adenosyl methionine                      |
| STS            | Silver thiosulfate                                 |
| TEA            | Triethylamine                                      |
| THF            | Tetrahydrofuran                                    |
| TMSMS          | Trimethylsulphonium methanesulphonate              |
| TP             | [1,2,3]Triazolo[1,5- <i>a</i> ]pyridine            |
| Trisyl         | 2,4,6-Triisopropylbenzenesulfonyl hydrazide        |

# Chapter 1 – Introduction

## 1.1 Horticultural produce industry and food wastage

The global food industry was worth \$1.46 trillion<sup>1</sup> annually in 2014, producing over 1.75 billion metric tonnes<sup>2, 3</sup> of fruits and vegetables worldwide. The Australian production in 2013-14 achieved gross values of \$6.70 billion for vegetables, fruits and nuts, which included production of near 3 million tonnes of commodities. In 2019/2020, a report from Horticulture Innovation has valued vegetables, fruits and nuts production at \$14.3 billion, increasing over \$1 billion annually.<sup>4</sup> Unfortunately, due to high water content of horticultural produce they are perishable and a significant amount of losses occur on transportation and storage from the farm to the consumer. The wastage occurs at all stages of the food supply chain, during production, post-harvest processing, retail and finally with the consumer, generally resulting in ~50% wastage across the entire world.<sup>5</sup> The amount of wastage varies between products cultivated and storage technologies used, thus significant variations between regions of the world are observed (Figure 1). In particular, wastage during processing and consumer stages vary significantly between developed and less developed areas. Developed areas are characterised by high consumption losses i.e. wastage by consumers. On the contrary, less developed areas have significantly lower consumption losses, however significantly greater wastage in processing, likely due to the less developed supply chains.

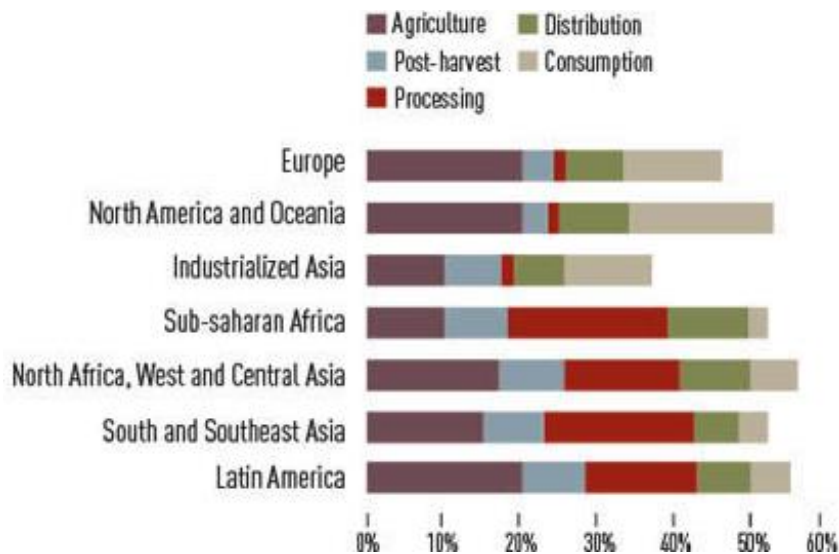


Figure 1 Distribution of horticultural produce wastage between global areas and sectors of food industry<sup>6</sup>

In Australia, an estimated 30-44% of fresh fruit and vegetables that leaves the farm is wasted before it reaches the consumer, resulting in around \$2-3 billion losses annually.<sup>7</sup> Not only are these losses financial but are also a waste of land and water resources. Importantly, this wastage occurs with the current preservation techniques such as refrigeration. A number of factors affect the storage life of fresh fruits and vegetables (temperature, humidity and postharvest diseases) but the plant hormone ethylene **1** is the major contributor causing up to 50% of the total losses (Figure 2).<sup>8</sup> Ethylene **1** is a ubiquitous plant hormone, and regulates growth in various plant cells. The ethylene-specific losses occur in particular in climacteric produce, where it triggers ripening.

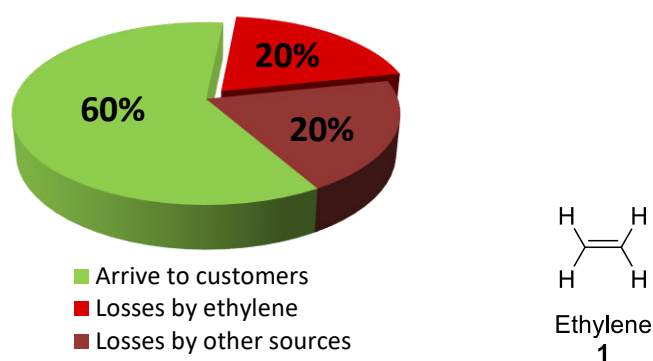


Figure 2 Approximate produce losses between the farm and a customer<sup>8</sup>

The horticultural produce sector has been developing at particularly fast rate since the industrial revolution in mid-1700s. Storage, transportation, fertilisers, and genetically modified crops have all significantly contributed to growth of this industry, with storage and transportation technologies allowing access to food products grown anywhere around the world. Horticultural produce have high water content and have relatively short shelf-lives but can be greatly extended under appropriate storage conditions. The two key parameters are temperature and relative humidity, which both can be achieved using modern equipment. Metabolism of fruits and vegetables continues to operate after harvest,<sup>9</sup> thus for appropriate storage environment various parameters must be considered. The optimal conditions vary from one produce to another, but they can be commonly classified as temperate, tropical and subtropical produce. Temperate produce can be stored at near 0 °C while tropical produce are commonly chill-sensitive i.e. exposure to low temperature may result in damage or loss of visual quality. Effectiveness of storage of food under lower temperatures was known since ancient times however readily accessible cold storage became only available with development

of refrigerators in mid-1750s. Over the last 200 years, the effects of low temperatures in storage of fresh food have been identified. When temperatures are decreased, the respiration rate is decreased, water loss is reduced and microbial development is slowed. More importantly, ethylene production is suppressed and sensitivity to ethylene is also reduced.<sup>9-13</sup> Alongside low temperature, maintaining storage environments at a high relative humidity is commonly used in storage of horticultural produce. Humidifiers were invented after refrigerators, with patents of large building/factory humidifiers being made as early as 1913,<sup>14</sup> while first ever patent of a room humidifier appearing only in 1964 by Raymond Banks.<sup>15</sup> Storage at high humidity greatly reduces water loss which affects the quality of a produce (wilting, shrivelling, weight loss). However, high humidity can only be used with low temperatures as otherwise it promotes growth of fungi and bacteria.<sup>16</sup> Paull has tabulated the optimal storage conditions for a number of fruits and vegetables (Table 1).<sup>17</sup> These and other storage considerations allow for significantly extended shelf life and allow the transportation of produce to global markets.

*Table 1 Optimal storage conditions for selected fruits and vegetables<sup>17</sup>*

| <b>Commodity</b> | <b>Temperature (°C)</b> | <b>Relative humidity %</b> |
|------------------|-------------------------|----------------------------|
| Banana           | 13-14                   | 90-95                      |
| Strawberry       | 0                       | 90-95                      |
| Apple            | -1-4                    | 90-95                      |
| Mango            | 13                      | 85-90                      |
| Asparagus        | 0-2                     | 95-100                     |
| Cucumber         | 10                      | 95                         |
| Bell pepper      | 7-13                    | 90-95                      |

## 1.2 Climacteric produce and spoilage by ripening

There are two classifications of fruit and vegetables, climacteric and non-climacteric (Figure 3). Climacteric produce can ripen after harvest and non-climacteric produce cannot. The ripening of climacteric produce by ethylene **1** was first proposed in 1935 by Crocker et al.<sup>18</sup> Climacteric commodities produce ethylene even after harvest, which binds to a receptor and triggers a signalling pathway to activate ripening process. Although ripening is essential for fresh fruit and vegetables to fully develop into a palatable product, it also accelerates ageing, known as senescence. Non-climacteric produce also generate ethylene, however their ripening does not depend on increase in ethylene production and are not as affected.<sup>19</sup>

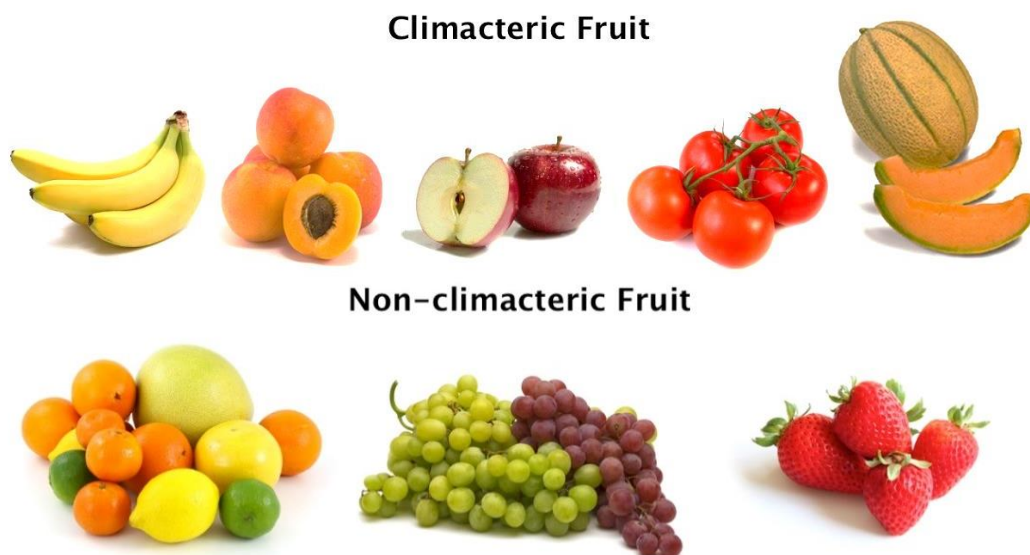


*Figure 3 Examples of climacteric and non-climacteric fruits<sup>20</sup>*

Climacteric produce are harvested prior to ripening, allowing for an extended storage period, and ripen on the shelf. Several methods, including refrigeration, are being used to delay the ripening process of climacteric commodities. Even though refrigeration slows the ripening process, the presence of ethylene is a major problem. Lack of appropriate ventilation in the storage area can result in the ethylene concentration being high enough to trigger ripening of produce and shorten shelf life. While ventilation can be partially effective in delaying the ripening of fruits, it is not ideal since ethylene is produced by other fruit or by combustion engines used in transportation vehicles and processing equipment.<sup>21</sup> While ethylene **1** is a key hormone in ripening, other plant hormones have specific functions in life cycles of plants as well as their products.

### 1.3 Ethylene as one of the 5 major plant hormones

Ethylene **1** is one of the five major plant hormones, signal molecules used in control and regulation of all systems in plants. The five major hormones are gibberellin **2**, ethylene **1**, abscisic acid **3**, auxin **4**, and cytokinin **5** (Figure 4). They are produced by the plant at small concentrations and used by cells to communicate and manage all aspects of plant's life. Their presence or lack thereof triggers reactions of cells, many of which are still not fully understood due to the complexity of the plant systems.<sup>22-25</sup> Out of the 5 major hormones, only gibberellin **2** is involved in plants' germination. Gibberellin **2**, auxin **4** and cytokinin **5** have prevalent functions in the growth of plants including flowering and fruit development. Ethylene **1** is also involved in the flowering and fruit development. Abscission of plant organs is regulated by ethylene **1** and abscisic acid **3**. Abscissic acid **3** also is involved in seed dormancy. (Figure 5).

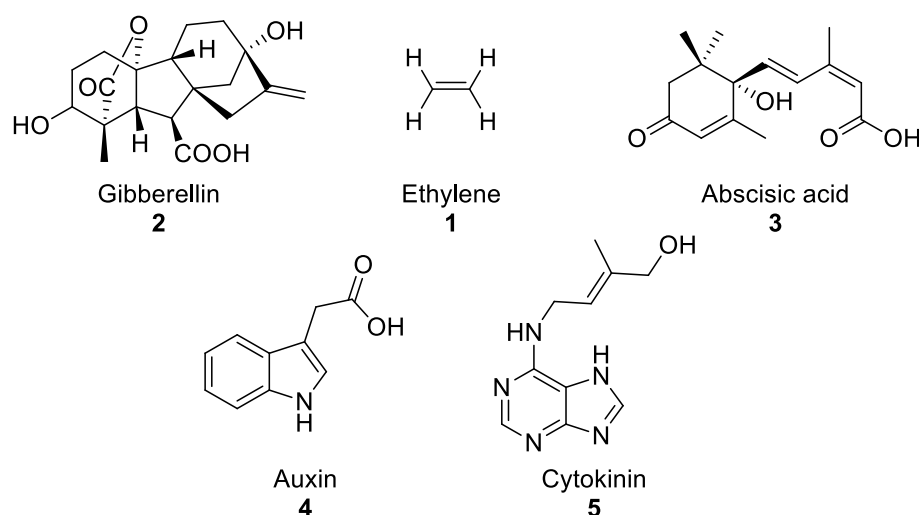


Figure 4 5 Major plant hormones

|               | Germination | Growth to Maturity | Flowering | Fruit Development | Abscission | Seed Dormancy |
|---------------|-------------|--------------------|-----------|-------------------|------------|---------------|
| Gibberellin   | ✓           | ✓                  | ✓         | ✓                 | -          | -             |
| Auxin         | -           | ✓                  | ✓         | ✓                 | -          | -             |
| Cytokinins    | -           | ✓                  | ✓         | ✓                 | -          | -             |
| Ethylene      | -           | -                  | ✓         | ✓                 | ✓          | -             |
| Abscisic Acid | -           | -                  | -         | -                 | ✓          | ✓             |

Figure 5 Involvement of the five major plant hormones life stages of a plant based on summary by B. Cornell<sup>26</sup>

Ethylene **1** is the only gaseous plant hormone. This allows it to be easily diffused throughout the tissue of the plant, reaching all cells within the plant and even affect surrounding plants. As with all plant hormones, the concentration required for it to have an effect is extremely low. Abeles has shown that inhibition of growth of various plants (tomatoes, beans, cucumber, petunias and other) occurred on exposure to ethylene **1** at concentrations as low as 0.5ppm.<sup>27</sup> A study by Burg and Burg showed sensitivity of various fruits and vegetables to ethylene **1** at concentrations as low as 0.02ppm.<sup>28</sup> Ethylene **1** has various functions in plant growth e.g. it controls leaf expansion in growth, it inhibits cell elongation while promoting stem thickening and it even inhibits plants geotropic response. While ethylene **1** is biosynthesised in plants, there are other sources contributing to ethylene **1** in atmosphere, the most prominent being a side product of combustion engines in cars and industrial machinery.<sup>29</sup> Due to the extremely low limits of ethylene **1** necessary to have effect on horticultural produce, these additional sources contribute significantly to produce wastage.<sup>30</sup>

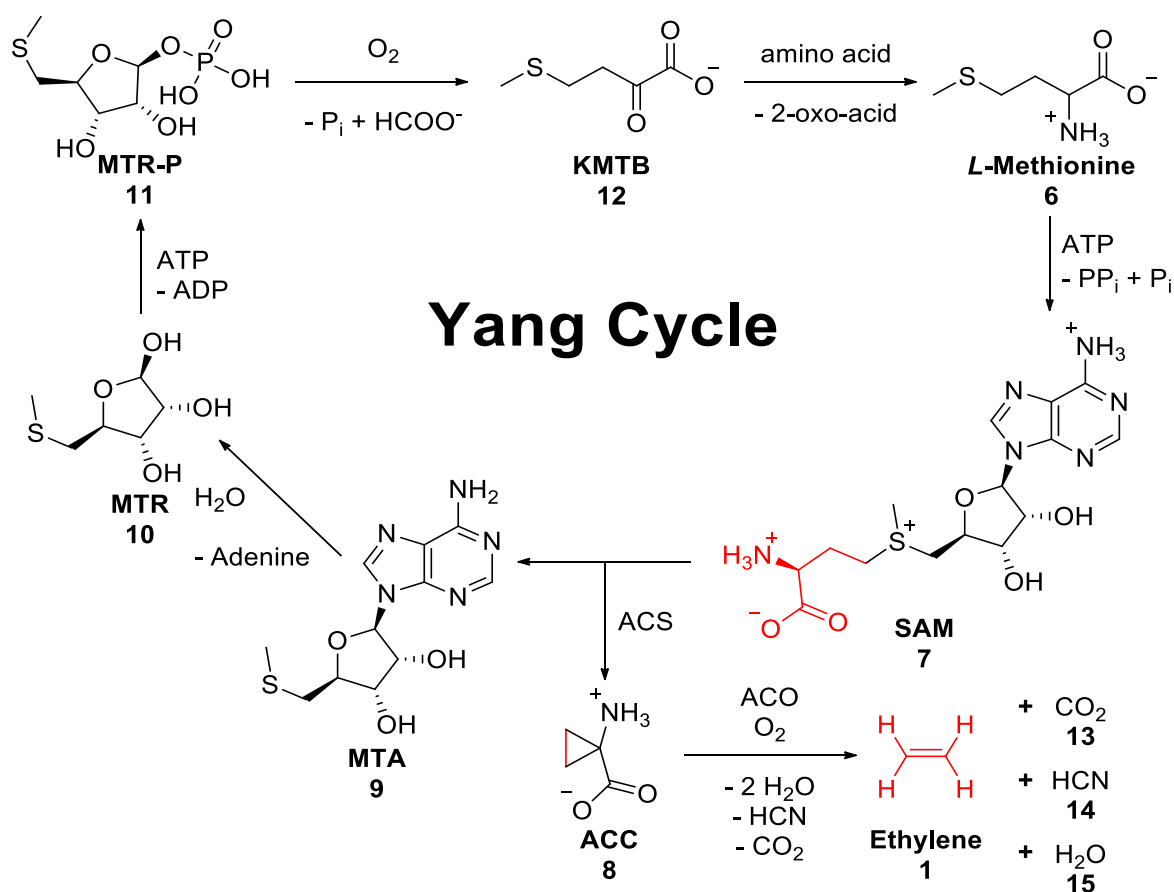
### **1.3.1 Ethylene history and storage of climacteric products**

The effects of ethylene **1** on plants have been observed by humans for thousands of years. In ancient Egypt, unripe sycamore figs were gashed with special tools which injured the fruit, causing a release of ethylene **1** and thus ripening the figs.<sup>31, 32</sup> With the development of modern analytical technologies, it became possible to identify ethylene **1**. Ethylene **1** was discovered and produced as early as 1700s, but the first demonstration of its involvement with plants is attributed to Neljubow in 1901. He demonstrated that ethylene **1** (present in gasoline exhaust) caused shedding of flowers and buds of pea plants in a greenhouse.<sup>33</sup> Discovery of the main effect of ethylene **1**, namely promotion of ripening and senescence in flowers and fruits, took place in 1930s, where ethylene **1** was confirmed to be produced by various fruits and vegetables, thus causing ripening in nearby produce. The effects of ethylene **1** on plants were investigated.<sup>34-38</sup> Presence of ripe apples stored alongside potatoes caused abnormal sprouting of the potatoes. Presence of ripe apples, pears, peaches, tomatoes and bananas alongside unripe fruits stimulated onset of ripening in these fruits. Presence of ethylene **1** hastened flowering and development of flowers as well. The analysis of ethylene **1** produced in plants could be inferred after the emergence of gas chromatography in 1950s by Cremer and Müller, who separated ethylene **1** from a mixture containing acetylene.<sup>39</sup>

These discoveries improved storage techniques, in particular for climacteric produce, by elimination of ethylene from the storage atmosphere. The techniques used to mitigate effects of ethylene **1** in atmospheric storage included decrease of temperature to slow down chemical processes and ventilation to decrease ethylene **1** concentration in storage. In the 1920s, Franklin Kidd investigated effects of temperature and altered atmosphere on storage of apples.<sup>40</sup> Storage atmosphere with different oxygen (O<sub>2</sub>) and carbon dioxide (CO<sub>2</sub>) concentrations were investigated. A decrease in temperature was shown to delay ripening. An increase in CO<sub>2</sub> concentration was harmful to the apples while change in O<sub>2</sub> concentration did not have significant effect on the fruits. In 1951, S.W. Porritt discussed the concept of ethylene **1** as a ripening hormone and his work was hotly debated at the time, with various apparent evidence shown, such as use of ethylene **1** to hasten change in skin colour of lemons from green to yellow.<sup>41</sup> Gas chromatography allowed confirmation of this concept in studies by Burg and Burg,<sup>42-44</sup> who investigated methods to lower ethylene **1** in produce to lower its effect and decrease wasteful ripening. Their studies involved ventilated storage of various fruits and vegetables at below atmospheric pressure, showing decrease in ethylene action under these conditions. Horticultural products can only be cooled down to specific temperatures to avoid damage (see Table 1 – optimal storage conditions), thus the suppression of ethylene **1** in storage is limited. Unfortunately, the amount of ethylene **1** needed to trigger ripening in produce is extremely small and the commodities generate it under these conditions, limiting the effectiveness of this type of storage. In order to develop greater understanding of the ethylene **1** in plants, it is essential to analyse its biosynthesis and action.

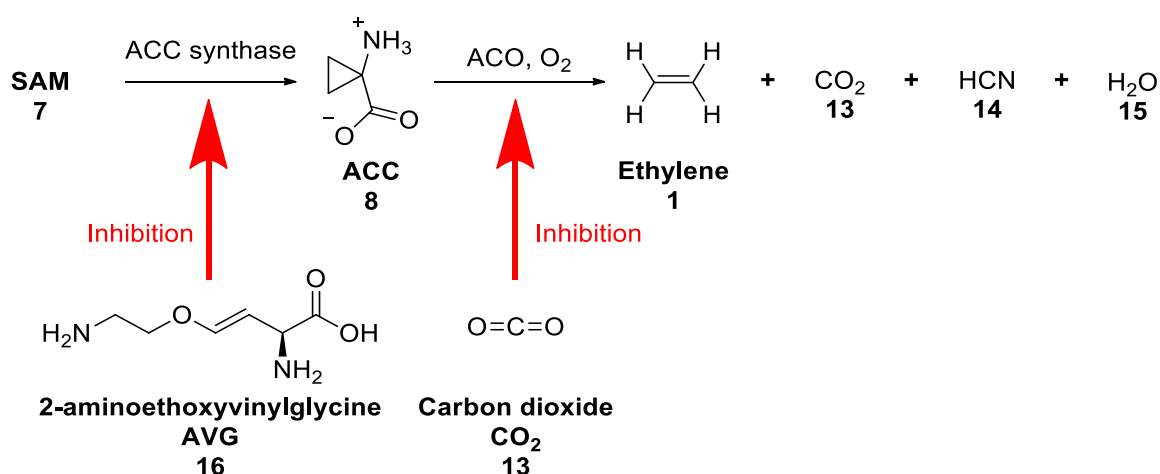
### 1.3.2 Ethylene biosynthesis

The biosynthesis of ethylene **1** in plants is well documented and is made from the common biochemical intermediate *S*-adenosyl methionine **7** (SAM).<sup>45-47</sup> The amino acid *L*-methionine **6** is converted to SAM **7** in a process called the Yang cycle (Scheme 1).<sup>48-64</sup> *L*-methionine **6** undergoes substitution reaction with adenosine 5'-triphosphate (ATP), catalysed by SAMe synthetase to form *S*-adenosyl methionine **7** (SAM). SAM **7** is an essential cosubstrate in the physiological functions of the plant, participating in a wide range of biological reactions including methyl group transfers, transsulfuration, and aminopropylation reactions.<sup>65, 66</sup> In the Yang cycle, ACC synthetase (ACS) converts SAM to 1-aminocyclopropane-carboxylate **8** (ACC) and 5'-methylthioadenosine **9** (MTA). MTA **9** is then converted back to *L*-methionine **6** in 4 steps to complete the Yang cycle. ACC **8** is oxidised in presence of O<sub>2</sub> catalysed by ACC oxidase (ACO) to form ethylene **1**, carbon dioxide **13**, cyanide **14**, and water **15**.



Scheme 1 Ethylene biosynthesis through the Methionine (Yang) cycle<sup>63</sup>

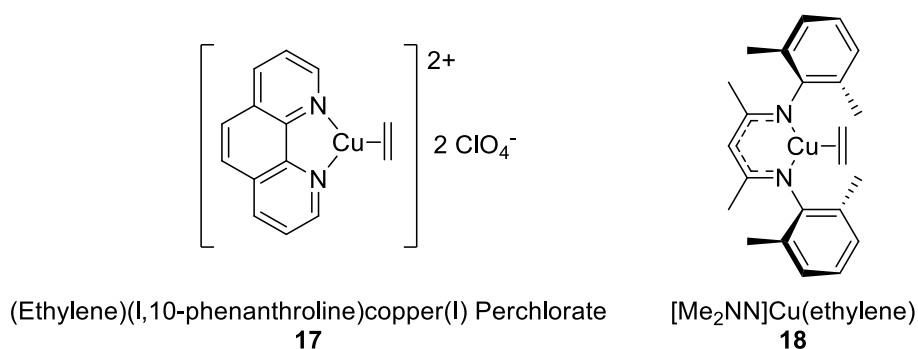
One way to prevent the action of ethylene **1** in plants is to inhibit its production. While production of ACC **8** could be inhibited to prevent production of ethylene **1**, ACC **8** has various other uses in plants such as precursor to synthesis of MACC or GACC enzymes by conjugation with malonic acid or glutathione.<sup>67</sup> In a similar manner inhibition of the methionine cycle would have significant effects on plants systems beyond synthesis of ethylene as SAM **7** is a common intermediate in many biosynthetic pathways.<sup>68</sup> Ethylene production by ACC oxidase can be inhibited by increasing the concentration of carbon dioxide **13**, however this affects other functions in plants thus is not viable on an industrial scale.<sup>69</sup> A brief exposure of Granny Smith apples with 20% CO<sub>2</sub> **13**, reduced the formation of ethylene **1** for a period of time. An increase in the concentration of ACC **8** was also noted suggesting that CO<sub>2</sub> **13** inhibited the enzymatic conversion of ACC **8** to ethylene **1** (Scheme 2).<sup>70</sup> 2-aminoethoxyvinylglycine **16** (AVG) is one of the most common ethylene biosynthesis inhibitors and it competitively inhibits the ACC synthase. It is also significantly less toxic for plants than carbon dioxide **13**. In order for this inhibition to be effective, a continuous exposure to the antagonist is required due to continuous productions of ACC **8**.<sup>71, 72</sup> While inhibition of ethylene biosynthesis may be effective in delaying the ethylene response, it also has a range of undesirable side effects on plants and produce. This approach has no effect on exogenous ethylene **1** and is not a commonly used technique in horticultural industry.



Scheme 2 Biosynthesis of ethylene from SAM and antagonists of ethylene biosynthesis<sup>63, 71</sup>

### 1.3.3 The ethylene receptor

The first observation of ethylene action is referred to as the ‘triple response’,<sup>73</sup> and is the alteration of growth of etiolated pea (*Pisum sativum*) seedlings. The three responses are elongation and thickening of the stem, and a change of direction of growth. The triple response is also observed in *Arabidopsis thaliana*,<sup>74-77</sup> a commonly used plant model for genome studies.<sup>73, 78-80</sup> Even though the role of ethylene **1** as a plant hormone has been known for over a century,<sup>81</sup> its interaction with the ethylene receptor is still poorly understood. It is believed ethylene receptor (ETR-1) contains a copper(I) cofactor allowing for binding of ethylene **1** to the protein. Rodriguez determined the copper content of a purified protein ETR1(1-128)GST fusion protein (obtained from *Arabidopsis*). It was done by graphite furnace atomic absorption spectroscopy.<sup>82</sup> It was further developed by Schott-Verdugo into a structural model of the transmembrane sensor domain of ETR1 by *ab initio* structure prediction and coevolutionary information. Their model was refined and validated by comparing to experimental data of protein-related copper stoichiometries on purified receptor preparations and tryptophan scanning mutagenesis.<sup>83</sup> To further understand the role of Cu(I) binding of ethylene, Cu(I)-ethylene complexes (e.g. **17** and **18**) have been extensively investigated (Scheme 3).<sup>84-89</sup> The insight obtained from the chemical model can be applied alongside experimental data based on years of studies of reactivity between olefins and plants to further understand the ethylene receptor.

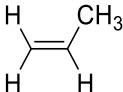
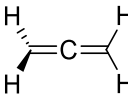
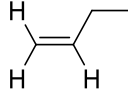


Scheme 3 Examples of Cu(I)-ethylene complexes<sup>85, 87</sup>

## 1.4 Agonists of the ETR-1

Ethylene **1** is not the only compound that triggers the ethylene response. In 1967, Burg and Burg<sup>90</sup> studied the response of ethylene **1** and its derivatives (**19-26**) in peas and discovered that compounds with a terminal alkene have similar effect on plants to ethylene **1**, i.e. acting as agonists of the ethylene receptor (Table 2). A number of key parameters have been discovered to trigger the ethylene response. Only terminal unsaturated compounds are active, and the strength of the agonist is inversely proportional to molecular size. These authors also postulated the ethylene receptor operates through a metal containing site based on the common reactivity patterns of carbon monoxide **21** in plants.

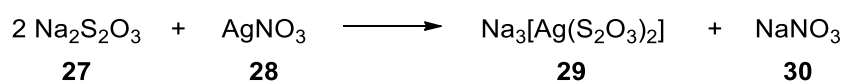
*Table 2 Biological Activity of Ethylene 1 and other unsaturated compounds as determined by the pea straight growth test by Burg and Burg in 1967<sup>90</sup>*

| No.       | Compound         | Structure   | $K'_A$ relative to ethylene | Gas phase for half-maximum activity (ppm) |
|-----------|------------------|---|-----------------------------|---|
| <b>1</b>  | Ethylene         |   | 1                           | 0.1                                       |
| <b>19</b> | Propylene        |  | 130                         | 10  |
| <b>20</b> | Vinyl chloride   |  | 2,370                       | 140                                       |
| <b>21</b> | Carbon monoxide  | $:\equiv\text{O}:$  | 2,900                       | 270                                       |
| <b>22</b> | Vinyl fluoride   |  | 7,100                       | 430                                       |
| <b>23</b> | Acetylene        | $\text{H}-\equiv\text{H}$   | 12,500                      | 280                                       |
| <b>24</b> | Allene           |  | 14,000                      | 2,900                                     |
| <b>25</b> | Methyl acetylene | $\text{H}-\equiv\text{C}-\text{H}$  | 45,000                      | 800                                       |
| <b>26</b> | 1-Butene         |  | 140,000                     | 27,000                                    |

## 1.5 Preventing ethylene action

### 1.5.1 Substitution of the copper ion in ETR-1

Silver(I) ions block ethylene **1** perception as it replaces copper(I) within the ethylene receptor.<sup>91</sup> Rodriguez et al. showed silver ions can replace the copper in the ethylene receptor in a mutant *etr1-1(1-128)*GST fusion protein in yeast. The functionality of the Ag(I) bound receptor was altered, as ethylene **1** does not cause an activation of its signalling pathway.<sup>92</sup> Therefore, Ag(I) ions can be considered as an indirect ethylene antagonists, with a single exposure necessary for an extended period of insensitivity to ethylene **1**. One of the first examples of silver ions as effective ethylene antagonists was shown in 1976 by Beyer.<sup>93</sup> Silver nitrate **28** was found to be an effective blocker of the ethylene action in a range of horticultural products (peas, cotton, orchids). The salt solutions (10 - 240 mg/L) containing the surfactant Tween 20 were applied to pea, cotton and orchid plants. Afterwards, the plants were exposed to ethylene **1**, however no ethylene action was observed, indicating inhibition of the ethylene action. Beyer hypothesised the silver ions acted by replacing the Cu(I) cofactor in the ethylene receptor.<sup>93</sup> This study was followed by Halevy and Kofranek in 1976<sup>94</sup> which pointed out the potential toxicity of silver ions as a heavy metal thus not applicable to edible crops. Silver nitrate **28** and other silver salt solutions were also found to be poorly mobile in plant vascular systems causing black spotting of petals and leaves. In 1978, a breakthrough in this area was found in the use of silver thiosulphate **29** (STS) (Scheme 4).<sup>95</sup> STS **29** is made by reacting sodium thiosulphate **27** with silver nitrate **28**. The negatively charged  $[\text{Ag}(\text{S}_2\text{O}_3)_2]^{3-}$  ion could be transported at significantly higher rates through a plant body while retaining its 'antiethylene action'. STS **29** was found to be an excellent treatment for cut carnations to keep them fresh longer by preventing ethylene action and thus abscission of petals. STS **29** has been effectively used ever since its discovery. Unfortunately, STS **29** like other silver salts could not be used for edible products.



*Scheme 4 Preparation of silver thiosulphate<sup>96</sup>*

## 1.6 Inhibitors of ethylene action

### 1.6.1 Olefins

With existence of agonists for the ethylene receptor other than ethylene **1**, it was hypothesised antagonists could exist as well, thus could be used to delay ripening of climacteric produce. In 1965, Burg and Burg postulated a correlation between the ethylene receptor and the reactivity of transition metals (such as silver<sup>97-99</sup>) with olefins (such as ethylene **1**).<sup>100</sup> Amongst the tested olefins, 1-butene derivatives were found to act as antagonists to ethylene action i.e. could occupy the binding site of the receptor without triggering a response.<sup>90, 101</sup> 1-Alkenes were shown to decrease in the agonistic response with extended carbon chain; 1-butene **26** and longer alkenes (**31-35**) were found to exhibit antagonistic response instead (Table 3).<sup>90</sup> This suggested an antagonistic binding site near the copper cofactor in the receptor. The antagonistic effect of these compounds was not long lasting, implying competitive binding mode with the ethylene receptor.

Table 3 Effect of ethylene and 1-alkenes on etiolated pea growth by Sisler in 2008<sup>102</sup>

| No.       | Compound   | Structure | Effect on ethylene action $\mu\text{L}$                   |
|-----------|------------|-----------|---|
| <b>1</b>  | Ethylene   |           | Agonist<br>$0.1 \pm 0.02$                                 |
| <b>19</b> | Propene    |           | Agonist<br>$10 \pm 0.5$                                   |
| <b>26</b> | 1-Butene   |           | Agonist      Antagonist<br>$27000 \pm 500$ $3300 \pm 100$ |
| <b>31</b> | 1-Pentene  |           | Antagonist<br>$2300 \pm 80$                               |
| <b>32</b> | 1-Hexene   |           | Antagonist<br>$1100 \pm 50$                               |
| <b>33</b> | 1-Octene   |           | Antagonist<br>$400 \pm 35$                                |
| <b>34</b> | 1-Decene   |           | Antagonist<br>$300 \pm 5$                                 |
| <b>35</b> | 1-Dodecene |           | Antagonist<br>$246 \pm 10$                                |

In 1973, 2,5-norbornadiene **36** was shown to be the first olefin found to significantly counteract ethylene action.<sup>101</sup> 2,5-Norbornadiene **36** is a competitive antagonist, able to counteract 0.3  $\mu\text{L/L}$  of ethylene **1** at 600  $\mu\text{L/L}$ . The antagonistic effect of 2,5-norbornadiene **36** was shown to be reversible, similarly to 1-butene analogues. In a later study, the scope of ethylene antagonists was expanded.<sup>103</sup> (Table 4). Most alkenes were active ethylene antagonists to some degree. Benzene **44** and cyclohexane **43** were not active, which was expected based on their chemistry. Interestingly, the strain of the tested molecules was proportional to their inhibition of ethylene action. Sisler and Yang theorised that an olefin will only show an ethylene-like agonist response if its double bond has an unsubstituted methylene group.<sup>104</sup> The most strained of the compounds tested was 2,5-norbornadiene **36**, which also was the most potent, showing the greatest efficacy in comparison to other cyclic olefins (**37-42**) (Table 4). A variety of further studies also have showed its potency.<sup>105, 106</sup> While effective as an ethylene antagonist at low concentrations, it was toxic to plants in greater amounts, limiting its industrial use.

Table 4 The inhibition of ethylene action by various compounds by Sisler and Yang in 1984<sup>103</sup>

| No.       | Compound            | Structure   | $K_i$ $\mu\text{L/L}$ |
|-----------|---------------------|---|-----------------------|
| <b>36</b> | 2,5-Norbornadiene   |  | 170                   |
| <b>37</b> | Norbornene          |  | 360                   |
| <b>38</b> | 1,3-Cyclohexadiene  |  | 488                   |
| <b>39</b> | 1,3-Cycloheptadiene |  | 870                   |
| <b>40</b> | Cyclopentene        |  | 1100                  |
| <b>41</b> | 1,4-Cyclohexadiene  |  | 4650                  |
| <b>42</b> | Cyclohexene         |  | 6060                  |
| <b>43</b> | Cyclohexane         |  | $\infty$              |
| <b>44</b> | Benzene             |  | $\infty$              |

\*The value of  $K_i$  was the concentration of inhibitor which will double the apparent  $K_m$  for ethylene. The smaller  $K_i$  is, the more effective an inhibitor it is.

In 1990, Sisler, Blankenship and Guest presented a study of cyclooctenes and cyclooctadienes (**45-50**) (Table 5) in an expansion of the library of cyclic olefins with ethylene antagonistic properties.<sup>107</sup> *trans*-Cyclooctene **46** was found to be a significantly more potent ethylene antagonist than *cis*-cyclooctene **50**, validating that strain is a requirement for potency. *trans*-Cyclooctene **46** was of particular interest as it could be easily applied to produce in storage due to its low boiling point that vaporizes at room temperature. Unfortunately, due to the competitive nature of the binding, it required a continuous exposure to maintain an antagonistic effect,<sup>108</sup> its toxicity as well as a strong and unpleasant odour, it was deemed commercially unusable.<sup>107</sup>

Table 5 Competition of cyclooctenes and cyclooctadienes with ethylene **1** for binding in tobacco leaves by Sisler, Blankenship and Guest in 1990<sup>107</sup>

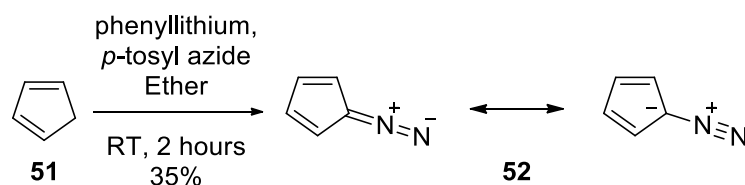
| No. | Compound                             | Structure  | K <sub>d</sub> (Gas)<br>μL/L |
|-----|--------------------------------------|--|------------------------------|
| 45  | <i>cis,trans</i> -1,3-Cyclooctadiene |   | 12                           |
| 46  | <i>trans</i> -Cyclooctene            |  | 22                           |
| 47  | <i>cis,trans</i> -1,5-Cyclooctadiene |  | 80                           |
| 36  | 2,5-Norbornadiene                    |  | 225                          |
| 48  | <i>cis,cis</i> -1,5-Cyclooctadiene   |  | 690                          |
| 49  | <i>cis,cis</i> -1,3-Cyclooctadiene   |  | 2400                         |
| 50  | <i>cis</i> -Cyclooctene              |  | 5000                         |

\*K<sub>d</sub> is the amount of compound that reduces ethylene binding by 50%. The smaller K<sub>d</sub> is, the more effective an inhibitor it is.

All of the presented olefins exhibited a competitive (reversible) inhibition of the ethylene receptor and thus require continuous exposure to effectively compete with ethylene generated by the plant.<sup>101, 107</sup> For an ethylene antagonist to be effective on an industrial scale it had to be effective on a single exposure to plant tissue, preventing ethylene action for an extended period of time.<sup>108, 109</sup> The next part of this review will address irreversible ethylene antagonist products.

### 1.6.2 Diazocyclopentadiene (DACP)

Most ethylene antagonists reported in this chapter are olefins, however there is one compound that stands out based on its functional group, diazocyclopentadiene **52** (DACP). Diazocyclopentadiene **52** was first synthesised in 1953,<sup>110</sup> by reacting lithiated cyclopentadiene **51** and tosyl azide by a diazo transfer reaction (Scheme 5).<sup>111</sup>



*Scheme 5 Synthesis of diazocyclopentadiene by Doering and DePuy<sup>110</sup>*

In 1992, in an attempt to identify the ethylene-binding site protein by a ‘tagging’ technique, Sisler and Blankenship found DACP **52** exhibited ethylene antagonistic properties.<sup>112</sup> The effects of DACP **52** were investigated under dark and light conditions on tobacco leaves and mung bean sprouts.<sup>113</sup> It was discovered DACP **52** inhibited ethylene action by continuous exposure, similar to various olefin compounds. The effectiveness of inhibition was increased when plants were exposed to UV light, which was hypothesised by the authors to be due to photodegradation of the DACP **52** to a more reactive carbene species. The most significant discovery however, was on exposure to fluorescent light, which caused photodegradation to a complex mixture of products with significantly different properties. The formed mixture was found to exhibit a ‘permanent’ inhibition of ethylene action i.e. affected the plants beyond the timeframe of the experiment. DACP **52** exhibited a partial ‘permanent’ effect when activated by fluorescent light prior to plant treatment. It was postulated by the authors DACP **52** forms a more reactive species that exhibits these particularly outstanding properties.<sup>113</sup> The single exposure treatment was a significant milestone as it

significantly lowered amounts of chemical used and prolonged the effective period of an ethylene antagonistic treatment. Unfortunately the development of DACP **52** as an ethylene antagonist was not continued due to its toxicity and explosive properties<sup>114, 115</sup> making it hazardous for large scale use, even though its production is relatively simple.

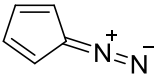
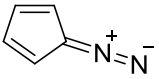
Further studies of ethylene antagonistic effects of DACP **52** have also shown high affinity and effectiveness on a wide range of products including: tomatoes,<sup>116, 117</sup> apples,<sup>118</sup> strawberries<sup>119</sup> and sweet pea flowers.<sup>120</sup> Irradiated DACP **52** has shown effective inhibition of the ethylene receptors on cut carnations at concentration as low as 9  $\mu\text{L/L}$ .<sup>113, 121, 122</sup> While this was a significantly weaker effect in comparison to 1-MCP **53** (5 nL/L, discovered at a later date),<sup>123</sup> unlike majority of other ethylene antagonists, the ‘permanent’ inhibition was an essential outcome for effective use of ethylene antagonists. The mode of action of DACP **52** has not been postulated in the literature, however the diazo group is the most reactive part of the molecule. DACP **52** has been known to photodegrade under UV light, resulting in formation of highly reactive carbene species. Diazo compounds can form complexes with transition metals through both nitrogen and carbon atom, allowing for a variety of addition and insertion reactions of the diazo group or form a reactive carbene intermediate.<sup>124</sup>

## 1.7 1-Methylcyclopropene (1-MCP)

### 1.7.1 History of 1-MCP

The greatest breakthrough to date was the discovery of 1-methylcyclopropene **53** (1-MCP), a low boiling point, highly reactive species and the only ethylene antagonist used commercially. The history of the commercial development of 1-MCP **53** was summarised in “A brief history of 1-methylcyclopropene”.<sup>125</sup> In 1984, Sisler *et al.* found that ring strain increases level of activity of ethylene antagonists<sup>104</sup> and investigated inhibition of ethylene action by various cyclopropenes.<sup>126</sup> Their structures are highly strained from the constraints of the alkene in a 3-membered ring. Sisler continued his studies and in 1996 with Dupille and Serek published a study on effectiveness of 1-MCP **53** in carnations.<sup>123</sup> The results suggested the inactivation of the ethylene receptors in plants with 1-MCP **53** are effective at concentrations as low as 0.5 nL/L. In 1999, Sisler and Serek presented a comparative study showing significantly greater potency of 1-MCP **53** in comparison to any other known ethylene antagonists at the time (Table 6).<sup>122</sup>

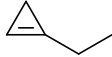
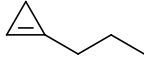
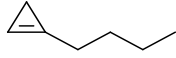
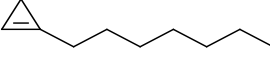
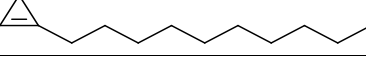
Table 6 Concentration of compound needed to protect plants against ethylene by Sisler and Serek in 1999<sup>122</sup>

| No. | Compound                                       | Structure   | Plant      | Concentration<br>μL/L |
|-----|--|---|------------|-----------------------|
| 52  | Diazocyclopentadiene<br>(in dark)              |  | Carnation  | 700000                |
| 50  | <i>cis</i> -Cyclooctane                        |  | Banana     | 512000                |
| 36  | 2,5-Norbornadiene                              |  | Banana     | 55000                 |
| 46  | <i>trans</i> -Cyclooctene                      |  | Banana     | 780                   |
| 54  | 3,3-Dimethylcyclopropene                       |  | Banana     | 700                   |
| 52  | Diazocyclopentadiene<br>(in fluorescent light) |  | Carnation  | 140                   |
| 53  | 1-Methylcyclopropene                           |  | Pea growth | 40                    |
| 53  | 1-Methylcyclopropene                           |  | Banana     | 0.7                   |
| 53  | 1-Methylcyclopropene                           |  | Carnation  | 0.5                   |

\*The smaller the Concentration is, the more effective an inhibitor it is.

Other derivatives of 1-MCP **53** were investigated by Sisler et al. in 2003, in particular the effect of length of the alkyl chain on potency of the compound.<sup>127</sup> For 1-alkyl cyclopropenes (**53**, **56-60**) up to 1-propylcyclopropene **57**, increasing the length of the carbon chain decreases the potency of the antagonist; however, for even longer chains up to 1-decylcyclopropene **60** the potency increased again (Table 7). Even though the length of the chain increased the potency, it also decreased compounds volatility, thus 1-MCP **53** remained the easiest to apply, resulting in its most common use.

Table 7 Minimal concentration of selected cyclopropenes and time of imposed insensitivity on banana fruits<sup>127</sup>

| No.       | Compound             | Structure  | Concentration (nL L <sup>-1</sup> gas) | Time of insensitivity (days) |
|-----------|----------------------|--|--|------------------------------|
| <b>55</b> | Cyclopropene         |     | 0.7 ± 0.05                             | 12                           |
| <b>53</b> | 1-Methylcyclopropene |     | 0.7 ± 0.05                             | 12                           |
| <b>56</b> | 1-Ethylcyclopropene  |    | 4.0 ± 0.4                              | 12                           |
| <b>57</b> | 1-Propylcyclopropene |   | 6.0 ± 0.3                              | 12                           |
| <b>58</b> | 1-Butylcyclopropene  |   | 3.0 ± 0.1                              | 12                           |
| <b>59</b> | 1-Heptylcyclopropene |   | 0.4 ± 0.01                             | 21                           |
| <b>60</b> | 1-Decylcyclopropene  |  | 0.3 ± 0.01                             | 36                           |

In 2006, Grichko performed a study on 21 known cyclopropene derivatives (**53**, **59-78**), assessing their ability to inhibit ethylene action (Figure 6).<sup>128</sup> The study included various volatile and water-soluble analogues. The compounds did not exhibit properties superior to 1-MCP **53**, however the study provided an insight into effect of various functional groups on potency of the chemicals. The effectiveness of the most water soluble compound was over 200 times weaker than 1-MCP **53**. The study also shown the compounds with molecular weight as high as 206 (16 carbon atoms) are able to inhibit ethylene action.

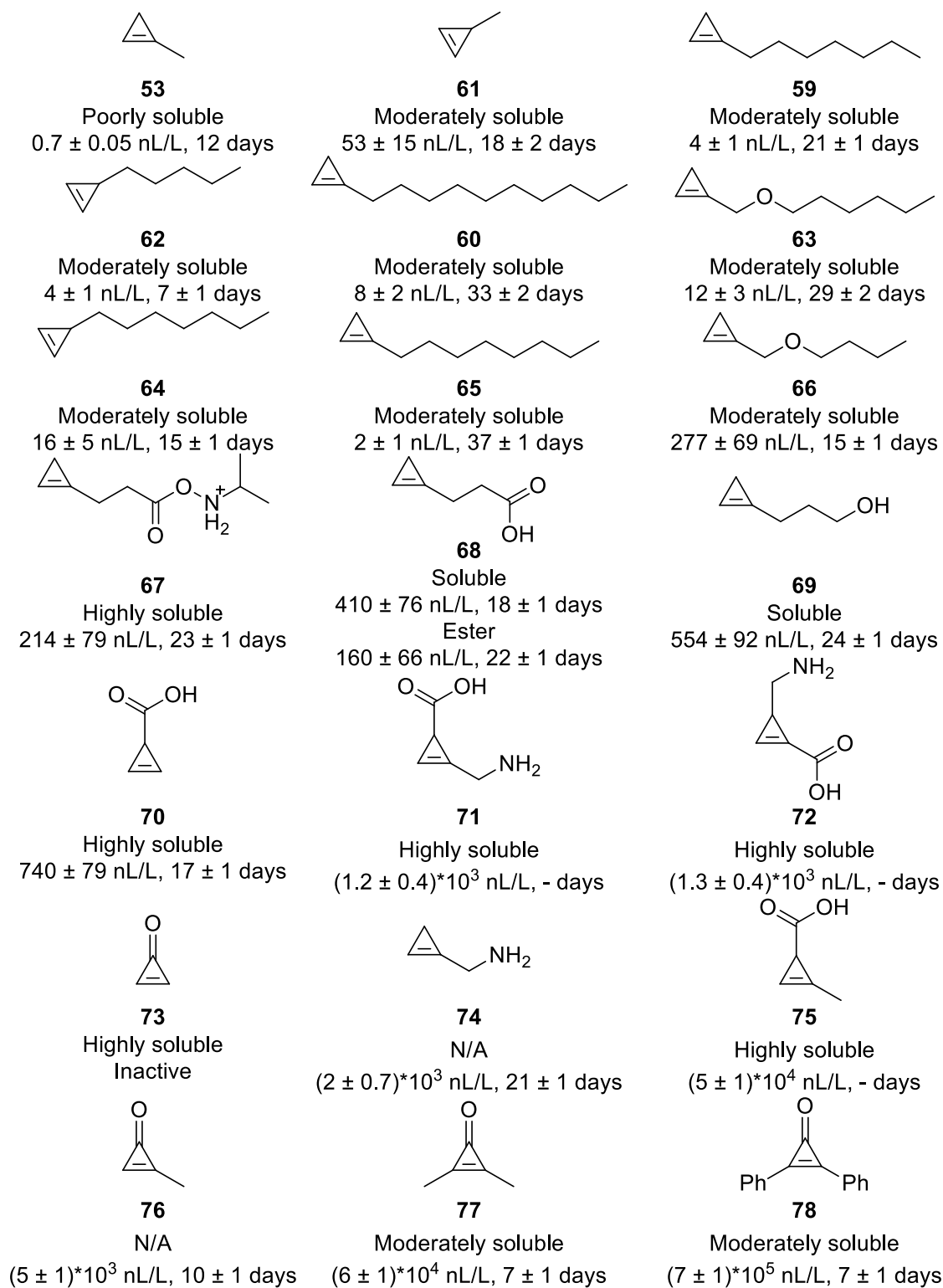
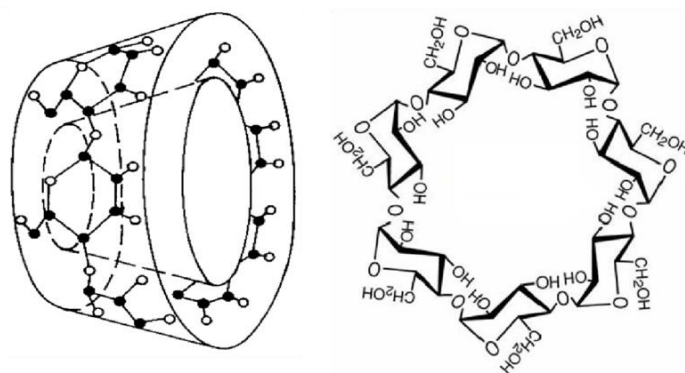


Figure 6 Inhibition of ethylene action by cyclopropene analogues in banana fruit peels.<sup>128</sup> The properties of each compound is noted below each structure (Solubility in water, Minimum apparent vapour concentration nL/L gas and Time of protection (days))

### 1.7.2 Application of 1-MCP

1-MCP **53** does not present a danger to environment, humans or animals and its by-products are easily degradable.<sup>129</sup> Its high volatility allows a quick dispersion of the remaining chemical, leaving no detectable traces on the products by the time it reaches customers. Due to high volatility of 1-MCP **53**, the compound must be introduced to produce through fumigation. This involved gassing of plants and produce in sealed tents and containers, a cumbersome method that optimally would be avoided and replaced with introduction of a water soluble ethylene antagonist as part of other processing steps such as watering of plants or washing of the produce. While potent, physical properties of 1-MCP **53** are unsatisfactory for ease of handling and application. High reactivity also translates into instability in storage. Pure 1-MCP **53** degrades in just a few hours at room temperature and cooling storage does not stop the degradation completely. An alternative method of storage and application of 1-MCP **53** was developed: an inclusion complex of 1-MCP **53** and cyclodextrin **79** (Figure 7). The inclusion complex is a powder, which releases 1-MCP **53** when it is dissolved in water.<sup>130, 131</sup> Under these conditions 1-MCP **53** remained stable for significantly longer period of time than in a neat solution. More recent studies proposed *in situ* synthesis of 1-MCP **53** as an alternative method of application, such as lithiation-borylation release<sup>132-135</sup>, discussed later. While these are more convenient solutions for storage, use of fumigation as the application method are not suboptimal.



79

Figure 7  $\beta$ -Cyclodextrin<sup>136</sup>

### 1.7.3 Synthesis of 1-MCP

1-MCP **53** was first synthesised by Fisher and Applequist in 1965 from methallyl chloride **80** and sodamide (Figure 8, path a).<sup>137</sup> Alternative bases (e.g. lithium amide, potassium amide or lithium alkoxide) were used successfully,<sup>138, 139</sup> and a large scale application was shown,<sup>140</sup> however more applicable synthesis strategies were developed. Based on synthesis pathways to 1-octyl-2-bromo-cyclopropene,<sup>141-143</sup> a more general route was envisioned by Pirrung et al.<sup>141-144</sup> The tribromocyclopropane **81** (made by the dibromocarbene addition to a vinyl bromide) is reacted with an alkyl lithium to give the cyclopropene organolithium **82** by debromination and lithium-halogen exchange (Figure 8, path b).<sup>144</sup> The organolithium **82** formed 1-MCP **53** upon hydrolysis. More recently, Sarker et al. developed a synthesis of 1-MCP **53** from a boron precursor **84**, which released 1-MCP **53** on contact with water (Figure 8, path c).<sup>132, 145</sup> The synthesis involved lithiation of methylene cyclopropane **83** followed by the reaction with boron trichloride, to form the organoboron **84**. This organoboron **84** is an improved delivery method of 1-MCP **53** in comparison to use of cyclodextrin **79** compounds. It is easy to handle and offers a sustained and selective release of 1-MCP **53**. A downside of the method is that the compound is water sensitive.

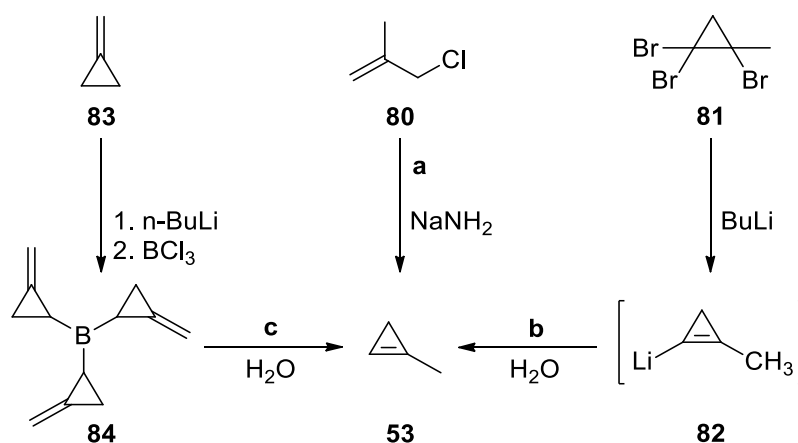
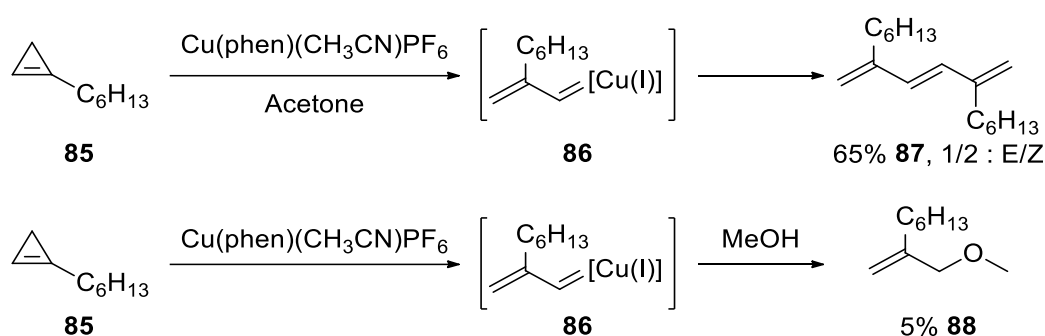


Figure 8 Synthesis methods of 1-methylcyclopropene **53** a) from methallyl chloride **80** and sodamide<sup>137</sup> b) reductive debromination of the tribromocyclopropane **81**<sup>141-144</sup> c) by lithiation-borylation release<sup>132, 145</sup>

### 1.7.4 Pirrung's mode of action

The mode of action of 1-MCP **53** was initially postulated as a consequence of the strain of the cyclopropene,<sup>127</sup> however later studies have shown similarly strained analogues such as cyclopropene **55** or 3,3-dimethyl-cyclopropene **54** are less potent than 1-MCP **53**. In 2008, Pirrung et al. proposed a more realistic mode of action for cyclopropenes based on their reactivity with copper(I) complexes.<sup>144</sup> The key model reaction is shown in Scheme 6. The reaction of 1-hexylcyclopropene **85** with a copper(I) complex gave the dimer **87**. This reaction suggested the copper complex reacted with the cyclopropene **85** to form a copper carbenoid species **86** which dimerised. This reaction was also shown to react with alcohols, affording a methyl ether **88** (Scheme 6).<sup>146</sup>



Scheme 6 Dimerization of 1-hexylcyclopropene and reaction between 1-hexylcyclopropene and methanol, in presence of copper(I) complex<sup>147</sup>

Based on these reactions, the proposed mode of action of 1-MCP **53** is as follows, it reacts with the copper(I) cofactor **89** in the receptor to form a copper carbenoid species **90** which then inserts into the ethylene receptor forming a covalent bond **91** and deactivating it permanently (Figure 9).

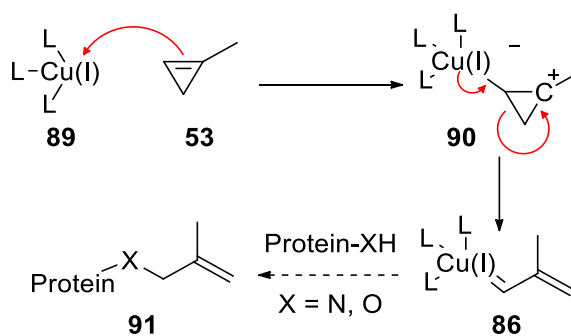


Figure 9 Proposed mechanism of 1-MCP action by Pirrung et al.<sup>144</sup>

## 1.8 Cycloproparenes

### 1.8.1 Discovery of antagonistic effects of cycloproparenes

Since the discovery of 1-MCP **53** as an effective ethylene antagonist, no new antagonists other than cyclopropenes have been reported. Recently, a collaborative project at Curtin University has shown that the cycloproparenes: benzocyclopropene **92** and 1*H*-naphtho[*b*]cyclopropene **93** (Figure 10) are also effective ethylene antagonists.<sup>148</sup> To understand how these molecules work, a brief review of their unique chemistry will be discussed.

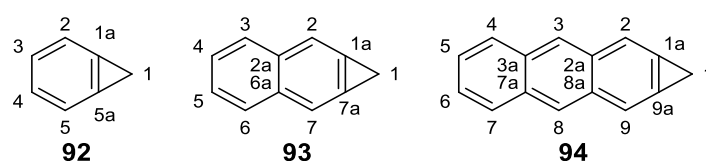


Figure 10 benzocyclopropene **8**, 1*H*-naphtho[*b*]cyclopropene **9** and 1*H*-cyclopropa[*b*]anthracene **10**

The fusion of a cyclopropene with an aromatic ring have been theoretically interesting molecules since the first stable exemplar was successfully synthesised in 1964 by Anet and Anet.<sup>149</sup> The studies of cycloproparenes were dominated by exploration of their reactivity due to inherent high strain energy: benzocyclopropene **92** (68 kcal/mol), 1*H*-naphtho[*b*]cyclopropene **93** (67.8 kcal/mol) and 1*H*-cyclopropa[*b*]anthracene **94** (69 kcal/mol).<sup>150-152</sup> Cycloproparenes are more reactive species in comparison to cyclopropenes (1-MCP **53**, 53 kcal/mol), while simultaneously being more stable due to aromatic stabilization effects. The effects of the strain of the three-member ring onto the aromatic structures have been of great interest and the strain induced localization was experimentally analysed for many cycloproparenes (e.g. Figure 11). The strain of the ring fusion was shown to cause bond shortening due to bent bond phenomenon, particularly near the site of the fusion, however the bond localization was commonly found negligible away from the ring-fusion.<sup>153-161</sup>

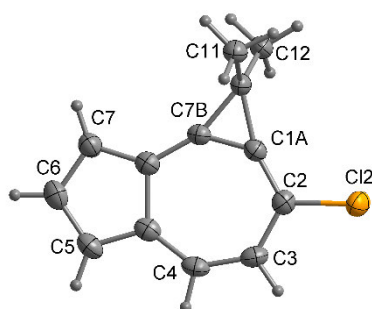


Figure 11 Molecular structure of 2-chloro-1,1-dimethyl-1*H*-cycloprop-[*e*]azulene, by permission of John Wiley and Sons publisher<sup>162</sup>

## 1.8.2 Synthesis

The high reactivity of cycloproparenes makes their synthesis a significant challenge. Nevertheless, several synthetic methods to obtain cycloproparenes have been developed.<sup>163, 164</sup> The synthesis methods of cycloproparenes presented below were extensively reviewed by Halton, first in 1973 and updated over the decades in 1980, 1989 and 2003 (Figure 12) and only key reactions will be highlighted.<sup>152, 165-167</sup>

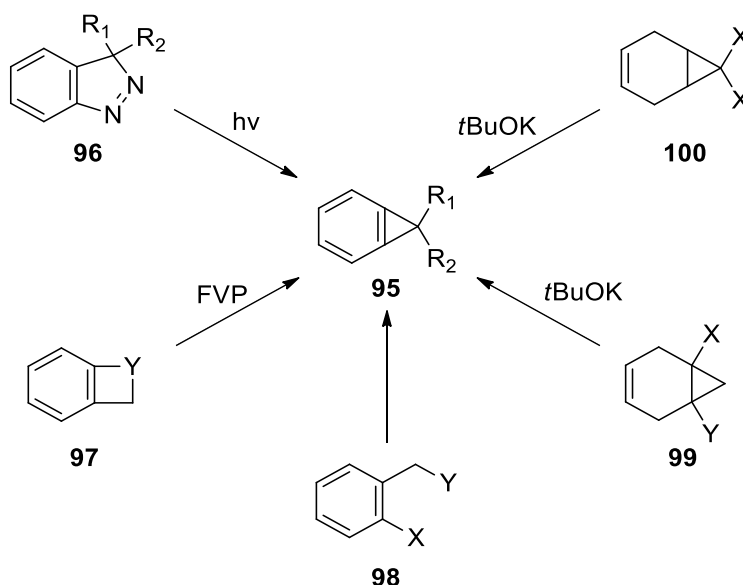
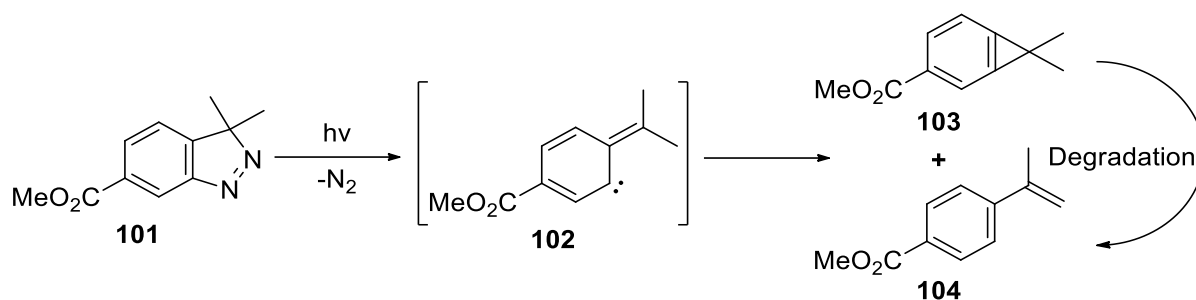
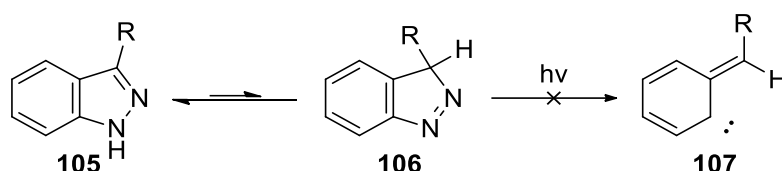


Figure 12 Pathways to cycloproparenes<sup>152</sup>

The photolysis of 3*H*-indazoles was the very first reported synthesis of a cycloproparene. Irradiation of 3*H*-indazole **101** caused a loss of the nitrogen (Scheme 7), to form a carbene reactive intermediate **102** which undergoes ring closure to form the cycloproparene **103** or hydrogen abstraction to give the alkene **104**. The photolysis reaction commonly favours formation of alkene **104** over the cycloproparene **103**. The photolysis was shown effective for various 3,3-dimethyl 3*H*-indazoles, however no aryl derivatives have been synthesised by this method. Little progress was made in recent years in synthesis of cycloproparenes using photolysis. The limitation to the 3,3-disubstituted indazoles is due to an alternative and preferential 1*H*-tautomeric form of the 3-monosubstituted indazoles, **105** (Scheme 8) that inhibits the photochemical reaction.

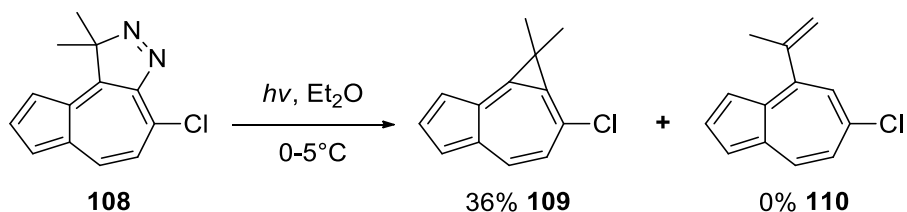


Scheme 7 First synthesis of a cycloproparene<sup>149</sup>



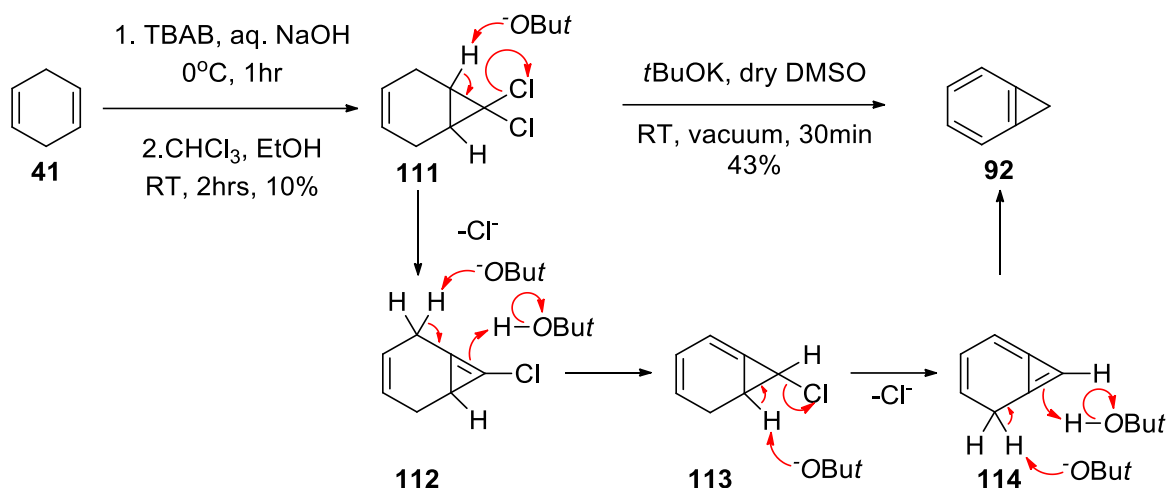
Scheme 8 Equilibrium of 3-monosubstituted indazoles<sup>129</sup>

The first application of this method to a nonbenzoid cycloproparene was shown by Payne and Wege.<sup>168</sup> The photolysis of the pyrazole **108** at low temperature gave cycloproparene **109** as the only product (Scheme 9). Unlike other cycloproparenes made by this method, 2-chloro-1,1-dimethyl-1*H*-cycloprop-*[e]*azulene **109** was significantly more stable, characterised by distinct lack of degradation to the ring open alkene **110**.



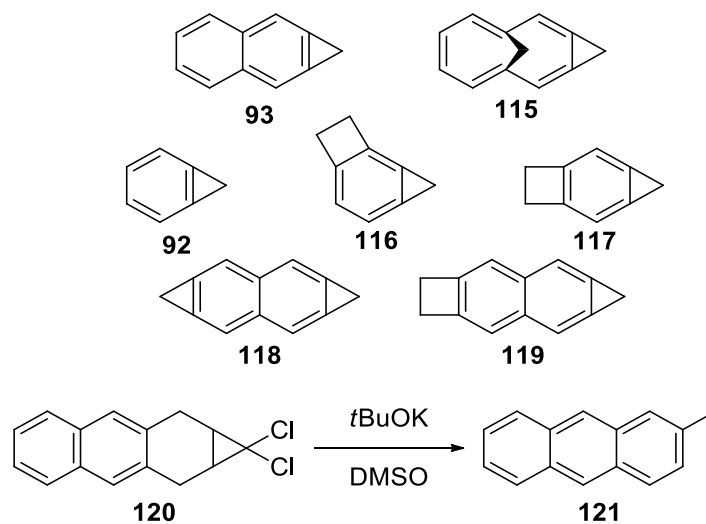
Scheme 9 Synthesis of 2-chloro-1,1-dimethyl-1*H*-cycloprop-*[e]*azulene **109** by photolysis<sup>168</sup>

The Billups synthesis method<sup>169-171</sup> was of particular interest to this study due to its simplicity and is exemplified by the synthesis of the parent compound benzocyclopropene **92** (Scheme 10). Addition of dichlorocarbene (made from  $\text{CHCl}_3$  and  $\text{NaOH}$ ) to 1,4-cyclohexadiene **41** gives 7,7-dichlorobicyclo[4,1,0]hept-3-ene **111**. Slow addition of this compound **111** to cold potassium *tert*-butoxide in dry DMSO produces the benzocyclopropene **92** which can be separated from the reaction mixture by distillation under reduced pressure. In this reaction, chlorine substituents (**111-113**) are sequentially eliminated and the double bonds rearrange into the 6-membered ring, aromatizing the ring (Scheme 10). By using potassium *tert*-butoxide, a strong bulky base, the E2 reaction is favoured, minimising amount of possible side reactions and by-products.



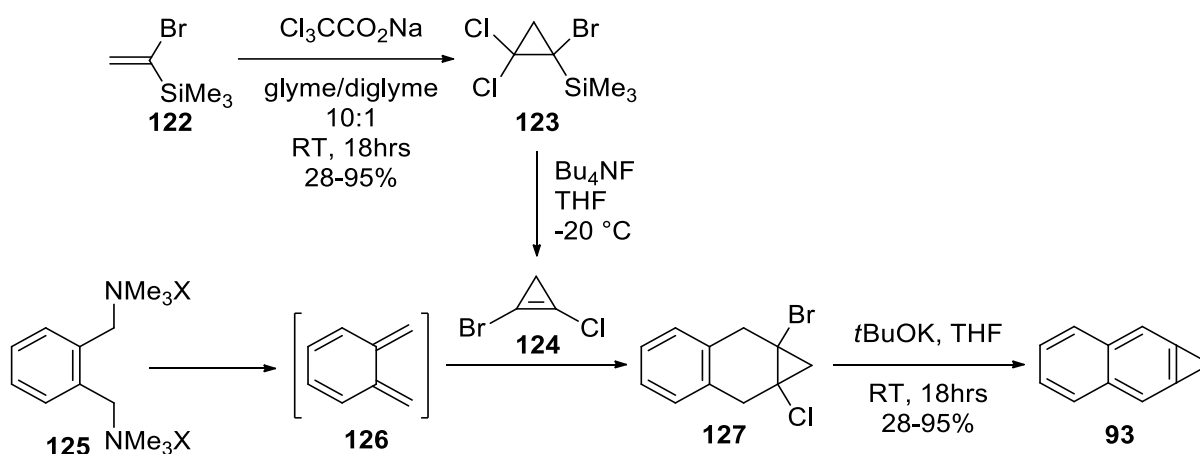
Scheme 10 Synthesis of benzocyclopropene **92** by double dehydrohalogenation of 7,7-dichloro-bicyclo[4.1.0]heptane **111**<sup>172</sup>

Billups synthesis was used in synthesis of various benzo- and naphtho- based cycloproparenes **115-119** (Scheme 11), however its scope is limited to a relatively small number of compounds. This method is only applicable for structures with no more than two fused aromatic rings. Attempts at double dehydrochlorination of larger structures like the anthracene derivative **120** resulted in only a ring open product **121** (Scheme 11).<sup>173, 174</sup>

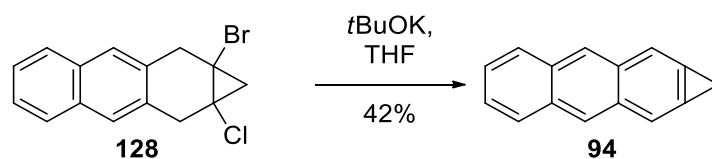


Scheme 11 Cycloproparene structures synthesised by double dehydrochlorination of a 7,7-dihalo precursor<sup>172</sup> and an ineffective synthesis target – 1H-cyclopropa[b]anthracene<sup>173, 174</sup>

In 1984, Billups et al. developed a convenient synthesis of 1-bromo-2-chlorocyclopropene **124**, using a fluoride source to eliminate TMSCl from the dichlorocarbene adduct **123** (Scheme 12).<sup>175</sup> The Diels-Alder reaction between the 1,2-dihalocyclopropene **124** and an appropriate diene **126** yields a necessary adduct **127**. Unlike the Billups reaction, the cyclopropene **93** is formed directly without the need for isomerisation, allowing more reactive cyclopropenes to be synthesised and allowed access to compounds otherwise unachievable by other synthetic methods.<sup>132</sup> An example of this is 1*H*-cyclopropa[*b*]anthracene **94**, which was obtained in 42% yield by double dehydrohalogenation from the cyclopropene adduct **128** (Scheme 13).<sup>176</sup> In contrast, the dichlorocarbene adduct **120** did not yield the target compound **94** and formed the ring-opened product **121** instead (Scheme 11).

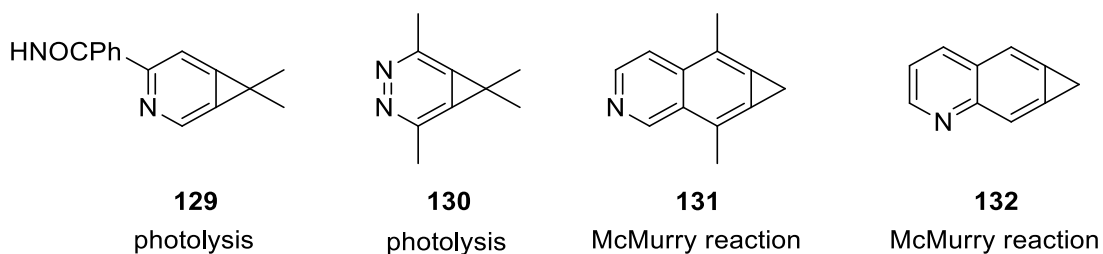


Scheme 12 Synthesis of 1*H*-cyclopropa[*b*]naphthalene **93** derived from the 1*a*-bromo-7*a*-chlorocyclopropene **127**<sup>172, 175, 177</sup>



Scheme 13 Comparison between double dehydrohalogenation of 7,7-dihalo and 1,6-dihalo precursors<sup>176, 178</sup>

The key drawbacks of the cycloproparenes as ethylene antagonists is their poor solubility in water and thus difficulty in application, requiring mixed solvents (normally water:ethanol) which is not an ideal in processing of horticultural produce. Synthesis and reactivity of cycloproparenes has been investigated in the past,<sup>165, 179, 180</sup> however the chemistry of more polar cycloproparenes is limited. Studies of pyridyl cycloproparenes **129-132** are the most relevant to this subject. Insertion of a nitrogen into the cycloproparene structure has significant effect on its physical properties, including water solubility. Unfortunately, the studies have shown it also affects its stability negatively, thus the number of successfully synthesised pyridyl derivatives is very limited (Scheme 14).<sup>181-183</sup>



*Scheme 14 Pyridyl derivatives of cycloproparenes and their methods of synthesis<sup>181-183</sup>*

### 1.8.3 Reactions

A brief summary of the reactivity of cyclopropenes is presented below. The reactivity of cyclopropenes mostly focuses on the highly strained cyclopropene ring and its ring opening reactions. These reactions include addition of nucleophiles, electrophiles and radicals as well as dimerization (Figure 13). Cyclopropenes may undergo other reactions as well, such as cycloadditions and a wide array of transition metal catalysed reactions.

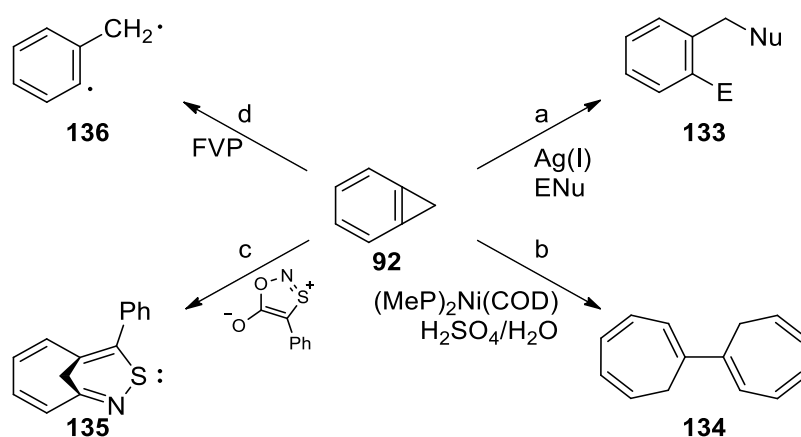
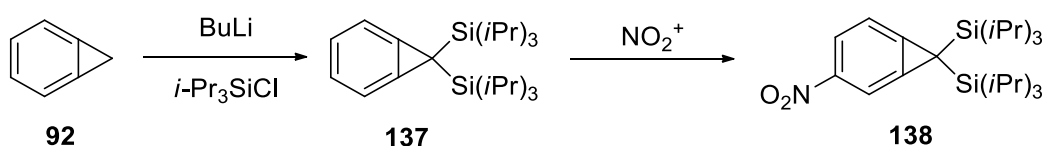
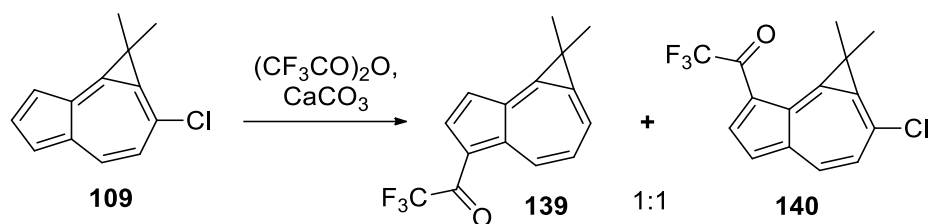


Figure 13 Chemistry of cyclopropenes<sup>172</sup> a) with electrophiles and nucleophiles, b) with transition metal complexes, c) in cycloadditions, d) upon flash vacuum pyrolysis

Electrophilic aromatic substitution of cyclopropenes is severely limited by the highly reactive three-membered ring, thus only kinetically stabilised derivatives are able to undergo classic substitution reactions. An example of a classical electrophilic aromatic nitration can be seen on bis-silated benzocyclopropene **137**, using bulky chlorotris(isopropyl)silane (Scheme 15), but these are rare.<sup>184</sup> The unusual stability of the 1,1-dimethylcyclopropazulene derivative **109** also allowed a nitration reaction.<sup>162</sup> Treatment of azulene with trifluoroacetic anhydride is known to readily form trifluoroacetylated products, and application of this reaction to the compound **109** yielded a 1:1 mixture of two trifluoroacetylated products **139** and **140** (Scheme 16). Interestingly, no ring open products were formed in the reaction, indicating low reactivity of the three membered ring, so prevalent in cyclopropenes.

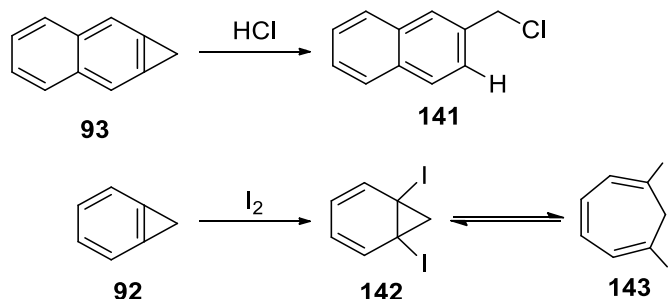


Scheme 15 Nitration of bicyclo[4.1.0]hepta-1,3,5-triene-7,7-diylbis(triisopropylsilane) **49**



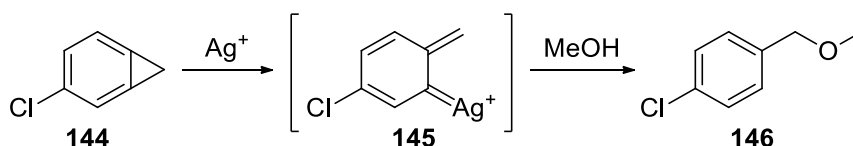
*Scheme 16 Trifluoroacetylation of 2-chloro-1,1-dimethylcycloprop[e]azulene **109**<sup>162</sup>*

The three-membered ring of the cycloproparenes is highly strained, thus reacts with electrophiles, so cycloproparenes are sensitive to acids,<sup>185</sup> halogens<sup>174, 186</sup> and other electrophiles. Opening of the three-membered ring and reaction with an electrophile such as an acidic hydrogen results in formation of a benzylic cation that may then capture a nucleophile (Scheme 17).<sup>153</sup> Depending on the cycloproparene and the reagents used (e.g. **93** vs **92**), the cyclopropyl cation formed prior to the ring opening may be sufficiently stable to allow capture of a nucleophile instead of ring opening **141**, thus yielding a norcaradiene-cycloheptatriene equilibrated compound **142-143** (Scheme 17).<sup>186, 187</sup>

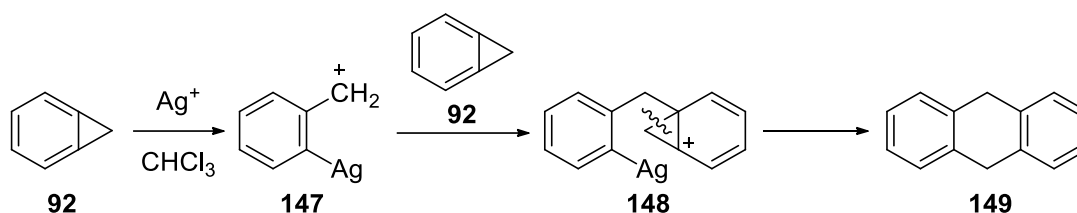


*Scheme 17 General benzyl reaction of the 1H-cyclopropa[b]naphthalene **93**<sup>153, 188</sup> and formation of norcaradiene-cycloheptatriene equilibrium from benzocyclopropene **92**<sup>186, 187, 189</sup>*

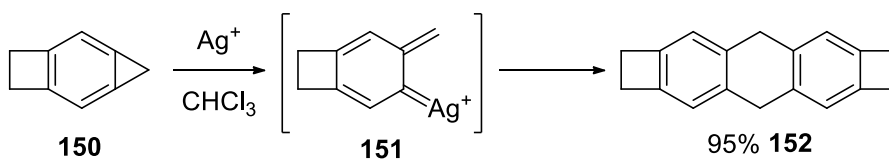
Silver(I) complexes have shown to be efficient catalysts for benzylation reaction using cyclopropenes. The silver ion mediated benzylation of cyclopropenes was shown effective with broad range of alcohols, amines and thiols, effective for a variety of derivatives, enhancing yield as well as enabling formation of previously unattained products e.g. ether **146** (Scheme 18).<sup>190</sup> When silver salts were applied in inert conditions, cyclopropenes were shown to dimerize,<sup>191, 192</sup> as in case of rocketene **150** (Scheme 20). Billups proposed a mechanism of such dimerization as a facile reaction arising from an addition of silver ion to the sigma electrons of the cyclopropenyl ring **147** to form cationic intermediate **148** (Scheme 19). Unfortunately, no further studies have been performed on this application of silver(I) complexes, leaving a significant gap in the literature knowledge.



Scheme 18 Reaction between 3-chlorobicyclo[4.1.0]hepta-1,3,5-triene **144** and methanol in presence of silver(I) complex<sup>190</sup>



Scheme 19 Proposed mechanism of dimerization of benzocyclopropene **92** in presence of silver(I) complex, by Billups et al.<sup>192</sup>

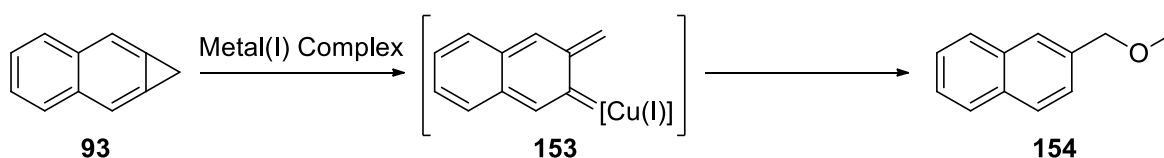


Scheme 20 Dimerization of rocketene **150** in presence of silver(I) complex<sup>192</sup>

## 1.9 Cycloproparenes as ethylene antagonists

Cycloproparenes react with transition metals, in particular silver(I) to form reactive intermediates.<sup>190</sup> These reactions are reminiscent of the Pirrung's proposed reaction between 1-MCP **53** and the copper(I) complex in Scheme 6.<sup>127</sup> Degradation of the 1*H*-cyclopropa[*b*]naphthalene **93** was assessed against multiple copper(I) complexes (Table 8) and suggested that cycloproparenes could have the same reactivity as 1-MCP **53** in plants.

Table 8 Ring opening of **93** in presence of various metal(I) complexes, by Musa<sup>193</sup>



| Complex  | Co-solvent                      | Time   | Yield |
|--|---------------------------------|--------|-------|
| None   | -                               | 2 hrs  | N.R.  |
| AgNO <sub>3</sub>  | CH <sub>2</sub> Cl <sub>2</sub> | 30 min | 50%   |
| Cu(PPh <sub>3</sub> )I   | CH <sub>2</sub> Cl <sub>2</sub> | 30 min | 23%   |
| Cu(1,10-phen)(CH <sub>3</sub> CN)I   | CH <sub>2</sub> Cl <sub>2</sub> | 30 min | 66%   |
| [Cu((3,5-Me <sub>2</sub> Pz) <sub>3</sub> CH)(CH <sub>3</sub> CN)PF <sub>6</sub> | CH <sub>3</sub> CN              | 30 min | 60%   |

### 1.9.1 Effectiveness of cycloproparenes as ethylene antagonists

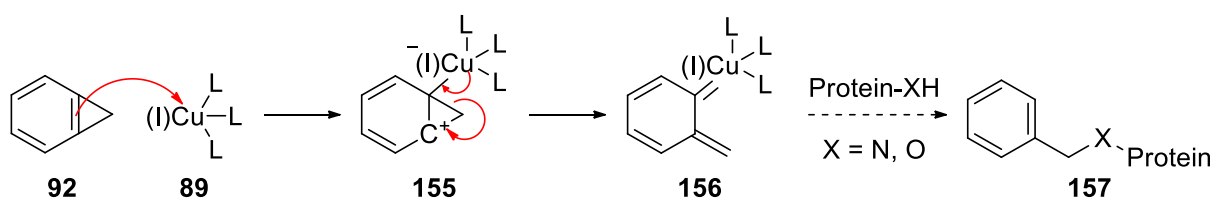
Geraldton Wax ('Purple Pride' variation, *Chamelaucium uncinatum*), a wax flower endemic to Western Australia, was used as model plant to test ethylene antagonists. These flowers were effectively used in various past studies of ethylene antagonists.<sup>194-200</sup> Wax flowers are known to undergo flower abscission when exposed to ethylene **1** thus provide a convenient model for observation of inhibition of ethylene action.<sup>195, 199, 201</sup> When 1*H*-naphtho[*b*]cyclopropene **93** and 1-MCP **53** were applied to Geraldton wax (Figure 14), a 69-80% reduction in flower abscission for naphthocyclopropene **93** and 48-49% reduction in flower abscission for 1-MCP **53** was observed, clearly showing an antagonistic effect of these compounds against ethylene action. Benzocyclopropene **92** and naphthocyclopropene **93** were also effective against plums, nectarines and apples.<sup>193, 202, 203</sup>



Figure 14 In-vivo test of 1H-naphtho[b]cyclopropene (left) in comparison to 1-MCP (middle), effect on Geraldton wax vs an ethylene control (right), experiment performed by Abdalghan<sup>204</sup>

### 1.9.2 Proposed Mode of action of cycloproparenes

The cycloproparene **92** was shown to be an effective antagonist of ethylene action, and Cu(I) reactivity can be a preliminary indicator of inhibition of ethylene action.<sup>144</sup> This reactivity was observed for known ethylene antagonists, and not observed for poor antagonists like tetrachlorocyclopropene.<sup>144</sup> Cycloproparenes have shown a single exposure inhibition of ethylene action in *in vivo* studies, similar to 1-methylcyclopropene **53**.<sup>205</sup> The mode of action of inhibition of the ethylene receptor is yet to be fully understood, however based on their structural similarity to cyclopropenes and model reactions, a similar mechanism to that of 1-MCP **53** is suspected (Scheme 21). This implies reaction with the copper cofactor **89** of the ethylene receptor forms an organocopper intermediate **156**, which reacts with the ethylene receptor to form a covalent bond **157**.

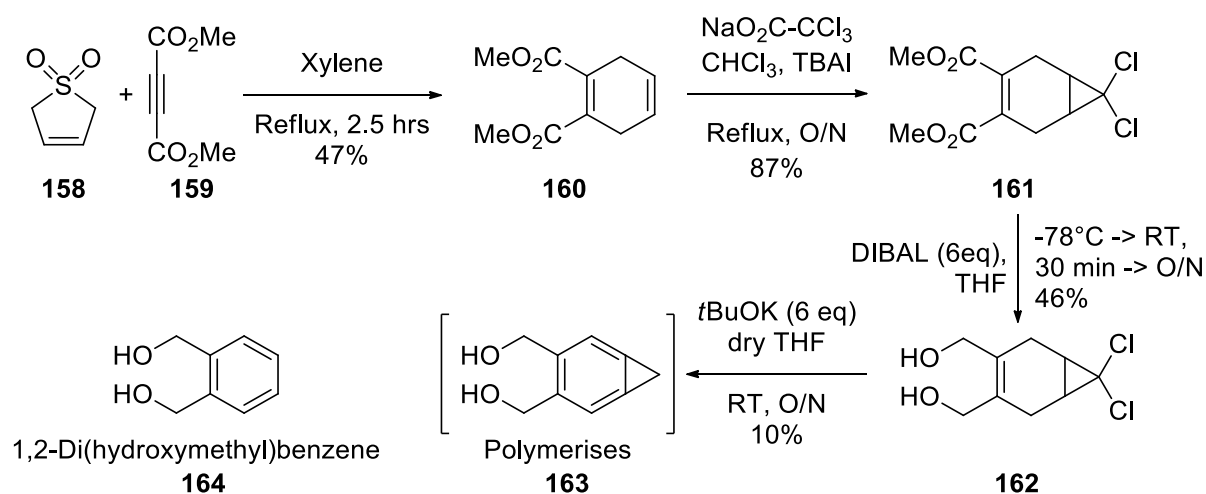


Scheme 21 Proposed mode of action of benzocyclopropene **16** on ETR-1 receptor

### 1.9.3 Attempts to prepare water-soluble cycloproparenes

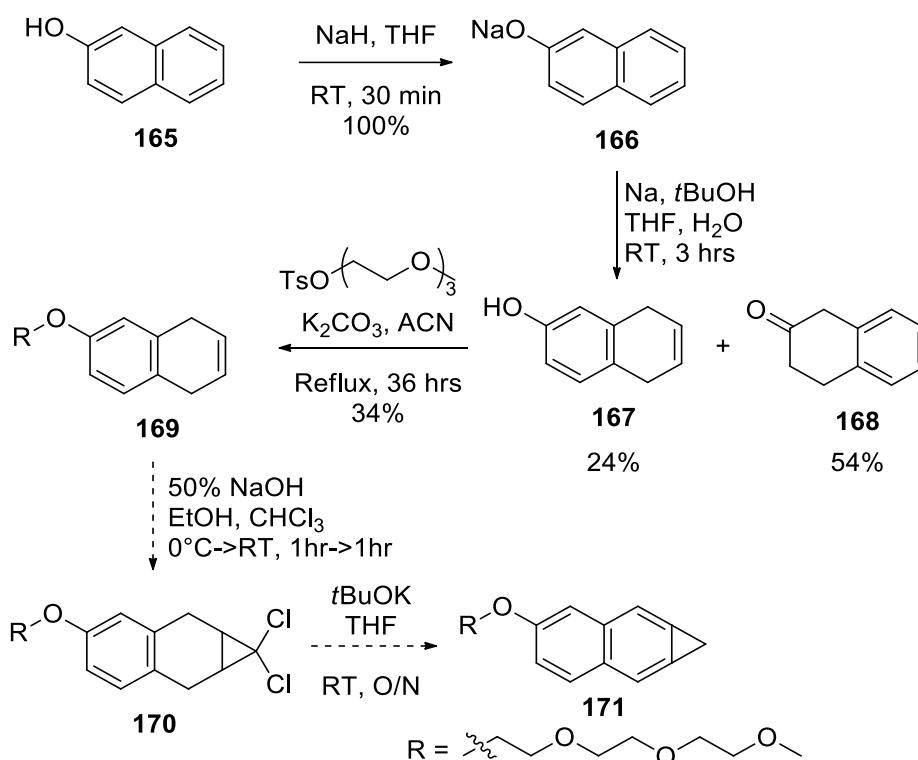
The current ethylene antagonist 1-MCP **53** is potent, yet its application is cumbersome, involving additional processing steps, resulting in additional overhead costs for production. Development of a water-soluble ethylene antagonist is a key target to reducing these costs. Ideally, a water-soluble ethylene antagonist would be introduced as part of the existing processing chain e.g. washing of the produce which includes spraying and dipping produce in water. This next section will highlight some attempts towards making water-soluble cycloproparenes within the Payne group.

The synthesis of a benzocyclopropene diol derivative **163** was first attempted by Musa (Scheme 22).<sup>193</sup> 1,2-Di(hydroxymethyl)benzene **164** is soluble in water, so the proposed cycloproparene **163** compound should be reasonably soluble in water. The reaction of 1,3-butadiene (made *in-situ* from 3-sulfolene **158**) and dimethyl acetylenedicarboxylate **159** gave dimethyl 1,4-cyclohexadiene-1,2-dicarboxylate **160**. Dichlorocarbene generated from sodium trichloroacetate was added to the most electron rich alkene to afford the desired adduct **161**. Reduction of **161** using DIBAL yielded the diol **162** in a relatively short reaction sequence. When the diol **162** was reacted with potassium *tert*-butoxide in THF, the cycloproparene **163** was isolated but polymerized within several hours. This made it too reactive to test on horticultural products.



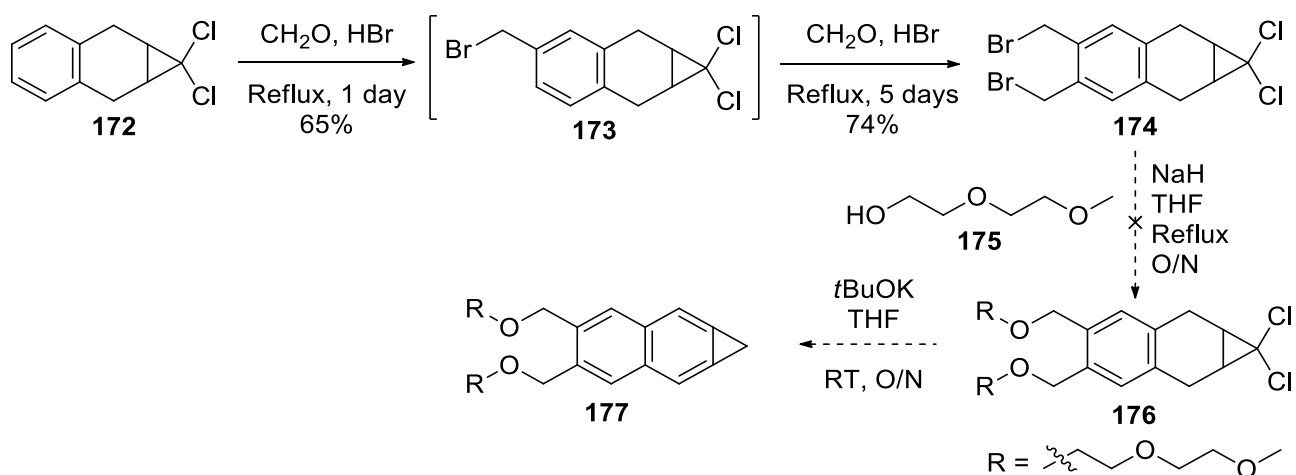
Scheme 22 Synthesis pathway of bicyclo[4.1.0]hepta-1,3,5-triene-3,4-diyl dimethanol **163**<sup>193</sup>

Introduction of a hydrophilic polyglycol chain to 1*H*-cyclopropa[*b*]naphthalene **93** also was attempted by Musa (Scheme 23).<sup>193</sup> Initial dissolving metal reduction of the 2-naphthol **165** gave 2-tetralone **167**. When reduction was performed on the sodium naphthoxide salt **166**, a 2:1 ratio of tetralone **167** and 5,8-dihydro-2-naphthol **168** was obtained. The glycol chain was introduced by reaction with tri(ethylene glycol) monomethyl ether tosylate. Unfortunately, the attempts at introduction of the dichloroadduct into the structure yielded only trace amounts of the target precursor **170** thus an alternative synthesis target was pursued.



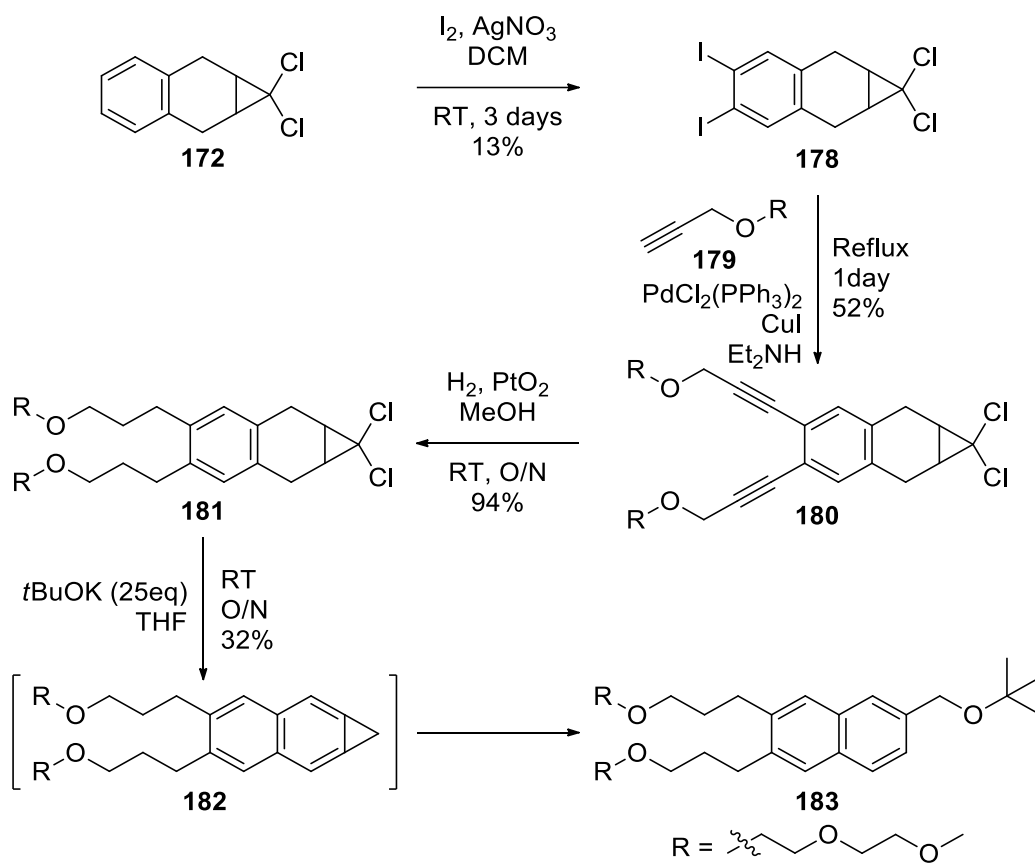
Scheme 23 Attempted synthesis pathway of 4-(2-(2-(2-methoxyethoxy)ethoxy)ethoxy)-1*H*-cyclopropa[*b*]naphthalene **171**<sup>193</sup>

An introduction of two glycol chains to 1*H*-cyclopropa[*b*]naphthalene **93** was attempted by Musa (Scheme 24).<sup>193</sup> Treatment of the dichloroadduct **172** with hydrobromic acid and formaldehyde gave the double bromomethylated product **174** by electrophilic aromatic substitution. For substitution of the bromine with glycol ether chain **175**, only trace amounts of the compound **176** were observed.



Scheme 24 Attempted synthesis pathway of 4,5-bis((2-(2-methoxyethoxy)ethoxy)methyl)-1*H*-cyclopropa[*b*]naphthalene **177**

Based on the previous failed attempts, an alternate method to introduce polyethylene glycol chains by a Sonogashira coupling reaction was envisioned (Scheme 25).<sup>206</sup> The insertion of a propyl chain between the glycol chain and the cycloproparene was thought to improve the stability of the final cycloproparene. The dichloroadduct precursor **172** was diiodinated **178** by an electrophilic aromatic iodination, albeit at low yield. The 1-propyl-glycol chains **179** were attached by the Sonogashira cross-coupling reaction, and the introduced alkynes were subsequently hydrogenated with  $\text{PtO}_2$  catalyst, to form the target propane-glycol chains **181**. When the dichloride **181** was reacted with potassium *tert*-butoxide, only the ring open by-product **183** was observed, with no evidence of the target cycloproparene **182** being formed.



Scheme 25 Attempted synthesis pathway of 4,5-bis(3-(2-(2-methoxyethoxy)propyl)-1H-cyclopropa[b]naphthalene **182**<sup>206</sup>

## **1.10 Project aims**

### **1.10.1 Optimal properties of an ethylene antagonist**

In order for the ethylene antagonists to be commercially viable, they have to meet a range of criteria. An ideal antagonist would be potent, stable, safe and easy to apply. While many compounds were investigated as potential ethylene antagonists, only 1-MCP **53** met the industry standards thus far. While a range of developed theories guides in development of new ethylene antagonists, the understanding of the mechanism of inhibition remains not fully understood. An ideal antagonist needs to be effective across a large range of produce. The antagonist needs to be applied effectively to minimise reapplication requirements. The stability of the antagonist in storage and application method are essential for ease of handling, and lack of degradation also ensures repeatable effectiveness. The ethylene antagonists must be nontoxic, as well as their degradation products. Difficulty of application of the antagonist results in additional overhead costs for the production of a produce, such as 1-MCP **53** applied by fumigation. Ideally, an ethylene antagonist would be introduced as part of the already existing post-harvest processing chain e.g. washing of the produce which includes spraying and dipping produce in water. Water solubility is thus an essential target for future development. The aim of this work is to develop new approaches to an ideal ethylene antagonist.

### 1.10.2 Synthesis of water soluble cycloproparenes

Out of the ideal criteria described above, the only used ethylene antagonist, 1-MCP **53**, is highly effective and safe, however it is not user friendly as it is unstable and difficult to apply. Cycloproparenes are equally potent and safe, while being easier to make and store due to their increased stability. Unfortunately, they are poorly water soluble, which limits their application. Synthesis of water soluble cycloproparenes has proven challenging (1.9.3 Attempts to prepare water-soluble cycloproparenes), and was not successful thus far. This suggests an alternative pathway to water soluble cycloproparenes has to be considered. Attaching a salt to a cycloproparene could increase its water solubility. These salts include  $\text{CO}_2\text{K}$ ,  $\text{SO}_3\text{K}$ ,  $\text{SO}_2\text{NHK}$  or  $\text{PO}_3\text{K}_2$  (Figure 15). A water-soluble cycloproparene would allow easier application of the antagonists onto the produce by spraying and dipping methods. Moreover, handling of the chemicals in salt form would be also beneficial for storage. This project will initially focus on synthesis of the water-soluble cycloproparenes in Figure 15.

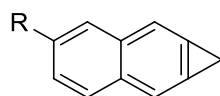


Figure 15 Potential salt analogues of 1H-naphtho[b]cyclopropane **93**

### 1.10.3 Synthesis of diazo-active triazolopyridines

A new class of compound will also be investigated as ethylene antagonists. [1,2,3]Triazolo[1,5-a]pyridines exhibit a masked diazo reactivity through an equilibrium favouring the closed ring form. Diazo compounds are known to form reactive carbenes, exhibiting reactivity with transition metals that akin to cyclopropenes. This project investigated synthesis of triazolopyridine derivatives with electron withdrawing groups (Figure 16) in search for diazo-reactive analogues.

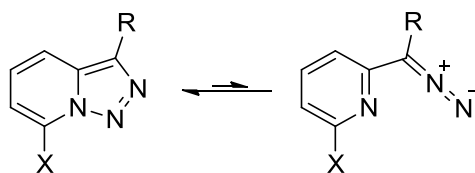
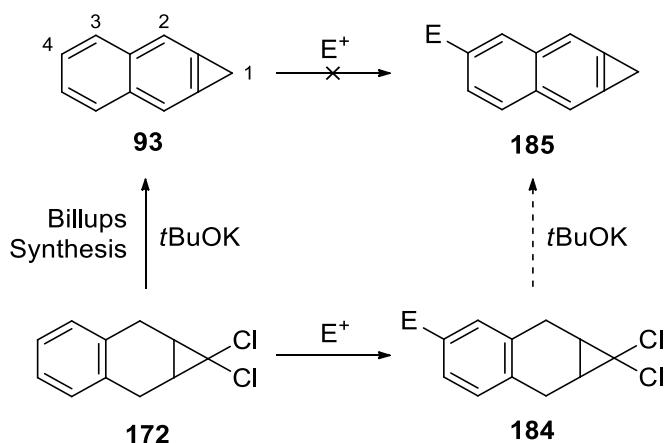


Figure 16 Potential analogues of [1,2,3]Triazolo[1,5-a]pyridine

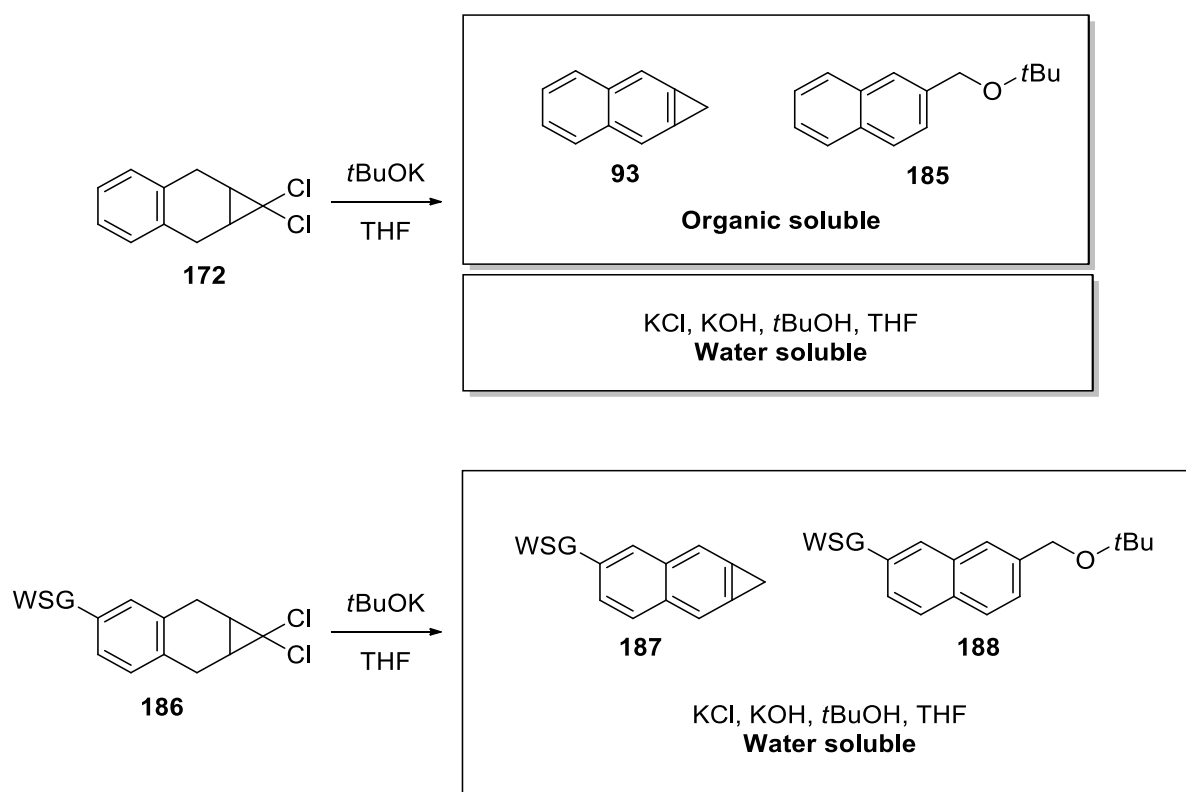
## Chapter 2 – Water soluble cycloproparenes

Cycloproparenes are inherently difficult to make due to their high reactivity towards acids, electrophiles and transition metals. This restricts the synthetic pathways when attempting to make water-soluble derivatives. One requirement for ethylene antagonism in cycloproparenes is that position 1 is unsubstituted, which renders only two synthesis methods suitable: dehydrohalogenation of a dihalocarbene adduct (Billups synthesis) or dehydrohalogenation of 1,1-dihalo-cyclopropene adducts. Theoretically, the most efficient way to add a solubilising group to a cycloproparene is through an electrophilic aromatic substitution. However, these reactions are rare for cycloproparenes (see Chapter 1.8.4) and only highly hindered or unreactive cycloproparenes remain intact. An alternative is to perform the electrophilic aromatic substitution before the formation of the cycloproparene, which would circumvent some of these issues (Scheme 26). 1*H*-cyclopropa[*b*]naphthalene derivatives were chosen for this study due to ease of synthesis and the good potency of the parent compound **93**. The approach that will be taken is to make the dichlorocarbene adduct **172**, perform an electrophilic aromatic substitution **184** and the dehydrochlorination reaction to give target cycloproparenes **185** (Scheme 26).



Scheme 26 Potential synthesis of substituted 1*H*-cyclopropa[*b*]naphthalenes via electrophilic aromatic substitution<sup>152, 176</sup>

The synthesis of these molecules was expected to be challenging. Most cycloproparenes reported are non-polar which facilitates the workup after the Billups synthesis by a simple partitioning between the pentane and water. The organic phase contains only the cycloproparene **93** and any degradation products (e.g. **185**). The aqueous phase contains salts and water soluble solvents. If the synthesised cycloproparene is water soluble **187** (i.e. with a Water Soluble Group) instead, all the products of the reaction will be located in the aqueous phase, making isolation of these sensitive compounds even more difficult (Scheme 27).



Scheme 27 Comparison of products of the Billups synthesis between organic and water soluble analogues of the 1H-cyclopropa[b]naphthalene

## 2.1 Carboxylate analogues

To overcome some of the expected isolation issues, the carboxylate salt **191** was chosen as a target. It is a salt of a weak acid **192**, what may allow isolation through acid-base chemistry. To validate the choice of solubilising group, potassium 2-naphthoate **189** was tested for solubility in water, and was found fully soluble. The similarity in structures between **189** and **191** suggests the target carboxylate **191** should be soluble in water as well and thus could potentially be isolated through acid-base chemistry (Figure 17).

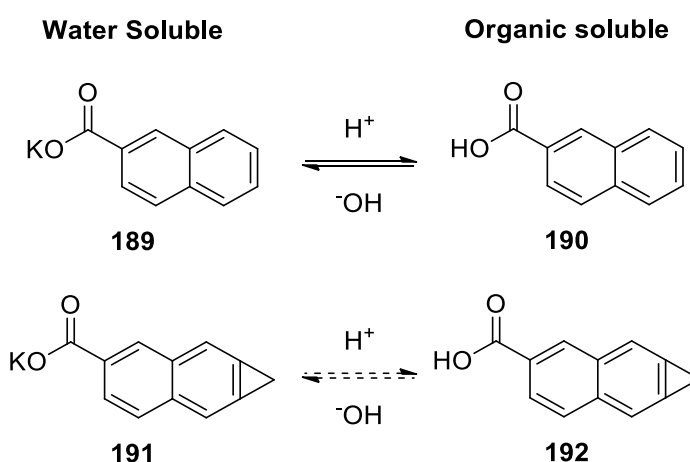
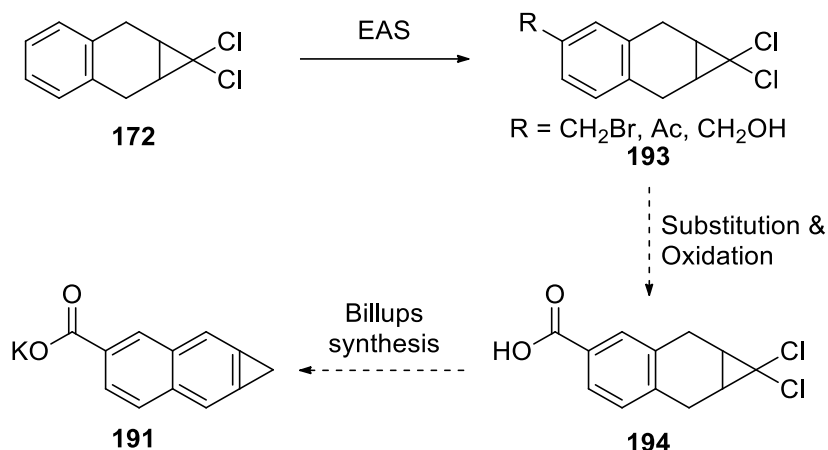


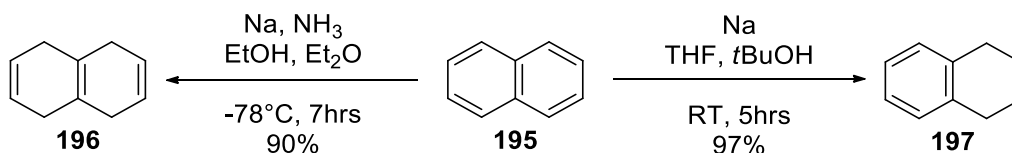
Figure 17 Acid/Base equilibria of 2-naphthoic acid **190** as well as 1H-cyclopropa[b]naphthalene-4-carboxylic acid **192**

There is no direct way to introduce a carboxylic acid through an electrophilic aromatic substitution but a two-step approach could be envisaged. A functionalised methyl (e.g. bromomethyl, acetate or methanol) can be introduced to the dichlorocarbene adduct **172** through an electrophilic aromatic substitution instead. These groups **193** can undergo substitution and oxidation reactions to form the carboxylic acid **194**. Under basic conditions, **194** can be deprotonated and undergo double dehydrohalogenation to form the target potassium naphtha[b]cyclopropenoate **191** (Scheme 28).



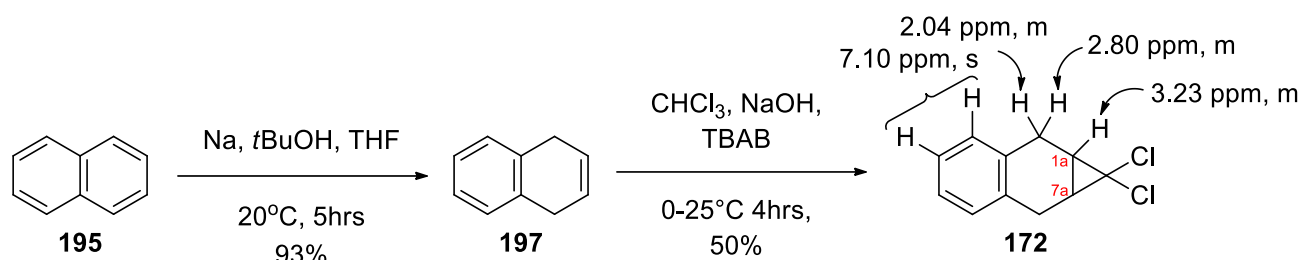
*Scheme 28 Proposed synthesis pathway of potassium naphtha[b]cyclopropenoate through EAS*

The starting material for the proposed synthesis is the dichlorocarbene adduct **172** and is made by a simple two-step synthesis from naphthalene **195**. The reduction of **195** can selectively produce a number of products depending on the conditions used. A birch reduction using sodium, ammonia and ethanol yields 1,4,5,8-tetrahydronaphthalene **196**<sup>207</sup> (Scheme 29). Naphthalene **195** has also been reduced to 1,4-dihydronaphthalene **197** using sodium and ethanol in benzene, developed in 1940 by Cook et al.<sup>208</sup> More recent synthesis by Menzek et al.<sup>209</sup> uses sodium and *tert*-butanol in tetrahydrofuran at room temperature, yielding the expected product **197** in good yield and purity.



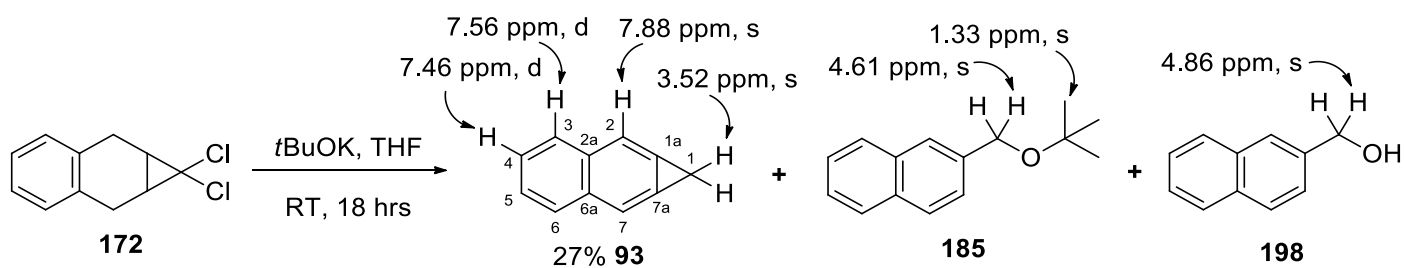
*Scheme 29 Reductions of naphthalene<sup>207, 209</sup>*

1,4-Dihydronaphthalene **197** was synthesised in 40 g scale, using sodium and *tert*-butanol in tetrahydrofuran, and was used without further purification in the next step. The 1,1-dichlorocarbene adduct **172** was made using classical conditions. 1,4-Dihydronaphthalene **197** was reacted with chloroform and sodium hydroxide using tetrabutylammonium bromide as a phase transfer catalyst (Scheme 30).<sup>210</sup> The product was purified by silica gel filtration using petroleum spirits yielding the expected adduct **172** in 50% yield. Using this method, 40 g of the adduct **172** could be easily obtained. The <sup>1</sup>H NMR spectrum was identical to that reported by Billups et al.<sup>163</sup> and had a singlet at 7.10 ppm (2H) and three multiplets at 3.23 (1H), 2.80 (2H) and 2.04 ppm (2H).



Scheme 30 Synthesis pathway of 1,1-Dichloro-1a,2,7,7a-tetrahydro-1H-cyclopropa[b]naphthalene

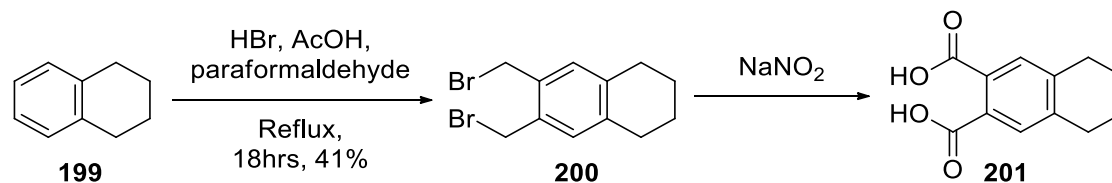
The dichlorocarbene adduct **172** is used to synthesise 1*H*-cyclopropa[*b*]naphthalene **93** which was used as the parent compound of this study.<sup>169-171</sup> When the adduct **172** was reacted with potassium *tert*-butoxide in tetrahydrofuran, three products were obtained from the reaction: 1*H*-naphtho[*b*]cyclopropane **93**, 2-(*tert*-butoxymethyl)naphthalene **185** and 2-hydroxymethylnaphthalene **198** (Scheme 31). 1*H*-naphtho[*b*]cyclopropane **93** is moderately stable and was purified by chromatography. The <sup>1</sup>H NMR spectrum of the cycloproparene **93** had three signals in the aromatic region, two apparent doublets and a singlet at 7.88, 7.56 and 7.46 ppm indicative of substitution at the position 1a and 7a. A singlet at 3.52 ppm was indicative of the cyclopropene ring hydrogens. In the <sup>1</sup>H NMR spectrum of the 2-(*tert*-butoxymethyl)naphthalene **185**, a 2H singlet at 4.61 ppm and a 9H singlet at 1.33 ppm were indicative of the *tert*-butoxymethyl ether. The <sup>1</sup>H NMR spectrum of the 2-naphthalenemethanol **198** had a 2H singlet at 4.86 ppm indicative of the hydroxymethyl group.



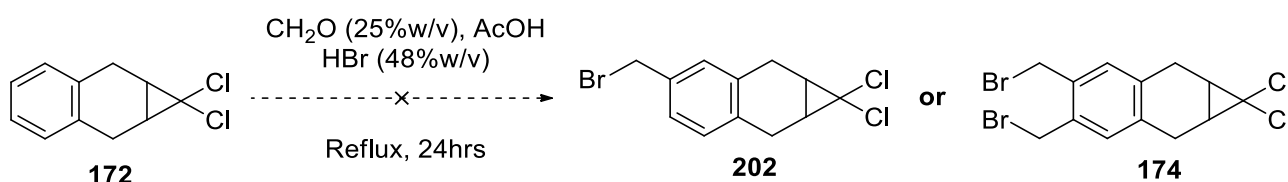
Scheme 31 Synthesis of 1*H*-naphtho[*b*]cyclopropane

As the dichlorocarbene adduct **172** is a tetralin derivative, electrophilic aromatic substitution of tetralin **199** was used as an exemplar reaction pathway. Bromomethylation of tetralin **199** gives the dibromide **200** (Scheme 32). Bromomethyl derivatives can be converted to a carboxylic acid **201** by substitution and oxidation with NaNO<sub>2</sub> in a method developed by Matt et al.<sup>211</sup> Bromomethylation of the adduct **172** was observed by Musa,<sup>193</sup> however Mattison could not reproduce this result.<sup>206</sup> When

the dichlorocarbene adduct **172** was heated to reflux in aqueous formaldehyde, hydrobromic acid and acetic acid mixture, only starting material **172** and degradation products were obtained (Scheme 33) and an alternative pathway was examined.

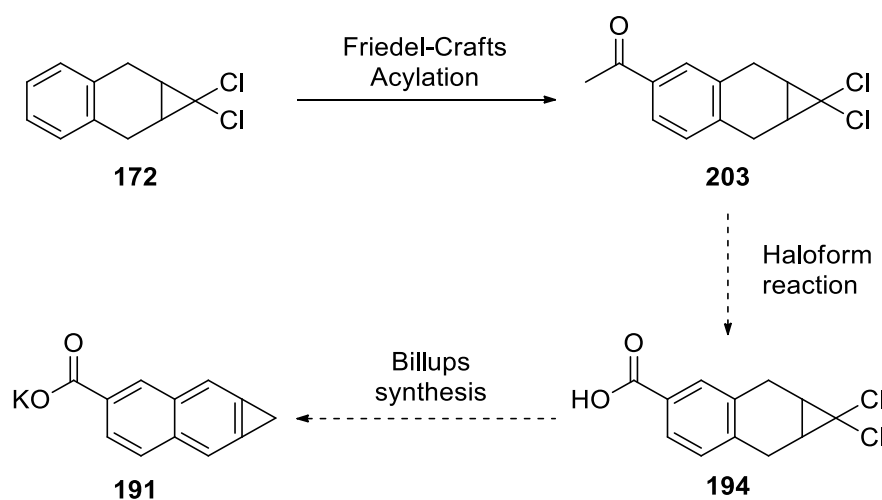


*Scheme 32 Dibromomethylation of tetralin 199 by Matt et al.<sup>211</sup>*



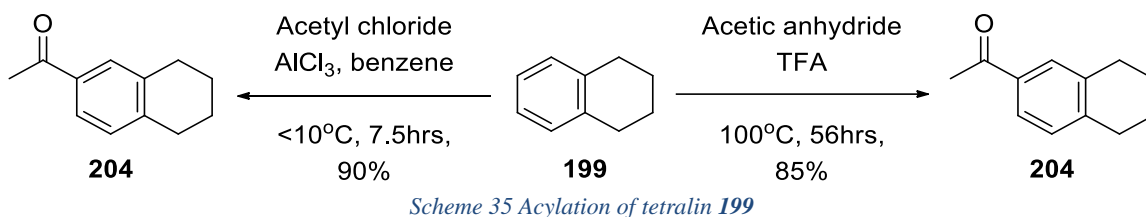
*Scheme 33 Attempted synthesis of 4-(bromomethyl)-1,1-dichloro-1a,2,7,7a-tetrahydro-1H-cyclopropa[b]naphthalene 202*

As the bromomethylation route was unsuccessful, an alternative synthesis was attempted (Scheme 34). A Friedel-Crafts acylation should be a clean reaction as the product of the first acylation, the ketone would deactivate the aromatic ring to further reactions. A haloform reaction could convert the newly formed acetyl group **203** into the carboxylic acid **194**. Finally, reacting the carboxylic acid **194** with potassium *tert*-butoxide would first deprotonate the carboxylic acid to form the salt, followed by a dehydrochlorination to give the cycloproparene **191** following the Billups protocol.

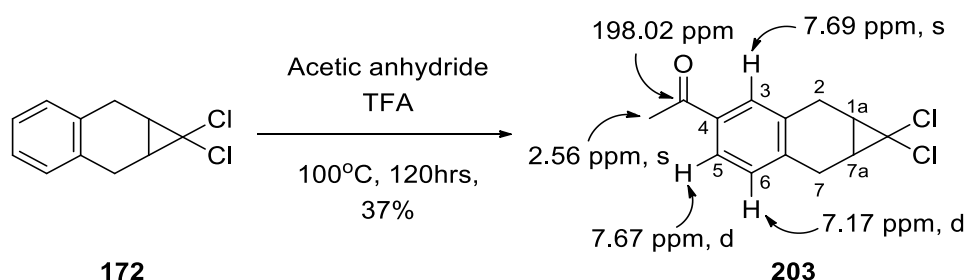


*Scheme 34 Proposed synthesis pathway of potassium naphtha[b]cyclopropenoate 191 through acetylation*

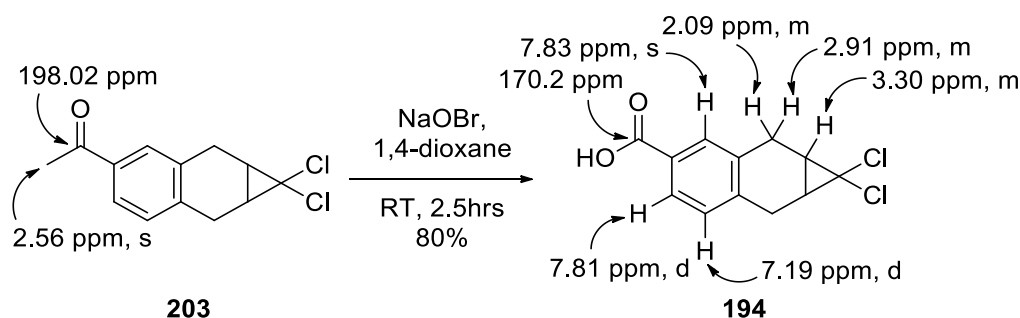
Friedel-Crafts acylation requires a Lewis acid catalyst and a source of the acetyl group such as acyl chlorides or anhydrides. A commonly used catalyst is aluminium trichloride, which was effectively used in acylation of tetralin **199** with acetyl chloride in benzene (Scheme 35).<sup>212</sup> Due to acid sensitivity of the cyclopropane ring present in the adduct **172**, a milder catalyst was needed. Liu and Xu acylated tetralin **199** in 85% yield by using acetic anhydride in trifluoroacetic acid at 100 °C (Scheme 35).<sup>213</sup>



When the dichlorocarbene adduct **172** was heated in acetic anhydride and TFA at 100°C in a sealed tube for 120 hours, a 50:50 mixture of starting material **172** and the acetyl derivative **203** was obtained (Scheme 36). Column chromatography gave the acetyl derivative **203** in a 37% yield. The <sup>1</sup>H NMR spectrum of the **203** had three aromatic signals: two doublets at 7.67 and 7.17 ppm and a singlet at 7.69 ppm indicating a substitution at position 4 had occurred. Three multiplets at 3.28, 2.89 and 2.07 ppm were reminiscent of the positions 1a, 2, 7 and 7a in the starting material **172** and suggested the cyclopropane ring was intact. A 3H singlet at 2.56 ppm was indicative of the newly substituted acetyl group, confirmed by the IR spectrum strong absorbance at 1677 cm<sup>-1</sup> indicating the C=O ketone stretch.

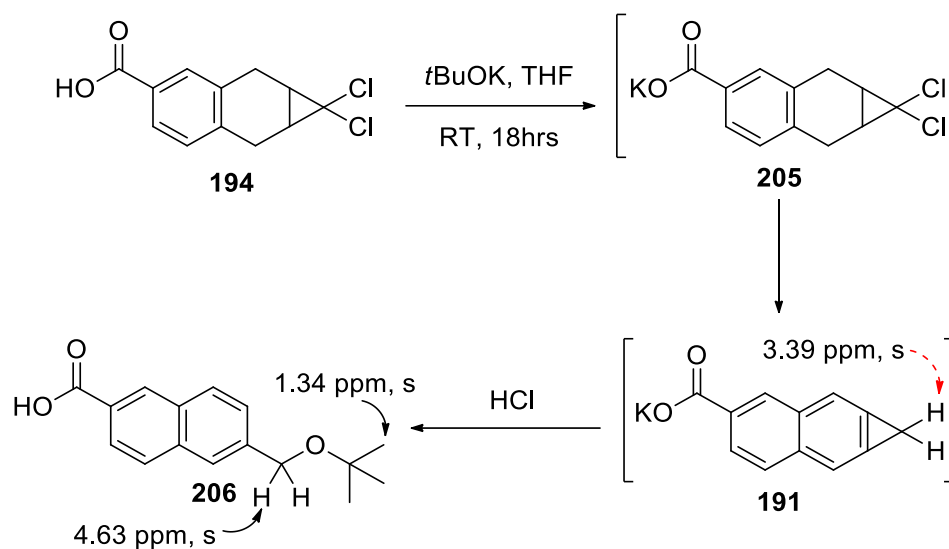


The acetyl group of **203** was oxidised to the carboxylic acid **194** using a haloform reaction, a reaction reported to transform 1-(5,6,7,8-tetrahydronaphthalen-2-yl)ethanone to its carboxylic acid.<sup>214</sup> Treatment of the acetyl **203** using sodium hypobromite in 1,4-dioxane over 2.5 hours at room temperature gave an excellent yield of **194** with no need for further purification (Scheme 37). The <sup>1</sup>H NMR spectrum of carboxylic acid **194** had three aromatic signals, two doublets at 7.83 and 7.20 ppm and a singlet at 7.85 ppm, indicating the aromatic ring was unchanged. The three multiplets at 3.30, 2.91 and 2.09 ppm were characteristic for the hydrogens at positions 1a/7a and 2/7 in the starting material and confirmed the cyclopropane was intact. The methyl group at 2.56 ppm of the starting material was missing. The presence of a carboxylic acid was consistent with the <sup>13</sup>C NMR spectrum signal at 170.2 ppm and the IR spectrum, a broad O-H stretch from 3200-2400 cm<sup>-1</sup>, a strong C=O stretch at 1678 cm<sup>-1</sup> and a strong C-O stretch at 1293 cm<sup>-1</sup>.



Scheme 37 Synthesis of 1,1-dichloro-1a,2,7,7a-tetrahydro-1H-cyclopropa[b]naphthalene-4-carboxylic acid **194**

With the carboxylic acid **194** successfully synthesised, it was subjected to potassium *tert*-butoxide in tetrahydrofuran (Scheme 38). The carboxylic acid **194** was reacted with 1 eq. of *t*BuOK in THF for 18 hours. The reaction mixture was concentrated under reduced pressure, the residue dissolved in water, acidified with hydrochloric acid to pH <3 and extracted with ethyl acetate. The <sup>1</sup>H NMR spectrum of the organic layer showed significant amount of the starting material **194** and a mixture of side products. The absence of signals between 3.40–3.60 ppm suggested that either cycloproparene **96** had not formed or it had fully degraded to ring-opened product **206** upon protonation. Presence of ring-opened product **206** was consistent with the presence of six aromatic signals, as well as two singlets at 4.63 and 1.34 ppm (2:9 integration ratio) in the <sup>1</sup>H NMR spectrum.



*Scheme 38 Attempted synthesis of potassium 1H-naphtho[b]cyclopropen-4-oate 191*

As the ring opened product **206** could be a result of the acid workup, the reaction was reattempted under the same conditions but with an altered workup. To neutralise the excess base in the reaction mixture without introduction of strong acids, a buffer solution was used instead. A pH 7 phosphate buffer (**208-210**) was added to the crude reaction mixture to neutralise any remaining base and the solution was concentrated under reduced pressure (Figure 18). The  $^1\text{H}$  NMR spectrum of the crude solid had a complex mixture of products containing two major products. Gratifyingly, a singlet at 3.39 ppm was within the expected spectrum range for the target cyclopropene **191**, taking into account the chemical shift differences between  $\text{CDCl}_3$  and  $\text{D}_2\text{O}$  as solvents. No alternative structure could be envisioned to match this signal. Unfortunately, despite numerous attempts, the compound could not be further isolated without complete degradation to the ring-opened product **206**.

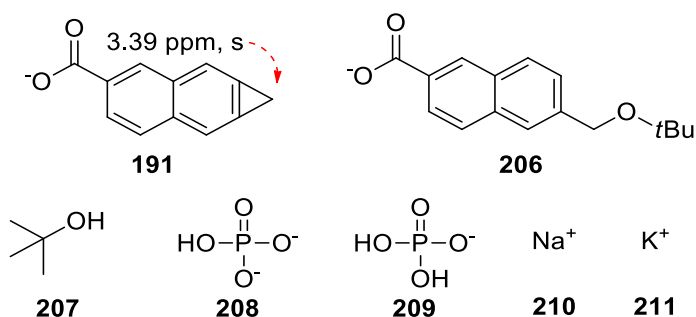
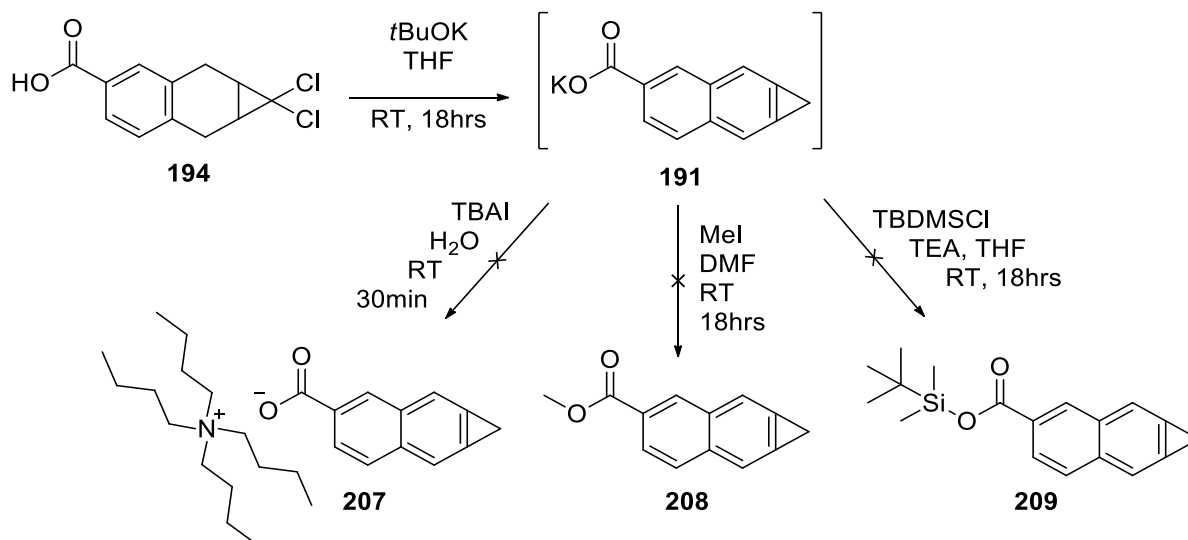


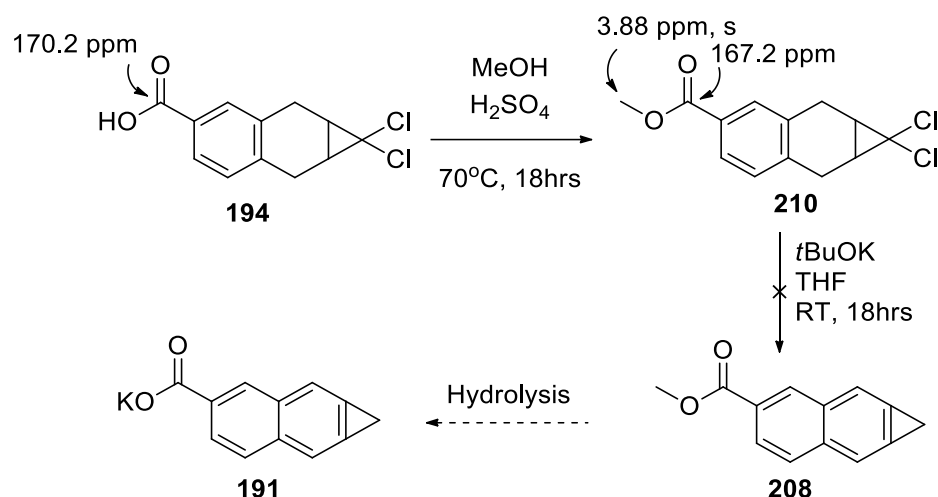
*Figure 18 Salt mixture of the potassium 1H-cyclopropa[b]naphthalene-4-carboxylate 191 buffer workup*

A number of methods were investigated to isolate the cycloproparene **191** with little success (Scheme 39). Using tetrabutylammonium iodide as lipophilic cation did allow some salt to be extracted into the organic phase but only ring opened products of **207** were recovered. Using iodomethane instead gave ring opened methyl esters of **208**. Similarly, esterification using *tert*-butyldimethylsilyl chloride gave ring opened products of **209** as well.



Scheme 39 Attempts at isolation of potassium 1H-cyclopropa[b]naphthalene-4-carboxylate **191**

Due to lack of success in separation of the carboxylate salt **191**, a modified pathway was envisioned. The carboxylic acid **194** could be esterified to a methyl ester **210**. Formation of the cycloproparene analogue **208** by the Billups synthesis and subsequent hydrolysis would give the desired carboxylate salt **191**. When the acid **194** was heated under reflux in methanol and catalytic amount of sulfuric acid,<sup>215</sup> the expected ester **210** was obtained in quantitative yield (Scheme 40). The <sup>1</sup>H NMR spectrum was near identical to the starting material except for the new methyl signal at 3.88 ppm. The presence of a methyl ester was consistent with the IR spectrum, a strong C=O stretch at 1713 cm<sup>-1</sup>, a strong C-O stretch at 1275 cm<sup>-1</sup>. Unfortunately, when potassium *tert*-butoxide was added to a solution of methyl ester **210** and tetrahydrofuran, only degradation products were observed.

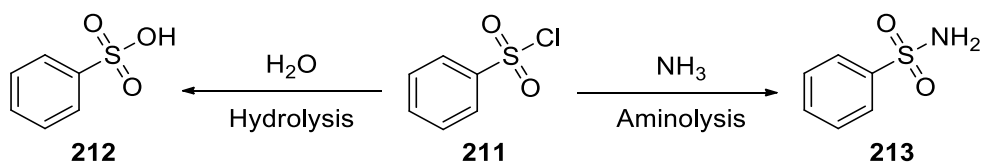


Scheme 40 Attempted synthesis of methyl 1H-cyclopropa[b]naphthalene-4-carboxylate 208

Although circumstantial evidence for the synthesis of the cycloproparene carboxylate salt **191** was observed, all efforts to isolate the compound were unsuccessful. The results of this series of experiments indicate either the ring-opening is favoured on introduction of the carboxylate, or the product formed is significantly less stable and degrades rapidly. Based on these findings alternative analogues were targeted for further study of water soluble cycloproparenes.

## 2.2 Sulfonate analogues

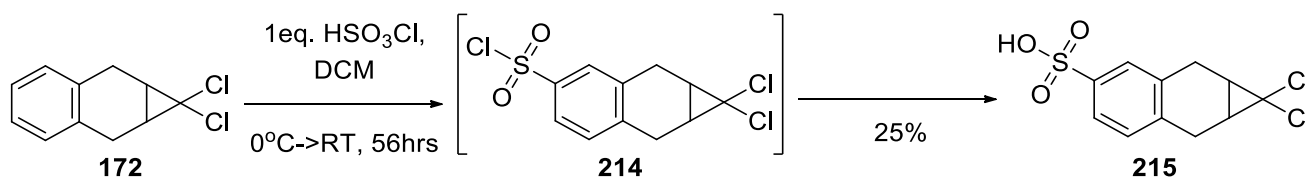
As only fleeting evidence of the potassium 1H-cyclopropa[b]naphthalene-4-carboxylate **191** was observed, an alternative salt was targeted. Sulfonic acids are stronger acids when compared to carboxylic acids (benzenesulfonic acid vs benzenecarboxylic acid pK<sub>a</sub> in water -2.6 vs 4.2).<sup>216</sup> Sulphonamides are weaker acids than carboxylic acids. Both of these groups of compounds easily form water soluble or partially soluble salts. Sulfonic acid derivatives can be introduced through a chlorosulfonation, which is accessible by an electrophilic aromatic substitution. Like the Friedel-Craft acylation, sulfonyl chlorides are deactivating so a clean reaction was expected. Sulfonyl chlorides (e.g. **211**) are very flexible functional groups and can be readily transformed to a range of products through hydrolysis (**212**) or aminolysis (**213**) (Scheme 41).



Scheme 41 Hydrolysis and aminolysis of sulfonyl chloride 211

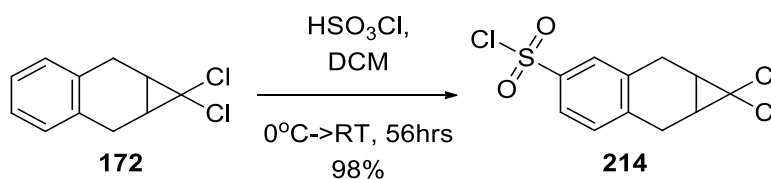
### 2.2.1 Hydrolysis approach

Based on the chlorosulfonation of tetralin by Anderson et. al.,<sup>217</sup> the adduct **172** was treated with 1 equivalent of chlorosulfonic acid in dichloromethane. The crude product mixture did not contain the expected sulfonyl chloride **214** but a single major side product was present (Scheme 42). The <sup>1</sup>H NMR spectrum showed three 1H aromatic signals, two doublets (7.54 and 7.11 ppm) and a singlet (7.58 ppm), indicating a substitution at the position 4 had occurred. A broad signal was present in the 7.1-6.9 ppm region. The multiplets at 3.17, 2.74 and 1.97 ppm were characteristic for the hydrogens at positions 1a and 2 in the adduct **172** and suggested that the cyclopropane was intact. The compound was identified as 1,1-dichloro-1a,2,7,7a-tetrahydro-1H-cyclopropa[b]naphthalene-4-sulfonic acid **215**. While the sulfonic acid **215** was the target of the synthesis pathway, the yield of the reaction was poor, thus further chlorosulfonation reaction conditions were attempted.



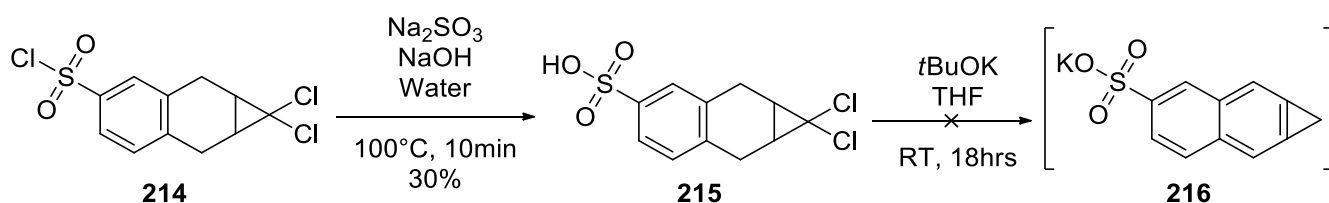
*Scheme 42 Attempted synthesis of 1,1-dichloro-1a,2,7,7a-tetrahydro-1H-cyclopropa[b]naphthalene-4-sulfonyl chloride **214***

When the chlorosulfonation reaction was repeated using 10 equivalents of the chlorosulfonic acid, the expected sulfonyl chloride **214** was obtained in excellent yield and did not require purification (Scheme 43). The <sup>1</sup>H NMR spectrum had three aromatic signals each integrating for 1H, two doublets (7.75 and 7.34 ppm) and a singlet (7.77 ppm), indicating a substitution at the position 4 had occurred. The three multiplets at 3.36, 2.95 and 2.13 ppm were characteristic for the hydrogens at positions 1a and 2 in the starting material and confirmed the cyclopropane was intact. The IR spectrum had absorbance indicative for a sulfonyl chloride at 1370, 1165 and 583 cm<sup>-1</sup>.



*Scheme 43 Synthesis of 1,1-dichloro-1a,2,7,7a-tetrahydro-1H-cyclopropa[b]naphthalene-4-sulfonyl chloride **214***

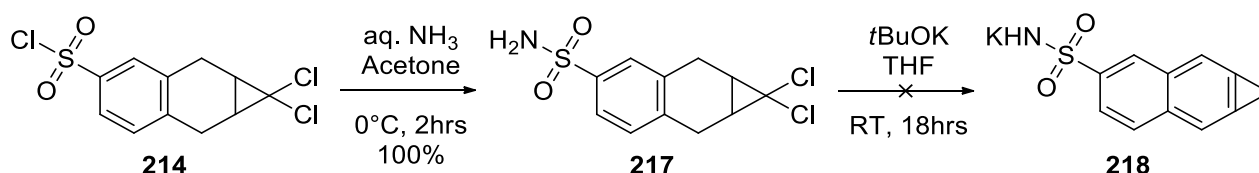
Hydrolysis of aryl sulfonyl chlorides is well documented in the literature as reviewed by Zoller.<sup>218</sup> The method developed by Liu et al.<sup>219</sup> used sodium hydroxide and sodium sulfite for the hydrolysis of 2-naphthalenesulfonyl chloride. When the sulfonyl chloride **214** was reacted under the same conditions, a complex mixture of products including significant amount of starting material was obtained (Scheme 44). Sulfonic acid **215** was separated by titration with 1:99 petroleum spirits:dichloromethane at -20 °C. No starting material was recovered after titration, suggesting hydrolysis had occurred to give the expected product. The <sup>1</sup>H NMR spectrum of compound **215** had three 1H aromatic signals, two doublets (7.59, 7.17 ppm) and a singlet (7.63 ppm), indicating a substitution at the position 4 had occurred. A broad signal shifting between 8 – 6.5 ppm was present, suggesting presence of the sulfonic acid. The multiplets at 3.25, 2.84 and 2.05 ppm were characteristic for the hydrogens around the cyclopropane. The IR spectra were inconsistent across multiple scans, however study of Warren et al. showed this behaviour of sulfonic acids was due dissociation with variations in humidity.<sup>220</sup> One of the IR spectra included signals characteristic for the sulfonic acid at 3401, 1717 cm<sup>-1</sup> as well as at 2900 and 1683 cm<sup>-1</sup>. When the sulfonic acid **215** was reacted with potassium *tert*-butoxide under the standard conditions (Scheme 44), the <sup>1</sup>H NMR spectrum of the dichloromethane extract had a complex mixture of side products. No signals in the 3.60 – 3.40 ppm range indicated lack of the expected product **216**. The aqueous layer was evaporated with an acetonitrile azeotrope. The <sup>1</sup>H NMR spectrum of the aqueous layer had a complex mixture. The NMR analysis of the crude extracts did not have a signal characteristic for cycloproparenes, thus this reaction was not further investigated.



Scheme 44 Synthesis of 1,1-dichloro-1a,2,7,7a-tetrahydro-1H-cyclopropa[b]naphthalene-4-sulfonic acid **215** and attempted synthesis of potassium 1H-cyclopropa[b]naphthalene-4-sulfonate **216**

## 2.2.2 Aminolysis approach

As an alternative to the sulfonate, synthesis of a sulfonamide derivative was attempted. Sulfonyl chloride **214** can undergo aminolysis to form sulfonamide **217**. Following the method developed for a tetralin analogue,<sup>221</sup> the sulfonyl chloride **214** was stirred with aqueous ammonia in acetone at 0 °C for 2 hours to give the sulfonamide **217** after purification (Scheme 45). The <sup>1</sup>H NMR spectrum had three aromatic signals, two doublets (7.64, 7.24 ppm) and a singlet (7.67 ppm), indicating a change in the functional group at the position 4. A new singlet was present at 4.91 ppm indicating the sulfonamide. The multiplets at 3.29, 2.90 and 2.09 ppm were characteristic of the hydrogens of the region surrounding the cyclopropyl group. The presence of sulfonamide was further confirmed by IR spectrum absorbance signals: moderate and strong N-H stretches at 3345 cm<sup>-1</sup> and 3253 cm<sup>-1</sup>, strong S=O stretch at 1312 cm<sup>-1</sup> and 1151 cm<sup>-1</sup>. This sulfonamide **217** was reacted with potassium *tert*-butoxide in tetrahydrofuran (Scheme 45). The reaction mixture was diluted with water, extracted with petroleum spirits, neutralised with the pH 7 buffer solution and extracted with dichloromethane. The NMR analysis of the crude extracts did not have a signal characteristic for cycloproparenes, thus this reaction was not further investigated.



Scheme 45 Synthesis of 1,1-dichloro-1a,2,7,7a-tetrahydro-1H-cyclopropa[b]naphthalene-4-sulfonamide **217** and attempted synthesis of potassium ((1H-cyclopropa[b]naphthalen-4-yl)sulfonyl)amide **218**

Due to similar difficulties across synthesis of various cycloproparene salts, this approach appeared to be a synthetic dead end and a different family of compounds was targeted for further research of water-soluble ethylene antagonists.

## **Chapter 3 – Development of an *in vivo* assay as a preliminary assessment of ethylene antagonism in water soluble compounds**

### **3.1 Preface**

The collaboration between Prof. Zora Singh and Dr. Alan Payne combined their respective fields: horticulture and chemistry. Initial plans for this thesis included focus on organic synthesis and preparation of novel ethylene antagonists, which were to be tested for their biological activities by Singh's group. Unfortunately, within the first year of the project the horticulture laboratory at Curtin University was shut down and could no longer perform the required ethylene antagonist studies. The original, purely synthetic, scope was expanded to include a series of basic *in vivo* experiments in addition to a Cu(I) reactivity chemical model as a preliminary method for determination of ethylene antagonistic properties of the compounds synthesised. Three plants were considered as candidates: pea seedlings, birch leaves and Geraldton wax flowers.

### 3.1.1 Pea seedlings

In search of an appropriate plant model for a preliminary assessment of ethylene antagonistic properties of compounds, a number of test subjects was considered. Green pea (*Pisum sativum*) seedlings were originally considered due to their characteristic triple response on exposure to ethylene **1**.<sup>222, 223</sup> Ethylene treated seedlings show reduction in elongation, thickening of the stem, as well as change of direction of growth. These properties were extensively reviewed and used in studies of ethylene signalling in plants.<sup>224-229</sup> It was envisioned potential ethylene antagonist compounds would be introduced to the pea seedlings prior to gassing with ethylene **1**, resulting in decrease of the triple response as in comparison to a control.

The preliminary experiments were performed to observe the control response of green pea (*Pisum sativum*) seedlings to ethylene **1** (1.4  $\mu\text{mol/L}$  of container), which showed a clear decrease in stem length, increase in diameter and change of direction as was expected (Figure 19). On further consideration, the system was considered too complex for the model to be further developed, due to slow growth rate of the peas, expecting for a single test to take at least 1 week. With this consideration in mind, a more rapid response test subject was considered.

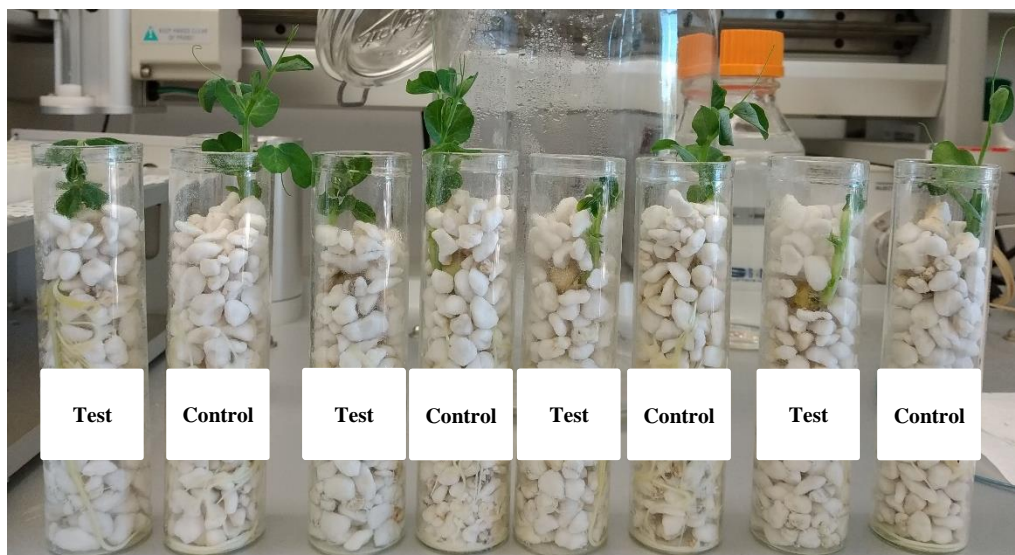


Figure 19 Preliminary samples of ethylene action on green peas, “Controls” are procedural blanks, “Tests” are ethylene exposed

### 3.1.2 Birch leaves

Silver birch (*Betula pendula*) is known to undergo ethylene-induced leaf abscission.<sup>230, 231</sup> Upon exposure of high concentrations of ethylene **1**, silver birch leaves separate from the branches, allowing for a clear observation of ethylene action on the plant. To assess the potential of silver birch as a model subject, preliminary testing was performed. Silver birch cuttings (>10 leaves each) were gassed with ethylene **1** (1.4  $\mu\text{mol/L}$  of container) and abscission of leaves was observed. Unfortunately, the abscission was not clear; the leaves remained attached to the main branch (Figure 20), albeit separating on gentle touch, indicating weakening of the connection between the two. In comparison, the leaves of a fresh cutting were firmly attached to the branch and required a firm pull to separate. The sample size was also unsatisfactory; the amount of leaves per cutting was insufficient for relevant statistical analysis and unscaleable due to the laboratory space limits. A plant providing a larger sample size while remaining more compact was required.



Figure 20 Preliminary assay of a silver birch cutting

### 3.1.3 Geraldton wax

Cuttings of Geraldton wax (*Chamelaucium uncinatum*) were chosen as the plant model for this *in vivo* model. Geraldton wax is a flowering plant endemic to Western Australia (local), known to undergo flower abscission when exposed to ethylene **1**.<sup>195, 199, 201</sup> Geraldton wax is seasonal, bearing flowers only between June to October, thus limiting their potential use as an assay. Nevertheless, the flower abscission in this plant provides a convenient, easily quantifiable model for observation of inhibition of ethylene action thus were deemed appropriate for this simple and preliminary assessment of compounds as potential ethylene antagonists. Flower abscission occurs in Geraldton wax on exposure to ethylene **1**, naturally produced by the plant or from an outside source such as traffic or industry gas emissions.<sup>232-234</sup> Grown plants and cuttings can be also gassed

with ethylene **1** in a laboratory setting to observe the effects directly.<sup>195, 199</sup> The ethylene action in Geraldton wax can be prevented by application of an ethylene antagonists and thus comparison in the flower drop between a sample and a control allows for a preliminary assessment of inhibition of ethylene action by tested compounds. These flowers were effectively used in many past studies of ethylene antagonists,<sup>194-200</sup> including their use on cycloproprenes.<sup>148</sup> Prior to development of 1-MCP **53**, silver thiosulfate complex **29** was commonly used as a spray-able solution for flowers, including Geraldton wax.<sup>232, 233</sup> Its use was replaced over time with 1-MCP **53** as a significantly more potent and environmentally friendly compound. Since only a few ethylene antagonists ever found industrial use, majority of studies focused on 1-MCP **53** as the gold standard. Due to high volatility of the compound, it is used by fumigation, both on industrial and laboratory scale (Figure 21).<sup>194, 196, 197, 200</sup> 1-MCP **53** was shown to reduce abscission of Geraldton wax flowers and buds caused by ethylene **1** by over 97% when applied before application of ethylene **1**. When applied simultaneously with ethylene **1** the reduction was not as powerful, yet still significant. Lack of abscission caused by 1-MCP **53** showed lack of cytotoxic effects by the product.

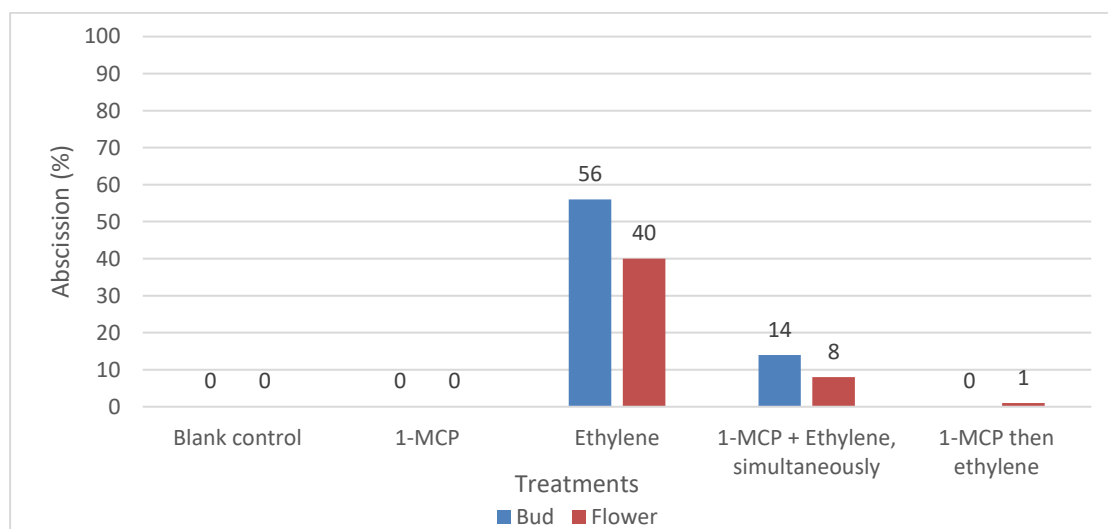


Figure 21 Effect of ethylene **1** (2  $\mu\text{L/L}$ ) and 1-MCP **53** (200 nL/L) on bud and flower abscission (%) from freshly harvested Geraldton waxflower, by Serek<sup>194</sup>

Fumigation is considered impractical for produce requiring application of ethylene antagonist while still on the plant. A more practical application is through spraying, and studies into spray-able compounds were developed.<sup>235-237</sup> The developed analogues of 1-MCP **53** (e.g. 3-cyclopropyl-1-enyl-propanoic acid sodium salt **68**) shown decrease in potency in comparison to the parent compound **53** (required minimum concentration  $410 \pm 76$  nL/L vs 0.7 nL/L for banana peels),<sup>128</sup> however the ease of application by spraying is an important factor to consider and strongly favours water soluble compounds for industrial use. The application of ethylene antagonists as feed solutions to plants or as dipping solutions for produce is limited due to solubility and stability issues. This remains an important avenue to explore in development of novel ethylene antagonists, as incorporating them into current industrial practices would be extremely convenient for use.

### **3.2 Development of a simple in-house assay**

The aim and target of this study was development of a preliminary assessment method for compounds as potential ethylene antagonists. The scope and scale of this *in vivo* study was developed as a simple indicator of potential as ethylene antagonists only, and further studies are required for proper assessment of efficacy of tested compounds as ethylene antagonists. Furthermore, the study only involved Geraldton wax as the plant test subject thus the potency of ethylene antagonistic effect in other plants or produce cannot be ascertained without separate experiments performed on the target plants or produce.

This study focused on water soluble ethylene antagonists, thus application by the feed solution was chosen as the target mode of application. Preliminary assessment of the developed compounds found partial solubility in pure water for key compounds, and use of 3% ethanol allowed for full dissolution of all compounds tested. The use of low concentrations of ethanol in aqueous solutions have little to no effect on cut carnations,<sup>238</sup> and preliminary assessment of Geraldton wax for effects of 3% ethanol solution in comparison to pure water shown no significant differences in flower abscission, indicating it was viable to use in this model. For all of the assays performed, the control samples used procedural blanks as feed solutions i.e. aqueous solutions with ethanol concentration identical to that used in the samples tested.

### 3.2.1 Containers for sealed ethylene exposure

In the horticultural laboratory, assays on Geraldton wax were performed on sprigs 30-40 cm in 60 L barrels. Clearly, this was not suitable for the space in a chemistry laboratory. A smaller sample size had to be considered and thus appropriately sized containers had to be chosen. Sistema KLIP IT™ 2.35L Cookie Tub containers were found to be of optimal size and quality for these tests (Figure 22). With 163 mm height, the containers allowed for a Geraldton wax cutting of up to 50 flowers to stand freely. These containers also had a rubber seal and a clipping sealing mechanism, ensuring containment of ethylene **1** inside the container without leaking. The test were to be run in triplicates to conform with statistical norms and to more easily identify potential outliers and assays with results affected by miscellaneous external influence. Initial preliminary tests of the containers have shown a consistent Geraldton wax abscission from ethylene **1**, however it was noted the results became less consistent after multiple assays were run in the same containers.



Figure 22 Sistema 2.35L containers used for Geraldton wax testing of potential ethylene antagonists

On investigation, it was considered the plastic material of the containers may absorb ethylene **1** on prolonged exposure, thus affecting the results. Literature review has shown permeability of plastic polymers can occur,<sup>239, 240</sup> thus a washing regiment was proposed to ensure removal of any residue from the test containers. After each test was performed, the containers were filled with 0.025% sodium hypochlorite solution and

left sitting overnight. Bleach, as a strong oxidiser would react with the organic residue remaining after a test, and easily washed out with deionised water on the following day. Application of this washing regiment gave more consistent results in these tests (Figure 23).

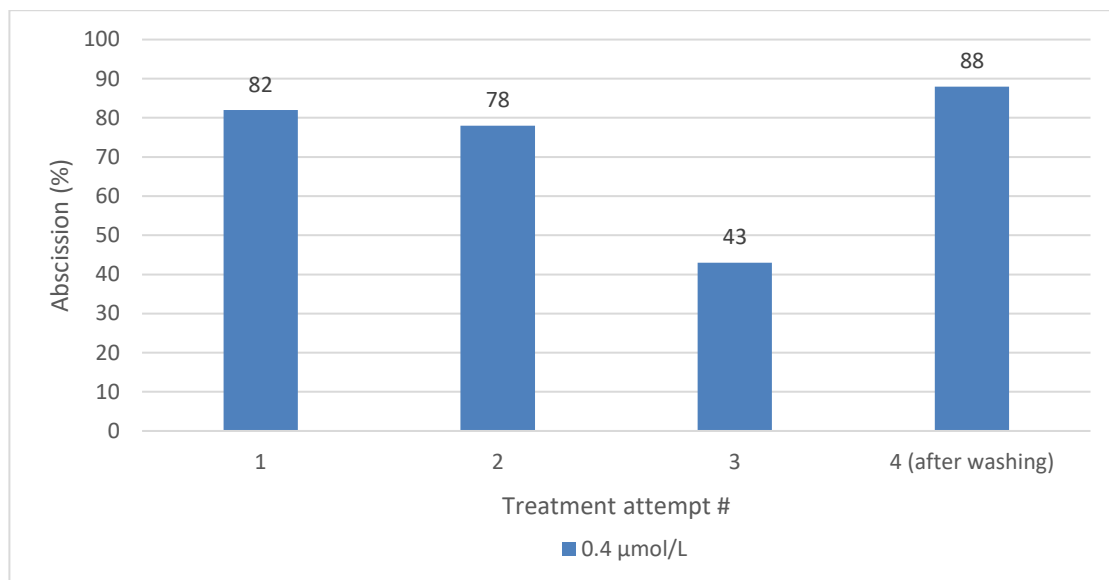
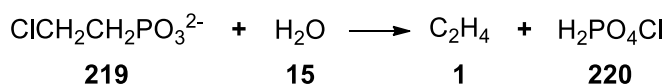


Figure 23 Variability of control (ethylene **1** alone) abscission of Geraldton wax on repeated container use

### 3.2.2 Optimisation of ethylene exposure amount

Studies by Wen and Tucker were followed as a basis for development of the in-house study model.<sup>241</sup> Ethylene can be handled in gas form in pressurised gas cylinders, however appropriate equipment is necessary for safe use and accurate dose application. As a more convenient alternative on small scale, ethylene can be generated *in situ* by a chemical reaction of (2-chloroethyl)phosphonic acid **219** (or ethephon).<sup>241, 242</sup> Ethephon **219** is a stable solid, generally bought and stored in an acidic (pH ~2.3) aqueous solution in the form of monoanion. By increasing the pH of the solution, it forms an unstable dianion which degrades to ethylene **1**, being entirely deprotonated at pH 9 (Scheme 46). This allows for a simple and accurate application of ethylene **1** to a closed container due to delayed decomposition. Sodium hydroxide was used as the base, with solution of 10 g in 10 mL of water, ensuring excess of base for complete deprotonation of the ethephon and thus quantitative release of ethylene **1**.



Scheme 46 Decomposition of ethephon **219** to ethylene **1** under basic conditions

The amount of ethylene **1** sufficient to reliably cause flower abscission in Geraldton wax was assessed. Four cuttings of the plant were placed into tap water in individual 2.35 L closed containers and each gassed with ethylene **1** overnight (16 hours). Four concentration of ethylene **1** were tested: 141.4, 14.1, 1.41 and 0.14  $\mu\text{mol/L}$ . After the 16 hours, the containers were opened and the amount of flower abscission was observed over two days (Figure 24). Samples 141.4, 14.1 and 1.41  $\mu\text{mol/L}$  had an over 90% abscission after 1 day with no change on the second day, while the last sample of 0.14  $\mu\text{mol/L}$  had only 24% abscission on the first day, going up to 90% on the second day. This indicated a concentration of 0.14  $\mu\text{mol/L}$  was too low to reliably trigger ethylene action in the plant cuttings. Further tests in the range between 1.41 and 0.14  $\mu\text{mol/L}$  allowed to optimise the ethylene **1** concentration to 0.43  $\mu\text{mol/L}$ , which was used in the model study. For convenience of application, the ethephon **219** was applied as an aqueous solution at concentration of 3.32 mmol/L and volume of 300  $\mu\text{L}$  with a mechanical pipette for the 2.35 L containers.

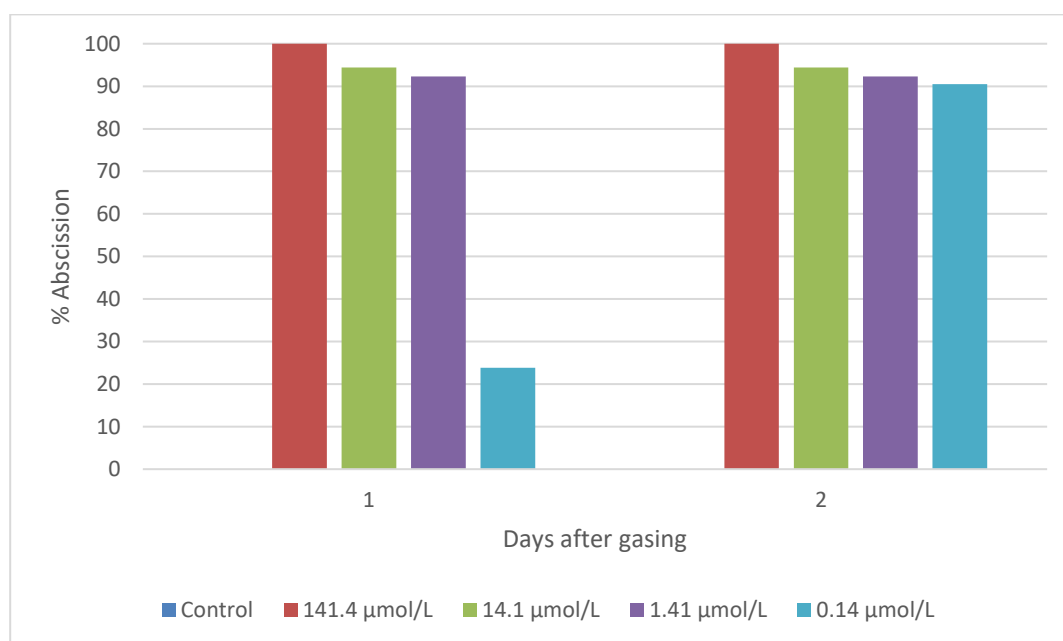


Figure 24 Effect of ethylene **1** concentration on abscission of Geraldton wax

### 3.2.3 Validation of ethylene controls used across all assays

On completion of all of the *in vivo* assays, the controls were collectively assessed against literature values for Geraldton wax abscission of flowers.<sup>194-200, 232, 233</sup> The procedural blank control (plants not exposed to ethylene **1**) showed no flower abscission in all samples with 0 - 5% ethanol **1** solutions. Twenty triplicates of gassed control (0.42  $\mu\text{mol/L}$ ) were run for a total sample size of 60. None of the triplicates failed to cause flower abscission. The average flower abscission was 71% with standard deviation of 22%. The distribution of the samples in 20% abscission range brackets (Figure 25) showed a clear pattern in the distribution, with abscission of over 40% for majority of control samples. This was consistent with the literature referenced tests, (Figure 21) which shown abscission at 56% and 40% for ethylene controls. Only 4/60 samples were in the bottom two range brackets (i.e. below 40%) and considered outliers, thus based on the sample distribution, control samples with abscission below 40% indicate a presence of an outside influence on the results and the test was considered invalid.

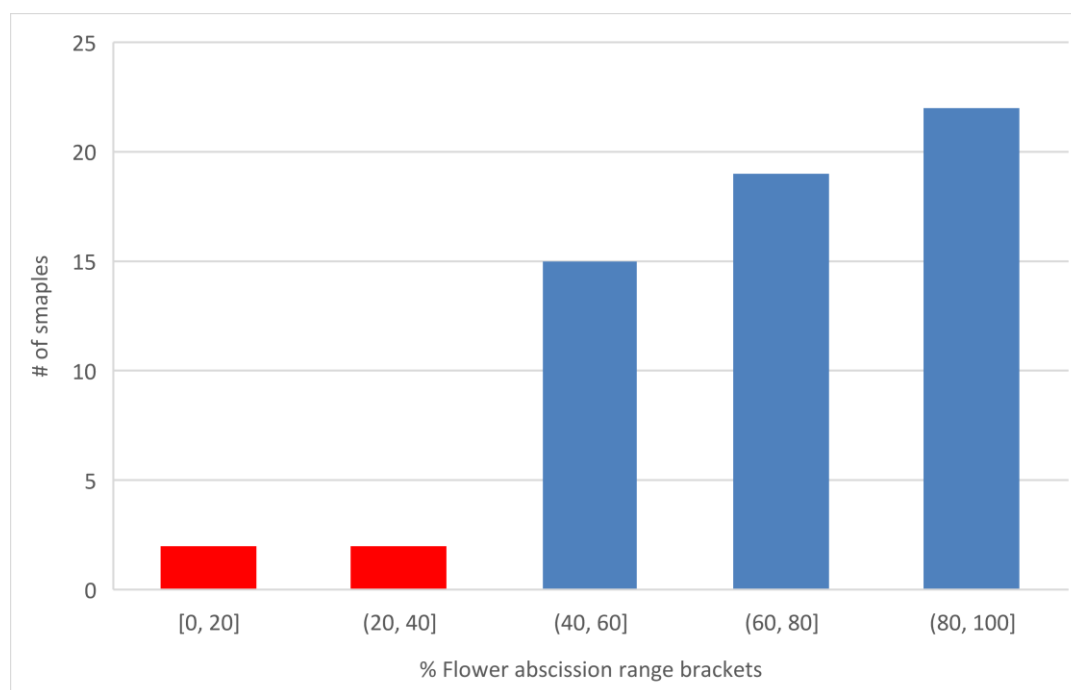


Figure 25 Distribution of results for ethylene gassed control samples of Geraldton wax

### 3.2.4 Finalised model assay

A standardized model assay was developed (Figure 26). A complete assay model was prepared based on series of preliminary experiments. The sprigs of Geraldton wax were taken from the same bush to minimise cultivar variations. Blank and gas control samples were run alongside tested samples. All samples were tested in triplicates.

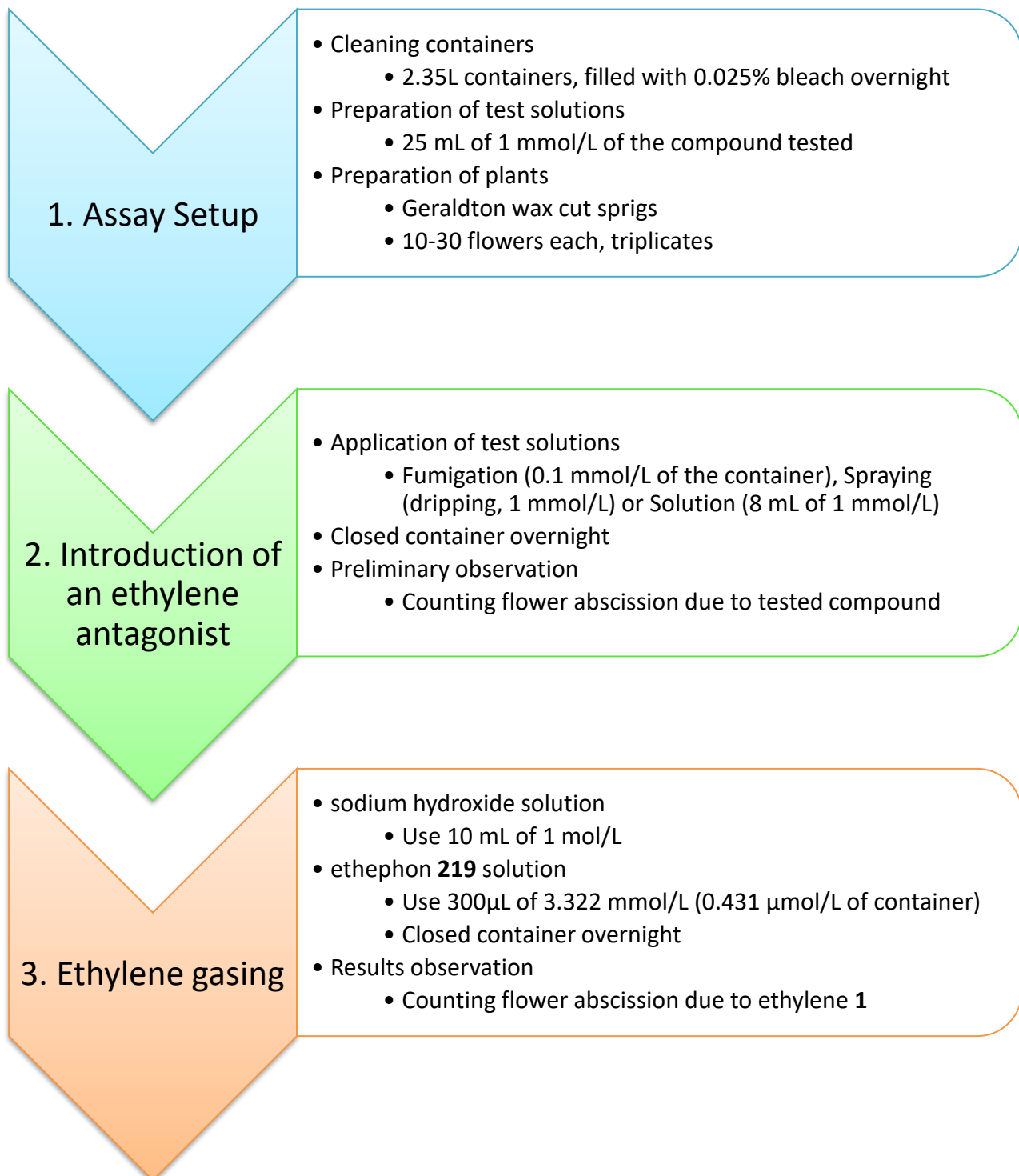


Figure 26 Geraldton wax assay model

### 3.2.5 Preliminary attempts of the in-house assay

The model assay was used with 1*H*-naphtho[*b*]cyclopropene **93**, a known ethylene antagonist. **93** was dissolved in a 5% ethanol solution for spraying and fumigation. Spraying showed a 51% decrease in abscission in comparison to the gassed control, while the fumigation showed over 76% decrease in abscission, indicating greater potency of the fumigation method. These attempts indicate presence of antagonism against ethylene action. (Figure 27).

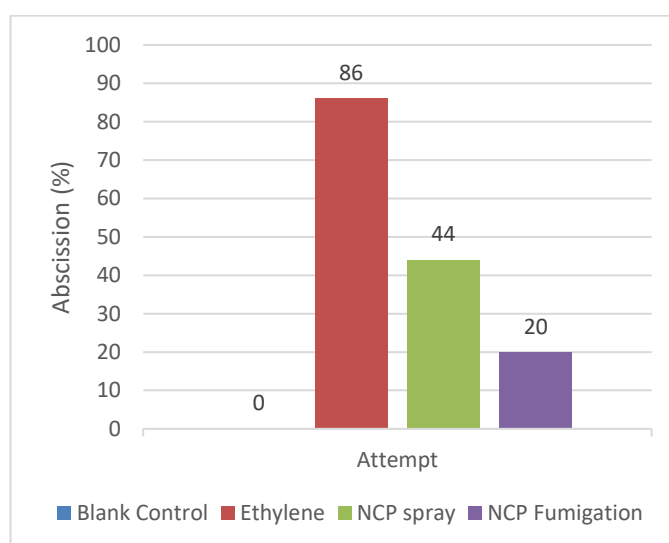


Figure 27 Geraldton wax flower abscission on treatment with 1*H*-naphtho[*b*]cyclopropene **93**

Limonene is a known ethylene antagonist as a fumigant.<sup>201, 243, 244</sup> Two independent attempts at fumigation with 1M limonene were performed following the model assay (Figure 28). The results shown reduction in abscission, 15% and 37% as compared to 83% and 64% of the controls, indicating significant antagonism against ethylene action at high concentration.

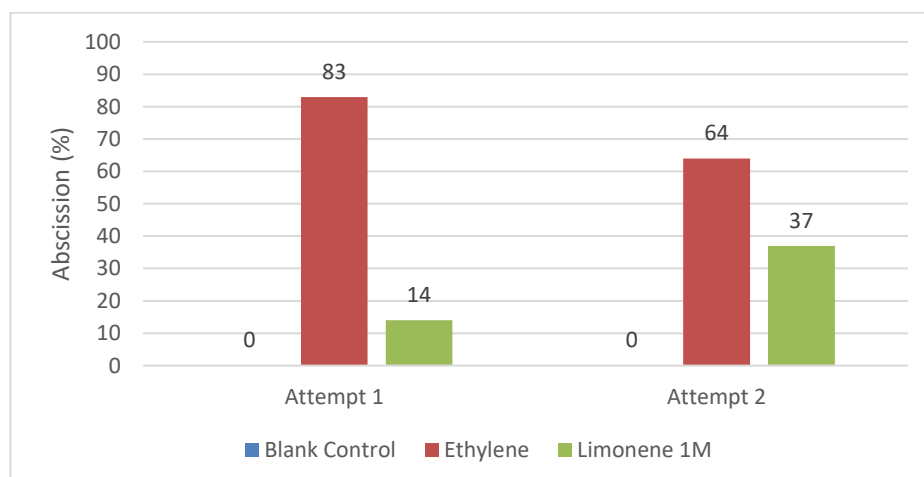


Figure 28 Geraldton wax flower abscission on treatment with limonene

### 3.2.6 Differences between fumigation, spray, dipping and watering

Current practices in horticultural industry involve application of 1-MCP **53** by fumigation.<sup>196</sup> This method is very efficient due to the volatile compound being easily introduced throughout the entire plant. On the other hand, fumigation is more involved in application as it requires tightly regulated atmosphere of storage of the produce. For the developed in-house assay using Geraldton wax, fumigation is also effective due to type of containers used for the testing. This method is applicable to volatile compounds such as 1-MCP **53**, 1*H*-cyclopropa[*b*]naphthalene **93** or limonene, however could not be used for less volatile compounds, which would be the case for more water soluble compounds. For water-soluble compounds, spraying and dipping would be more practical. Both of these methods introduce an ethylene antagonist in a solution directly to the surface of the produce, allowing for straightforward access into the plants systems. Method of application of 1-MCP **53** by spraying was also developed, in which its solubility was improved.<sup>245, 246</sup> In context of the in-house assay, spraying is also applicable to cut carnations, albeit more messy in application.<sup>247, 248</sup> Dipping of produce in solutions of water-soluble ethylene antagonists were shown to be also effective method of application,<sup>249, 250</sup> especially practical and easy to be introduced into the washing of the produce as a regular process in industry. Dipping is also effective for cut carnations as it is similar in technique to spraying. Finally, introduction of ethylene antagonists through watering of a plant or a cut carnation has not been as extensively studied due to lack of effective water-soluble ethylene antagonists. It is hypothesised a water-soluble ethylene antagonists introduced into a plant through watering could travel through a plant to reach the ethylene receptors. Compounds in this study were assessed based on application by watering and some by fumigation and spraying.

## Chapter 4 – Diazo-active [1,2,3]Triazolo[1,5-*a*]pyridines

### 4.1 Background

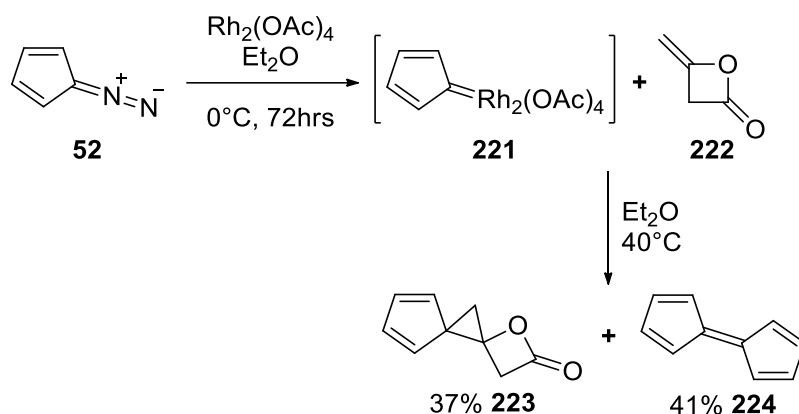
#### 4.1.1 Diazocyclopentadiene (DACP)

Although tentative evidence of a water soluble cyclopropene was observed, it was too difficult to isolate, characterise and test for its antagonism of ethylene action in plants. A new, more user-friendly structure was needed to further this investigation. Of all the compounds tested for the antagonistic activity against ethylene action, one molecule stood out as a relatively unique, diazocyclopentadiene **52** (Scheme 47, See Chapter 1.6.2 ). The compound was a reasonable inhibitor of ethylene action in carnations (9  $\mu\text{L/L}$ ).<sup>113, 121, 122</sup> Tomatoes,<sup>116, 117</sup> apples,<sup>118</sup> strawberries<sup>119</sup> and sweet pea flowers<sup>120</sup> have also been shown to be effectively protected from ethylene action by fumigation with DACP **52**. Other than initial publications mentioned, DACP **52** appears to have been forgotten by the horticultural community. This is not surprising due to the high toxicity and potential explosive nature of the molecule, and effectiveness of 1-MCP **53**.

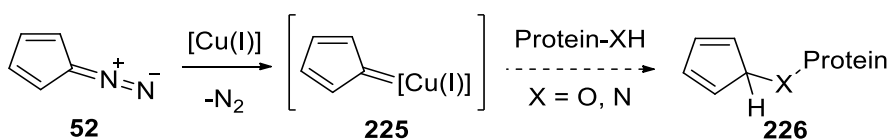


*Scheme 47 Resonance structures of diazocyclopentadiene 2<sup>251</sup>*

Intriguingly, DACP **52** can react through a metal-carbenoid species with loss of nitrogen. When DACP **52** and diketene **222** were reacted with  $\text{Rh}_2(\text{OAc})_2$ , the spiro cyclopropane **223** and the dimerised product, the fulvalene **224**, were isolated (Scheme 48).<sup>251, 252</sup> The obvious similarities of the chemistry of 1-MCP **53** (Scheme 6) and DACP **52** and the limited but reported antagonistic effect of DACP **52** warranted further investigation. The same reaction could occur in the ethylene receptor as for 1-MCP **53**, where DACP **52** reacts with the copper(I) cofactor in ETR-1, forming the copper carbenoid intermediate **225** which then disables the receptor by forming a covalent bond **226** (Scheme 49).



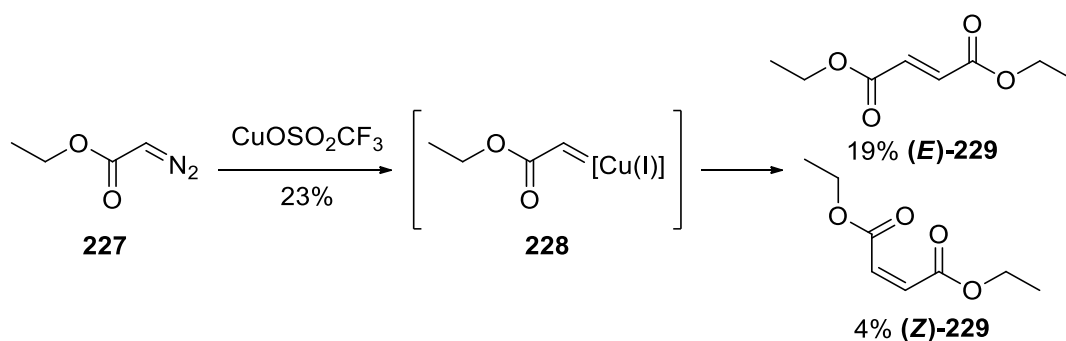
Scheme 48 Reactivity of diazocyclopentadiene **52** in presence of a rhodium catalyst<sup>251</sup>



Scheme 49 Proposed mode of action of diazocyclopentadiene **52** as an ethylene antagonist

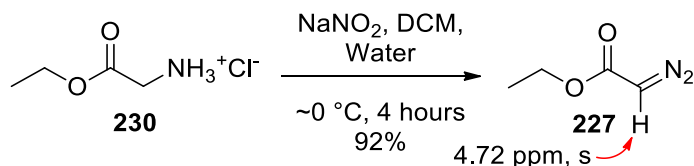
#### 4.1.2 Ethyl diazoacetate

All diazo-compounds should perform in a similar way to DACP **52**, so the simplest diazo-compounds should also have antagonistic effect on ethylene action. To test this hypothesis, a proof-of-concept experiment was developed using ethyl diazoacetate **227**. Like DACP **52**, ethyl diazoacetate **227** reacts with transition metals to form metal carbenoids and react with a range of molecules. Ethyl diazoacetate **227** also reacts with copper(I) salts. Scheme 50 shows the dimerisation of ethyl diazoacetate **227** with copper(I) triflate to give a mixture of diethyl fumarate (*E*)-**229** and diethyl malonate (*Z*)-**229**.<sup>253</sup> To date, ethyl diazoacetate **227** has not been tested for its antagonistic properties against ethylene action.



Scheme 50 Dimerisation of ethyl diazoacetate **227** catalysed by copper(I) triflate by Reck et al.<sup>253</sup>

Ethyl diazoacetate **227** was prepared using the standard method of reacting glycine ethyl ester hydrochloride **230** in DCM with an aqueous solution of sodium nitrite.<sup>254</sup> After stirring the reaction mixture for 4 hours at 0 °C and a simple workup, a yellow oil was obtained (Scheme 51), and stored at -20°C until used. The <sup>1</sup>H NMR spectrum of the crude product had a 1H singlet at 4.72 ppm characteristic for the diazo group as well as a 2H quartet at 4.22 ppm and a 3H triplet at 1.28 ppm characteristic for the ethyl ester.



*Scheme 51 Synthesis of ethyl diazoacetate 227<sup>254</sup>*

Geraldton wax was fumigated with ethyl diazoacetate **227** (Figure 29) according to the procedure discussed in Chapter 3. When Geraldton wax was fumigated with ethyl diazoacetate **227** (1 mmol/L) for 16 hours, a complete decolouration of the petals occurred and general browning of leaves and petals indicated plant death (Table 9). Interestingly, no flower abscission occurred. This demonstrated the known high toxicity of ethyl diazoacetate **227**. The application at lower concentration (0.1 mmol/L) followed by ethylene **1** (0.43 μmol/L) gave a different result. Partial decolouration still occurred in the petals but the plant was alive and there was a reduction of bud and flower drop (29%) compared to the control (80%). Ethyl diazoacetate **227** also cause partial flower abscission (19%) with no ethylene **1** present. These results suggest ethyl diazoacetate **227** may exhibit an antagonistic effect on ethylene action, however is also extremely toxic to the plant.



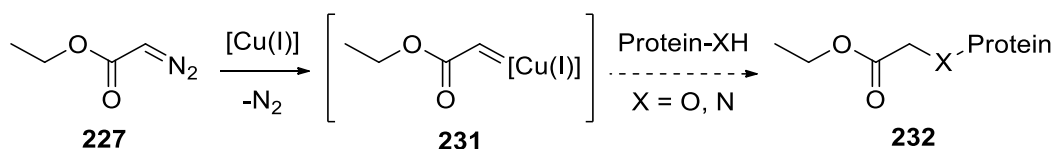
*Figure 29 Loss of colour and senescence in Geraldton wax after fumigation: ethyl diazoacetate 227 + ethylene 1 (left), ethylene 1 (middle) and a procedural blank (right)*

Table 9 Effectiveness of ethyl diazoacetate **227** as ethylene antagonist in Geraldton wax

|                                    | Flower abscission (% drop) |          |
|------------------------------------|----------------------------|----------|
|                                    | No ethylene                | Ethylene |
| Control                            | 0%                         | 80%      |
| Ethyl diazoacetate<br>(0.1 mmol/L) | 19%                        | 29%      |
| Ethyl diazoacetate<br>(1 mmol/L)   | 0%*                        | 0%*      |

\*Plant death occurred

The above experiment demonstrates that diazo-compound could be a promising lead as inhibitors of ethylene action. The mode of action of ethyl diazoacetate **227** is proposed to be similar to 1-MCP **53** based on the reactivity of diazo-compounds with transition metals (Scheme 52). The diazo group reacts with the copper(I) cofactor, generating a reactive intermediate **231** which then incapacitates the receptor by forming a covalent bond **232**. However, if this avenue is pursued, the toxicity of diazo compounds needs to be addressed.



Scheme 52 Proposed mode of action of ethyl diazoacetate **227** as an ethylene antagonist

#### 4.1.3 [1,2,3]Triazolo[1,5-*a*]pyridine

The previous experiment showed that ethyl diazoacetate **227** may provide a protective effect against ethylene, however less toxic compounds needed to be designed. If the diazo functionality could be masked, there could be an avenue for development to circumvent the toxicity issues. [1,2,3]Triazolo[1,5-*a*]pyridines **233** are bicyclic, aromatic heterocycles containing three nitrogens. This class of compounds is in equilibrium with an open ring form, 2-(diazomethyl)pyridine **234** (Figure 30). The closed ring isomer is the dominant structure in the parent compound, however different analogues exist where the open ring form is preferred. For example, *tert*-butyl 7-fluoro-[1,2,3]triazolo[1,5-*a*]pyridine-3-carboxylate **235** remains in an open ring form **236** under standard conditions (Figure 31).<sup>255</sup> If a “Goldilocks” compound could be found,

a molecule that is just reactive enough to react with the transition metals but stable enough to be not toxic, it may be a good antagonist of the ethylene action.

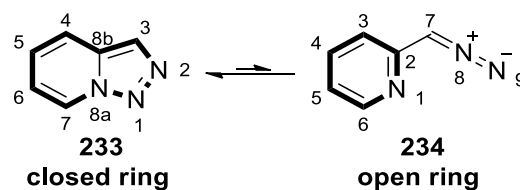


Figure 30 Equilibrium of [1,2,3]triazolo[1,5-a]pyridine **233** with 2-(diazomethyl)pyridine **234**

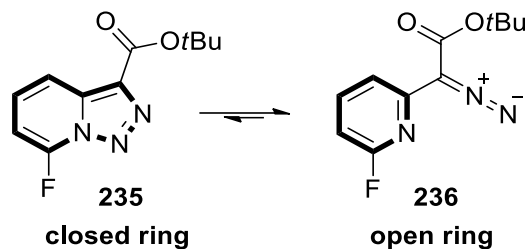


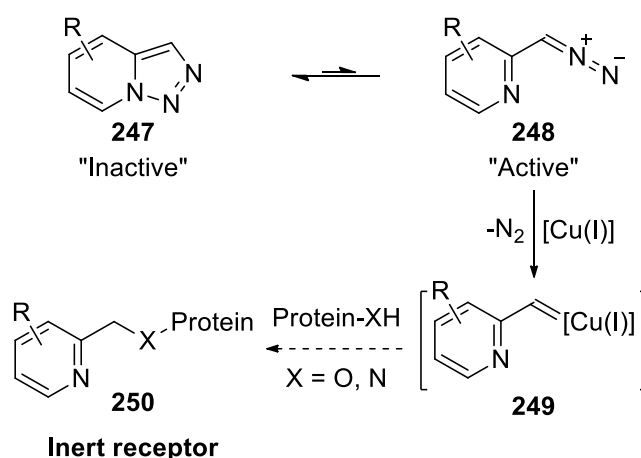
Figure 31 Equilibrium of tert-butyl 7-fluoro-[1,2,3]triazolo[1,5-a]pyridine-3-carboxylate **235** with tert-butyl diazo-2-(6-fluoropyridin-2-yl)acetate **236**<sup>255</sup>

Triazolopyridines have not been investigated as ethylene antagonists in the past and only a few studies in relation to plants were performed. In particular, Egner et al.<sup>256</sup> investigated potential of triazolopyridines (amongst other families of compounds) as herbicides. The compounds **237-246** were tested *in vivo* for activity against D1 protein of photosystem II in plants, a known herbicide binding niche. A broad range of activity was found for triazolopyridines, dependent on substitution of the triazolopyridine skeleton structure (Figure 32). In particular, introduction of a halogen at position 7 shown significant increase in reactivity (**238**, **239**, **245**, **246** each  $IC_{50} < 0.1 \mu M$ ), more than double than any other active functional group tested such as  $SCH_3$  or  $OCH_3$ . In comparison, the analogue with a methyl group at position 7 (**237**) was less potent, further presenting halogens as key in activating reactivity of triazolopyridines.

| Compound   | R                                  | X                              | $IC_{50}(\mu M)$ |
|------------|------------------------------------|--------------------------------|------------------|
| <b>237</b> | CH <sub>3</sub>                    | H                              | 2.3              |
| <b>238</b> | Br                                 | H                              | <b>0.024</b>     |
| <b>239</b> | Cl                                 | H                              | <b>0.095</b>     |
| 240        | OCH <sub>3</sub>                   | H                              | 0.46             |
| 241        | SCH <sub>3</sub>                   | H                              | 0.16             |
| 242        | NHN(CH <sub>3</sub> ) <sub>2</sub> | H                              | 0.47             |
| 243        | Si(CH <sub>3</sub> ) <sub>3</sub>  | H                              | 1.2              |
| 244        | Br                                 | C <sub>6</sub> H <sub>5</sub>  | 0.18             |
| <b>245</b> | Br                                 | OC <sub>6</sub> H <sub>5</sub> | <b>0.085</b>     |
| <b>246</b> | Br                                 | CH <sub>3</sub>                | <b>0.065</b>     |

Figure 32 Substituted triazolopyridines  $IC_{50}$  Inhibition of D1 proteins belonging to photosystem II of plants<sup>256</sup>

The proposed mode of action of [1,2,3]triazolo[1,5-*a*]pyridines **247** would be as follows. The “unmasked” ring opened diazo compound **248** would react with a copper(I) cofactor of the ethylene receptor (**249**) and inhibit ethylene action by forming a covalent bond **250**. Based on these considerations, a mode of action for [1,2,3]triazolo[1,5-*a*]pyridines is proposed below (Scheme 53). Appropriate functionalisation of the triazolopyridine may shift the equilibrium to the ring open form sufficiently to activate the diazo reactivity with copper(I) cofactor to form a carbenoid reactive intermediate and bind to the receptor protein.



Scheme 53 Proposed mode of action of [1,2,3]Triazolo[1,5-*a*]pyridines as ethylene antagonists

Three key components can be considered to shift the equilibrium of [1,2,3]triazolo[1,5-*a*]pyridine **233** (Figure 33). Firstly, the aromaticity of both structures in the equilibrium. Secondly, stabilisation of the diazo group in the open ring form will affect the shift in equilibrium. Thirdly, the change between the two forms happens through bond breaking/formation between the nitrogen 1 and 8a atoms, thus change in the strength of this bond should affect the equilibrium.

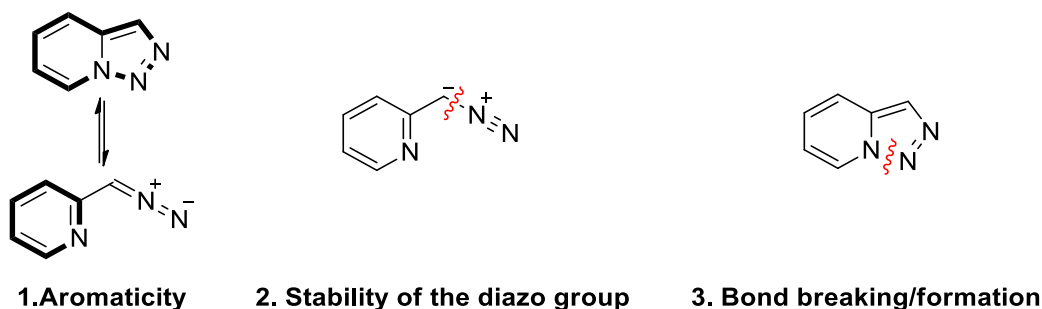
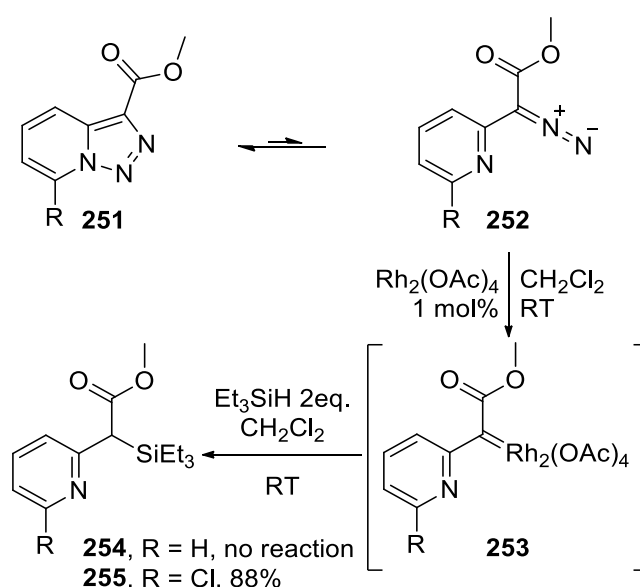


Figure 33 Three key components of shifting equilibrium of the triazolopyridines

Chuprakov et al.<sup>257</sup> showed that methyl 7-chloro-[1,2,3]triazolo[1,5-*a*]pyridylacetate **251** did not show a diazo absorbance in the IR spectrum but reacted in carbene-like reaction in presence of rhodium(II) catalyst, demonstrating the reactivity of the ‘masked’ diazo group **252** (Scheme 54). The closed ring methyl ester **251** is in equilibrium with an open ring methyl ester **252** to form a metal carbenoid intermediate **253** with the rhodium catalyst to give either insertion products **255** or cyclopropenes. More recent articles show effective use of further catalysts including rhodium<sup>258, 259</sup> and copper<sup>260, 261</sup> (including copper(I) complexes which are most relevant to this study). Interestingly, the compound without chlorine (**254**) showed no reactivity.



Scheme 54 Reaction of 7-chloro-[1,2,3]triazolo[1,5-*a*]pyridylacetate **251** catalysed by rhodium(II) complex<sup>257</sup>

Study of Lv et al.<sup>255</sup> highlights the change in reactivity of different halogen substituents of triazolopyridine *tert*-butyl esters **256-258** (Figure 34). The <sup>1</sup>H NMR spectrum of the fluorine derivative **258** showed significantly different spectrum compared to the bromo- and chloro- analogues **256** and **257**. The fluorine derivative **258** was determined to be in the open ring form under standard conditions. This illustrated the greater electro negativity of the fluorine atom compared to bromine and chlorine atoms, being sufficient to shift the equilibrium from the closed form to the open form.

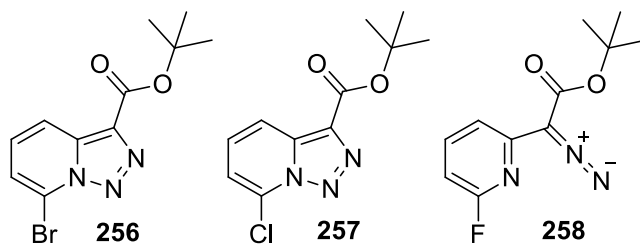


Figure 34 Halogen variations of tert-butyl 7-halo-[1,2,3]triazolo[1,5-a]pyridine-3-carboxylate<sup>255</sup>

A computational study by Blanco et al. looked at the substitution effect on the isomeric equilibrium of [1,2,3]triazolo[1,5-*a*]pyridines.<sup>262</sup> DFT calculations were performed for the [1,2,3]triazolo[1,5-*a*]pyridine **233** ring opening to identify relative energy changes in ring-chain isomerism (Figure 35). This study discussed the ring opening as a ‘moderately endothermic process’ and compared a number of analogues to identify which substituents have a more significant effect on this equilibrium. The mechanism of the ring-opening process is shown in Figure 35.

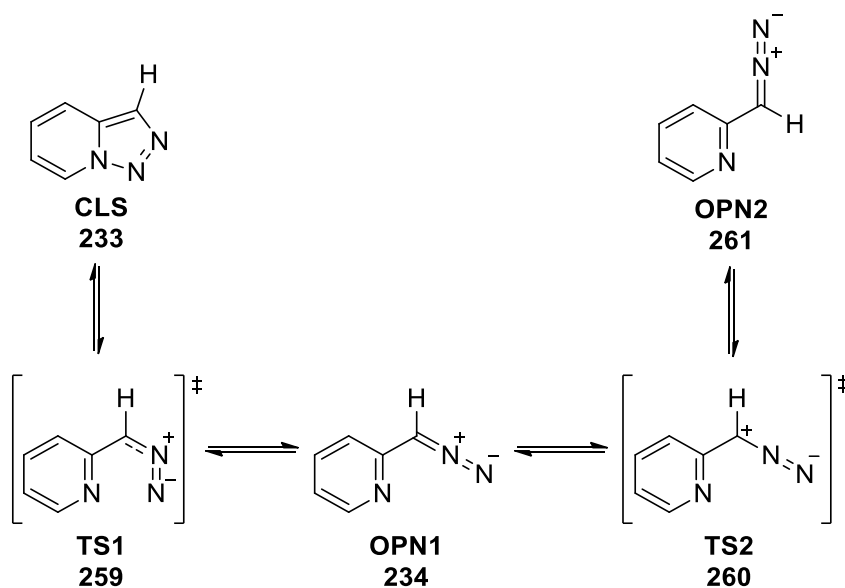


Figure 35 Ring-chain isomerism of [1,2,3]triazolo[1,5-*a*]pyridine **233**<sup>262</sup>

The study also found 7-halo-analogues **155-157** have significantly lower relative energies of the open ring forms compared to the parent compound (Table 10). Moreover, the negative relative energy of the 7-fluoro derivative **157** at OPN1 and OPN2 indicated the ring opening to be instead a mildly exothermic process, which is observed in tert-butyl 7-fluoro-[1,2,3]triazolo[1,5-*a*]pyridine-3-carboxylate **153** (Figure 34).

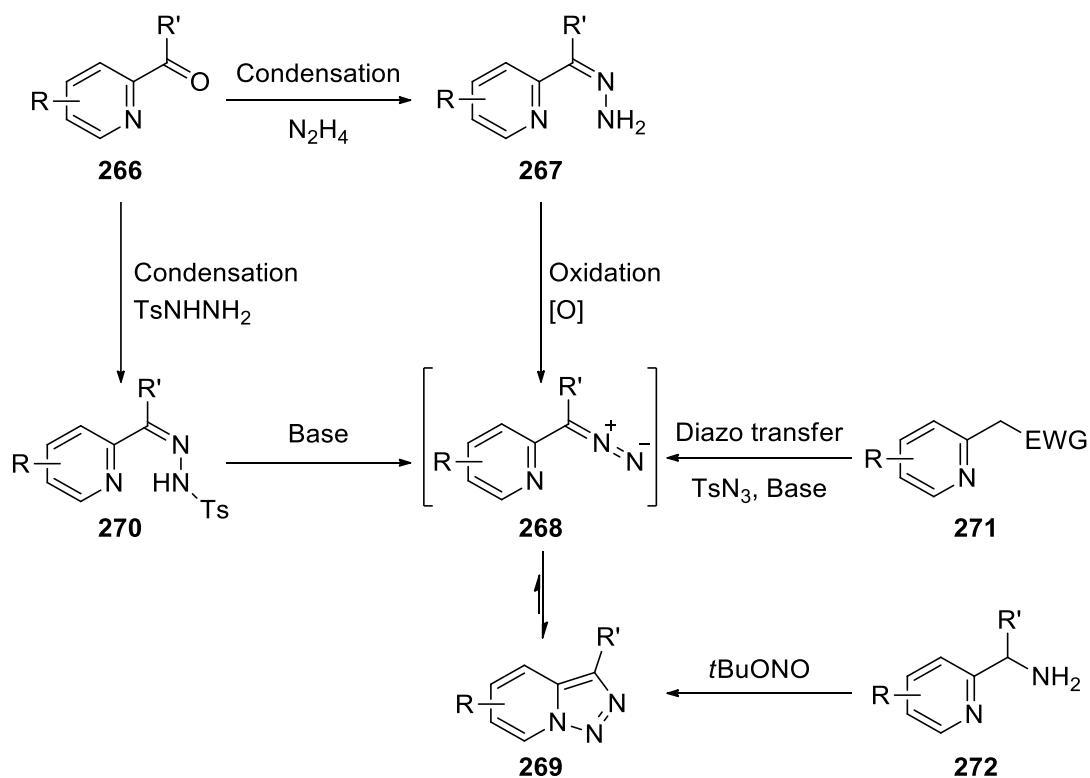
Table 10 Calculated relative energies (kJ mol<sup>-1</sup>) of the [1,2,3]triazolo[1,5-*a*]pyridine structures<sup>262</sup>

|             | <b>7-H</b>     | <b>3-SiH<sub>3</sub></b> | <b>7-Br</b>    | <b>7-Cl</b>    | <b>7-F</b>     |
|-------------|----------------|--------------------------|----------------|----------------|----------------|
| <b>Form</b> | <br><b>233</b> | <br><b>262</b>           | <br><b>263</b> | <br><b>264</b> | <br><b>265</b> |
| <b>CLS</b>  | 0.0            | 0.0                      | 0.0            | 0.0            | 0.0            |
| <b>TS1</b>  | 81.6           | 76.6                     | 64.3           | 62.7           | 53.0           |
| <b>OPN1</b> | 30.9           | 24.4                     | 4.9            | 1.4            | -14.4          |
| <b>TS2</b>  | 71.3           | 54.8                     | 47.9           | 43.7           | 28.3           |
| <b>OPN2</b> | 34.0           | 16.6                     | 7.7            | 4.6            | -11.1          |

Based on these findings, 7-halo-[1,2,3]triazolo[1,5-*a*]pyridine derivatives were chosen as an appropriate starting point for development of new ethylene antagonists. Out of the 7-halo-[1,2,3]triazolo[1,5-*a*]pyridines (Table 10), only the 7-bromo analogue **263** has been synthesised to date. Based on the computational study, it was of interest to investigate whether the bromine atom of the 7-bromo derivative **263** weakens the N-N bond sufficiently to enable diazo reactivity of triazolopyridine. As the 7-fluoro derivative **265** would exist in the ring open form, it would exhibit typical properties of diazo compound toxicity and thus not a viable target of the study. The calculations by Blanco have also shown the position 3 on the [1,2,3]triazolo[1,5-*a*]pyridine **233** affects the ring opened/ring closed equilibrium inversely to position 7. Electron withdrawing groups at position 3 shift the equilibrium towards the closed ring form while electron donating groups shift the equilibrium towards the ring open form. This implies a combination between a halogen at the position 7 and another functional group at position 3 could be used to carefully optimise reactivity of the triazolopyridine. With the shift towards the open ring form, it is anticipated the reactivity of the compound will increase, thus enabling potential ethylene antagonistic effect.

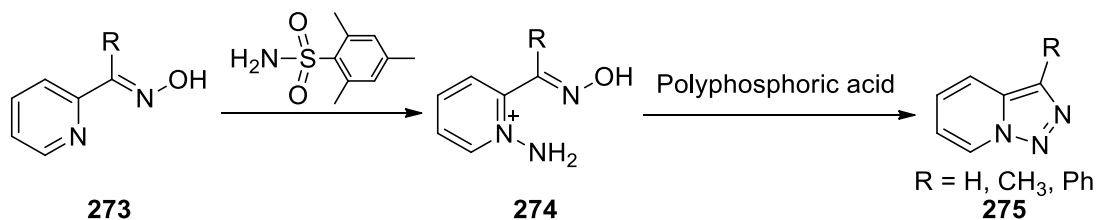
#### 4.1.4 Synthesis pathways to [1,2,3]triazolo[1,5-*a*]pyridines

The general synthesis of the [1,2,3]triazolo[1,5-*a*]pyridines was reviewed by Ballesteros and will be covered here briefly.<sup>263</sup> There are three main synthetic pathways towards [1,2,3]triazolo[1,5-*a*]pyridines, all through formation of a key diazo intermediate **268** (Scheme 55).<sup>264-267</sup> The first known synthesis was developed by Boyer et al.<sup>268</sup> in 1957, by oxidation of hydrazones **267** using Ag<sub>2</sub>O. Other oxidants were also shown to be effective, Bower and Ramage<sup>269</sup> used potassium ferrocyanide while Jones<sup>270-272</sup> and Sliskovic<sup>270, 273</sup> demonstrated effective use of nickel peroxide, lead tetraacetate and copper(I) salts. Boyer and Goebel<sup>274</sup> demonstrated an alternative synthetic pathway avoiding need for oxidation. Condensation of tosylhydrazines with aldehydes or ketones yielded hydrazones **270**, which gave a diazo compound **269** when treated with base (sodium hydroxide, potassium hydroxide, or morpholine).<sup>268, 275, 276</sup> An alternative method of synthesis of triazolopyridine derivatives uses the Regitz's diazo transfer reaction, incorporating insertion of a diazo group by tosylazide under basic conditions (**271**) (using sodium ethoxide).<sup>277, 278</sup> Further studies by Abarca,<sup>275</sup> Jones,<sup>279</sup> Balli et al.<sup>280</sup> or Monteiro<sup>281</sup> have shown other diazo transfer reagents (e.g. 2-azido-1-ethylpyridinium tetrafluoroborate, 2-azido-3-ethylbenzothiazolium tetrafluoroborate) and bases (NaH, EtONa, BF<sub>4</sub><sup>-</sup>, PhLi) can be used. An electron withdrawing group on the methyl group of a pyridine precursor **271** allows for targeted introduction of the diazo group at the alpha carbon, thus only analogues with electron withdrawing group on the position 3 can be synthesised by this method. More recently, Cai et al. presented an alternative pathway to triazolopyridines from 2-pyridine amines **272** in a one-step reaction using *tert*-butyl nitrite (Scheme 55).<sup>282</sup> The reaction is catalyst free and occurs at room temperature, achieving moderate yields. As proposed mechanism, the 2-pyridine amine **272** and *t*BuONO undergo diazotation/1,3-H migration/cyclization sequences, followed by dehydration to give the desired triazolopyridine **269**. The reaction was reported to work on various analogues, including 7-bromo derivative **263** as well as 3-phenyl derivatives. Unfortunately, a 7-methoxy derivative was not achieved. Overall, this novel pathway to substituted triazolopyridines is promising, however its limitations go against the target compounds of this study. Method of Lv et al.<sup>255</sup> was used throughout this study as it was shown effective on 7-halo -3-EWG- derivatives of triazolopyridine, which was a target of this study.



Scheme 55 Synthesis of [1,2,3]triazolo[1,5-a]pyridine by: a) oxidation of a hydrazone,<sup>263-273</sup> b) elimination of a sulfonylhydrazone,<sup>268, 274-276</sup> c) diazo transfer reaction<sup>275, 277-281</sup> and d) diazotation by *t*BuONO<sup>282</sup>

A less common synthetic pathway to triazolopyridines was reported by Tamura et al.,<sup>283</sup> using oximes in an intramolecular cyclization to *N*-amine salts **274** followed by treatment with polyphosphoric acid (Scheme 56). *N*-amination of the pyridine ring **273** with a sulfonamide yields an oxime salt **274** which under acidic conditions causes cyclization and loss of water. Required use of strong acids limits this synthesis method to only more stable triazolopyridines (**275**). No other studies were undertaken on this method of synthesis of triazolopyridines, thus this method was not used in this study.

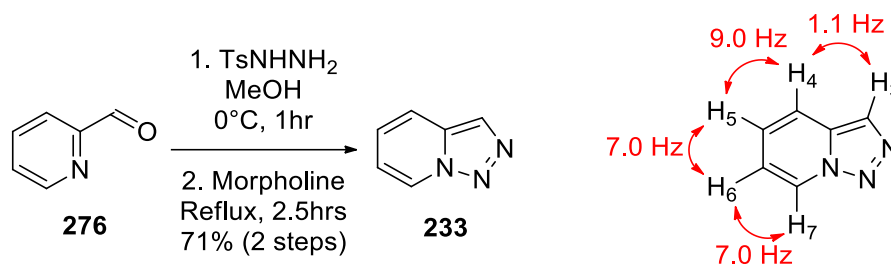


Scheme 56 Synthesis of [1,2,3]triazolo[1,5-a]pyridines by Tamura et al.<sup>283</sup>

## 4.2 Synthesis of [1,2,3]triazolo[1,5-*a*]pyridine derivatives

### 4.2.1 [1,2,3]Triazolo[1,5-*a*]pyridine

[1,2,3]Triazolo[1,5-*a*]pyridine **233** was made from the commercially available 2-pyridinecarboxaldehyde **276** (Scheme 57).<sup>284</sup> The aldehyde **276** was stirred with *p*-toluenesulfonylhydrazide in methanol and the tosylhydrazone was collected by filtration. Elimination of the tosyl group with morpholine yielded [1,2,3]triazolo[1,5-*a*]pyridine **233** in 71% yield over 2 steps. The <sup>1</sup>H NMR spectrum of the [1,2,3]triazolo[1,5-*a*]pyridine **233** (Figure 36) had five aromatic signals and matched the data of Roy et al.<sup>285</sup> The <sup>1</sup>H NMR spectrum indicated presence of only the closed ring product. The characteristic spectrum of the parent compound **233** is reasonably consistent in known derivatives and was used as an indicator for the formation of other triazolopyridines.



Scheme 57 Synthesis of [1,2,3]triazolo[1,5-*a*]pyridine **233**

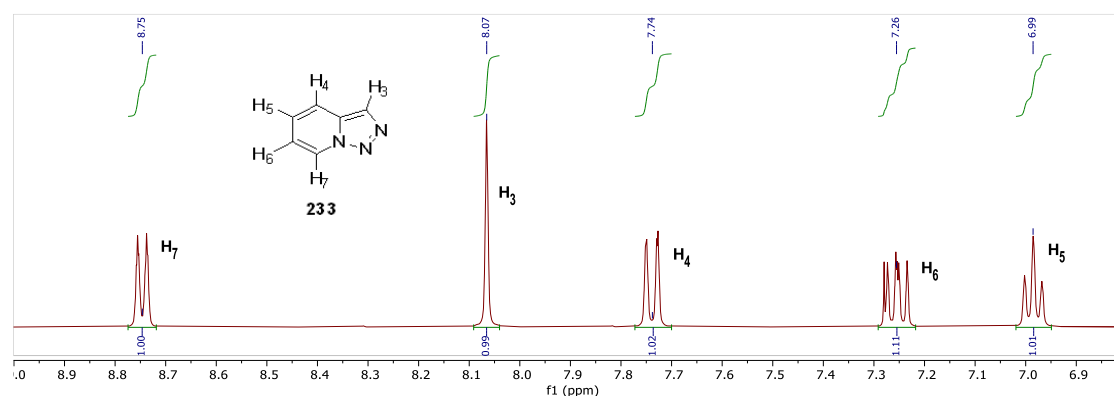
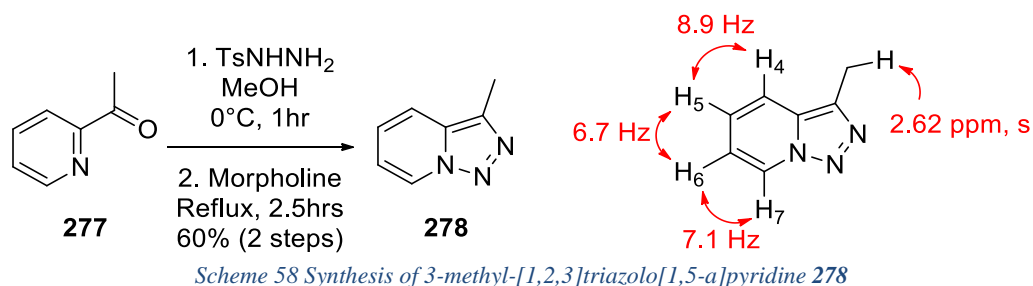
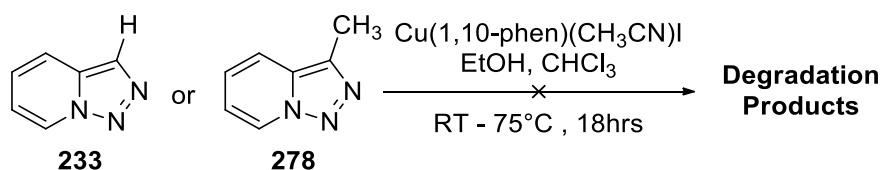


Figure 36 <sup>1</sup>H NMR expanded spectrum of [1,2,3]triazolo[1,5-*a*]pyridine **233**

It was of interest to compare reactivity of the easily accessible 3-methyl derivative **278** to the parent compound **233**. In a similar manner to **233**, synthesis of 3-methyl-[1,2,3]triazolo[1,5-*a*]pyridine **278** was attempted. Synthesis of Liu et al.<sup>286</sup> was followed and **278** was synthesised from 2-acetylpyridine **277** through a hydrazone formation with tosyl hydrazine followed by reaction with morpholine (Scheme 58). The <sup>1</sup>H NMR spectrum of the purified product **278** was very similar to the parent compound **233** and had four aromatic signals and a singlet at 2.62 ppm assigned to the methyl group. The spectrum matched the data of Lamaa et al.<sup>260</sup> and is similar to the parent compound **233**, except for the singlet at 8.06 ppm missing in the aromatic region, replaced with a singlet at 2.62 ppm.



The reactivity of the parent triazolopyridine **233** and 3-methyl derivative **278** were tested with Cu(1,10-phen)(CH<sub>3</sub>CN)I in ethanol (Scheme 59). This proved to be a useful tool as it could be conducted throughout the year whereas Geraldton wax only flowers between months of July to September. When compounds **233** and **278** were stirred at room temperature, no reaction took place. Reaction repeated at 75 °C also recovered starting material. These results indicate the equilibrium between [1,2,3]triazolo[1,5-*a*]pyridine **233** and 2-(diazomethyl)pyridine **234** is strongly favoured towards the closed ring product. The methyl group of the 3-methyl derivative **278** is weakly electron donating but had no effect on the open/closed ring equilibrium to “unmask” the diazo group.



The compounds **233** and **278** were tested in the *in vivo* assay as described in Chapter 3. Both compounds were fully dissolved in 3% ethanol to form 1M solutions and used as stock solutions. No abscission of flowers or other toxic effects were observed when Geraldton wax was treated with the compounds. Upon exposure to ethylene **1**, less than 30% reduction in flower abscission for both tested compounds was observed, suggesting lack of significant antagonism against ethylene action (Figure 37). Based on the Cu(I) reactivity and *in vivo* results, other more reactive analogues were investigated instead.

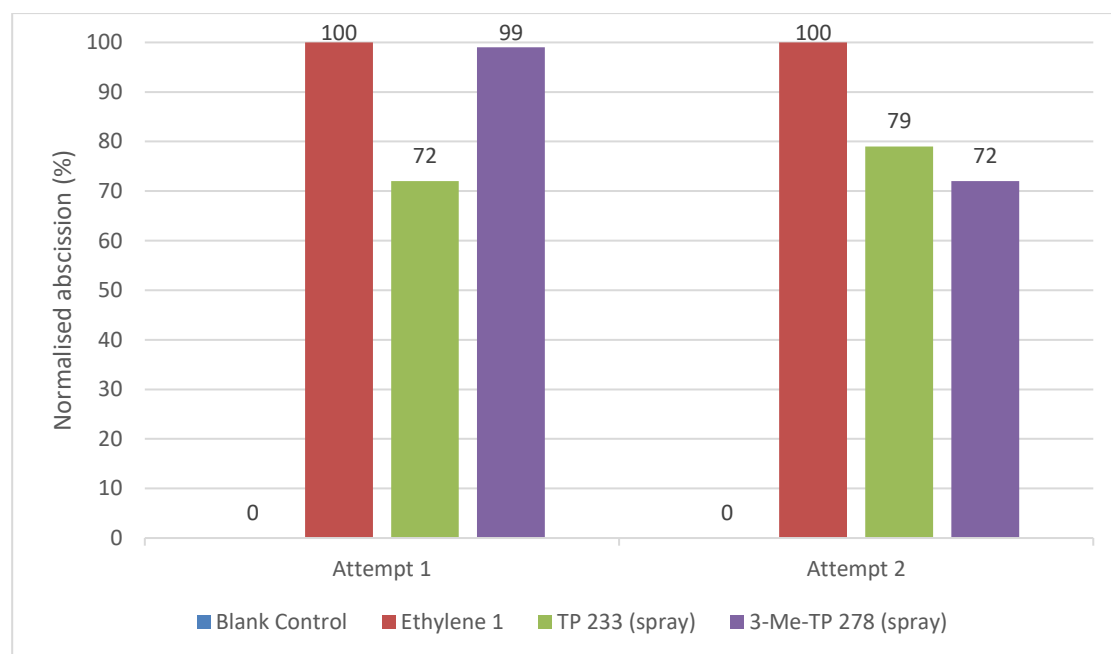
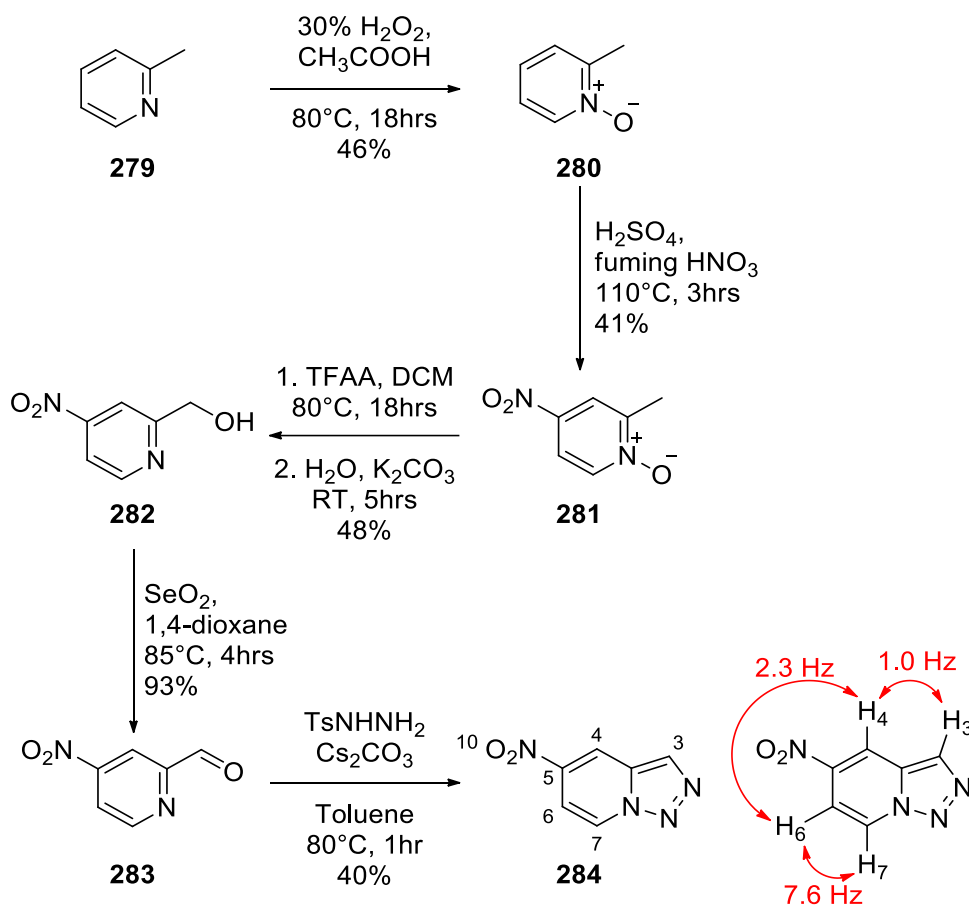


Figure 37 Geraldton wax flower abscission on treatment with [1,2,3]triazolo[1,5-a]pyridine **233** and 3-methyl-[1,2,3]triazolo[1,5-a]pyridine **278** at 1M solution concentration

### 4.3 5-EWG-[1,2,3]triazolo[1,5-*a*]pyridines

The nitro group is a significantly more electron withdrawing than fluorine, thus insertion at the position 7 which would utilise both inductive and resonance withdrawal effects was expected to favour the open ring product. Insertion at another position on the pyridine ring e.g. position 5, para to the nitrogen atom of the ring, would minimise the inductive effect of the EWG group. This could potentially lower to a level sufficient for the closed ring form being favoured, while enabling reactivity of the ring open form. Based on these considerations, synthesis pathway for 5-nitro-[1,2,3]triazolo[1,5-*a*]pyridine **284** was envisioned (Scheme 60). A synthesis using a condensation reaction between tosyl hydrazone and the previously reported (4-nitro-2-pyridyl)-1-carboxaldehyde **283** was undertaken.<sup>287</sup> (4-Nitro-2-pyridyl)-1-methanol **282** was made from picoline **279** in 3 steps using literature procedures.<sup>287, 288</sup> Oxidation of the alcohol **282** with activated manganese dioxide in DCM was unsuccessful, so selenium dioxide in 1,4-dioxane<sup>287</sup> was used to produce the (4-nitro-2-pyridyl)-1-carboxaldehyde **283**. When the aldehyde was reacted with *p*-toluenesulfonyl hydrazide and caesium carbonate, 5-nitro-[1,2,3]triazolo[1,5-*a*]pyridine **284** was produced without the need for further purification. The <sup>1</sup>H NMR spectrum (Figure 38) had a total of four signals, which were deshielded compared to the parent compound, due to the anisotropic effect of the nitro group: 8.86 (d, *J* = 7.6 Hz), 8.76 (dd, *J* = 2.3, 1.0 Hz), 8.44 (d, *J* = 1.0 Hz) and 7.80 (dd, *J* = 7.6, 2.3 Hz) ppm. The small coupling constant of 2.3 Hz between H<sub>4</sub> and H<sub>6</sub> ppm indicated a *meta* coupling and confirmed the orientation of the nitro group. The <sup>13</sup>C NMR spectrum of **284** had a total of six signals, all in the aromatic region and no signal was present for a typical diazo carbon (20-50 ppm), indicating the closed ring form is the dominant structure in the equilibrium.



Scheme 60 Synthesis pathway of 5-nitro-[1,2,3]triazolo[1,5-a]pyridine **284**

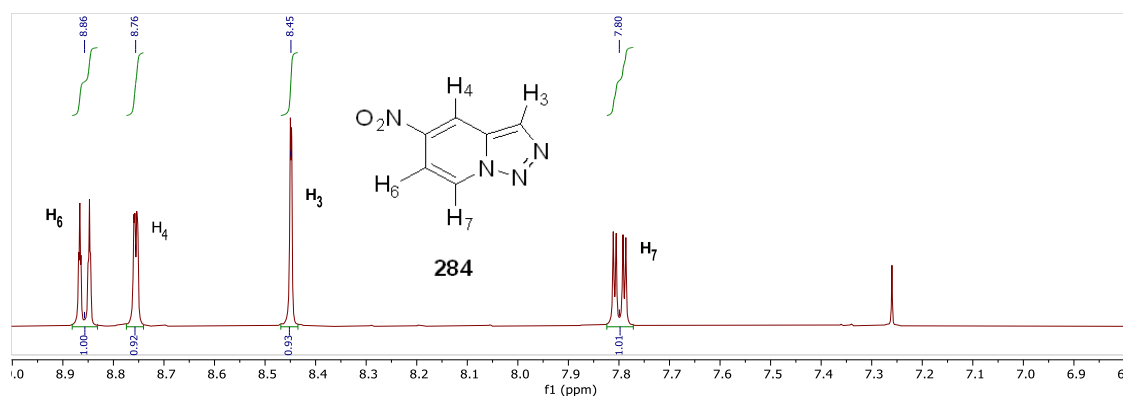
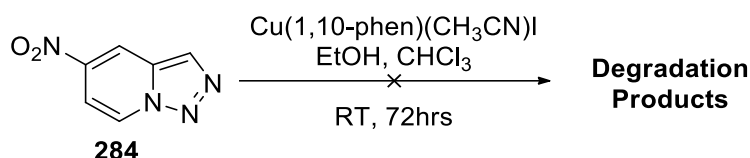


Figure 38 <sup>1</sup>H NMR spectrum of 5-nitro-[1,2,3]triazolo[1,5-a]pyridine **284**

When 5-nitro-[1,2,3]triazolo[1,5-*a*]pyridine **284** was tested for degradation with Cu(1,10-phen)(CH<sub>3</sub>CN)I in ethanol (Scheme 61), the starting material was recovered, indicating the open ring form is not a contributing structure. Based on the strength of the nitro group, it can be hypothesised the mesomeric effect of an electron withdrawing group on the position 5 will not be sufficient to cause a more significant shift in the triazolopyridine equilibrium to enable a diazo activity.



*Scheme 61 Degradation of 5-nitro-[1,2,3]triazolo[1,5-*a*]pyridine **284** catalysed by copper(I) complex in ethanol*

The nitrotriazolopyridine **284** was tested in the Geraldton wax assay. Compound **284** was fully dissolved in 3% ethanol solution and sprayed as a 1M solution. No abscission of flowers or other toxic effects were observed during the pre-treatment process. Although a modest reduction in flower abscission was observed, the lack of reactivity with copper(I) suggests this observation may have occurred through a different pathway (Figure 39). Based on these findings, derivatives with EWGs at position 7 and 3 were targeted instead.

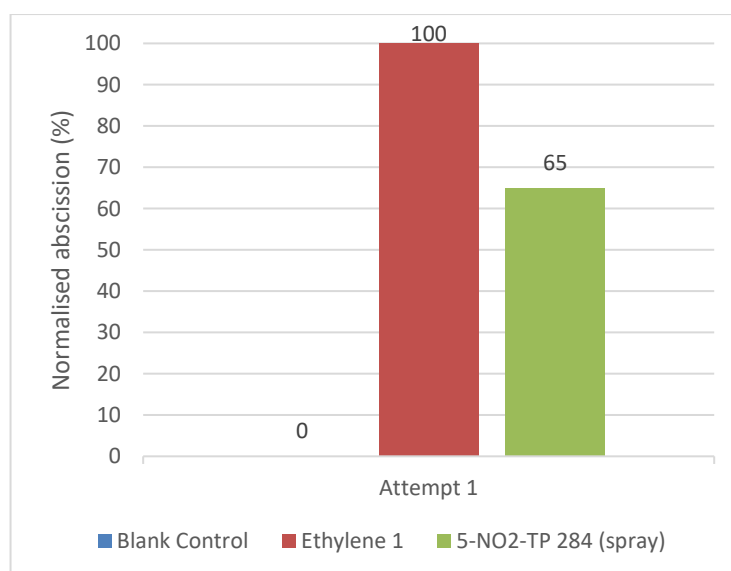
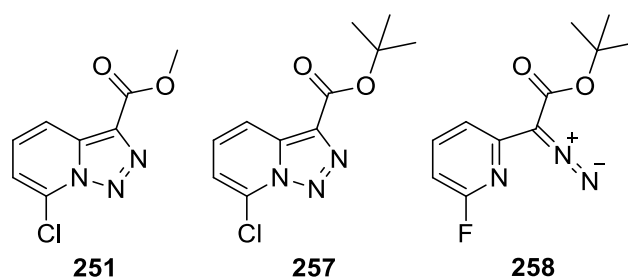


*Figure 39 Geraldton wax flower abscission on treatment with 5-nitro-[1,2,3]triazolo[1,5-*a*]pyridine **284** at 1M solution concentration*

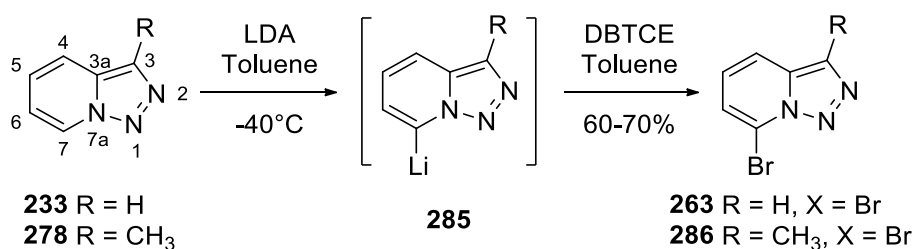
#### 4.4 7-Halo-[1,2,3]triazolo[1,5-*a*]pyridines

7-Chloro-[1,2,3]triazolo[1,5-*a*]pyridylacetate **251** can be considered a literature exemplar for the reactivity of triazolopyridines with transition metals.<sup>257</sup> Moreover, replacing the chlorine substituent with a fluorine, a more electronegative atom, results in a ring-opened product **258** at ambient conditions (Scheme 62).<sup>255</sup> These considerations suggest halogens at the position 7 have a key role in shift towards an activated diazo group and enabled reactivity of triazolopyridines. Thus, 7-halo-derivatives of triazolopyridine needed to be prepared.



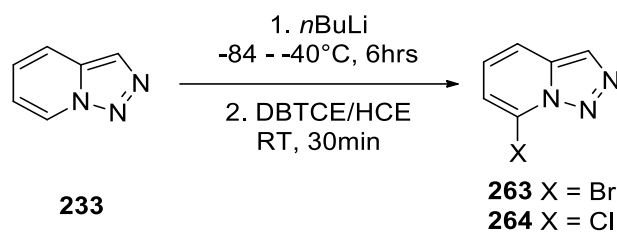
*Scheme 62 Halogen variations of triazolopyridine esters*

In 1980, Jones and Sliskovic<sup>289</sup> reported regioselective lithiation of [1,2,3]triazolo[1,5-*a*]pyridine **233** at position 7 when using lithium diisopropylamide. The lithiated species **285** reacted with electrophiles (e.g. formaldehyde, TMSCl, D<sub>2</sub>O) giving access to a wide range of 7-substituted analogues.<sup>270, 289</sup> The lithiated triazolopyridine **285** also reacts with dibromotetrachloroethane (DBTCE) to give bromides **263** and **286** (Scheme 63).<sup>290</sup> Bromination by method of Abarca et al.<sup>290</sup> proved challenging and only a small amount of the 7-bromo-[1,2,3]triazolo[1,5-*a*]pyridine **263** was obtained in a complex mixture. The product was successfully purified by flash chromatography, however the lower yield than anticipated, indicated degradation during purification. The <sup>1</sup>H NMR spectrum of **263** had four signals in the aromatic region that matched the reported spectrum.<sup>290</sup>



*Scheme 63 Bromination of [1,2,3]triazolo[1,5-*a*]pyridines by Abarca et al.<sup>290</sup>*

An alternative procedure for metalation was attempted, using *n*BuLi in toluene at -84 °C. While difficult to get consistent results (See Scheme 64), an improved yield of the 7-bromo derivative **263** was obtained and the 7-chloro-[1,2,3]triazolo[1,5-*a*]pyridine **264** was also successfully synthesised by using hexachloroethylene instead of dibromotetrachloroethylene. Purification of the products was problematic, with the products degrading during chromatography. The <sup>1</sup>H NMR spectrum of the 7-chloro-[1,2,3]triazolo[1,5-*a*]pyridine **264** (Figure 41) was very similar to the 7-bromo-[1,2,3]triazolo[1,5-*a*]pyridine analogue **263** and had four aromatic signals: 8.17 (s), 7.72 (dd), 7.24 (dd) and 7.08 (dd) ppm. The upfield shift of the 7.72 doublet and downfield shift of the 7.24 triplet as compared to the bromo derivative **263**, can be attributed to the greater electron withdrawing effect of the chlorine atom.



| Target halogen | Equivalents of <i>n</i> BuLi | Additives | Solvent | T (°C) | Yield* |
|----------------|------------------------------|-----------|---------|--------|--------|
| Br             | 1                            | DIPA      | Ether   | -40    | 0-25%  |
| Cl             | 1                            | DIPA      | Ether   | -40    | 0%     |
| Br             | 0.31                         | -         | Toluene | -84    | 0-32%  |
| Cl             | 0.31-0.5                     | -         | Toluene | -84    | 0-32%  |
| Cl             | 2                            | -         | Toluene | -84    | 66%    |
| Cl             | 4                            | -         | Toluene | -84    | 7-19%  |

\*Based on [1,2,3]triazolo[1,5-*a*]pyridine **233**

Scheme 64 Synthesis of 7-halo-[1,2,3]triazolo[1,5-*a*]pyridine analogues **263** and **264**

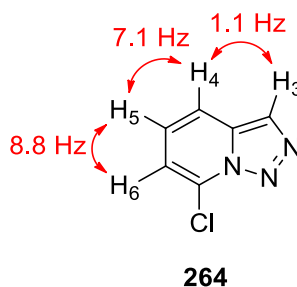


Figure 40 <sup>1</sup>H NMR splitting of 7-chloro-[1,2,3]triazolo[1,5-*a*]pyridine **264**

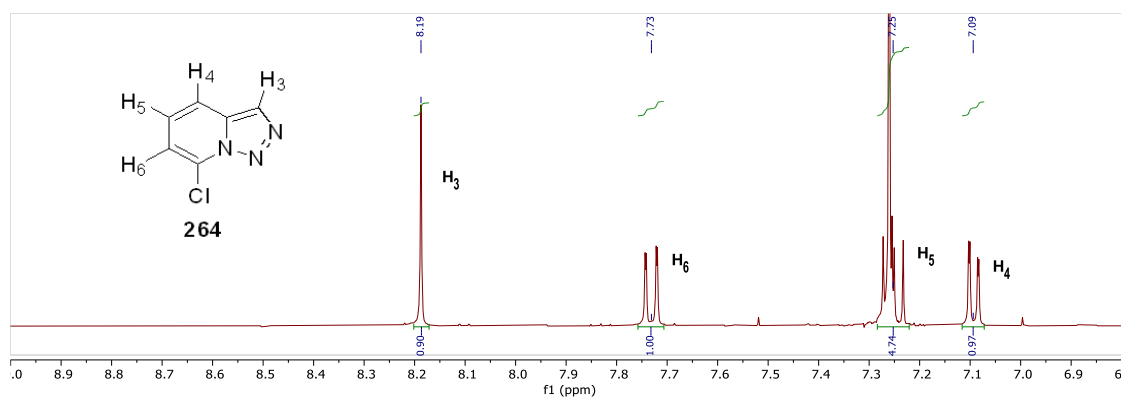
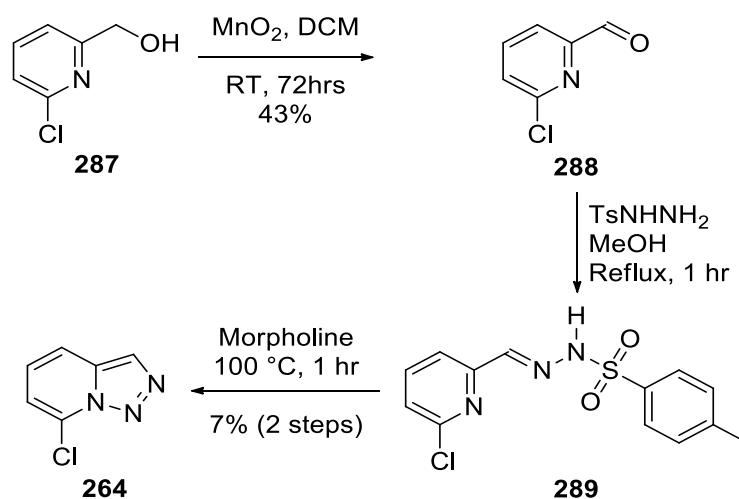


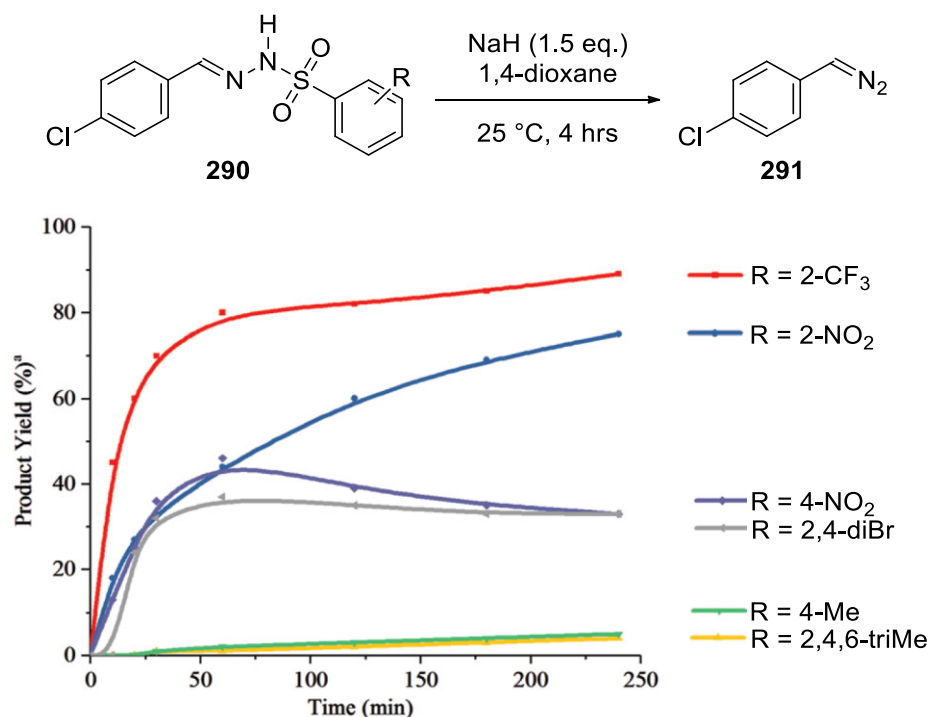
Figure 41  $^1\text{H}$  NMR spectrum of 7-chloro-[1,2,3]triazolo[1,5-*a*]pyridine **264**

Due to the low yield and inconsistencies of the lithiation reaction, an alternative synthesis pathway for the 7-chloro-[1,2,3]triazolo[1,5-*a*]pyridine **264** was pursued (Scheme 65). The hydrazone formation pathway was chosen due to its simplicity and starting material, (6-chloropyridin-2-yl)methanol **287** was available. Following method of Aoyama et al.,<sup>291</sup> the alcohol **287** was oxidised using activated manganese dioxide in dichloromethane to give pure (6-chloro-2-pyridyl)-1-carboxaldehyde **288** in a good yield. Due to high volatility of the product, a weak vacuum ( $\sim 5$  torr) and a liquid nitrogen trap were used to concentrate the product solution. (6-Chloro-2-pyridyl)-1-carboxaldehyde **288** was stirred with tosyl hydrazide in methanol to yield the expected hydrazone **289** as a white solid, which was used directly in the next reaction. When the hydrazone was heated in morpholine, a complex mixture of products was obtained. The  $^1\text{H}$  NMR spectrum of the complex mixture had identifiable signals of 7-chloro-[1,2,3]triazolo-[1,5-*a*]pyridine **264**, and purification by flash chromatography gave a poor yield, indicating degradation of the target compound.

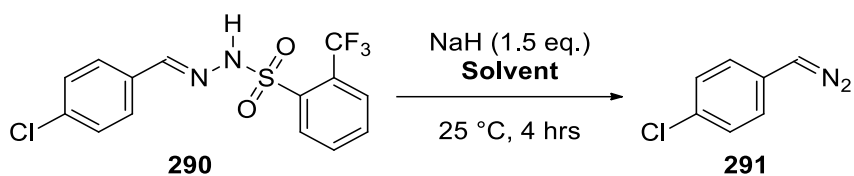


Scheme 65 Synthesis of 7-chloro-[1,2,3]triazolo[1,5-*a*]pyridine **264**

A recent study by Liu et al. showed the influence of the arylsulfonyl substituents, various bases, solvents and temperature on the yield of diazo compounds obtained by from sulfonylhydrazones.<sup>292</sup> Aryl groups containing strongly electron withdrawing groups (**290**) increased product yield, in particular with an EWG group at the *ortho* position, due to the inductive effects (Scheme 66). Nine aprotic solvents were tested and all except DMSO have shown satisfactory results (Scheme 67). The best yields were achieved at room temperature. Cooling the reaction to 0 °C significantly reduced the rate of reaction and thus yield, while heating to 40 °C increased decomposition of the diazocompound. From the range of bases investigated caesium carbonate gave the best yield (93%), with other bases also giving satisfactory yields (NaH 89%, LiOMe 75%, K<sub>3</sub>PO<sub>4</sub> 75%) (Scheme 68). Only two bases performing poorly, namely potassium *tert*-butoxide (43%) and lithium *tert*-butoxide (11%), indicating steric hindrance has a negative effect on the yield.

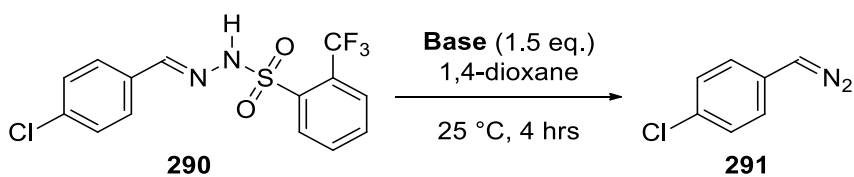


Scheme 66 Synthesis of diazo compounds by Liu et al.<sup>292</sup>



| Solvent            | NMR yield (%)    |               |
|--------------------|------------------|---------------|
|                    | Recovery (178aa) | Yield (179aa) |
| DMSO               | 14               | 20            |
| DMF                | 0                | 70            |
| CH <sub>3</sub> CN | 0                | 86            |
| 1,4-Dioxane        | 0                | 89            |
| THF                | 5                | 76            |
| PhCl               | 24               | 68            |
| DCE                | 20               | 65            |
| DCM                | 24               | 69            |
| Toluene            | 0                | 70            |

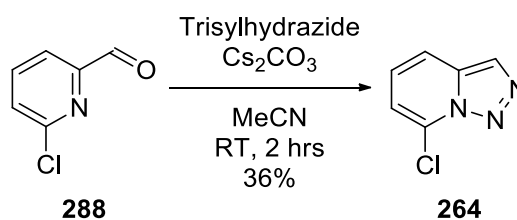
*Scheme 67 Effect of solvents on elimination of sulfonylhydrazones by Liu et al.<sup>292</sup>*



| Base                            | NMR yield (%)    |               |
|---------------------------------|------------------|---------------|
|                                 | Recovery (178aa) | Yield (179aa) |
| NaH                             | 0                | 89            |
| K <sub>3</sub> PO <sub>4</sub>  | 12               | 75            |
| K <sub>2</sub> CO <sub>3</sub>  | 15               | 63            |
| Cs <sub>2</sub> CO <sub>3</sub> | 0                | 93            |
| KOH                             | 0                | 65            |
| KOtBu                           | 10               | 43            |
| LiOtBu                          | 5                | 11            |
| LiOMe                           | 0                | 75            |

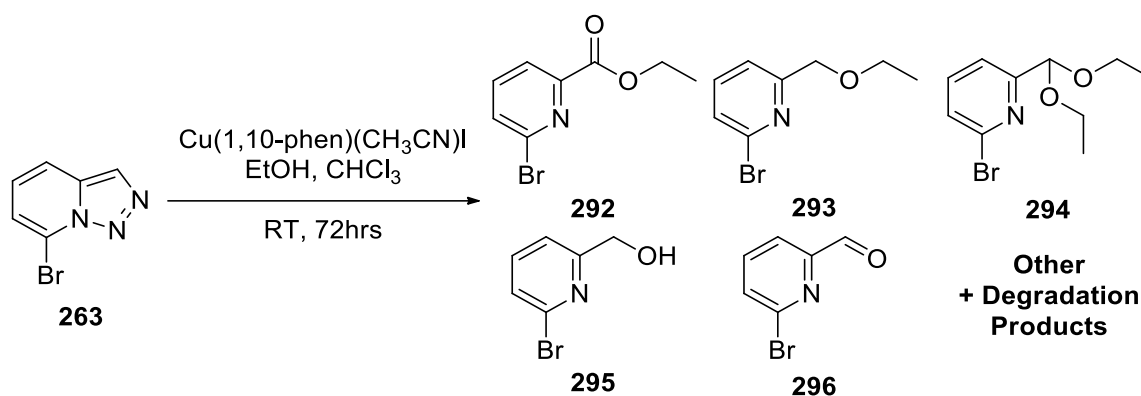
*Scheme 68 Effect of bases on elimination of sulfonylhydrazones by Liu et al.<sup>292</sup>*

The study by Liu did not include any pyridine derivatives, however these findings should be applicable to the synthesis of 2-(diazomethyl)pyridine **234** and thus [1,2,3]triazolo[1,5-*a*]pyridines. Based on the reported findings and available reagents, a one-pot synthesis procedure using 2,4,6-triisopropylbenzenesulfonyl hydrazide and caesium carbonate in acetonitrile was used for synthesis of triazolopyridine analogues.<sup>285</sup> When these reagents were used with 6-chloro-2-pyridinecarboxaldehyde **288** (Scheme 69), 7-chloro-[1,2,3]triazolo[1,5-*a*]pyridine **264** was isolated in ~40% crude yield, however column chromatography again resulted in significant degradation. Fortunately, titration using petroleum spirits and ethyl acetate yielded acceptably pure chloride **264**, in sufficient amounts for the chemical model and *in vivo* experiments. The <sup>1</sup>H NMR spectrum of 7-chloro-[1,2,3]triazolo[1,5-*a*]pyridine **264** matched the one previously obtained in Figure 41.<sup>293</sup>



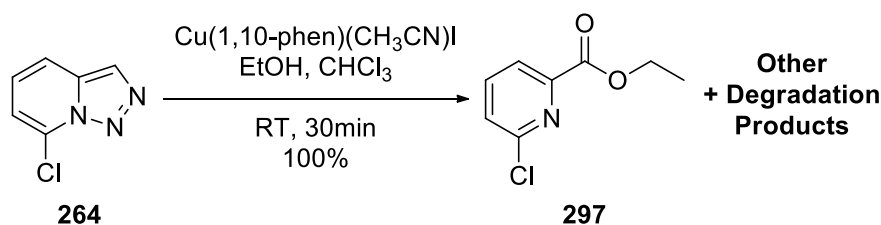
Scheme 69 Synthesis of 7-chloro-[1,2,3]triazolo[1,5-*a*]pyridine **264**

When the bromide **263** was reacted with Cu(1,10-phen)(CH<sub>3</sub>CN)I in ethanol (Scheme 70), the starting material was consumed over a period of 3 days. A number of compounds were isolated from the reaction: ethyl (6-bromopyridine)-2-carboxylate **292**<sup>294</sup> as the major product as well as minor amounts of (6-bromopyridin-2-yl)ethanol **295**,<sup>295</sup> 6-bromopicolinaldehyde **296**,<sup>296</sup> the ethyl ether **293** and the acetal **294**.<sup>297</sup> The mechanism of these transformations is not yet fully understood however. Alcohol **295** and ether **293** can be obtained by insertion reactions of carbenes into methanol and water.<sup>298, 299</sup> As the reaction was not degassed, oxygen was present in the reaction and Cu(I)/Cu(II) redox chemistry could give oxidised products akin to the Fehling's test for aldehydes.<sup>300</sup> These oxidation reactions could give the other products.



Scheme 70 Degradation of 7-bromo-[1,2,3]triazolo[1,5-a]pyridine **263** catalysed by copper(I) complex

It was expected 7-chloro derivative **264** would exhibit enhanced reactivity when compared to the 7-bromo derivative **263**. 7-Chloro-[1,2,3]triazolo[1,5-a]pyridine **264** was similarly reacted with  $\text{Cu}(1,10\text{-phen})(\text{CH}_3\text{CN})\text{I}$  in ethanol (Scheme 71). The starting material was consumed in 30 minutes, confirming significantly higher reactivity. Due to limited amount of material, only the ethyl ester **297** was isolated<sup>301</sup> from the complex mixture of products. While 7-chloro-[1,2,3]triazolo[1,5-a]pyridine **264** reacted with the Cu(I) complex, it also was inherently unstable.



Scheme 71 Degradation of 7-chloro-[1,2,3]triazolo[1,5-a]pyridine **264** catalysed by copper(I) complex

Both compounds **263** and **264** were fully dissolved in 3% ethanol to form 1M solutions and used as stock solutions. No abscission of flowers or other toxic effects were observed on introductions of the compounds to Geraldton wax over 24 hours. Disappointingly, 74% or more abscission was observed compared to the ethylene control, suggesting lack of significant antagonism against ethylene action (Figure 42). This may be due to the high reactivity of the compound which degrade prior to reacting with the ethylene receptor. This result suggests more stable analogues need to be prepared and tested, particularly based on the 7-chlorotriazolopyridine structure **264**.

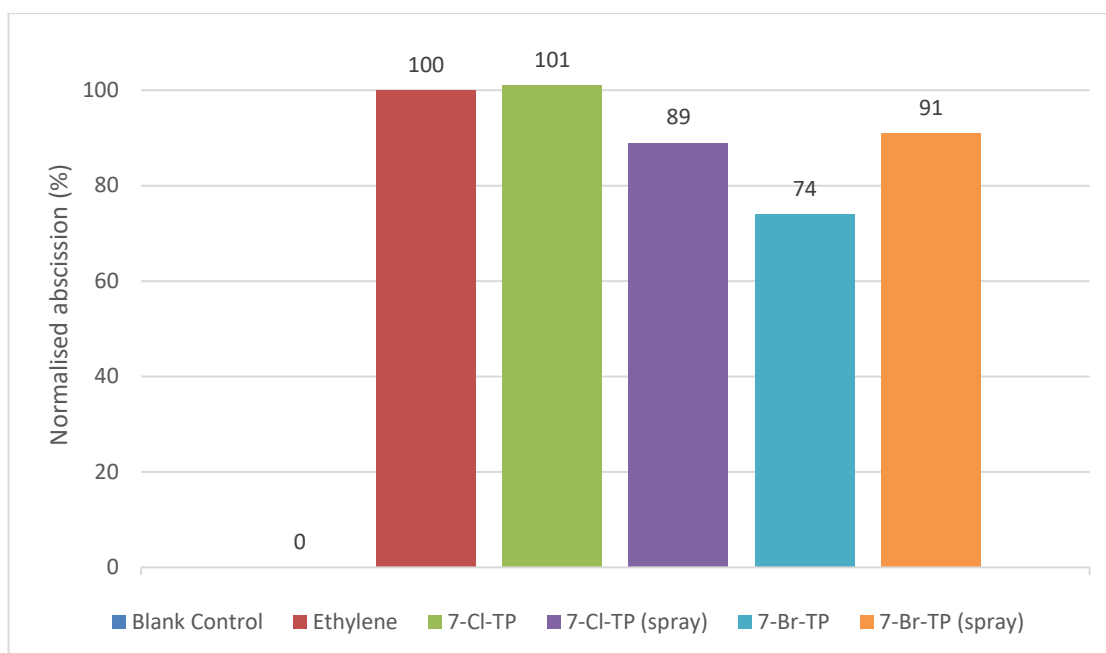


Figure 42 Geraldton wax flower abscission on treatment with 7-chloro-[1,2,3]triazolo[1,5-*a*]pyridine **264** and 7-bromo-[1,2,3]triazolo[1,5-*a*]pyridine **263** at 1M solution concentration

#### 4.5 7-Chloro-3-EWG-[1,2,3]triazolo[1,5-*a*]pyridines

Based on the work by Chuprakov et al.<sup>257</sup> the addition of an electron withdrawing group at position 3 to the 7-chloro-[1,2,3]triazolo[1,5-*a*]pyridine **264** should increase stability of the compound while potentially retaining appropriate level of reactivity. Position 3 of [1,2,3]triazolo[1,5-*a*]pyridines was identified as one also having substantial effect on the reactivity and stability of the diazo group as well as the open/closed ring equilibrium. 3-EWG-analogues **299** that are of particular interest in this study could be synthesised by diazo transfer reaction from their respective precursors. Three synthetic pathways were envisioned to make 7-chloro-[1,2,3]triazolo[1,5-*a*]pyridine derivatives **302** (Figure 43). The addition of an EWG to 2-methylpyridine **279** would give the pyridine **298**, which would allow for synthesis of the desired chloroderivative **302** by two pathways. Unfortunately, the halogenation by lithiation (Path 1) is incompatible with most EWG's (esters, nitro etc.) but does give access to unchlorinated derivatives **299**. Alternatively, the 2-EWG-pyridine precursor **300** could be halogenated prior to the diazo transfer reaction (Path 2). Methods for chlorination of substituted pyridines have been reported in the literature.<sup>302, 303</sup> Finally, an EWG (**301**) could be introduced to 6-chloro-2-methylpyridine **300** (commercially available), followed by a diazo transfer reaction to form the target disubstituted triazolopyridine **302** (Path 3).

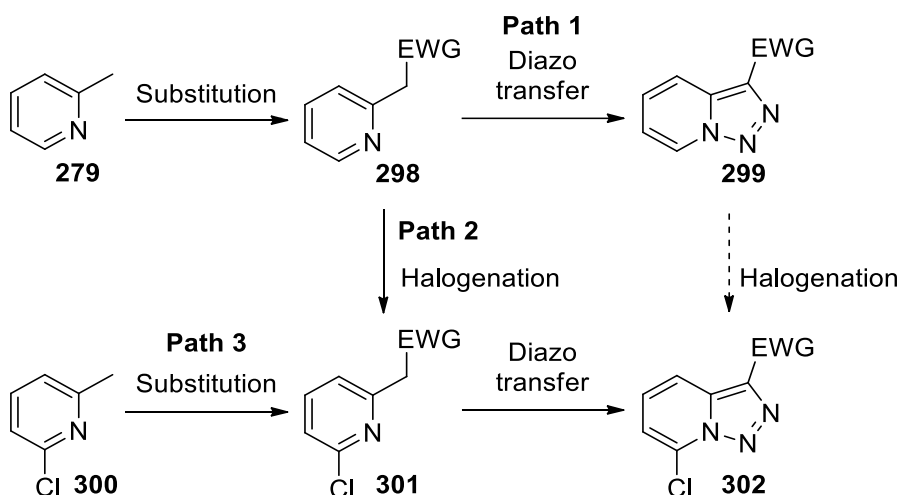
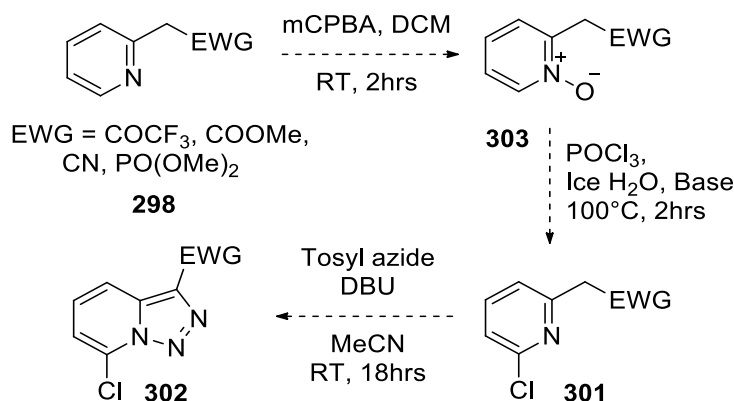


Figure 43 Proposed synthesis pathways of 3-Substituted-[1,2,3]triazolo[1,5-a]pyridine analogues **299** and **302**

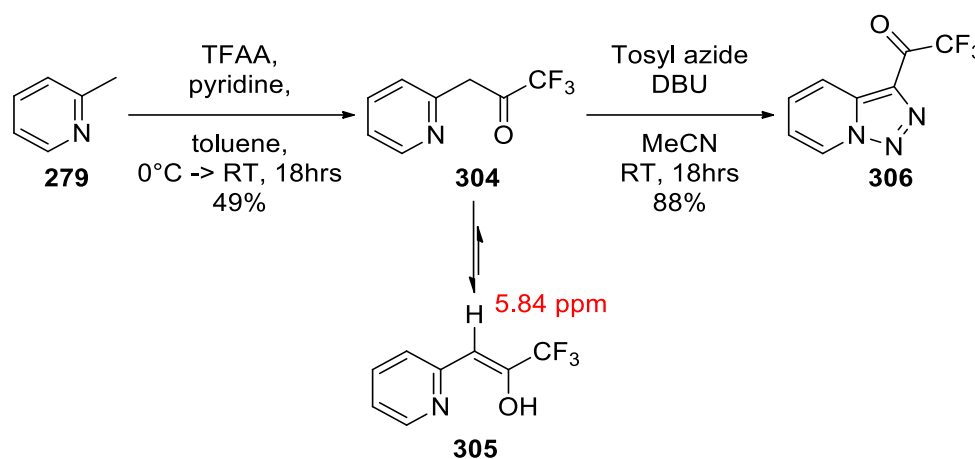
#### 4.5.1 3-EWG-[1,2,3]triazolo[1,5-a]pyridines

The 2<sup>nd</sup> synthetic pathway (Path 2) was initially explored as it gave access to both halogenated and non-halogenated version of triazolopyridine. A two-step halogenation of pyridine rings is well known: *N*-oxidation of the pyridine ring followed by deoxychlorination. The first example of *N*-oxidation of pyridine was accredited to Meisenheimer in 1926 using peracids.<sup>304</sup> *N*-Oxidation can be performed with a number of peroxide reagents such as *meta*-chloroperbenzoic acid, hydrogen peroxide, perfluorobutyryl peroxide or peracetic acid, generally in good yields.<sup>305-308</sup> Early examples of deoxychlorination of pyridine-*N*-oxides include use of phosphorus oxychloride.<sup>309</sup> It was envisioned *N*-oxidation of a substituted 2-methylpyridine **298** with *meta*-chloroperbenzoic acid, followed by deoxychlorination using phosphorus oxychloride would give the chlorinated pyridine precursor compound **301** (Scheme 72). Diazo transfer reaction using tosyl azide and DBU would transform the precursor into new disubstituted derivatives of [1,2,3]triazolo[1,5-*a*]pyridine **302**.



Scheme 72 Proposed synthesis pathway of 7-chloro-3-substituted-[1,2,3]triazolo[1,5-a]pyridine analogues **302**

Following the method of Kawase et al.,<sup>310</sup> 2-methylpyridine **279** was treated with trifluoroacetic anhydride in pyridine and toluene to give 3,3,3-trifluoro-1-(2-pyridinyl)-1-propen-2-ol **305**, the dominant tautomer of 1,1,1-trifluoro-3-pyridyl-2-propanone **304**, as indicated by a singlet at 5.84 ppm in the <sup>1</sup>H NMR spectrum (Scheme 73).<sup>311</sup> The diazo transfer on the purified compound **305** was performed using tosyl azide, DBU in acetonitrile gave the 1,1,1-trifluoro-2-([1,2,3]triazolo[1,5-*a*]pyridin-3-yl)ethanone **306** (Scheme 73). The compound **306** crystallised from dichloromethane at -20 °C. The <sup>1</sup>H NMR spectrum (Figure 44) had four aromatic signals in an isolated spin system reminiscent of the 6-membered ring of the parent triazolopyridine **233**. The <sup>13</sup>C NMR spectrum had 8 signals: 136.55 (C), 132.62 (CH), 131.85 (C), 126.79 (CH), 119.70 (CH) and 118.00 (CH) ppm indicative of the closed triazolopyridine ring. Signals at 173.99 (C) and 115.10 (C) ppm were coupled with fluorine in the <sup>13</sup>C NMR spectrum and indicated the trifluoroacetyl group.



Scheme 73 Synthesis pathway of 1,1,1-Trifluoro-2-([1,2,3]triazolo[1,5-*a*]pyridin-3-yl)ethanone **306**

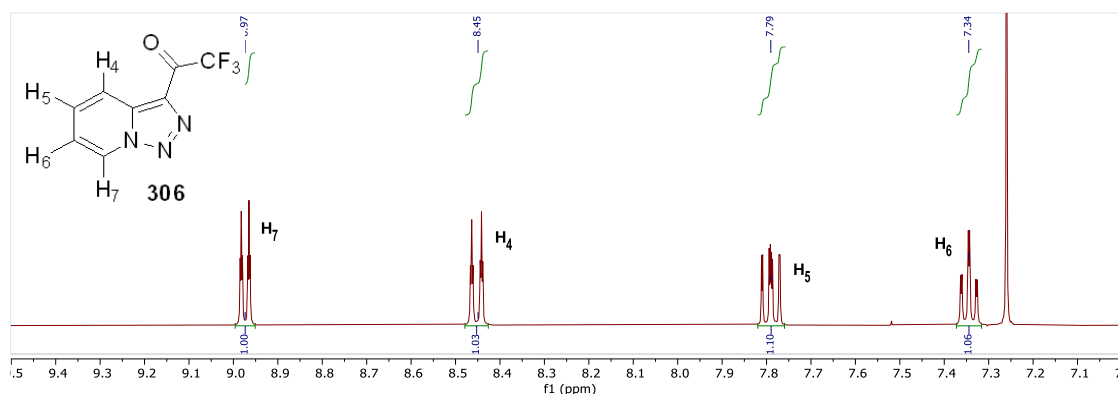
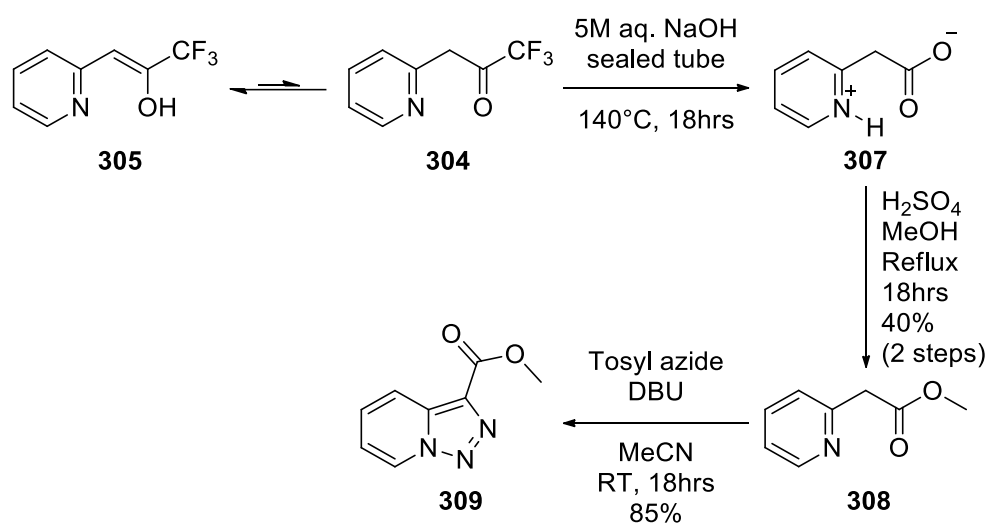


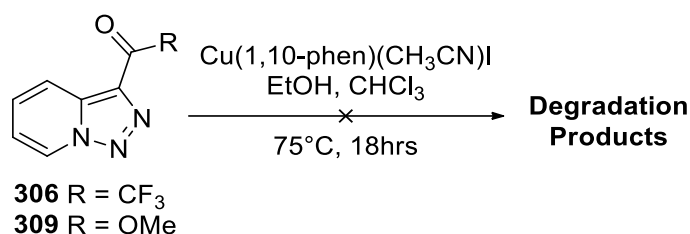
Figure 44 <sup>1</sup>H NMR spectrum of 1,1,1-Trifluoro-2-([1,2,3]triazolo[1,5-*a*]pyridin-3-yl)ethanone **306**

Trifluoroacetyl groups can be converted to a carboxylic acid by a reaction reminiscent of the final steps of a haloform reaction. Adapting the method of Park et al.,<sup>312</sup> 1,1,1-trifluoro-3-pyridyl-2-propanone **304** was hydrolysed under basic conditions to give the carboxylic acid **307** (Scheme 74). This compound existed as a zwitterion and was used directly in the next reaction. The carboxylic acid **307** was esterified with methanol and sulfuric acid to yield methyl 2-(pyridin-2-yl)acetate **308** (Scheme 74), which did not require further purification. The ester **308** was reacted with tosyl azide and DBU in acetonitrile to give methyl 3-([1,2,3]triazolo[1,5-*a*]pyridine)acetate **309** (Scheme 74). The NMR spectra matched the data of Allen et al.<sup>313</sup> and Chuprakov et al.<sup>257</sup>



Scheme 74 Attempted synthesis pathway of methyl 3-([1,2,3]triazolo[1,5-*a*]pyridine)acetate **309**

Compounds **306** and **309** were reacted with Cu(1,10-phen)(CH<sub>3</sub>CN)I in ethanol (Scheme 75), however only the starting material was recovered. This supports the hypothesis that introduction of EWGs on the position 3 of [1,2,3]triazolo[1,5-*a*]pyridine alone is not sufficient to “unmask” the diazo functional group.



Scheme 75 Attempted degradation of [1,2,3]triazolo[1,5-*a*]pyridine acetyl derivatives **306** and **309** in presence of copper(I) complex in ethanol

Both compounds **306** and **309** were fully dissolved in 3% ethanol and used at 1M as the stock solutions. No abscission of flowers or other toxic effects were observed on introductions of the compounds to Geraldton wax. Less than 20% reduction in flower abscission was observed for both tested compounds, suggesting lack of significant antagonism against ethylene action (Figure 45). The chemical reactivity and the *in vivo* results of **306** and **309** were consistent.

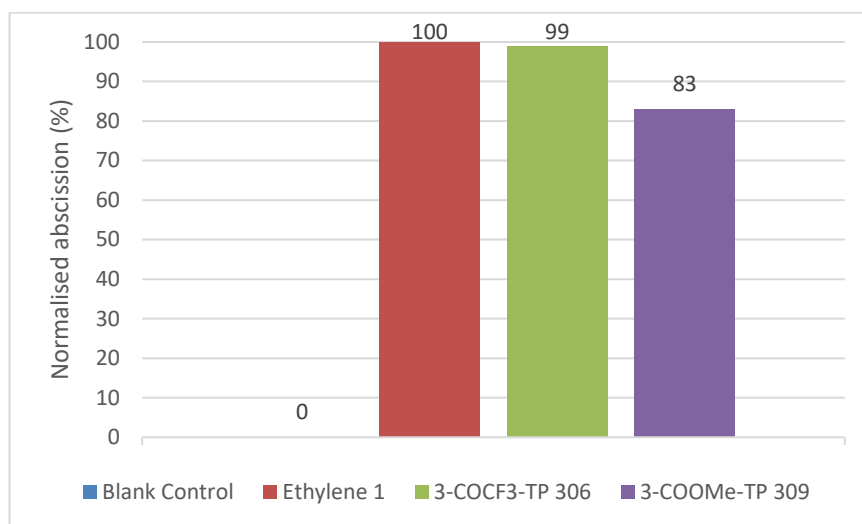
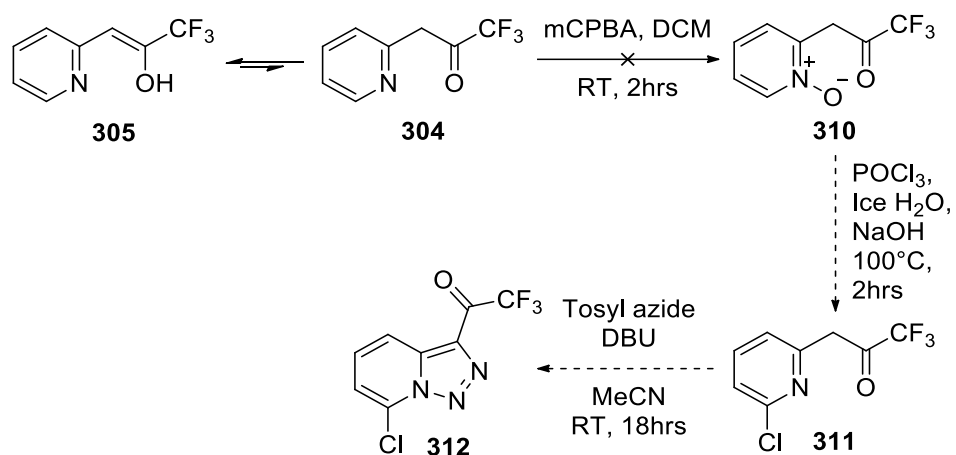


Figure 45 Geraldton wax flower abscission on treatment with 3-COCF<sub>3</sub>-[1,2,3]triazolo[1,5-*a*]pyridine **306** and 3-COOMe-[1,2,3]triazolo[1,5-*a*]pyridine **309** at 1M solution concentration

#### 4.5.2 Halogenation of EWG substituted triazolopyridines

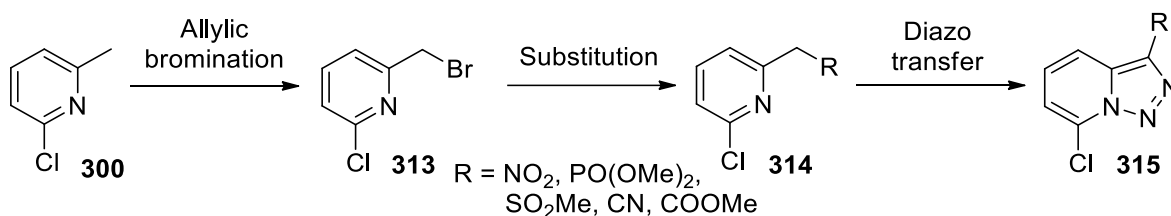
The introduction of a carbonyl at position 3 of triazolopyridines did not activate the diazo group, thus synthesis towards chlorinated derivatives was continued. The presence of a carbonyl functional group is not compatible with lithiation chemistry, thus a more classical approach to disubstituted triazolopyridines **312** was considered (Scheme 76). The reaction of pyridine *N*-oxides with POCl<sub>3</sub> is known to give 2-chloropyridines.<sup>309</sup> Synthesis of 1,1,1-trifluoro-(7-chloro-[1,2,3]triazolo[1,5-*a*]pyridin-3-yl)ethanone **312** by *N*-oxidation followed by deoxychlorination was attempted. When the trifluoropropanone **304** was reacted with *meta*-chloroperoxybenzoic acid in dichloromethane,<sup>305</sup> a complex mixture of side products was obtained after numerous attempts. The propensity of the ketone to enolize (it is effectively a masked 1,3-dicarbonyl compound **305**) is the likely cause of side reactions. When the same oxidation was attempted on the ester (a less reactive system), the expected *N*-oxide was not observed either, and a complex mixture of side products was present.



Scheme 76 Attempted synthesis pathway of 7-chloro-3-COCF<sub>3</sub>-[1,2,3]triazolo[1,5-a]pyridine derivative **312**

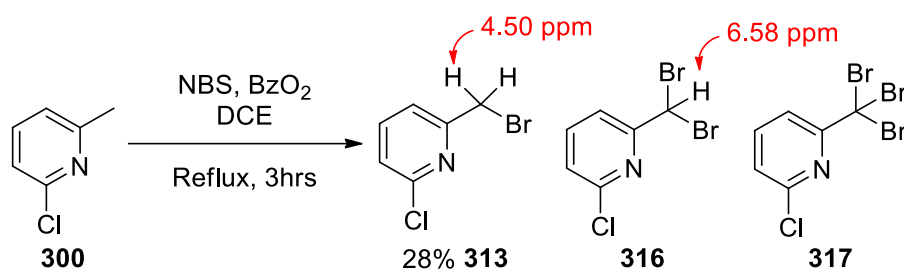
#### 4.5.3 EWG substitution of halogenated triazolopyridines

As the attempts at halogenation of the pyridine ring through an *N*-oxide were not successful, an approach using 2-chloro-6-methylpyridine **300** was considered (Scheme 77). A radical bromination would give the bromomethyl derivative **313**, which could then be substituted for a variety of electron withdrawing groups **314**. A diazo transfer reaction would then give the desired triazolopyridine analogues **315**.



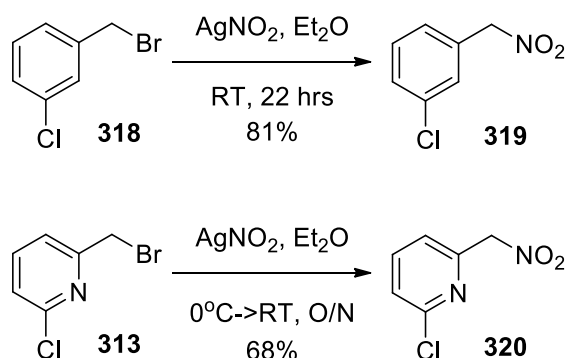
Scheme 77 Proposed synthesis pathway of disubstituted [1,2,3]triazolo[1,5-a]pyridine analogues **315**

2-Chloro-6-methylpyridine **300** was reacted with *N*-bromosuccinimide and benzoyl peroxide in dichloroethane as described by Ferjancic and Zard (Scheme 78).<sup>314</sup> The reaction mixture contained the expected product **313** along with starting material and over brominated products. A two-step purification was necessary to obtain the desired bromide **313**. The di and tri brominated compounds **316** and **317** were separated by flash chromatography, but the starting material co-eluted with bromide **313**. Fortunately, the expected product crystallised out from petroleum spirits at -20 °C, allowing for an easy and effective separation. The <sup>1</sup>H NMR spectrum had three aromatic signals at 7.66 (t), 7.38 (dd) and 7.26 (dd) ppm and a methylene singlet at 4.50 ppm. The spectrum matched the data of Jaafar et al.<sup>315</sup>



*Scheme 78 Synthesis of 2-(bromomethyl)-6-chloropyridine 313*

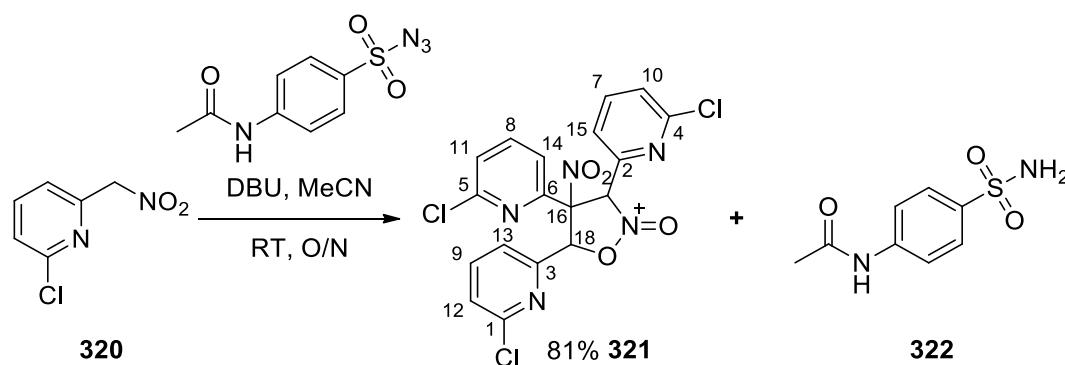
The nitrite anion can act as a nucleophile to give nitro groups. In a method developed for benzyl bromides **318**, silver nitrite was used as the source of  $\text{NO}_2^-$  (Scheme 79).<sup>316</sup> When the bromide **313** was reacted with  $\text{AgNO}_2$ , 2-chloro-6-(nitromethyl)pyridine **320** was obtained in good yield (Scheme 79). The  $^1\text{H}$  NMR spectrum of the purified nitromethyl **320** had a dd at 7.77 ppm and a two overlapping doublets at 7.42 ppm, indicating the disubstituted pyridine ring. The benzylic methylene was deshielded (5.59 ppm) compared to the starting material (4.50 ppm), indicating formation of the nitromethyl group. The presence of the nitro group was supported by absorbances at 1551 (N-O asym. Stretch) and 1371 (N-O symm. Stretch)  $\text{cm}^{-1}$  in the IR spectrum.



*Scheme 79 Synthesis of 1-chloro-3-(nitromethyl)benzene 319<sup>316</sup> and 2-chloro-6-(nitromethyl)pyridine 320*

When the diazo transfer reaction was attempted on the nitro derivative **320** using 4-acetamidobenzenesulfonyl azide (*p*-ABSA) and DBU in acetonitrile, the triazolopyridine was not formed. The reaction mixture contained an unknown product **321** and acetamidobenzenesulfonyl amine **322**. Acetamidobenzenesulfonyl amine **322** is the by-product of the diazo transfer reagent *p*-ABSA. When repeated the reaction produced the same products. The full information of the 2D NMR is given in the experimental but key correlations are given in Figure 47. The  $^{13}\text{C}$  NMR spectrum had 18 signals and  $^1\text{H}$  NMR spectrum had total of 11 signals (Figure 46); 2 singlets in 5.5-6.0 ppm region and 9 signals in aromatic region, out of which 3 were triplets and 6 were

doublets of doublets. The number of signals indicated a nonsymmetrical structure. Notably, while the proposed structure has 3 stereocenters, based on the NMR spectra only one product was identified, indicating high stereoselectivity of the reaction. The COSY spectrum shown 4 independent sections, suggesting presence of 3 pyridine rings connected by a three carbon bridge. The NMR spectra suggested a nitroisoxazolidinolate structure as the bridge, due to signal distribution on the  $^{13}\text{C}$  NMR spectrum (C16, C17 and C18). The HSQC and HMBC NMR spectra further corroborated the proposed bridge structure. The structure of this compound was tentatively proposed as 3,4,5-tris(6-chloropyridin-2-yl)-4-nitroisoxazolidin-2-olate **321** (Scheme 80). The lack of symmetry of the bridge indicated a substitution of at least one of the original nitro groups, which could be explained by formation of an isoxazolidinone.



*Scheme 80 Attempted synthesis of 7-chloro-3-nitro-[1,2,3]triazolo[1,5-a]pyridine 323*

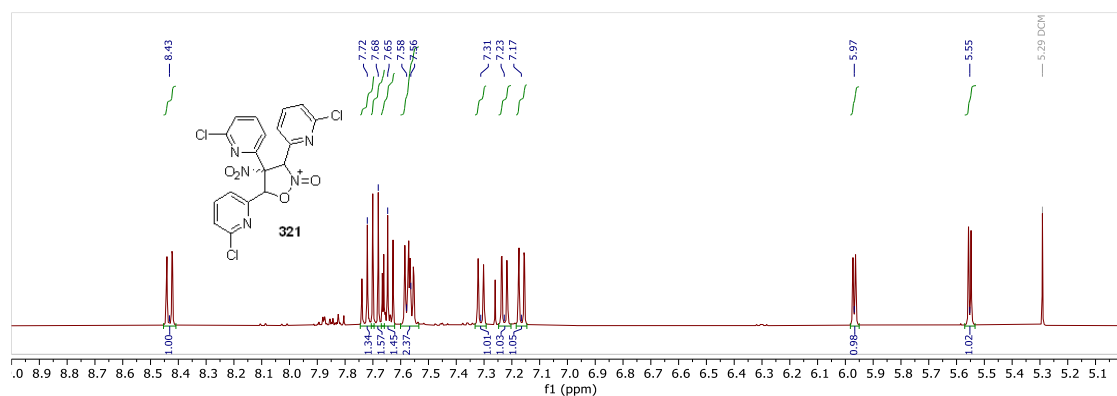


*Figure 46  $^1\text{H}$  NMR expanded spectrum of trimer 321*

The mechanism of formation of the trimer **321** from 2-chloro-6-(nitromethyl)pyridine **320** is proposed in Scheme 81. The nitrite **320** was deprotonated by DBU and the resulting nucleophile underwent an addition reaction to *p*-ABSA. By proton transfer, the sulfonamide was eliminated, forming the triazolopyridine **323**. The reactive triazolopyridine dimerizes to **325** then **327**, akin to a Michael addition reaction, followed by a substitution to form the nitroisoxazolidinolate **321**. While not identical, formation of isoxazolidinones from nitro groups have been reported in literature.<sup>317</sup> As the expected product **323** was not formed, an alternative triazolopyridine analogue was targeted.

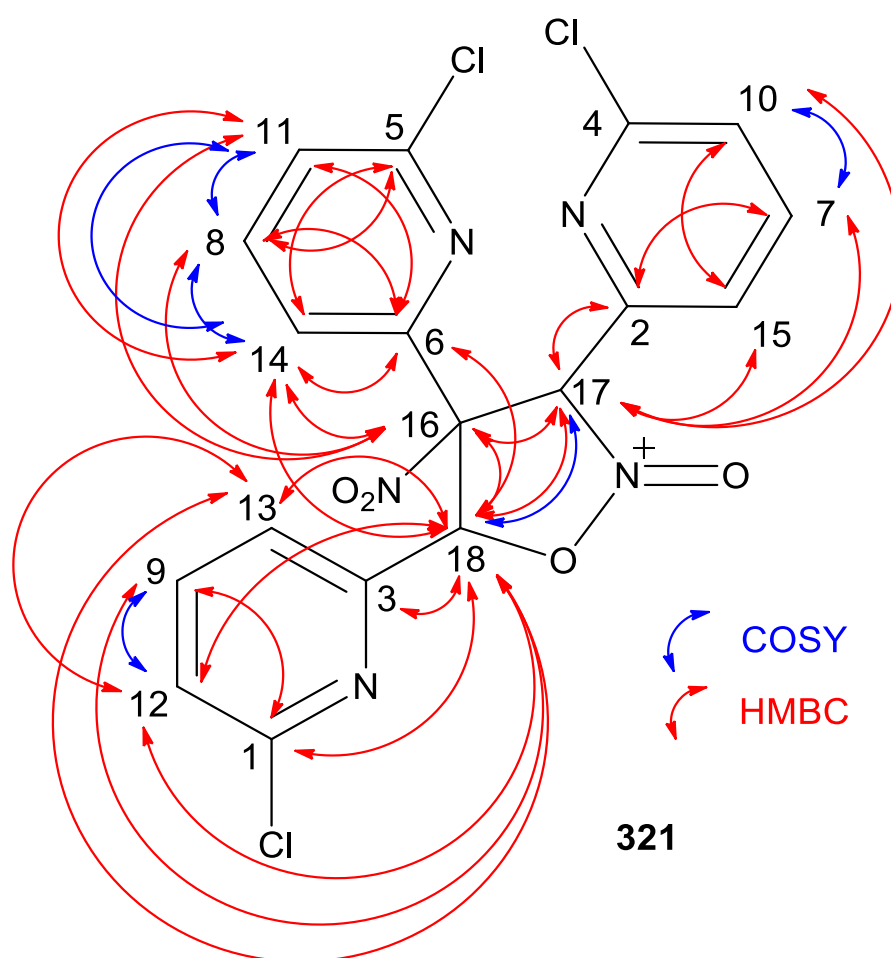
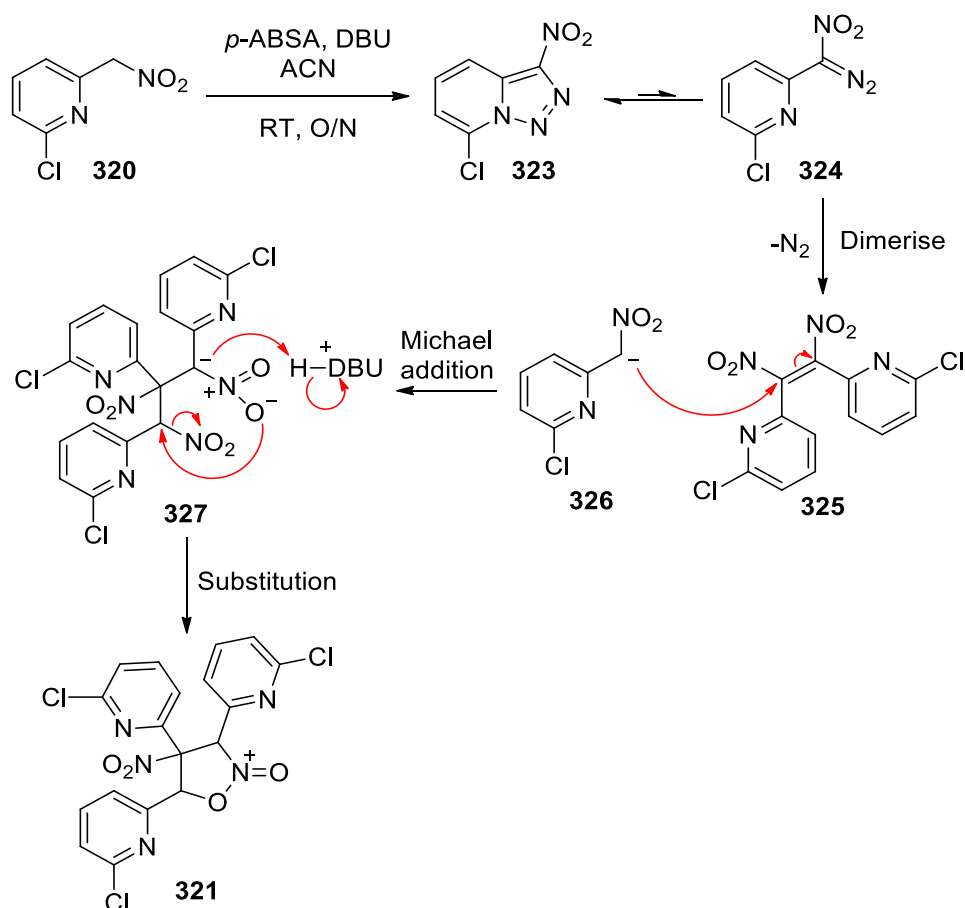
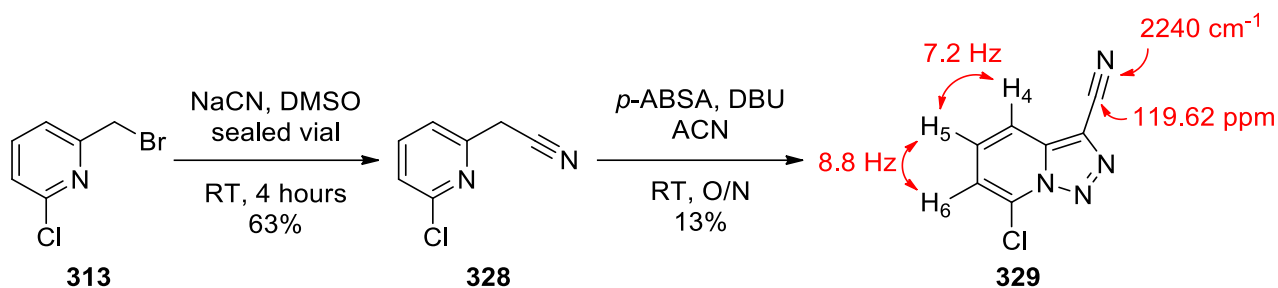


Figure 47 NMR analysis of proposed 3,4,5-tris(6-chloropyridin-2-yl)-4-nitroisoxazolidin-2-olate **321**



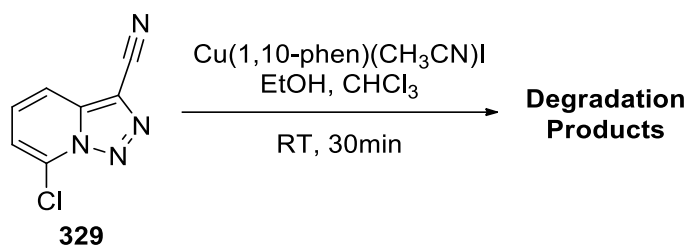
Scheme 81 Proposed mechanism of trimerization of 2-chloro-6-(nitromethyl)pyridine 320

In light of the problems associated with the nitro group, the synthesis of a nitrile derivative was investigated. Using a modified method of Altman et al.,<sup>318</sup> the bromide **313** was reacted with sodium cyanide in dimethylsulfoxide at room temperature for 4 hours to give the nitrile **328**.<sup>319</sup> The nitrile **328** was reacted under standard diazo transfer conditions, using *p*-ABSA and DBU (Scheme 82). The reaction was messy but contained 7-chloro-[1,2,3]triazolo[1,5-*a*]pyridine-3-carbonitrile **329** as the major product which was purified by titration as an unstable solid. The <sup>1</sup>H NMR spectrum of the triazolopyridine **329** had only three signals at 7.91, 7.63 and 7.33 ppm. <sup>13</sup>C NMR spectrum had 7 signals in the 130-100 region, which were characteristic of a triazolopyridine structure and a nitrile. The IR spectrum showed absorbance at 2240 (C≡N), supporting presence of the nitrile group.



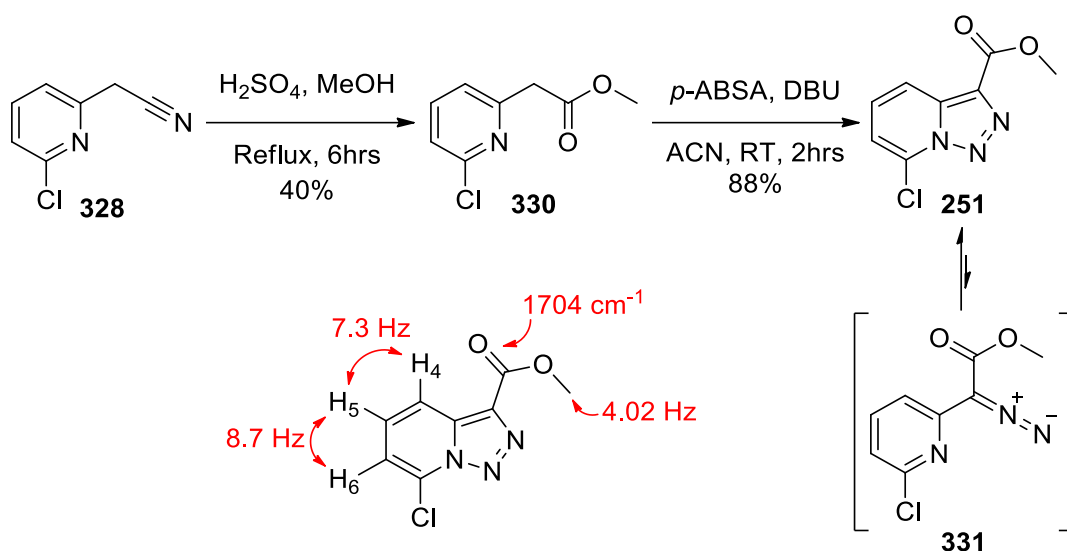
Scheme 82 Synthesis of (6-chloropyridin-2-yl)acetonitrile **328** and 7-chloro-[1,2,3]triazolo[1,5-*a*]pyridine-3-carbonitrile **329**

The nitrile **329** was reacted with Cu(1,10-phen)(CH<sub>3</sub>CN)I in ethanol (Scheme 83). The starting material was consumed entirely in 30 minutes (TLC). Due to limited starting material and complexity of the product mixture further analysis of the products was not undertaken. Affirming reactivity of the compound **329** with a copper(I) complex indicated its potential as an ethylene antagonist.



Scheme 83 Degradation of 7-chloro-[1,2,3]triazolo[1,5-*a*]pyridine-3-carbonitrile **329** in presence of copper(I) complex in ethanol

In an attempt to synthesise an ester analogue **251**, methanolysis of the nitrile **328** was attempted. The methanolysis was not attempted directly on the 7-chloro-[1,2,3]triazolo[1,5-*a*]pyridine-3-carbonitrile **329** due to its high reactivity, so the methanolysis was performed on the precursor **329**. Following method of Yoshimura et al.,<sup>320</sup> nitrile **328** was heated under reflux in methanol with sulfuric acid to yield the methyl 2-(6-chloropyridin-2-yl)acetate **330**.<sup>257</sup> When the ester **330** was subjected to diazo transfer conditions using *p*-ABSA and DBU, the reaction yielded pure methyl 7-chloro-[1,2,3]triazolo[1,5-*a*]pyridine-3-carboxylate **251** in good yield (Scheme 84). The <sup>1</sup>H NMR spectrum (Figure 48) matched the data of Chuprakov et al.<sup>257</sup> Broadening of the signals at 8.24 and 7.22 ppm as compared to the precursor compound and other triazolopyridine derivatives suggests a partial, yet not complete, shift in the equilibrium towards the open ring diazo compound **331**.



Scheme 84 Synthesis of methyl 2-(6-chloropyridin-2-yl)acetate **330** and methyl 7-chloro-[1,2,3]triazolo[1,5-a]pyridine-3-carboxylate **251**

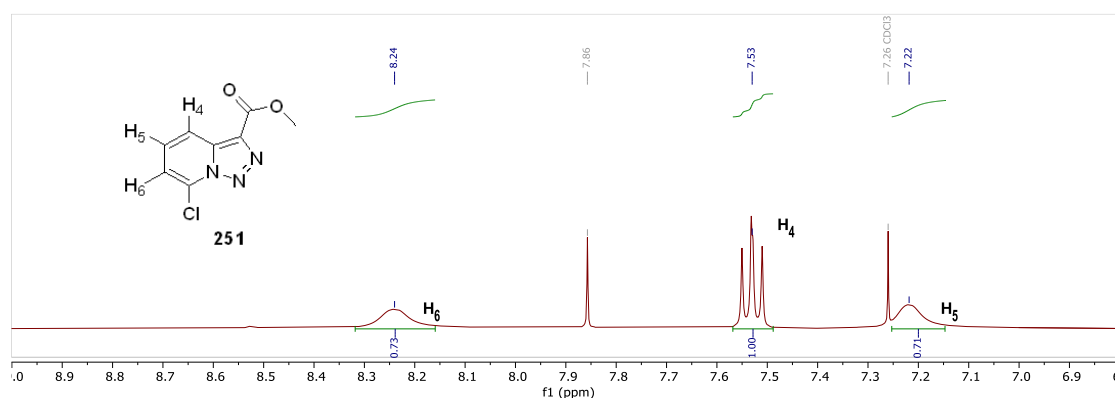
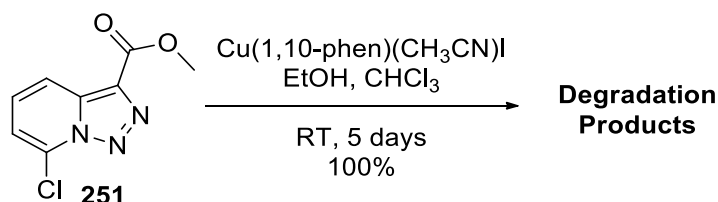


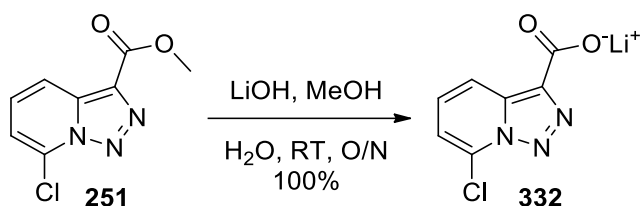
Figure 48  $^1\text{H}$  NMR expanded spectrum of 7-chloro-[1,2,3]triazolo[1,5-a]pyridine-3-carboxylate **251**

Methyl 7-chloro-[1,2,3]triazolo[1,5-a]pyridine-3-carboxylate **251** was reacted with  $\text{Cu}(1,10\text{-phen})(\text{CH}_3\text{CN})\text{I}$  in ethanol (Scheme 85). The starting material was consumed entirely in 5 days. Due to limited starting material and complexity of the product mixture further analysis of the products was not undertaken.



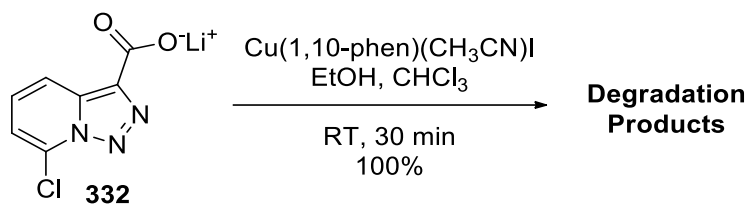
Scheme 85 Degradation of methyl 7-chloro-[1,2,3]triazolo[1,5-a]pyridine-3-carboxylate **251** in presence of copper(I) complex in ethanol

The formation of a carboxylate salt would give a more water soluble product. Due to acid sensitivity of the substituted triazolopyridine, a base promoted hydrolysis was attempted. When the methyl ester **251** was stirred with lithium hydroxide in methanol and water for 16 hours, pure lithium 7-chloro-[1,2,3]triazolo[1,5-*a*]pyridine-3-carboxylate **332** was obtained (Scheme 86).<sup>321</sup> The <sup>1</sup>H NMR spectrum of the carboxylate **332** in D<sub>2</sub>O was similar to that of the starting material except for the missing methyl singlet at 4.02 ppm. Minor shift of the signals was present due to different solvent.



*Scheme 86 Synthesis of lithium 7-chloro-[1,2,3]triazolo[1,5-*a*]pyridine-3-carboxylate **332***

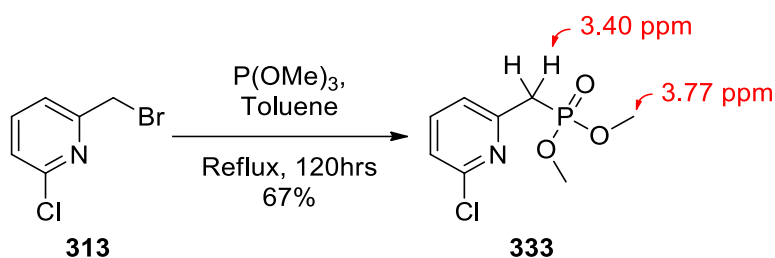
Lithium 7-chloro-[1,2,3]triazolo[1,5-*a*]pyridine-3-carboxylate **332** was reacted with Cu(1,10-phen)(CH<sub>3</sub>CN)I in ethanol (Scheme 87). The starting material was consumed entirely in 30 minutes to form a complex mixture of products. Reactivity of the compound **332** with a copper(I) complex indicated its potential as an ethylene antagonist.



*Scheme 87 Degradation of lithium 7-chloro-[1,2,3]triazolo[1,5-*a*]pyridine-3-carboxylate **332** in presence of copper(I) complex in ethanol*

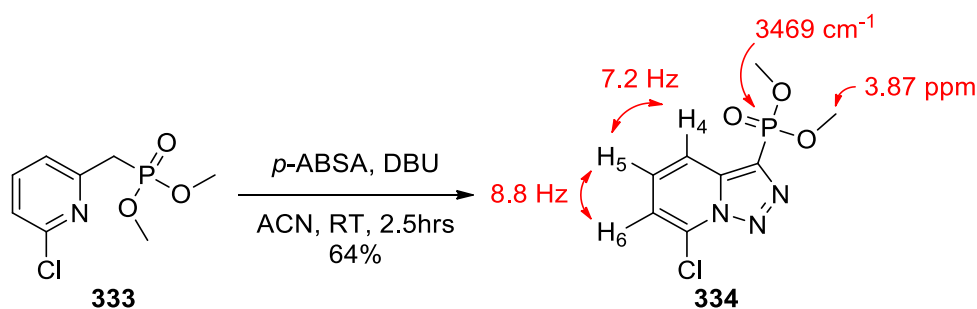
A synthesis of triazolopyridine phosphonate derivative **333** was also attempted using a modified method by Hinchliffe.<sup>322</sup> When the bromide **313** was heated under reflux with 0.95 equivalent of trimethyl phosphite in toluene for 120 hours, dimethyl (6-chloropyridin-2-yl)phosphonate **333** was obtained in a 1:1 mixture with the starting material (Scheme 88). The <sup>1</sup>H NMR spectrum of the purified product **333** had three signals in the aromatic region at 7.62 (dd), 7.32 (ddd) and 7.23 (ddd) ppm indicative of

the disubstituted pyridine ring. A 6H multiplet at 3.77 ppm was indicative of the two methyl phosphonate esters and a doublet centred at 3.40 ppm was indicative of the methylene coupling to the adjacent phosphorus atom. Splitting in the  $^{13}\text{C}$  NMR spectrum also was indicative of a phosphorous atom present in the structure. The presence of the phosphonate was further supported by absorbance at 3469 (broad, P-O), 1659 (C-O), 1437 (P=O), 1021 (P-O)  $\text{cm}^{-1}$  in the IR spectrum. The formula of the compound **333** ( $\text{C}_7\text{H}_{11}\text{PO}_3\text{Cl}$ ) was supported by HRMS (236.0231).



Scheme 88 Synthesis of dimethyl (6-chloropyridin-2-yl)phosphonate **333**

When the phosphonate **333** was treated with *p*-ABSA and DBU, a complex mixture containing dimethyl (7-chloro-[1,2,3]triazolo[1,5-*a*]pyridin-3-yl)phosphonate **334** as the major product was obtained (Scheme 89). The target compound was purified by titration as chromatography but led to significant degradation. The  $^1\text{H}$  NMR spectrum of the phosphonate **334** (Figure 49) had three signals at 8.20 (d), 7.45 (m) and 7.21 (d) ppm. The two singlets at 3.87 and 3.85 ppm were indicative of the phosphonate methyl esters.  $^{13}\text{C}$  NMR spectrum had 6 signals in the 140-110 region at 139.91 (C), 129.06 (CH), 128.36 (C), 117.54 (CH), 116.37 (CH) ppm, indicative of a triazolopyridine structure. A doublet centred at 53.70 ppm (2 x  $\text{CH}_3$ ) was indicative of the phosphonate methyl esters. The IR spectrum showed absorbance at 3469 (broad, P-O), 1625 (C-O), 1025 (P-O)  $\text{cm}^{-1}$ .



Scheme 89 Synthesis of dimethyl (7-chloro-[1,2,3]triazolo[1,5-*a*]pyridin-3-yl)phosphonate **334**

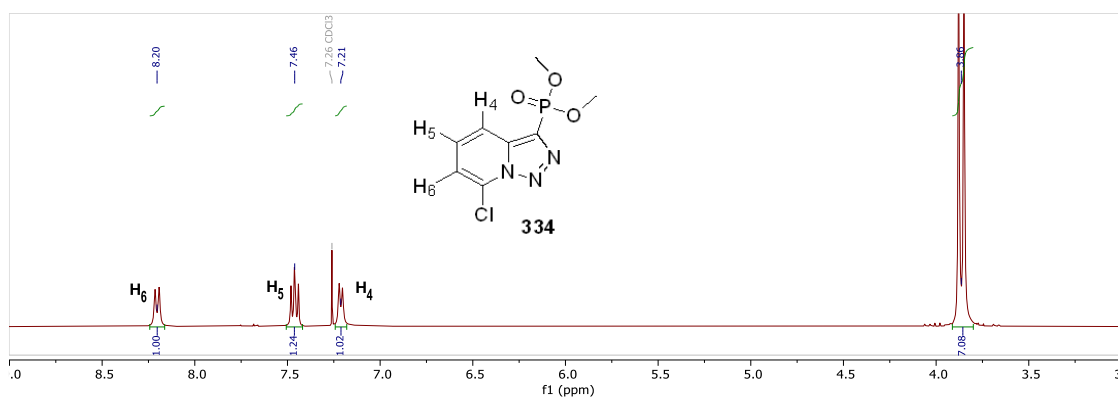
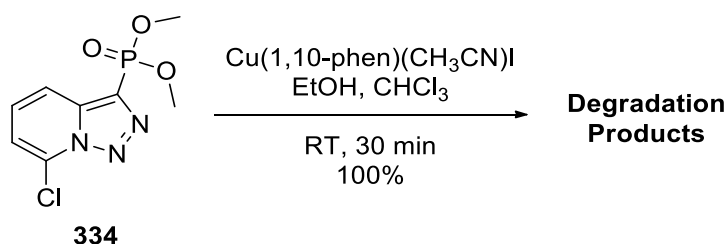


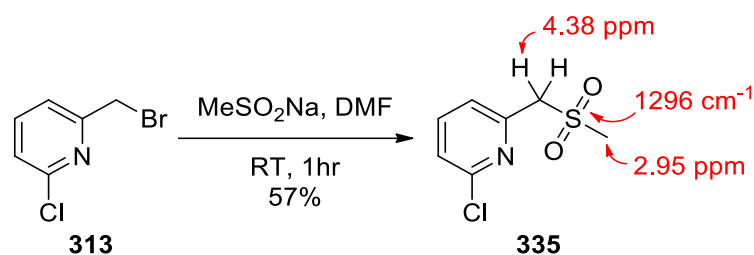
Figure 49  $^1\text{H}$  NMR expanded spectrum of dimethyl (7-chloro-[1,2,3]triazolo[1,5-*a*]pyridin-3-yl)phosphonate **334**

Dimethyl (7-chloro-[1,2,3]triazolo[1,5-*a*]pyridin-3-yl)phosphonate **334** was tested for degradation with  $\text{Cu}(1,10\text{-phen})(\text{CH}_3\text{CN})\text{I}$  in ethanol (Scheme 90). The starting material was consumed entirely in 30 minutes (TLC). Due to limited starting material and complexity of the product mixture further analysis of the products was not undertaken. Reactivity of the compound **334** with a copper(I) complex indicated its potential as an ethylene antagonist.



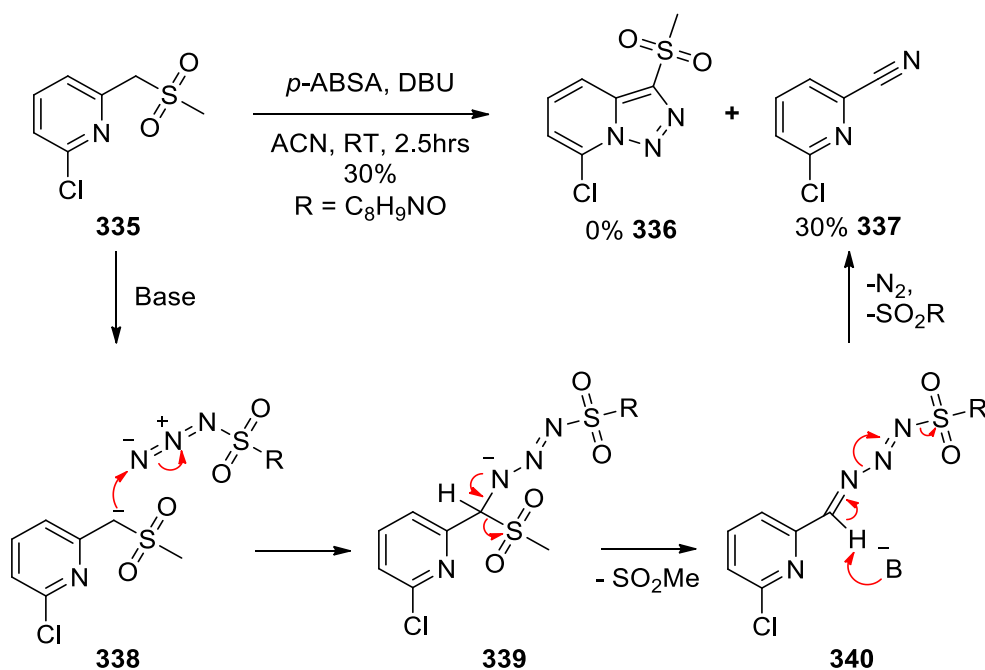
Scheme 90 Degradation of dimethyl (7-chloro-[1,2,3]triazolo[1,5-*a*]pyridin-3-yl)phosphonate **334**

Finally, the synthesis of 7-chloro-3-(methylsulfonyl)-[1,2,3]triazolo[1,5-*a*]pyridine **336** was attempted. A method by Tamayo et al. was followed.<sup>323</sup> The bromide **313** was stirred with sodium methanesulfinate in dimethylformamide to yield 2-chloro-6-((methylsulfonyl)methyl)pyridine **335** (Scheme 91). The  $^1\text{H}$  NMR spectrum of the purified product **335** had three aromatic hydrogens at 7.73 (dd), 7.63 (dd) and 7.43 (dd) ppm indicative of the disubstituted pyridine ring. The singlet at 4.38 ppm (2H) and a 3H singlet at 2.95 ppm were indicative of the methylsulfonyl group. The substitution was further supported by signals at 62.59 and 40.42 ppm in the  $^{13}\text{C}$  NMR spectrum, and the sulfone was supported in the IR spectrum with absorbance at 1296 (S=O) and 1115 (S=O)  $\text{cm}^{-1}$ . The molecular mass of the compound **335** was supported at 206.0034 by HRMS.

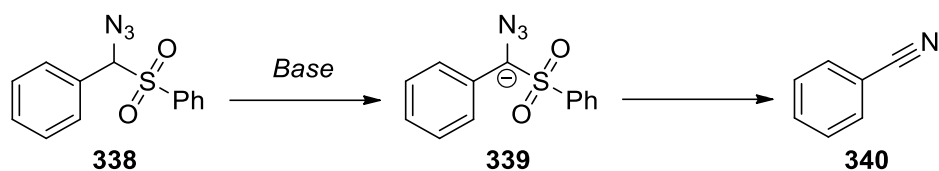


Scheme 91 Synthesis of 2-chloro-6-((methylsulfonyl)methyl)pyridine 335

Diazo transfer reaction was attempted on the methylsulfonylmethyl **335** using *p*-ABSA and DBU. The reaction yielded a complex mixture and unexpectedly 6-chloropicolinonitrile **337** as major product (Scheme 92). The <sup>1</sup>H NMR spectrum of the compound **337** had only three signals: 7.82 (dd), 7.65 (dd), 7.58 (dd) ppm and matched the data of Tsukamoto et al.<sup>324</sup> Mechanism of formation of 6-chloropicolinonitrile **337** from 2-chloro-6-((methylsulfonyl)methyl)pyridine **335** is proposed in Scheme 92. The sulfone **335** was deprotonated by DBU and the resulting nucleophile underwent an addition reaction to *p*-ABSA. Elimination of methyl sulfite gave the hydrazone, which upon the action of base eliminated nitrogen and the sulfonate, to give the nitrile **337**. Jarvis reported a similar transformation of  $\alpha$ -azido sulfones **338** into nitriles **340** under basic conditions at 55 °C (Scheme 93),<sup>325, 326</sup> however this room temperature transformation appears to be unique.



Scheme 92 Attempted synthesis of 7-chloro-3-(methylsulfonyl)-[1,2,3]triazolo[1,5-a]pyridine **336** and mechanism of 6-chloropicolinonitrile **337** formation



Scheme 93 Transformation of  $\alpha$ -azido sulfones **338** into nitriles **340** under basic conditions<sup>325, 326</sup>

The four halogenated triazolopyridine analogues **251**, **329**, **332** and **334** showed promising chemical reactivity and were tested in the Geraldton wax assay (See Chapter 3). Compounds **251** and **329** were fully dissolved in their respective 3% ethanol solutions, while compounds **332** and **334** were fully soluble in DI water. Two independent attempts were conducted for all four compounds (Figure 50 and Figure 51). For all four samples, no abscission of flowers or other toxic effects were observed upon pre-treatment of the compounds to Geraldton wax. The nitrile **329** and the ester **251** at 1M concentration showed reduction of abscission (average 31% and 40% respectively) greater than cyclopropene, as used in the preliminary model tests (Chapter 3). This suggests a significant antagonism against ethylene action for these two compounds. On the other hand, the free carboxylate **332** and the phosphonate **334** at 1M concentration were much less effective compared to the controls (average 81% and 68% respectively), suggesting lack of antagonism against ethylene action for these two compounds. As the nitrile **329** and methyl carboxylate **251** were tested at 0.1M concentration in two independent attempts to further assess their potency (Figure 51). The nitrile **329** shown abscission at 39% and 69%, indicating reduced potency in comparison to 1M concentration solution, yet still having a protective effect on flower abscission. The ester **251** similarly shown reduced potency at 41% and 73%, relatively similar in comparison to the nitrile **329**. This further suggests these two compounds possess significant antagonism against ethylene action.

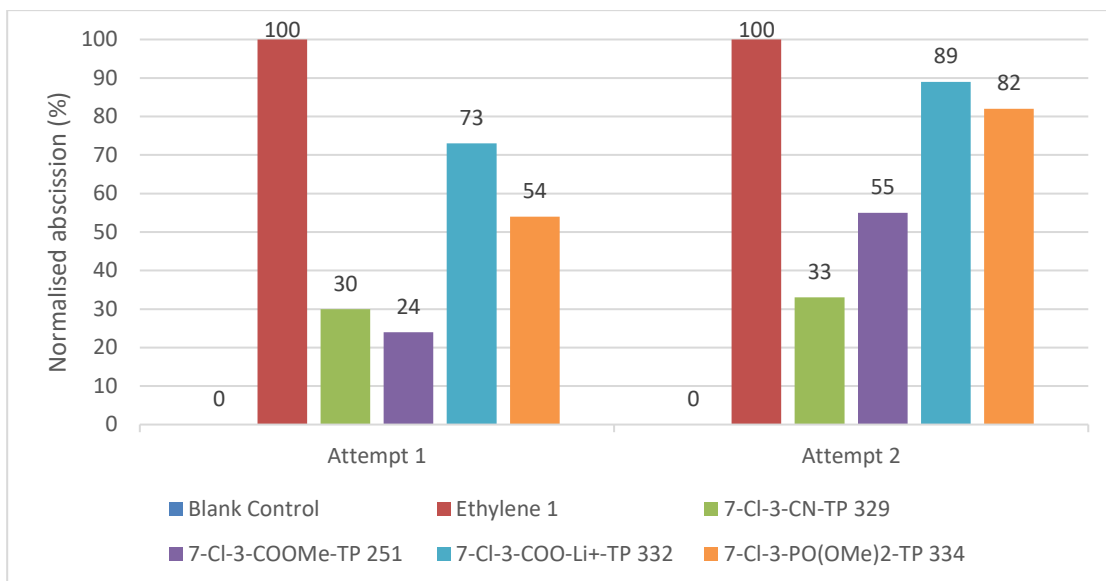


Figure 50 Geraldton wax flower abscission on treatment with 7-chloro-3-EWG-[1,2,3]triazolo[1,5-a]pyridines 251, 329, 332 and 334 at 1M solution concentration

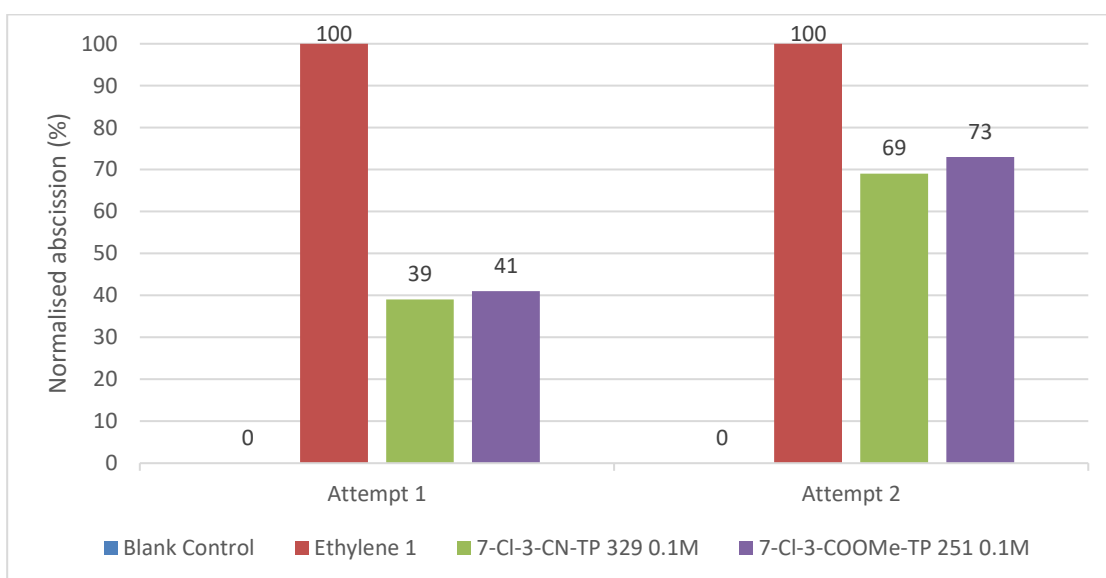


Figure 51 Geraldton wax flower abscission on treatment with 7-chloro-3-EWG-[1,2,3]triazolo[1,5-a]pyridines 251 and 329 at 0.1M solution concentration

## 4.6 [1,2,3]Triazolo[1,5]azines

Introduction of chlorine, as an electron withdrawing group, to position 7 of the triazolopyridine has shown activation of the diazo reactivity of the compound. In consideration of this functional group as an electronegative source causing decrease in basicity of the pyridine ring, an alternative ring structure was investigated. Nitrogen atoms are known to possess similar properties and their introduction into the aromatic ring significantly increases the  $\pi$ -deficiency of electrons and decreases basicity of the ring. Comparison of basicity of various nitrogen containing heterocycles **341-346** was shown below in Figure 52.

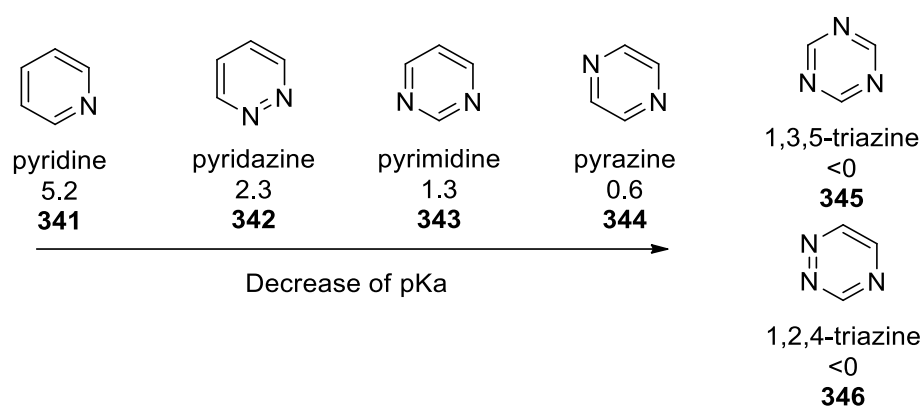


Figure 52 pKa values of various nitrogen containing heterocycles **341-346**

Based on the pKa values shown above, it can be hypothesised the reduction in resonance stabilisation caused by introduction of additional nitrogen atoms would weaken the N-N bond of the respective triazolopyridine analogues, thus shifting the equilibrium to the open ring form. Based on these findings, the [1,2,3]triazolo[1,5]azines **347** were envisioned as potential ethylene antagonists. The pyridine, pyrimidine and pyrazine analogues of [1,2,3]triazolo[1,5]azine were synthesised in the past, as shown by Maury et al.<sup>327</sup> The analysis of these compounds has shown each of them favours the closed ring form under standard conditions (Figure 53), what indicates masking of the diazo group. It can be hypothesised they exhibit decreased explosive and toxic properties in comparison to compounds with a free diazo group.

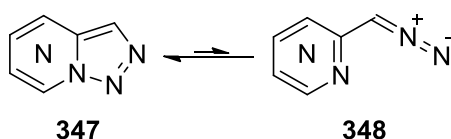
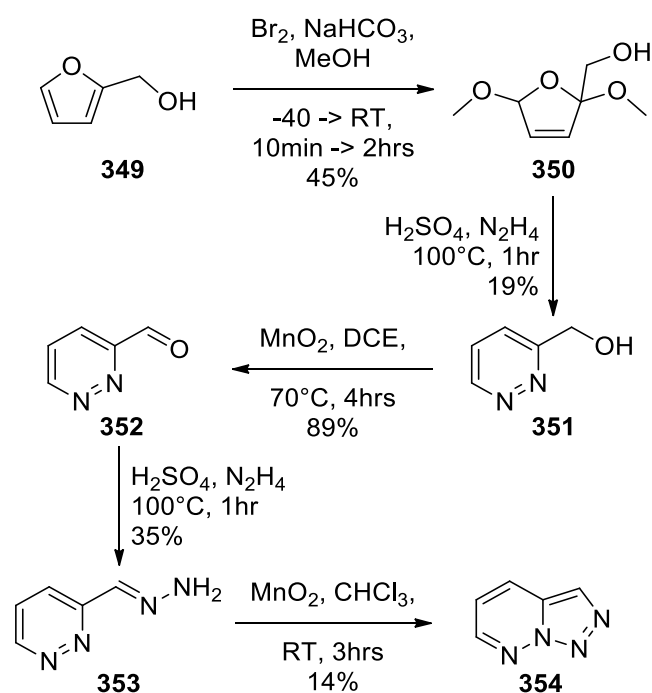


Figure 53 Proposed equilibrium of the [1,2,3]triazolo[1,5-a]azines **347**

#### 4.6.1 [1,2,3]Triazolo[1,5-*b*]pyridazine

As the first target of the 1,2,3-triazolo[1,5]azines, a five step synthesis of [1,2,3]triazolo[1,5-*b*]pyridazine **354** was attempted (Scheme 94), based on methods of Hammoud et al.,<sup>328</sup> Tsukamoto et al.<sup>329</sup> and Maury et al.<sup>327</sup> Furfuryl alcohol **349** was used as the starting material and was oxidised with bromine, sodium bicarbonate in methanol to form (2,5-dimethoxy-2,5-dihydrofuran-2-yl)methanol **350**. The compound **350** underwent condensation reaction with hydrazine and sulfuric acid to yield pyridazin-3-ylmethanol **351**. The compound **351** was oxidised with manganese dioxide in dichloroethane to yield pyridazine-3-carbaldehyde **352**. A second condensation with hydrazine with sulfuric acid gave (*E*)-3-(hydrazonomethyl)pyridazine **353** which was oxidised with manganese dioxide in chloroform to yield pure [1,2,3]triazolo[1,5-*b*]pyridazine **354**. The NMR spectra (Figure 54) matched the data of Hammoud et al.,<sup>328</sup> Tsukamoto et al.<sup>329</sup> and Maury et al.<sup>327</sup>



Scheme 94 Synthesis pathway of [1,2,3]triazolo[1,5-*b*]pyridazine **354**

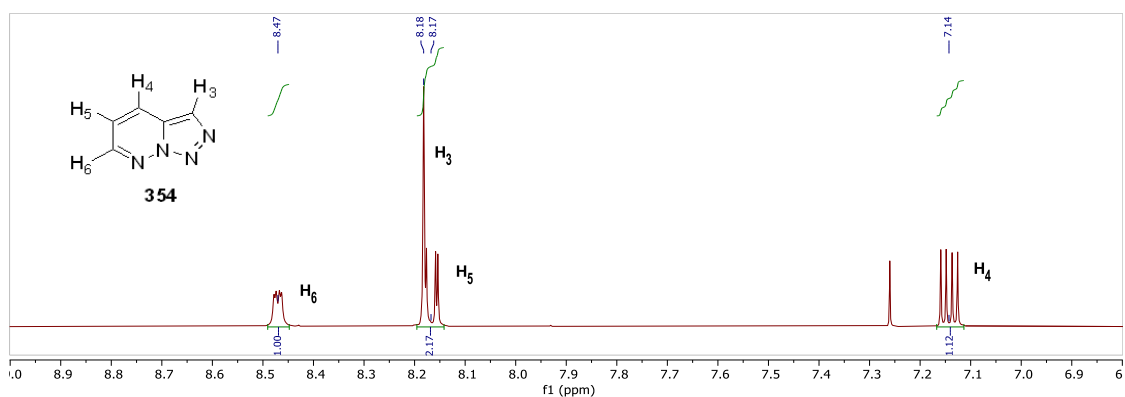
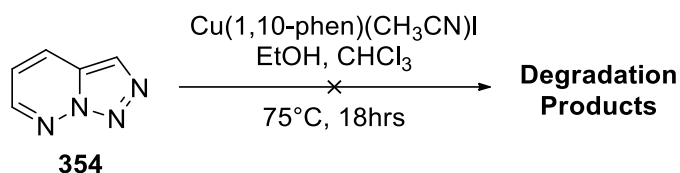


Figure 54  $^1\text{H}$  NMR expanded spectrum of [1,2,3]triazolo[1,5-*b*]pyridazine **354**

[1,2,3]Triazolo[1,5-*b*]pyridazine **354** was reacted with  $\text{Cu}(1,10\text{-phen})(\text{CH}_3\text{CN})\text{I}$  in ethanol (Scheme 95), however only the starting material was recovered, suggesting lack of significant antagonism against ethylene action. [1,2,3]Triazolo[1,5-*b*]pyridazine **354** was also tested in the *in vivo* assay. The pyridazine **354** was fully dissolved in 3% ethanol and used at 1M as the stock solutions. No abscission of flowers or other toxic effects were observed on introductions of the compound to Geraldton wax. No reduction in flower abscission was observed for the tested compound **354**, suggesting lack of significant antagonism against ethylene action (Figure 55). The chemical reactivity and the *in vivo* results were consistent.



Scheme 95 Degradation of [1,2,3]triazolo[1,5-*b*]pyridazine **354**

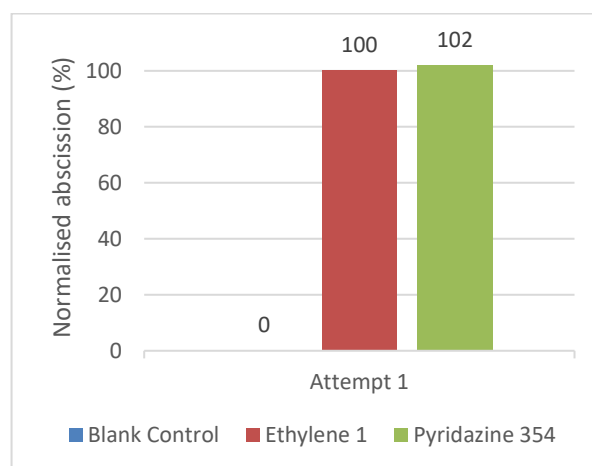


Figure 55 Geraldton wax flower abscission on treatment with [1,2,3]triazolo[1,5-*b*]pyridazine **354** at 1M solution concentration

## 4.7 Summary of Cu(I) reactivity and *in vivo* results

Unlike ethyl diazoacetate, no senescence or flower/bud abscission was caused purely by the tested triazolopyridines, indicating lack of toxicity towards plants. Clear trends were observed between the Cu(I) reactivity tests and Geraldton wax assays of the triazolopyridine analogues (Table 11). If the compounds were stable in the presence of a Cu(I) source, no antagonism was observed. Thus, copper(I) complex reactivity was shown to be an effective method for a preliminary determination of potential ethylene antagonists. Likewise, the simple in-house Geraldton wax assay has shown potential as a preliminary confirmation of ethylene antagonistic properties. These methods presented are a quick and simple in-house method of screening compounds for potential and allow chemists to find new antagonists of ethylene action. The results obtained, show some interesting conclusions. The introduction of a halogen at position 7 enabled reactivity of the compounds with copper(I) complex. The 5-nitro analogue **284** as well as pyridazine analogue **354** were found unreactive, indicating insufficient effect of the EWG introduced into the pyridine ring on the equilibrium of the parent structure. While the 7-chloro and 7-bromo analogues **264** and **263** were found to be very reactive, they have shown no reduction in ethylene action on Geraldton wax. Their ineffectiveness may be explained by their instability and high reactivity, and would decompose prior to reaching the ethylene receptors. Further functionalisation of 7-halo analogues with an EWG at position 3 was found to stabilise the compound while retaining its reactivity. The three synthesised 7-halo-3-EWG analogues **251**, **329**, **332** and **334** were found to react with copper(I) complexes as well as shown inhibition of ethylene action in Geraldton wax assays.



Figure 56 [1,2,3]Triazolo[1,5-*a*]pyridine derivatives

Table 11 Summary of the copper reactivity model tests and Geraldton wax in-house assays on triazolopyridine analogues

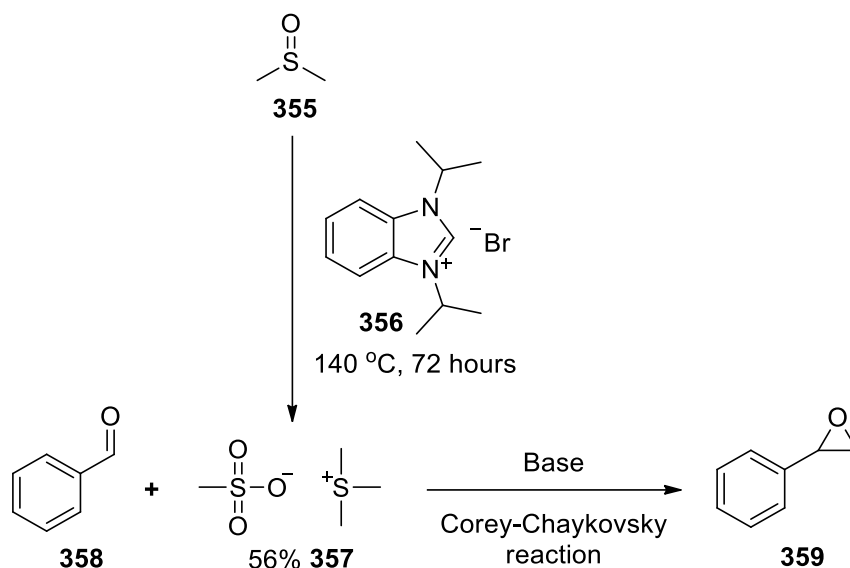
| No. | R<br>Position 7 | R'<br>Position 5 | R''<br>Position 3                  | Cu(I)<br>complex<br>reactivity | Inhibition<br>concentration<br>(mmol/L) |
|-----|-----------------|------------------|------------------------------------|--------------------------------|---|
| 233 | H               | H                | H                                  | ✗                              | ✗                                       |
| 278 | H               | H                | Me                                 | ✗                              | ✗                                       |
| 309 | H               | H                | COOMe                              | ✗                              | ✗                                       |
| 306 | H               | H                | COCF <sub>3</sub>                  | ✗                              | ✗                                       |
| 284 | H               | NO <sub>2</sub>  | H                                  | ✗                              | ✗                                       |
| 354 | N*              | H                | H                                  | ✗                              | ✗                                       |
| 263 | Br              | H                | H                                  | ✓                              | ✗                                       |
| 264 | Cl              | H                | H                                  | ✓                              | ✗                                       |
| 332 | Cl              | H                | COO·Li <sup>+</sup>                | ✓                              | ✗                                       |
| 334 | Cl              | H                | PO(OCH <sub>3</sub> ) <sub>2</sub> | ✓                              | 1                                       |
| 251 | Cl              | H                | COOMe                              | ✓                              | 0.1                                     |
| 329 | Cl              | H                | CN                                 | ✓                              | 0.1                                     |

\*Refers to [1,2,3]Triazolo[1,5-*a*]pyridazine 354

## Chapter 5 – Degradation of DMSO catalysed by benzimidazolium salts

### 5.1 Preface

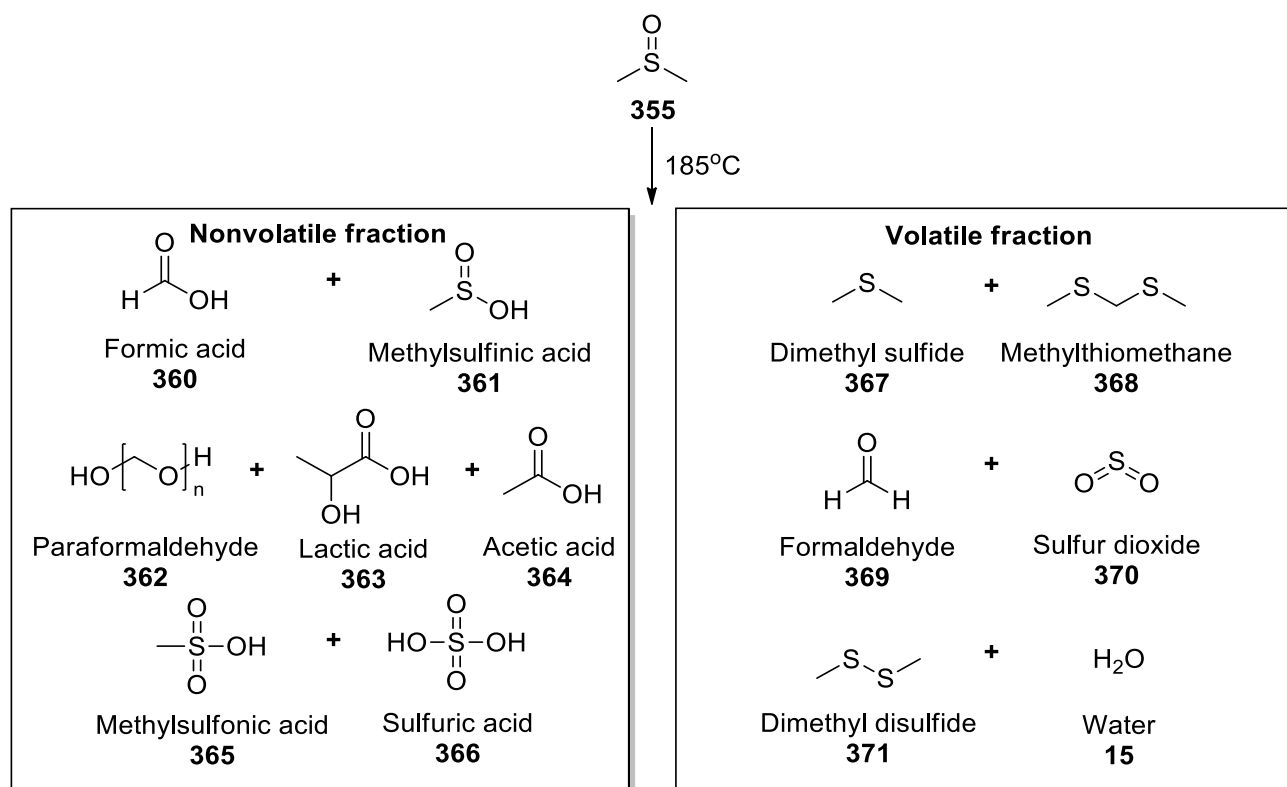
An internal internship at Curtin University gave the opportunity to work on a different project under guidance of Prof. Mark Ogden and Dr. Alan Payne. This project looked at the chemistry of the decomposition products of dimethyl sulfoxide **355** (DMSO) and initially started from an observation by Dr. David Brown in 2006, which was expanded by Chris Sealey (3<sup>rd</sup> year project) and Dr. Guy Travis as part of his PhD. The project was never fully completed, and this internship aimed to provide a closure to these studies. The project focused on the degradation of DMSO **355** catalysed by 1,3-diisopropylbenzimidazolium bromide **356**, forming trimethylsulfonium methanesulfonate (TMSMS) **357** (Scheme 96). This product is equivalent to trimethylsulfonium iodide, a reagent used in the Corey-Chaykovsky epoxidation reaction.<sup>330</sup>



Scheme 96 Epoxidation of benzaldehyde **358** with TMSMS **357**

## 5.2 Stability of DMSO

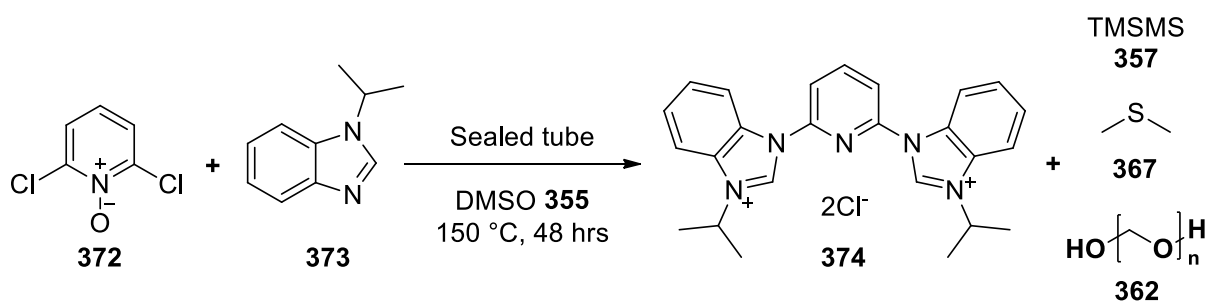
Dimethyl sulfoxide **355** (DMSO) is a polar aprotic solvent, commonly used for its ability to dissolve both polar and nonpolar compounds. It has a relatively high boiling point of 189 °C at atmospheric pressure and low toxicity. It is commonly used in substitution reactions requiring high temperature. DMSO **355** is considered safe and stable at room conditions, however there are reports that it degrades near its boiling point, as well as at lower temperatures when catalysed with oxidants, acids, halogens and other.<sup>331-333</sup> Recently, the decomposition of DMSO **355** was studied in presence of acids.<sup>333,334</sup> Several accidents were reported due to the excessive heating of DMSO **355**, commonly due to cooling failures.<sup>335-337</sup> DMSO **355** was shown to decompose when heated to near its boiling point with a long induction period (as little as 3.7% decomposition after 3 days of heating at reflux),<sup>338</sup> followed by a exothermic, rapid increase in decomposition rate, characteristic for autocatalysed decomposition reactions. The study found pure DMSO **355** undergoes this reaction even below its boiling point, at 185 °C, reaching a turning point at approximately 150 hours. IC and GC-MS analysis of the volatile and non-volatile fractions after DMSO **355** decomposition revealed a range of hydrocarbon and organosulfur compounds, including various methylated sulfides, acids as well as water, formaldehyde and paraformaldehyde (Scheme 97).



*Scheme 97 Various products of the autocatalysed degradation of pure DMSO **355**, by Deguchi<sup>333, 334</sup>*

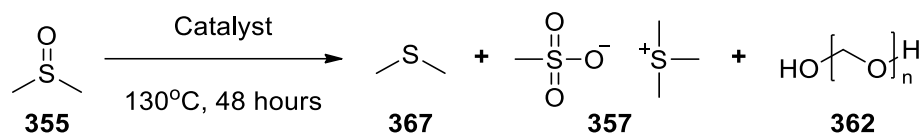
### 5.3 Catalytic degradation

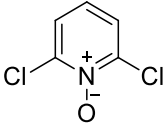
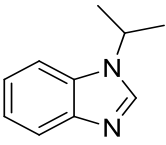
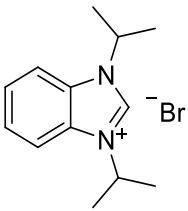
A side study by then PhD graduate, Dr. Guy Travers in 2015,<sup>339</sup> focused on analysis of the unknown degradation product of DMSO **355**, formed during preparation of an alkylated pincer compound **374** observed by Sealy and Brown in 2011 (Scheme 98).<sup>340</sup> On heating of dichloropyridine oxide **372** and isopropylbenzimidazole **373** in DMSO **355** in a sealed tube at 150 °C, degradation of DMSO **355** was observed. On cooling, the reaction mixture separated into two layers. The lower layer began boiling upon opening of the sealed tube and was identified as dimethyl sulphide **367** (Bp 37 °C). Dissolution of the remaining residue in diethylether, precipitated unknown white crystals. These crystals were characterised by IR, NMR and X-ray and identified as TMSMS **357**.



*Scheme 98 Attempted synthesis of alkylated pincer compound **374**, by Sealy and Brown<sup>340</sup>*

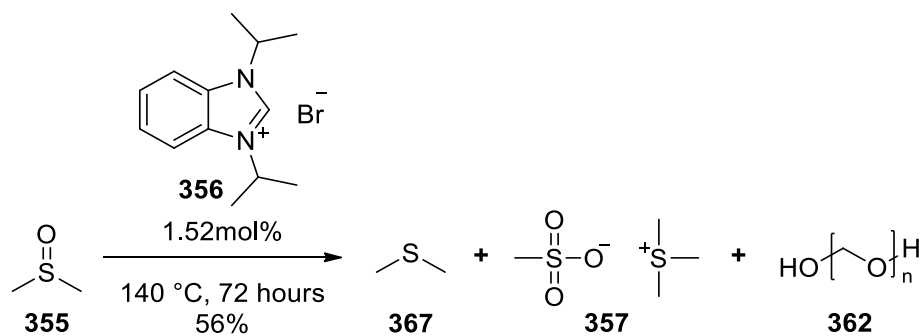
To determine the cause of this degradation of DMSO **355**, a series of control experiments were performed. Heating pure DMSO **355** at 140 °C over 3 days did not form the salt **357** in the product mixture (Scheme 99), so it was proposed the degradation was catalysed by one of the components of the reaction mixture in Scheme 98. When DMSO **355** was heated individually with the starting materials **372** or **373**, the decomposition of DMSO **355** was not observed. This suggested that the degradation was catalysed by the product of the reaction, the diimidazolium salt **374**. Due to limited availability of the product **374**, it was substituted for diisopropylbenzimidazolium bromide **356**, as it contained benzimidazolium salt moiety. Heating of DMSO **355** with compound **356** showed the formation of dimethyl sulphide **367** bubbles suggesting the diimidazolium salt **356** was the catalyst of DMSO degradation.



| Entry | Catalyst   | Result                       |
|-------|--|------------------------------|
| 1     | None   | No reaction observed.        |
| 2     | <br><b>372</b>  | No reaction observed.        |
| 3     | <br><b>373</b>  | No reaction observed.        |
| 4     | <br><b>356</b> | Bubbling in reaction vessel. |

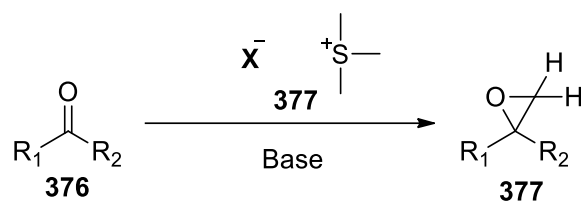
Scheme 99 Degradation of DMSO **355** catalysed by 1,3-diisopropylbenzimidazolium bromide **356**, by Travers<sup>339</sup>

The reaction with benzimidazolium bromide salt **356** was repeated under the same conditions shown in Scheme 98 i.e. 130 °C for 72 hours in a sealed vial. Work up of the reaction mixture with ethanol and diethyl ether gave the trimethylsulfonium salt **357** as white precipitate, confirming the benzimidazolium salts could degrade DMSO **355** to form TMSMS **357** (Scheme 100). The reaction was repeated with a condenser instead of a sealed vessel for safety reasons and gave comparable yields.



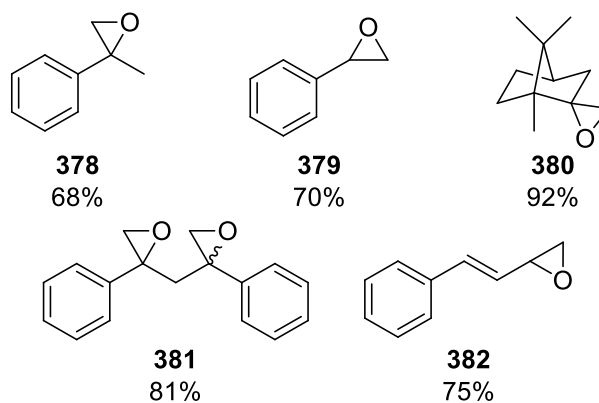
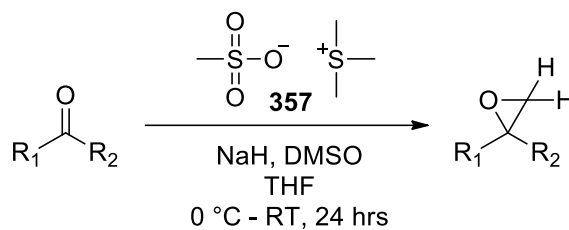
Scheme 100 Degradation of DMSO **355** catalysed by 1,3-Diisopropylbenzimidazolium bromide **356**, by Travers<sup>339</sup>





X = Br, Cl, I, BF<sub>4</sub>, TsO, HOSO<sub>3</sub>, CH<sub>3</sub>OSO<sub>3</sub>, CH<sub>3</sub>SO<sub>3</sub>

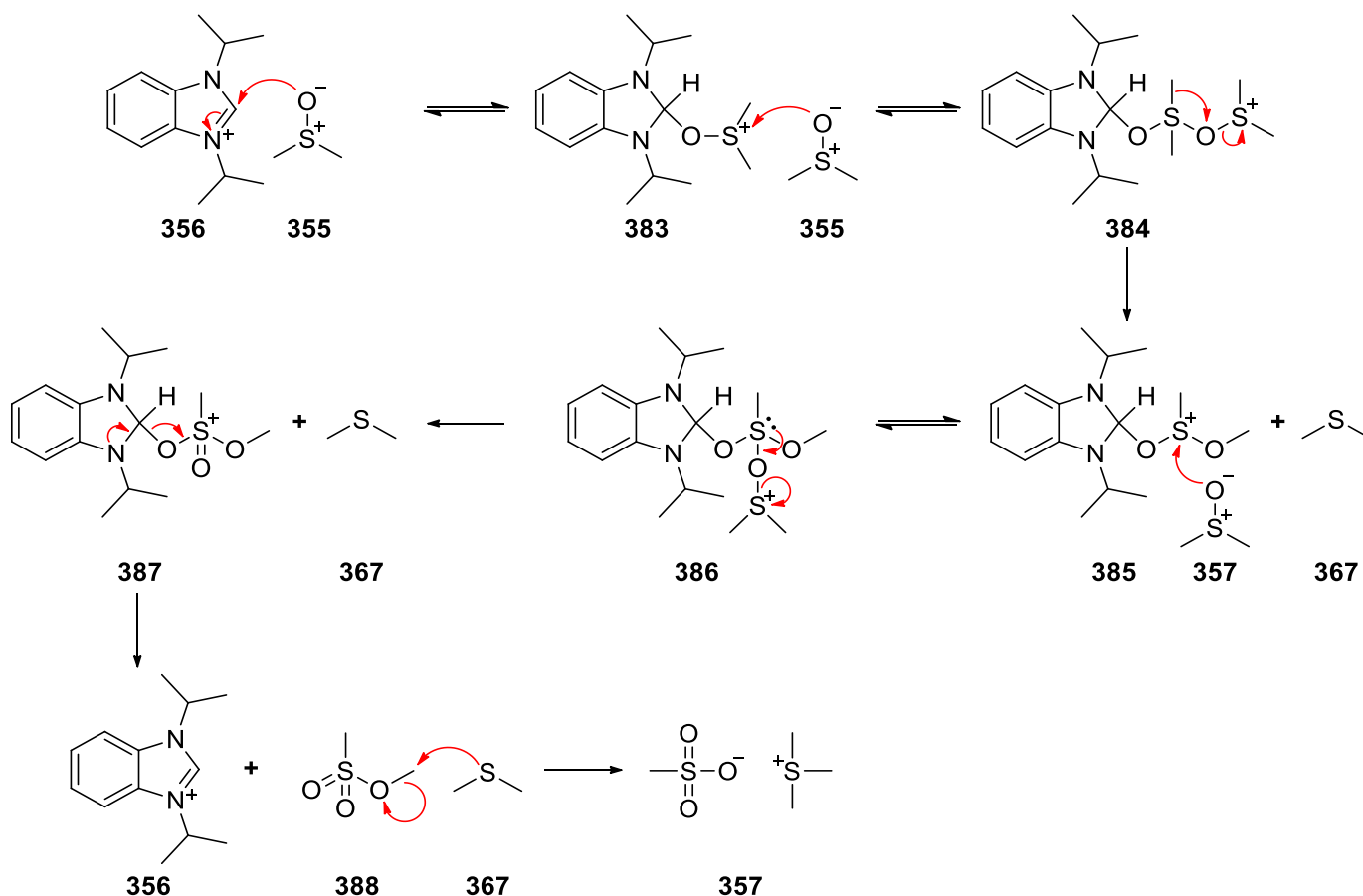
Scheme 104 Epoxidation with trimethylsulfonium cation<sup>339, 341, 348-355, 358</sup>



Scheme 105 Scope of epoxidation reaction with TMSMS 357, by Travers<sup>339</sup>

The efficiency and applicability of various trimethylsulfonium salts is comparable as reagents, however their synthesis has to be also considered in review of their usefulness. Trimethylsulfonium iodide, one of the most common of these salts, is synthesised from dimethyl sulphide **367**, a noxious low boiling liquid and methyl iodide, a known carcinogen.<sup>359</sup> Trimethylsulfonium methylsulfate, another commonly used salt, is synthesised from a highly toxic dimethyl sulfate and dimethyl sulphide **367**.<sup>360</sup> In comparison, trimethylsulfonium methanesulfonate **357** was shown to be catalytically synthesised from easily available and relatively safe to handle and use DMSO **355**.<sup>339</sup>

Based on the available information, an organocatalytic degradation of DMSO **355** to TMSMS **357** was proposed (Scheme 106).<sup>339</sup> In this mechanism, the benzimidazolium salt **356** acts as a Lewis acid to promote the disproportionation of DMSO **355** to dimethyl sulphide **367** (2x) and methyl methane sulfonate **388**, which forms TMSMS **357** through a substitution reaction. As dimethylsulfide **367** is essential for the reaction to proceed, the reaction required efficient cooling or a sealed system for it to be retained in the reaction.

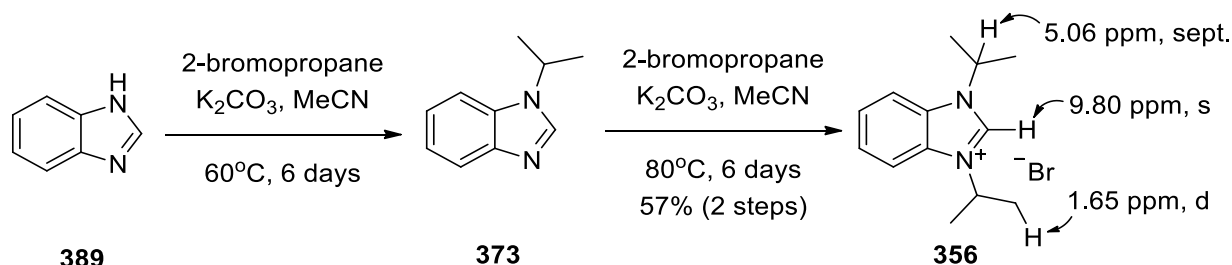


Scheme 106 Proposed mechanism of degradation of DMSO **355**, by Travers<sup>339</sup>

The aim of this study was to investigate the scope of catalysts yielding TMSMS **357** to further probe the mechanism of this reaction. A variety of compounds were chosen to further investigate the degradation mechanism, including a number of common ionic liquids. Ionic liquids are also considered as stable and inert solvents, while similarly to DMSO **355**, evidence of possible decomposition and reactivity was studied in recent years.<sup>361</sup> There is significant interest in the synthesis of deuterated compounds, particularly drugs,<sup>362-364</sup> so it was conceived a degradation of deuterated DMSO **405** should yield a unique deuterated TMSMS **406**, which could be used in preparation of deuterated epoxides, a simple (and cheap) entry into deuterated compounds.

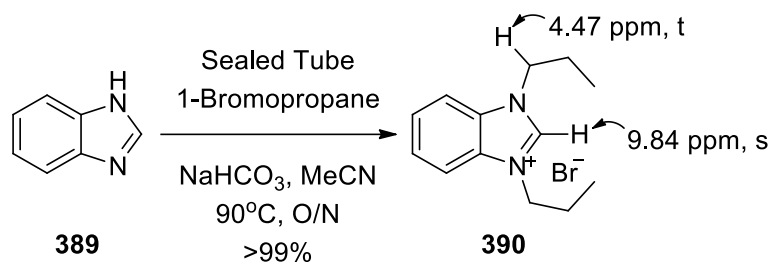
### 5.3.1 Preparation of benzimidazolium salts

Two salts were prepared, based on the procedure of Starikova et al.,<sup>365</sup> using benzimidazole **389** to synthesise 1,3-diisopropyl-1*H*-benzo[*d*]imidazol-3-ium bromide **356**. The starting material was heated with 2-bromopropane and potassium carbonate in acetonitrile for 6 days at 60 °C (Scheme 107). Accumulation of solid residue on the walls of the flask was noted. After workup, the <sup>1</sup>H NMR analysis of the product unexpectedly had signals matching the intermediate product 1-isopropyl-1*H*-benzo[*d*]imidazole **373** instead of the target product. It was theorised the white residue was the intermediate product **373** which due to accumulation and thus significant decrease of the reactive surface area did not react further to the target product **356**. The isolated intermediate **373** was resubjected to the reaction conditions at 80 °C, however in this attempt the white solid was scraped off multiple times every day. The reaction yielded the expected product **356** in good yield (Scheme 107). The <sup>1</sup>H NMR spectrum had a 1H singlet at 9.80 ppm indicative of the aromatic benzimidazolium hydrogen between the nitrogens, two 2H multiplets at 8.15 and 7.70 ppm of the ortho disubstituted benzene ring, and 2H septet at 5.06 ppm as well as a 12H doublet at 1.65 ppm, indicative of the two isopropyl groups.



Scheme 107 Synthesis of 1,3-diisopropyl-1*H*-benzo[*d*]imidazol-3-ium bromide **356**

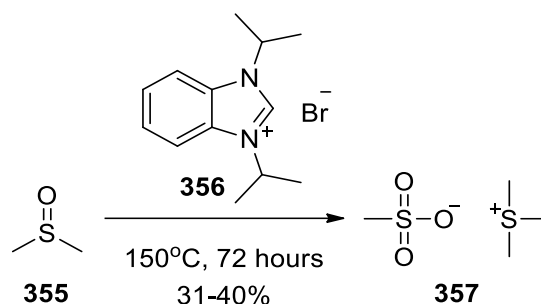
Synthesis of the 1,3-dipropyl-1*H*-benzo[*d*]imidazol-3-ium bromide **390** followed procedure of Starikova et al., using benzimidazole **389**, 1-bromopropane and sodium bicarbonate in acetonitrile in a sealed tube heated at 90 °C overnight (Scheme 108).<sup>366</sup> The reaction yielded the expected product **390** in a 99% yield. The <sup>1</sup>H NMR spectrum had a 1H singlet at 9.84 ppm, and two 2H doublets of doublets at 8.11 and 7.69 ppm, indicative of the benzimidazolium species. The 4H triplet at 4.47 ppm, a 4H multiplet at 1.94 ppm and a 6H triplet at 0.94 ppm were indicative of the propyl groups. Both salts were used in the degradation of DMSO reactions alongside a variety of common ionic liquids.



*Scheme 108 Synthesis of 1,3-dipropyl-1H-benzo[d]imidazol-3-ium bromide 390*

### 5.3.2 Catalysed degradation of DMSO

A procedure of DMSO degradation with benzimidazolium salts by Travers was followed.<sup>339</sup> In the initial attempt, DMSO **355** with a catalytic amount of 1,3-diisopropyl-1H-benzo[d]imidazol-3-ium bromide **356** (1.25 mol%) was heated at 130 °C for 72 hours, however no major change was observed and majority of DMSO **355** was recovered. The reaction was repeated at 150 °C and bubbling was observed after an induction period of 24 hours, indicating change in the reaction composition and start of formation of dimethyl sulphide **367** in the reaction mixture (Scheme 109). To minimise loss by evaporation, a double walled condenser was used, with a calcium chloride drying tube to allow gas exchange while ensuring dry conditions. The bubbling stopped after approximately 72 hours, indicating loss of dimethyl sulphide **367**. The reaction mixture turned black, white solid begun to accumulate on the walls of the condenser (identified as paraformaldehyde **362**) and a significant decrease in liquid volume was observed. Addition of ether followed by filtration gave trimethylsulfonium methanesulfonate **357** in good yield (32%) and purity. The <sup>1</sup>H NMR spectrum had two singlets at 2.86 and 2.41 ppm in a 3:1 ratio. The <sup>13</sup>C NMR spectrum had two singlets at 38.5 (overlap with DMSO signals) and 26.15 ppm. The reaction was repeated with a tenth of the catalyst load (0.125 mol%) and consistently yielded the expected product in similar yields (32% and 40%). This lower catalyst loading was considered the optimum conditions for this reaction.

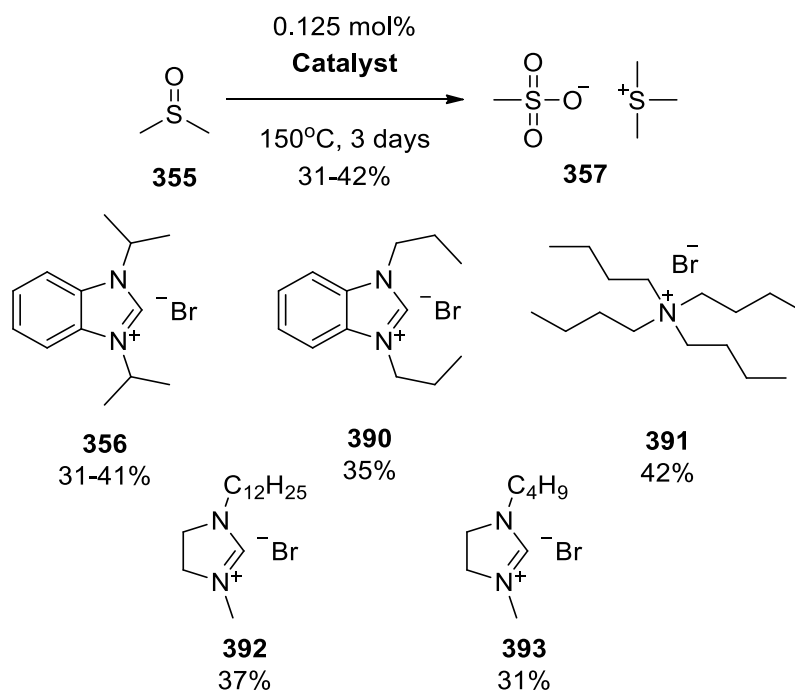


| Catalyst amount (mol%) | Additives     | Yield of TMSMS (%) |
|------------------------|---------------|--------------------|
| 0                      | -             | 0                  |
| 1.25                   | -             | 31                 |
| 0.125                  | -             | 32-40              |
| 0.125                  | TEA 1 mol%    | 8                  |
| 0.125                  | BHT 0.03 mol% | 7                  |

*Scheme 109 Degradation of DMSO **355** catalysed by 1,3-diisopropylbenzimidazolium bromide **356***

To probe the reaction, the optimum conditions were repeated with an addition of 1 mol% of triethylamine (TEA), to remove potential acid sources. A delay in the onset of the reaction was observed and after 72 hours yielded TMSMS **357** in an only 8% yield. The reaction was also repeated with an addition of 0.03 mol% of butylated hydroxytoluene (BHT), a free radical scavenger. Again, the reaction also shown a delay in the reaction onset and decreased yield (7%). TEA and BHT delayed the reaction onset, however did not prevent it completely. Based on these findings, it can be concluded the catalytic degradation of DMSO **355** with 1,3-diisopropylbenzimidazolium bromide **356** might involve an acid catalyst and have a radical component.

A series of other salts including common ionic liquids were reacted with DMSO **355** in search of potential trends in an attempt to determine a potential reaction mechanism. Five bromide salts **356** and **390-393** were effective catalysts for the conversion of DMSO **355** to TMSMS **357** in good yields (31-42%) (Scheme 110). Interestingly, tetrabutylammonium bromide **391** also catalysed the reaction which discounts the previously proposed, organocatalyst mechanism. The mechanism involved addition to the benzimidazole cation, however tetrabutylammonium cation cannot undergo such an addition.

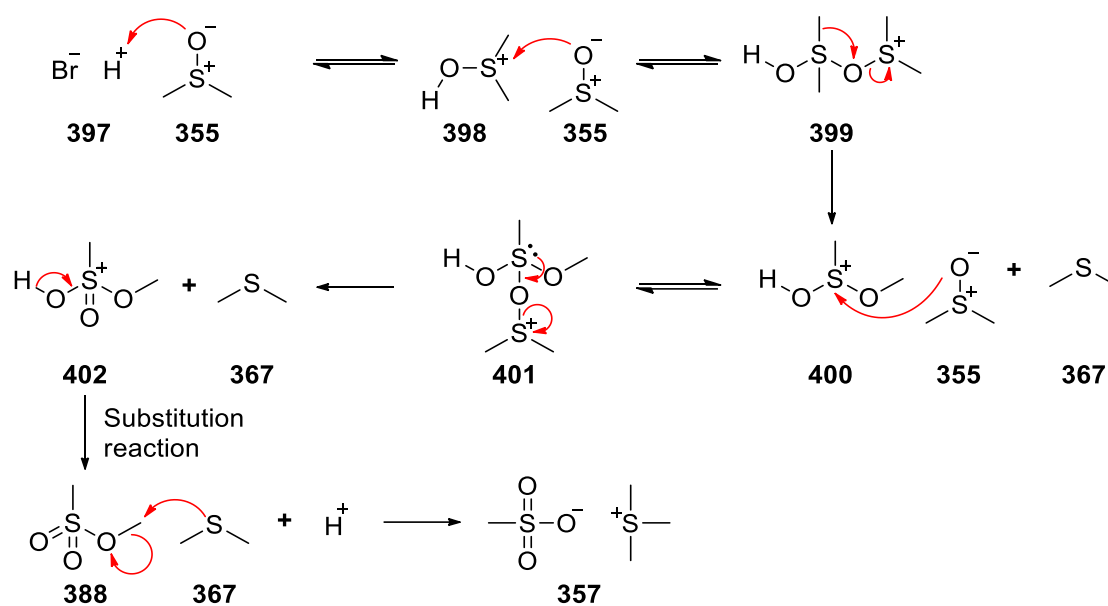


*Scheme 110 Degradation of DMSO 355 catalysed by bromic ionic liquids*

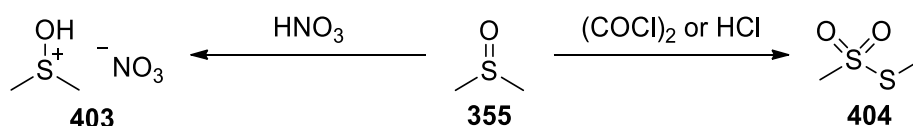
The comparable yield for both benzimidazolium and tetrabutylammonium salts was unexpected. All the salts tested had a common bromide counteranion, thus salts with alternative anions were tested as catalysts for degradation of DMSO **355**. Acetate **394**, tetrafluoroborate **395** or hexafluorophosphate **396** salts were chosen for the next series of experiments. Acetate as its conjugate acid, acetic acid, is a significantly weaker acid than hydrogen bromide. PF<sub>6</sub> and BF<sub>4</sub> counteranions are known to be more stable than halides in ionic liquids.<sup>367-369</sup> Ionic liquids may undergo thermal mass loss by ionic liquid vaporization and vaporization of the liquid phase thermal decomposition products. Ionic liquids with PF<sub>6</sub> and BF<sub>4</sub> counteranions show thermal decomposition and vaporization only under more severe conditions than their halide counterparts. Acetate, tetrafluoroborate or hexafluorophosphate salts of the compounds used in Scheme 110 were added to DMSO **355** under the same reaction conditions, but these reactions resulted in negligible amounts of TMSMS **357** formed (<1%) (Scheme 111).



Based on these findings, the proposed mechanism by Travers<sup>339</sup> was altered to involve HBr **397** (Scheme 113). The first step is the decomposition of the bromide salt to produce a small amount of HBr **397**. This degradation is very minor as the salt can be recovered from the reaction mixture. The small amount of HBr **397** produced then catalyses the disproportionation reaction. HBr **397** adds to DMSO **355** to produce hydroxydimethylsulfonium bromide **398** (Scheme 114). Formation of compounds **403** and **404** was previously proposed in a number of other DMSO degradation papers, in presence of nitric acid, HCl or phosgene, however the mechanisms are not fully known (Scheme 115).<sup>370-373</sup> Then hydroxydimethylsulfonium bromide **398** undergoes two redox reactions with 2 molecules of DMSO **355** to give methyl methanesulfonate **388** and two molecules of dimethyl sulphide **367**. Methyl methanesulfonate **388** is a methylating reagent and reacts with the produced dimethyl sulfide **367** to give the salt, a reaction known to occur quickly even at ambient conditions.<sup>330</sup>



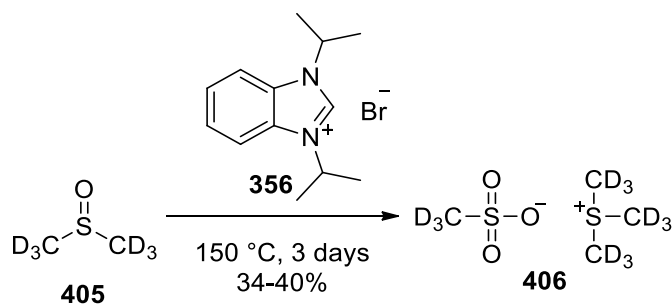
Scheme 114 Proposed mechanism of degradation of DMSO **355** by hydrobromic acid **397**



Scheme 115 Degradation of DMSO **355** catalysed by nitric acid,<sup>371</sup> phosgene or hydrochloric acid<sup>370</sup>

### 5.3.3 Deuterated DMSO

The degradation of DMSO **355** provides a valuable reagent in a synthesis significantly more user-friendly than the formation of other trimethylsulfonium salts. This reaction could be applied to deuterated DMSO **405** to make deuterated TMSMS **406**. This compound could be used to make deuterated epoxides. Degradation of  $d_6$ -DMSO **405** was attempted, following the procedure developed in this chapter, using 0.125 mol% of 1,3-diisopropyl-1*H*-benzo[*d*]imidazol-3-ium bromide **356** at 150 °C over 72 hours (Scheme 116). The reaction proceeded similarly to protio DMSO **355**, with evolution of gas, change of colour and decrease in volume. The reaction yielded comparable amounts (34 - 40%) of  $d_{12}$ -TMSMS **406**. Since  $d_{12}$ -TMSMS **406** is a fully deuterated compound, it was more complicated to analyse by spectroscopic methods. The  $^1\text{H}$  NMR spectrum shown no signals. The  $^2\text{H}$  NMR spectrum displayed two singlets at 2.86 and 2.33 ppm in a 3:1 ratio (Figure 57). The  $^{13}\text{C}$  NMR spectrum had two septets at 37.82 and 25.77 ppm, a splitting pattern characteristic for deuterated methyl groups (Figure 58). Repeated NMR analysis of the same sample did not show substitution of the deuterium with hydrogen atoms over time e.g. from solvent or moisture, indicating a stable product. This reaction has shown an easy and convenient access to deuterated TMSMS **406**, with minute impurities and minimal workup necessary.



Scheme 116 Degradation of  $d_6$ -DMSO **405** catalysed by 1,3-diisopropylbenzimidazolium bromide **406**

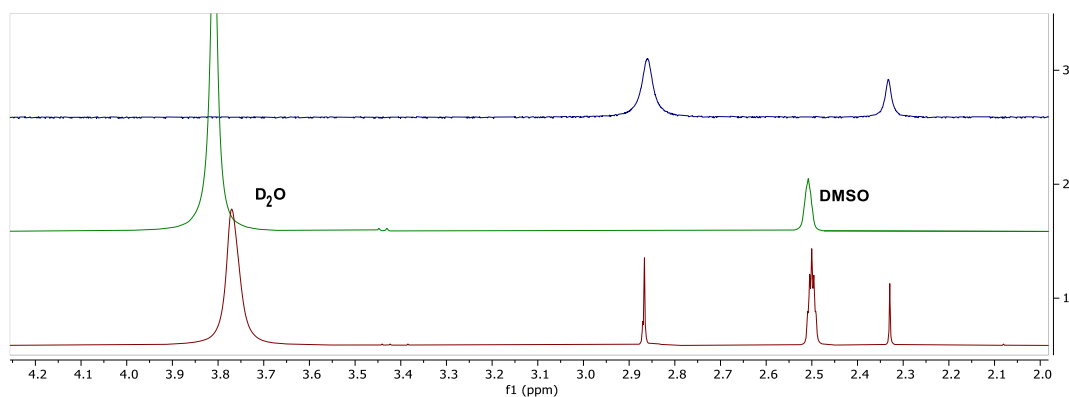


Figure 57 Comparison between spectra  $^2\text{H}$  NMR of  $d_{12}$ -TMSMS **406** (top),  $^1\text{H}$  NMR of  $d_{12}$ -TMSMS **406** (middle) and  $^1\text{H}$  NMR of TMSMS **357**

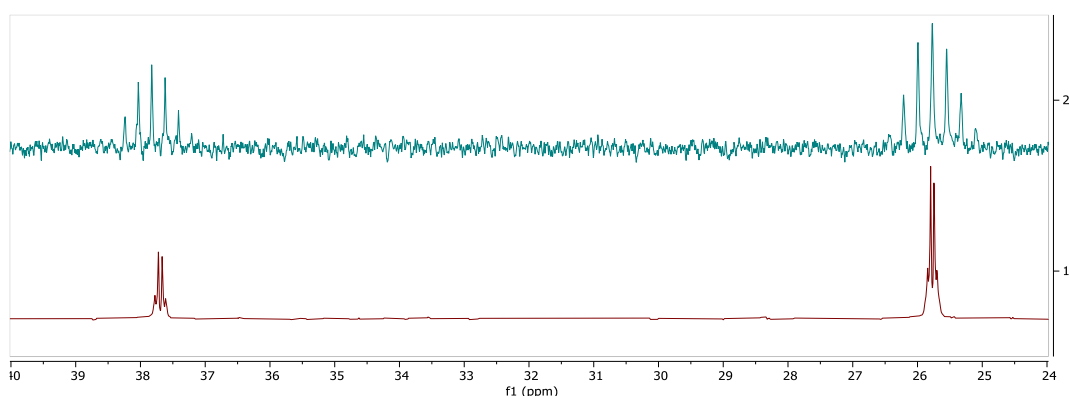
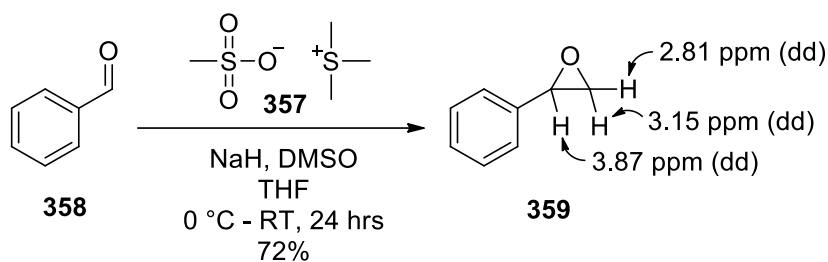


Figure 58 Comparison between  $^{13}\text{C}$  NMR spectra of  $d_{12}$ -TMSMS **406** (top) and TMSMS **357** (bottom) in  $\text{D}_2\text{O}$

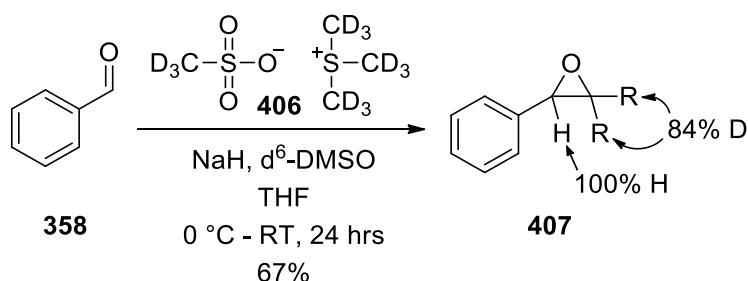
### 5.3.4 Epoxidation reactions with TMSMS and $d_{12}$ -TMSMS

Salts of the trimethylsulphonium cation, including TMSMS **357**, are well known epoxidation agents, effective for a wide range of aldehydes and ketones at mild conditions.<sup>330,339</sup> A procedure for epoxidation of benzaldehyde **358** was followed, using both TMSMS **357** and  $d_{12}$ -TMSMS **406**, in an attempt to obtain protio and deuterio epoxides. Benzaldehyde **358** was added to a solution of TMSMS and sodium hydride in DMSO and THF (Scheme 117). The epoxidation occurs by reaction between an aldehyde and dimethylsulfonylmethylide i.e. a trimethylsulphonium cation deprotonated by a strong base. The protio reaction yielded phenyloxirane **359** in good yield (72%). The  $^1\text{H}$  NMR spectrum had signals at 2.80 (dd, 1H), 3.14 (dd, 1H) and 3.86 (dd, 1H) characteristic of an unsubstituted epoxide as well as a multiple overlapping signals in the aromatic region 7.40 – 7.27 ppm indicative of the benzene ring.

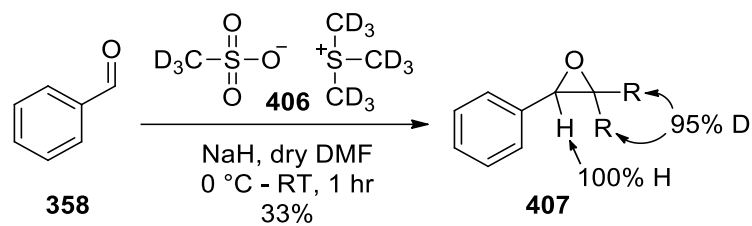


*Scheme 117 Epoxidation of benzaldehyde 358 with TMSMS 357*

The deuterio reaction was performed under the same conditions, using  $d_{12}$ -TMSMS **406** in deuterated DMSO **405**. Unexpectedly, the reaction yielded a mixture of deuterated **407** and protonated **359** product in a 84:16 ratio (Scheme 118). The epoxidation reaction was repeated in a different solvent system to ensure anhydrous conditions.<sup>374</sup>  $d_{12}$ -TMSMS **406** was dried under high vacuum (~1 torr) and used with sodium hydride in dry dimethylformamide to give phenyloxirane **407** with 95% deuterium at position 2 (Scheme 119). The  $^1\text{H}$  NMR spectrum had a singlet at 3.87 ppm and near identical set of signals in the aromatic region 7.40 – 7.27 ppm as in comparison to protio phenyloxirane **359**. The  $^2\text{H}$  NMR spectrum had two 1H singlets at 3.13 and 2.79 ppm reminiscent of the epoxide signals of protio phenyloxirane **359**. The  $^{13}\text{C}$  NMR spectrum had a 4 singlets in the aromatic region characteristic for phenyloxirane at 137.66, 128.53, 128.20 and 125.53 ppm. A doublet at 52.21 ppm and a pentet at 50.51 ppm indicate presence of the deuterated epoxide. The formation of protonated epoxides while using  $d_{12}$ -TMSMS **406** can be explained by the presence of unwanted water ( $\text{H}_2\text{O}$  **15**). As the ionic salt **406** is very hygroscopic, it absorbs water **15** from the air and in presence of a base allows for an exchange between deuterium and hydrogen atoms of the cation, thus resulting in protonated epoxides (Scheme 120).



*Scheme 118 Epoxidation of benzaldehyde 358 with  $d_{12}$ -TMSMS 407*



Scheme 119 Alternative epoxidation of benzaldehyde **358** with  $d_{12}$ -TMSMS **406**

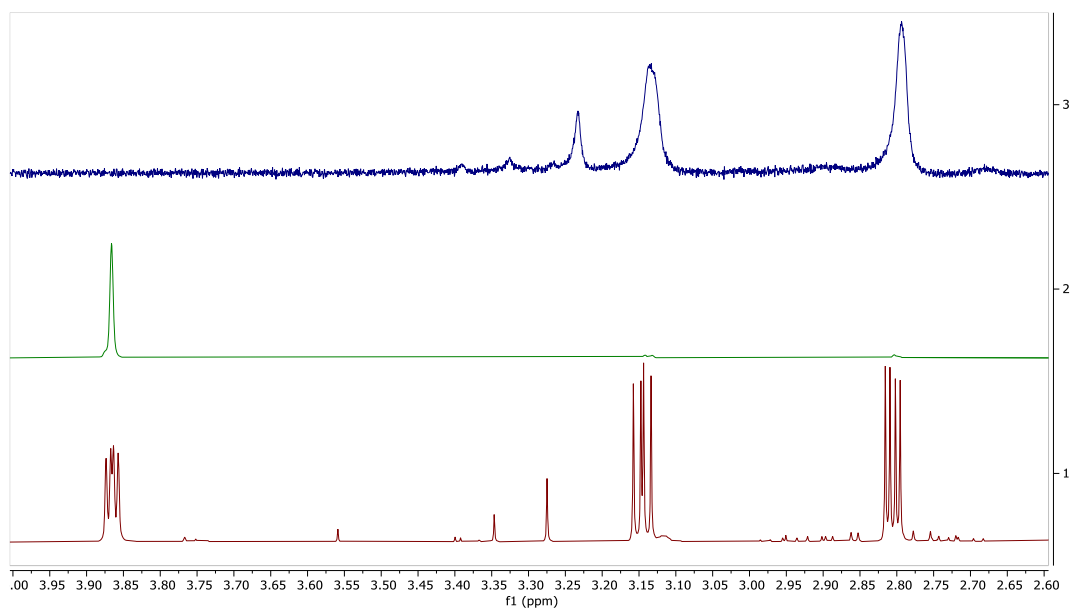
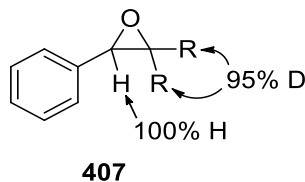


Figure 59 Comparison between spectra  $^2\text{H}$  NMR of phenyloxirane-3,3- $d_2$  **407** (top),  $^1\text{H}$  NMR of phenyloxirane-3,3- $d_2$  **407** (middle) and  $^1\text{H}$  NMR of phenyloxirane **359** (bottom)

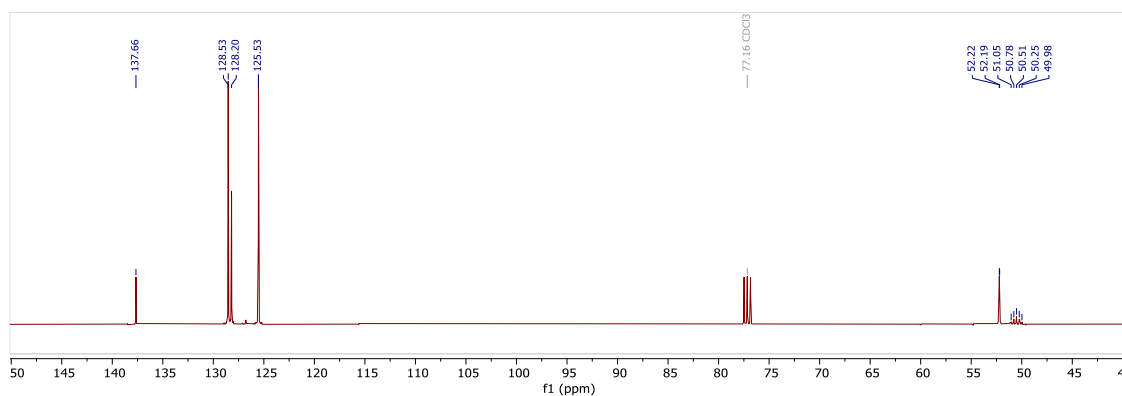
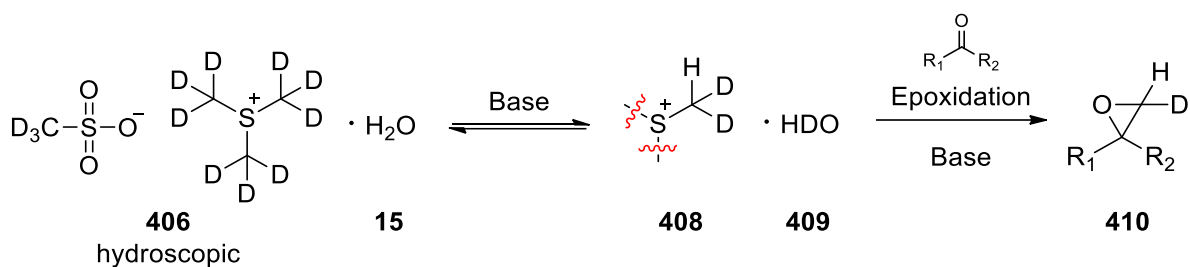


Figure 60  $^{13}\text{C}$  NMR Spectrum of phenyloxirane-3,3- $d_2$  **407**



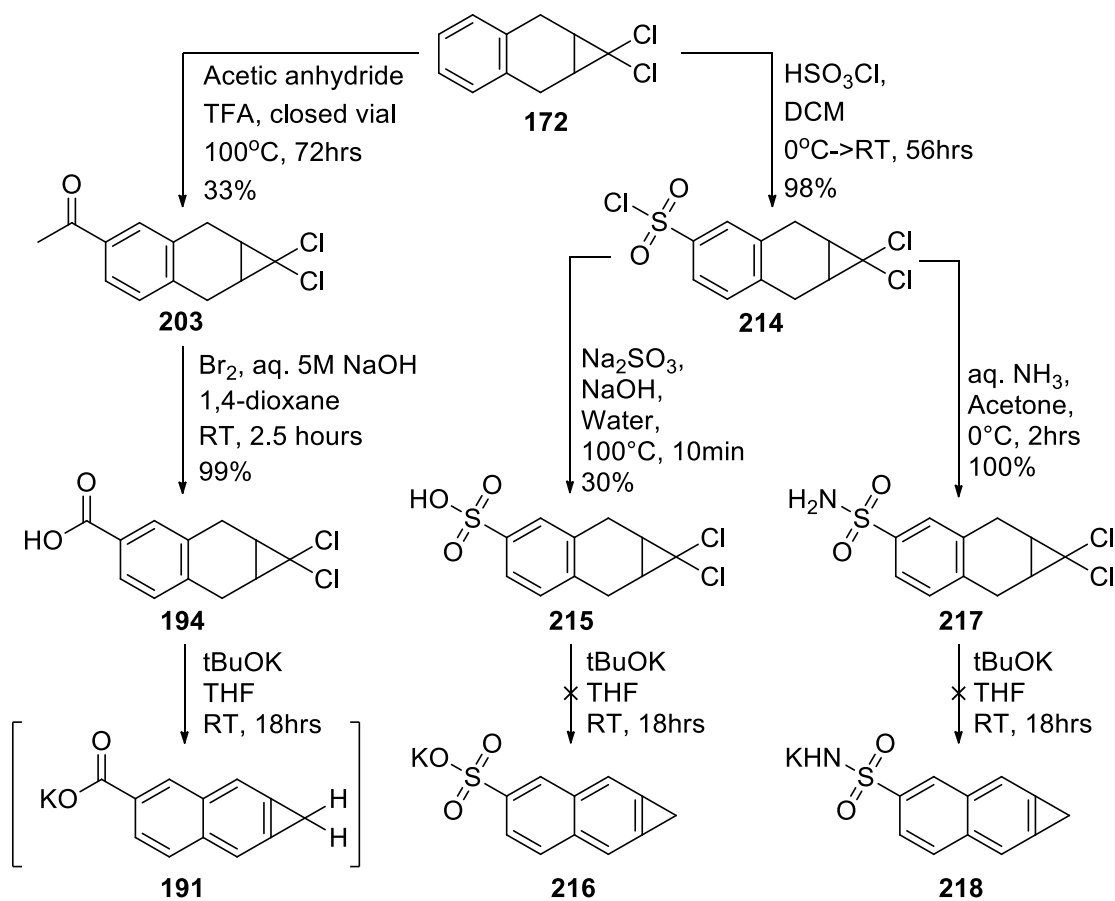
*Scheme 120 Epoxidation of benzaldehyde 358 with  $d_{12}$ -TMSMS 406*

## Chapter 6 – General conclusions

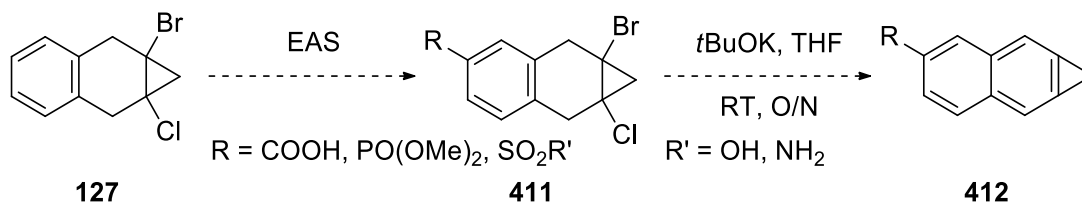
### 6.1 Cycloproparenes

The key goal of this study was to develop new chemical structures that could antagonise the action of ethylene **1** in plants. Using the proposed mode of action of 1-MCP **53**, a mechanistic approach could be adopted. Using this method, the cycloproparenes were previously found to be active. In this study, this approach was expanded to the triazolopyridines. These results demonstrate that (1) the proposed mode of action for 1-MCP **53** is reasonable and (2) a mechanistic approach based on the mode of action is a viable method to develop new antagonists.

The first part of this study was to make water soluble cycloproparenes using 1,1-dichloro-1a,2,7,7a-tetrahydro-1*H*-cyclopropa[*b*]naphthalene **172** as a starting material (Scheme 121). Carboxylic acid **191**, sulfonic acid **216** and sulfonamide **218** salts were targeted, but all produced ring opening products during the Billups synthesis. Only the carboxylate salt **191** was tentatively observed, however separation of the product from the reaction mixture was not successful. Alternatively, a synthesis of water soluble cycloproparene analogues in milder conditions could be attempted, using 1a-bromo-7a-chlorocyclopropane **127** precursors instead of the 1,1-dichloro-cyclopropane **172** precursors (Scheme 122), but these syntheses are longer and would not be suitable for commercialization.



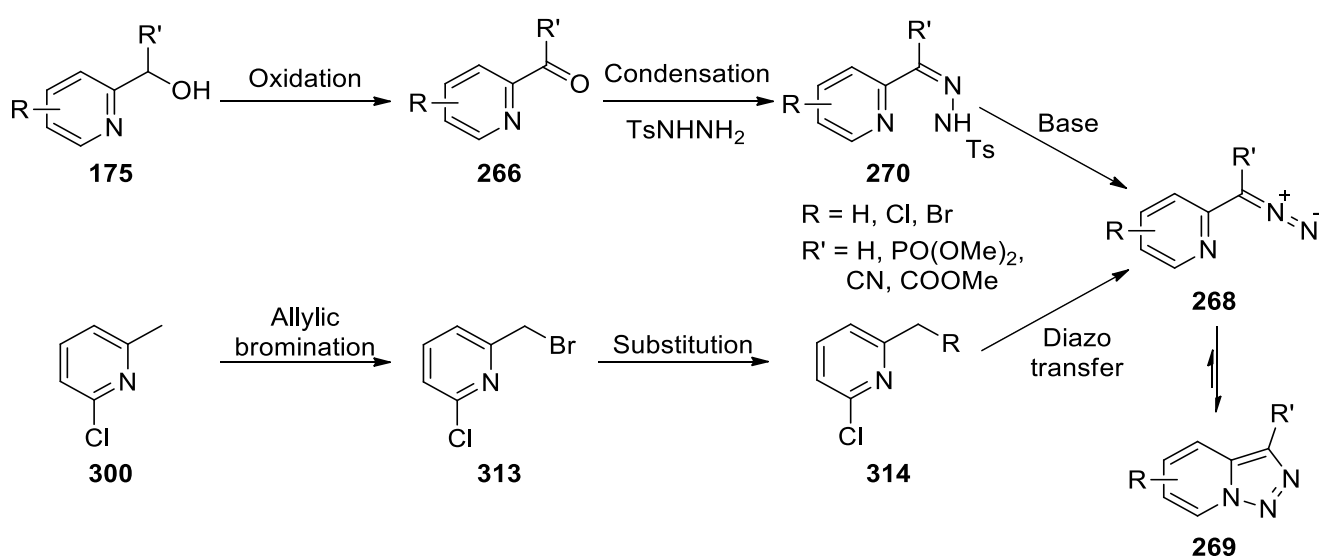
Scheme 121 Summary of attempts on synthesis of water soluble cycloproparenes



Scheme 122 Proposed synthesis of precursors to analogues of 1H-naphtho[b]cyclopropene

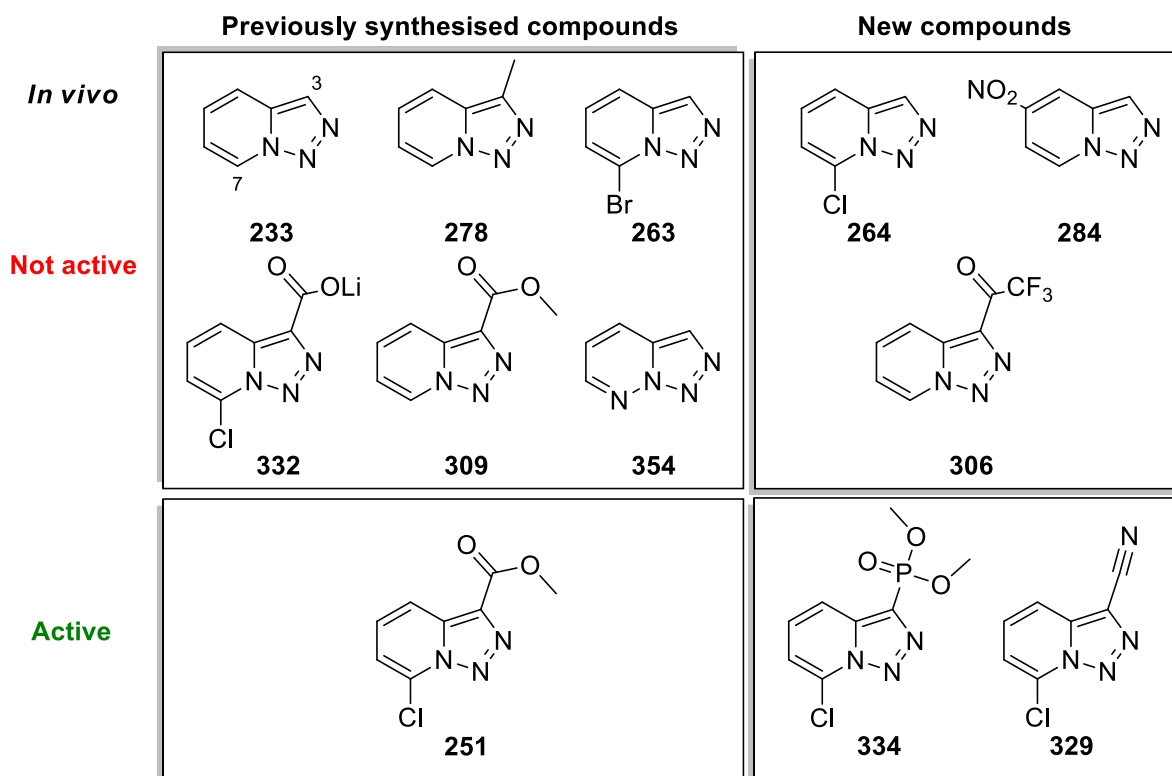
## 6.2 Triazolopyridines

Following the mechanistic approach in search of novel ethylene antagonists, triazolopyridines were investigated for their ‘masked’ diazo reactivity. Twelve analogues of [1,2,3]triazolo[1,5-*a*]pyridine were synthesised, out of which five were new (Scheme 124). The synthesis of substituted triazolopyridines through condensation was shown unreliable for reactive analogues due to stability issues. The most useful synthesis of triazolopyridines in this study was the use of the diazo transfer reaction and could be applied to further expand the library of these analogues (Scheme 123). The variability of synthetic yield indicated further optimisation is possible.



*Scheme 123 Synthesis pathway of [1,2,3]triazolo[1,5-*a*]pyridine analogues*

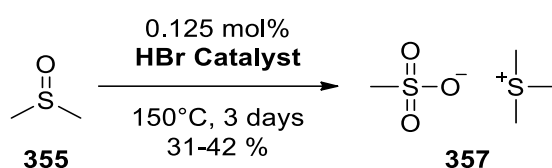
A simple, in-house assay for assessment of antagonism of ethylene action was developed using sprigs of flowering Geraldton wax and *in situ* generation of ethylene from ethephon. The assay was performed without specialised equipment and provides a simple way for chemists to test for assessment of potential ethylene antagonists in the synthetic laboratory setting. Insertion of bromine and chloride on position 7 of triazolopyridine ring activated the reactivity of the compound through the diazo functional group as shown by the Cu(I) reactivity tests. Insertion of EWGs at position 3 of the triazolopyridine ring did not activate the reactivity of the compound. Neither of these types of compounds displayed *in vivo* reactivity in the in-house assay, due to lack of stability or reactivity respectively. (Scheme 124). Insertion at both positions gave disubstituted species that was reactive both in the chemical model as well as in the in-house assay. The dimethyl phosphonate **334** displayed *in vivo* reactivity as a 1M solution while the methyl ester **251** and nitrile **329** displayed reactivity at as low as 0.1M concentration, indicating significantly greater efficacy. The assays could be further improved: greater sample size to increase statistical relevance; use of glass instead of plastic containers to minimise potential side effects and gas leakage as well as study of alternative plant subjects with alternative mechanisms of ethylene effect to observe, such as epinasty, tropistic behaviour, etiolated stem and others.



Scheme 124 Assessment of inhibition of ethylene action with analogues of [1,2,3]triazolo[1,5-a]pyridine

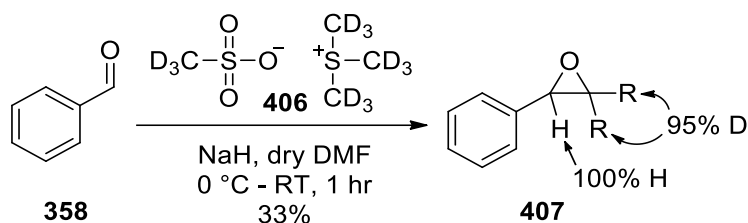
### 6.3 DMSO Degradation

The mechanism for the synthesis of trimethylsulfonium methanesulfonate **357** (TMSMS) by the degradation of dimethyl sulfoxide **355** (DMSO) was investigated. Six compounds were identified as catalysts of DMSO **355** degradation into TMSMS **357**, all containing a bromine anion. Three derivatives with a different counteranions did not catalyse the degradation. A base and a radical antioxidant were found to slow down the reaction onset. The conditions for degradation of DMSO **355** were optimised to 0.125 mol% catalyst, 150 °C for 72 hours with use of double-walled condenser and a calcium chloride drying plug (Scheme 125).



*Scheme 125 Degradation of DMSO 355 catalysed by bromic ionic liquids*

The preliminary findings indicated the degradation was catalysed by hydrobromic acid **397**. A greater spectrum of ionic liquids and other compounds should be studied for decomposition of DMSO **355** to obtain better understanding of the reaction mechanism. The degradation was found to be effective for the  $d_6$ -DMSO **405** to produce  $d_{12}$ -TMSMS **406**. The studies of epoxidation using  $d_{12}$ -TMSMS **406** produced deuterated epoxides (**407**) but further optimisation is needed. These studies would provide valuable data on comparison in effectiveness of the protio and deuterio analogues, and enable an easy access to deuterio epoxide products (Scheme 126).



*Scheme 126 Epoxidation of benzaldehyde 358 with  $d_{12}$ -TMSMS 406*

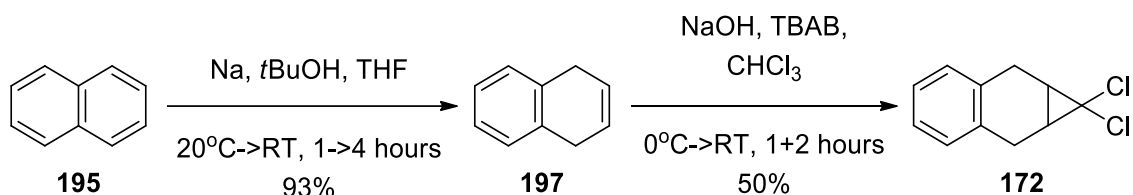
## Chapter 7 – Experimental

### General methods

All reactions involving moisture or air-sensitive reagents were performed under a positive pressure of nitrogen. Glassware was dried in an oven set at 120 °C for at least 30 minutes. Materials were obtained from commercial sources and used without further purification unless otherwise stated. NMR experiments were performed on a Bruker Ultra Shield Avance III 400 spectrometer ( $^1\text{H}$ , 400 MHz;  $^{13}\text{C}$ , 101 MHz). Chemical shifts ( $\delta$ ) are expressed in ppm with reference to the solvent resonances of chloroform-*d* ( $^1\text{H}$ , 7.26 ppm;  $^{13}\text{C}$ , 77.16 ppm). HRMS spectra were recorded at the School of Science, Edith Cowan University, Joondalup WA, using a Q Exactive™ Focus Hybrid Quadrupole-Orbitrap™ Mass Spectrometer (Thermo Fisher Scientific Corporation, US). Analytes ionisation was achieved using a heated electrospray ionisation source (HESI) operated in negative (-eV) mode. Samples were introduced into the HESI using a syringe pump operated at a flow rate of 5  $\mu\text{l min}^{-1}$ . The Q Exactive mass spectrometer was operated in full-scan mode from 70–1000  $m/z$  followed by isolation and full MS2 fragmentation of the parent compound in the HDC cell at variable collision energy. Infrared spectra were recorded on a Perkin Elmer Fourier Transform-IR spectrometer 100 equipped with a ZnSe-diamond crystal ATR accessory; spectra were acquired between 4000-650  $\text{cm}^{-1}$ . Melting points were determined on a Crown Scientific Barnstead Electrothermal 9100 apparatus. Column/flash chromatography was achieved using SiliaFlash® P60 silica gel (230-400 mesh, SiliaCycle, Canada) with the solvents stated. TLC was completed on Merck aluminium backed silica gel 60 F254 sheets and visualised by using short-wave UV light ( $\lambda = 254 \text{ nm}$ ). The ‘dry’ solvents tetrahydrofuran, dichloromethane, diethyl ether and acetonitrile were saturated with nitrogen and dried over activated alumina columns, *N,N*-dimethylformamide was saturated with nitrogen and dried over (5Å) molecular sieve columns (Innovative Technology PS-MD-5). Petroleum spirits 40-60 refers to the fraction of alkanes that boils between 40-60 °C.

## 7.1 Cycloproparenes

### 1,4-Dihydronaphthalene **197** and 1,1-Dichloro-1*a*,2,7,7*a*-tetrahydro-1*H*-cyclopropa[*b*]naphthalene **172**



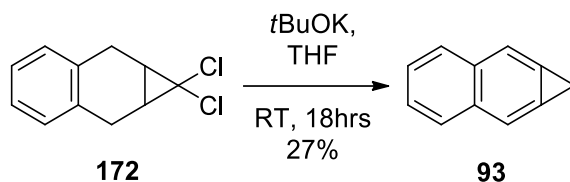
Small pieces of sodium metal (15 g, 650 mmol) were added in portions to a solution of naphthalene **195** (30 g, 234 mmol) in anhydrous tetrahydrofuran (400 mL) under nitrogen. *tert*-Butanol (62 mL, 653 mmol) was then added dropwise over 50 minutes, and the reaction mixture was stirred for 4 hours while kept at room temperature with a water bath. Petroleum spirits (200 mL) were added and the resulting mixture was filtered to remove excess sodium metal. The filtrate was washed with water (200 mL), dried over MgSO<sub>4</sub>, filtered and concentrated under reduced pressure, yielding 1,4-dihydronaphthalene **197** as a colourless oil (28.4 g, 93%) which was used in the next reaction. The NMR spectrum matched the data of Pétrier et al.<sup>375</sup>

**<sup>1</sup>H NMR (400 MHz, CDCl<sub>3</sub>)** δ 7.17-7.11 (m, 4H), 5.93 (t, *J* = 1.4 Hz, 2H), 3.40 (d, *J* = 1.4 Hz, 4H)

1,4-Dihydronaphthalene **197** (28.4 g, 218 mmol) and tetrabutylammonium bromide (0.501 g, 1.6 mmol) were added to an aqueous 25M sodium hydroxide solution (40 mL). To this mixture a solution of chloroform (40 mL, 499 mmol) and ethanol (4 mL) was added dropwise over 1 hour at 0 °C. The reaction mixture was stirred at 0 °C for 1 hour, then allowed to warm to room temperature over 2 hours. The reaction mixture was then diluted with water (200 mL) and chloroform (200 mL). The organic layer was separated and concentrated under reduced pressure, yielding a red/brown oil (40.16 g). The oil was purified by silica gel filtration (100% petroleum spirits) yielding pure 1,1-dichloro-1*a*,2,7,7*a*-tetrahydro-1*H*-cyclopropa[*b*]naphthalene **172** (16.44 g, 50%, 33% over 2 steps). The NMR spectrum matched the data of Billups et al.<sup>163</sup>

**<sup>1</sup>H NMR (400 MHz, CDCl<sub>3</sub>)** δ 7.10 (s, 4H), 3.26-3.20 (m, 2H), 2.81 (m, 2H), 2.06-2.03 (m, 2H)

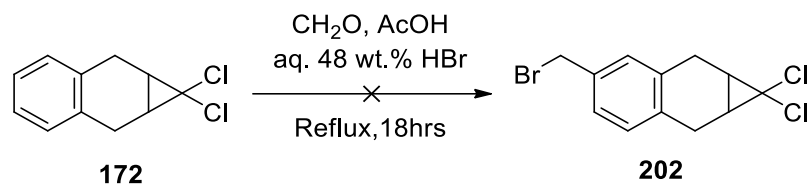
## 1*H*-Cyclopropa[*b*]naphthalene **17**



Potassium *tert*-butoxide (23.04 g, 205 mmol) was added in portions to a solution of 1,1-dichloro-1*a*,2,7,7*a*-tetrahydro-1*H*-cyclopropa[*b*]naphthalene **172** (9.61 g, 45.1 mmol) in anhydrous tetrahydrofuran (100 mL). The reaction mixture was stirred at room temperature for 18 hours, then concentrated under reduced pressure. The obtained solids were diluted with petroleum spirits (100 mL) and washed with water (100 mL), then the organic extract was concentrated under reduced pressure, yielding a brown oil (10.72 g). The product **93** was purified by flash chromatography (petroleum spirits) as a white solid (4.15 g, 27%). The NMR spectrum matched the data of Halton et al.<sup>167</sup>

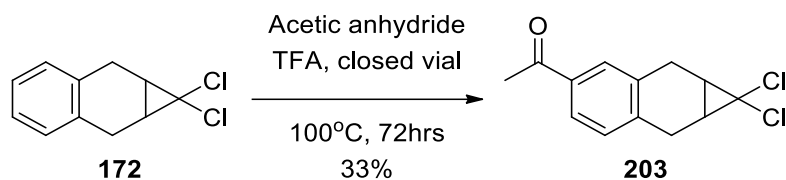
**<sup>1</sup>H NMR (400 MHz, CDCl<sub>3</sub>)**  $\delta$ : 7.88 (dd,  $J = 6.2, 3.3$  Hz, 2H), 7.58 (s, 2H), 7.46 (dd,  $J = 6.2, 3.3$  Hz, 1H), 3.52 (s, 2H)

**4-(Bromomethyl)-1,1-dichloro-1a,2,7,7a-tetrahydro-1H-cyclopropa[*b*]naphthalene 202 (attempted)**



A solution of 1,1-dichloro-1a,2,7,7a-tetrahydro-1H-cyclopropa[*b*]naphthalene **172** (0.5 g, 2.3 mmol) in glacial acetic acid (5 mL), aqueous 25 wt.% formaldehyde solution (0.21 g, 1.76 mmol) and aqueous 48 wt.% hydrobromic acid (0.85 g, 5.04 mmol) was heated under reflux overnight. The mixture was allowed to cool to room temperature and poured into ice cold water (50 mL). The resulting mixture was neutralised using sodium bicarbonate (0.42 g) and extracted using ethyl acetate (3 x 20 mL). The combined organic extracts were dried over MgSO<sub>4</sub>, filtered and concentrated under reduced pressure to give a complex mixture of side products as a brown oil.

## 4-Acetyl-1,1-dichloro-1a,2,7,7a-tetrahydro-1H-cyclopropa[*b*]naphthalene **203**



An oven dried pressure tube was charged with 1,1-dichloro-1a,2,7,7a-tetrahydrocyclopropa[*b*]naphthalene **172** (0.498 g, 2.34 mmol), acetic anhydride (0.361 g, 3.54 mmol) and trifluoroacetic acid (6.15 mL). The vial was sealed and stirred at 100 °C for 3 days. The reaction mixture was poured into a mixture of water (100 mL) and dichloromethane (30 mL) and was neutralised to pH>7 with solid sodium bicarbonate (~6 g). The organic layer was separated and the aqueous layer was extracted with dichloromethane (2 x 30 mL). The combined organic extracts were dried over MgSO<sub>4</sub>, filtered and concentrated under reduced pressure to yield a dark brown oil. The oil (0.517 g) was purified by flash chromatography (30:70 ethyl acetate:petroleum spirits), yielding pure product **203** as colourless crystals (0.2 g, 33%).

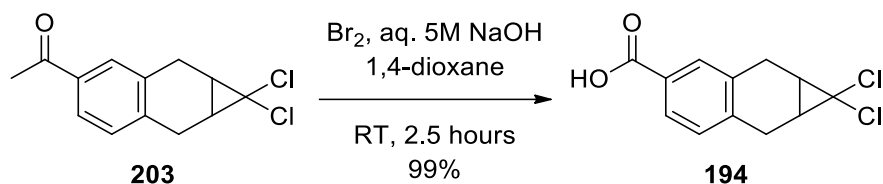
**<sup>1</sup>H NMR (400 MHz, CDCl<sub>3</sub>)** δ 7.69 (s, 1H), 7.67 (d, *J* = 7.8 Hz, 1H), 7.17 (d, *J* = 7.8 Hz, 1H), 3.32-3.24 (m, 2H), 2.92-2.86 (m, 2H), 2.56 (s, 3H), 2.08-2.06 (m, 2H)

**<sup>13</sup>C NMR (101 MHz, CDCl<sub>3</sub>)** δ 198.02 (C), 139.60 (C), 135.45 (C), 134.16 (C), 128.88 (CH), 128.65 (CH), 126.27 (CH), 65.70 (C), 27.07 (CH), 26.96 (CH), 26.70 (CH<sub>3</sub>), 25.21 (CH), 24.94 (CH)

**HRMS (Orbitrap) m/z:** [M+H]<sup>+</sup> C<sub>13</sub>H<sub>12</sub>Cl<sub>2</sub>O requires 255.0338, found 255.0338

**ATR IR** cm<sup>-1</sup> 1677 (C=O)

## 1,1-Dichloro-1a,2,7,7a-tetrahydro-1H-cyclopropa[b]naphthalene-4-carboxylic acid **194**



Bromine (1 mL, 39.03 mmol) was added to a stirred solution of an aqueous 5M sodium hydroxide (12 mL) at 0 °C. After 10 minutes, a 0.65 mL aliquot (2.11 mmol) was transferred to a separate flask, to which a solution of 4-acetyl-1,1-dichloro-1a,2,7,7a-tetrahydrocyclopropa[b]naphthalene **203** (47 mg, 0.184 mmol) in 1,4-dioxane (1 mL) was added dropwise. The reaction mixture was stirred at room temperature for 2.5 hours. An aqueous 5% w/v sodium metabisulfate solution (1 mL) was added to the reaction mixture, followed by aqueous 32% w/v hydrochloric acid until a pH <3 was achieved. The mixture was extracted with dichloromethane (3 x 5 mL). The combined organic extracts were dried over MgSO<sub>4</sub>, filtered and concentrated under reduced pressure, yielding pure 1,1-dichloro-1a,2,7,7a-tetrahydro-1H-cyclopropa[b]naphthalene-4-carboxylic acid **194** as a pale yellow solid (47 mg, 99%).

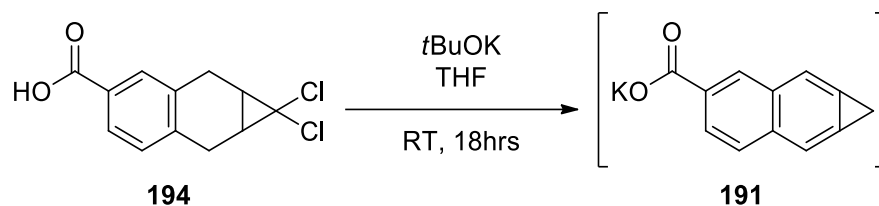
**<sup>1</sup>H NMR (400 MHz, CDCl<sub>3</sub>)** δ 7.83 (d, *J* = 1.7 Hz, 1H), 7.81 (dd, *J* = 7.9, 1.7 Hz, 1H), 7.19 (d, *J* = 7.9 Hz, 1H), 3.35 – 3.26 (m, 2H), 2.91 (d, *J* = 17.5 Hz, 2H), 2.09 (m, 2H) ppm.

**<sup>13</sup>C NMR (101 MHz, CDCl<sub>3</sub>)** δ 170.2 (C), 140.2 (CH), 134.1 (CH), 130.4 (C), 128.7 (C), 127.8 (C), 127.0 (CH), 65.6 (C), 26.9 (CH<sub>2</sub>), 26.8 (CH<sub>2</sub>), 25.2 (CH), 24.7 (CH) ppm.

**HRMS (Orbitrap) m/z:** [M-H]<sup>-</sup> C<sub>12</sub>H<sub>10</sub>Cl<sub>2</sub>O<sub>2</sub> requires 254.9985, found 254.9986

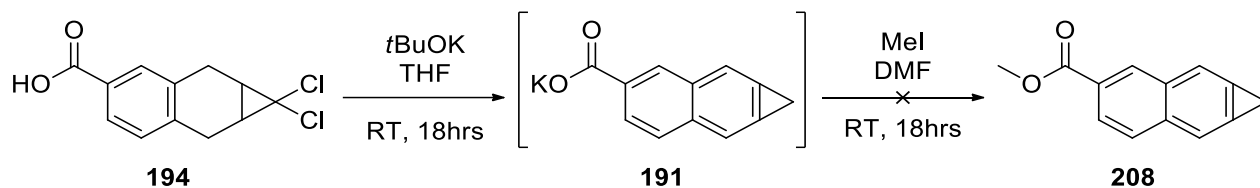
**ATR IR** cm<sup>-1</sup> 3200-2400 (O-H), 1678 (C=O), 1293 (C-O)

**Potassium 1*H*-cyclopropa[*b*]naphthalene-4-carboxylate 191  
(attempted)**



Potassium *tert*-butoxide (0.14 g, 1.25 mmol) was added in portions to a solution of 1,1-dichloro-1*a*,2,7,7*a*-tetrahydro-1*H*-cyclopropa[*b*]naphthalene-4-carboxylic acid **194** (0.064 g, 0.22 mmol) in anhydrous tetrahydrofuran (2 mL) under nitrogen. The mixture was stirred at room temperature for 18 hours, then evaporated. The NMR analysis of the crude did not have signals characteristic for cycloproparenes. Petroleum spirits (25 mL) and 0.1M pH 7 phosphate buffer solution (5 mL) were added to the crude product, then it was washed with water (2 x 25 mL). The organic layer was separated and concentrated under reduced pressure, yielding a brown oil (0.032 g). The <sup>1</sup>H NMR spectrum showed a complex mixture of products.

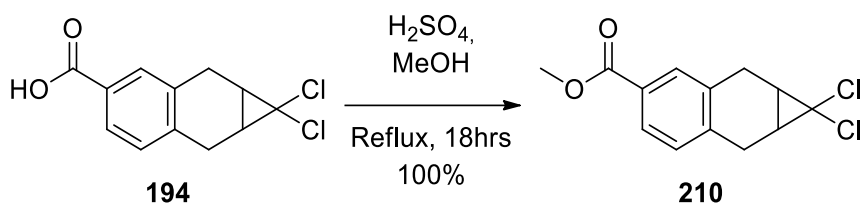
## Methylation of carboxylate to methyl naphtho[*b*]cyclopropenoate 208 (attempted)



Potassium *tert*-butoxide (0.109 g, 0.972 mmol) was added in portions to a solution of 1,1-dichloro-1a,2,7,7a-tetrahydro-1H-cyclopropa[*b*]naphthalene-4-carboxylic acid **194** (50 mg, 0.194 mmol) in anhydrous tetrahydrofuran (2 mL). The reaction mixture was stirred at room temperature for 18 hours and then concentrated under reduced pressure. The solids obtained were dissolved in water (20 mL) and acidified with aqueous 32% w/v hydrochloric acid (3 mL), resulting in a cloudy solution. The mixture was washed with ethyl acetate (3 x 10 mL) and the combined organic extracts were concentrated under reduced pressure, yielding a yellow solid (20 mg) which was used in the next reaction.

The solid was dissolved in tetrahydrofuran (3 mL) and triethylamine (2 mL), then cooled to 0 °C in an ice bath. Methyl iodide (0.377 g, 2.5 mmol) was added to the mixture and stirred overnight. The mixture was diluted with diethyl ether (20 mL) and washed with pH 7 buffer solution (sodium phosphate mono- and di-basic, 3 x 7 mL). The organic layer was concentrated under reduced pressure, yielding a colourless oil (0.172 g). The oil was diluted with petroleum spirits, precipitating white solid which was filtered off. The filtrate was concentrated under reduced pressure, yielding a complex mixture as a colourless oil (0.13 g). The <sup>1</sup>H NMR spectrum showed a complex mixture of products.

**Methyl 1,1-dichloro-1*a*,2,7,7*a*-tetrahydro-1*H*-cyclopropa[*b*]naphthalene-4-carboxylate **210****



A drop of concentrated sulfuric acid was added to 1,1-dichloro-1*a*,2,7,7*a*-tetrahydro-1*H*-cyclopropa[*b*]naphthalene-4-carboxylic acid **194** (30 mg, 0.117 mmol) dissolved in methanol (10 mL). The reaction mixture was stirred at reflux overnight, diluted with water (50 mL) then extracted with dichloromethane (3 x 20 mL) and the combined organic extracts were dried over MgSO<sub>4</sub>, filtered and concentrated under reduced pressure, yielding methyl 1,1-dichloro-1*a*,2,7,7*a*-tetrahydro-1*H*-cyclopropa[*b*]naphthalene-4-carboxylate **210** as a brown solid (30 mg, 100%).

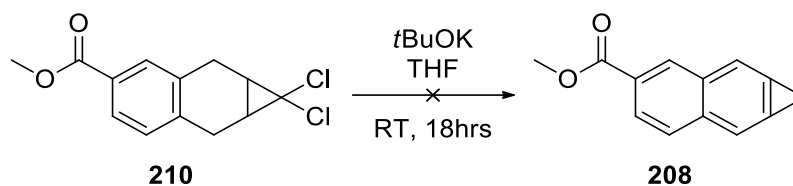
**<sup>1</sup>H NMR (400 MHz, CDCl<sub>3</sub>)** δ 7.79 (d, *J* = 1.7 Hz, 1H), 7.76 (dd, *J* = 8.0, 1.7 Hz, 1H), 7.15 (d, *J* = 8.0 Hz, 1H), 3.89 (s, 3H), 3.32 – 3.23 (m, 2H), 2.94 – 2.84 (m, 2H), 2.09 – 2.05 (m, 2H) ppm.

**<sup>13</sup>C NMR (101 MHz, CDCl<sub>3</sub>)** δ 167.2 (C), 139.3 (CH), 134.0 (CH), 129.9 (C), 128.7 (C), 128.2 (C), 127.3 (CH), 65.7 (C), 52.13 (CH<sub>3</sub>), 27.0 (CH<sub>2</sub>), 27.0 (CH<sub>2</sub>), 25.2 (CH), 24.8 (CH) ppm.

**HRMS (Orbitrap) m/z:** [M+H]<sup>+</sup> C<sub>13</sub>H<sub>12</sub>Cl<sub>2</sub>O<sub>2</sub> requires 271.0287, found 271.0287

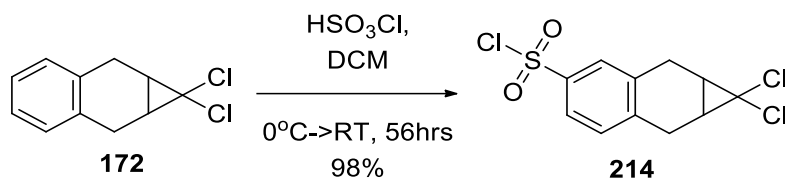
**ATR IR** cm<sup>-1</sup> 1713 (C=O), 1275 (C-O)

## Methyl naphtho[*b*]cyclopropenoate **208** (attempted)



Potassium *tert*-butoxide (16.1 mg, 0.143 mmol) was added in portions to a solution of methyl 1,1-dichloro-1a,2,7,7a-tetrahydro-1H-cyclopropa[*b*]naphthalene-4-carboxylate **210** (36 mg, 0.133 mmol) in anhydrous tetrahydrofuran (7 mL) under nitrogen. The mixture was stirred at room temperature for 18 hours. Petroleum spirits (15 mL) was added to the mixture, then it was washed with water (10 mL). The organic extract was separated and concentrated under reduced pressure, yielding a brown oil (15.4 mg). The <sup>1</sup>H NMR spectrum showed a complex mixture of products.

## 1,1-Dichloro-1a,2,7,7a-tetrahydro-1*H*-cyclopropa[*b*]naphthalene-4-sulfonyl chloride **214**



Chlorosulfonic acid (9 mL, 135 mmol) was added dropwise to a solution of 1,1-dichloro-1a,2,7,7a-tetrahydrocyclopropa[*b*]naphthalene **172** (2.4 g, 11.26 mmol) in dichloromethane (25 mL) at 0 °C. The reaction mixture was allowed to warm up to room temperature and stirred for 56 hours. The reaction mixture was diluted with dichloromethane (25 mL) and water (50 mL), neutralised with potassium bicarbonate and the aqueous layer was separated. The organic extract was washed with water (2 x 50 mL), dried over MgSO<sub>4</sub>, filtered and concentrated under reduced pressure to yield 1,1-dichloro-1a,2,7,7a-tetrahydro-1*H*-cyclopropa[*b*]naphthalene-4-sulfonyl chloride **214** as a brown oil (3.46, 98%).

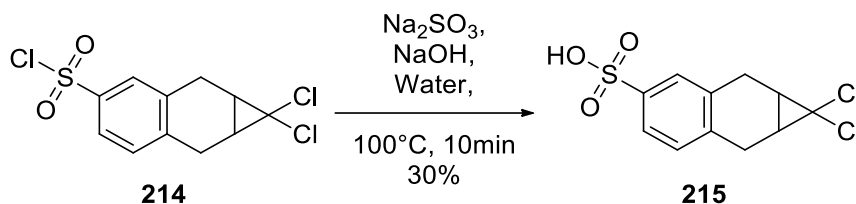
**<sup>1</sup>H NMR (400 MHz, CDCl<sub>3</sub>)** δ 7.77 (s, 1H), 7.75 (d, *J* = 8.5 Hz, 1H), 7.34 (d, *J* = 8.5 Hz, 1H), 3.36 (m, 2H), 2.95 (m, 2H), 2.13 (m, 2H)

**<sup>13</sup>C NMR (101 MHz, CDCl<sub>3</sub>)** δ 142.6 (C), 142.2 (C), 136.1 (C), 129.9 (CH), 127.1 (CH), 124.6 (CH), 65.1 (C), 26.7 (2xCH), 25.5 (CH<sub>2</sub>), 25.1 (CH<sub>2</sub>)

**HRMS (Orbitrap) m/z:** Sample degraded during testing

**ATR IR** cm<sup>-1</sup> 1370 (S=O), 1165 (S=O)

## 1,1-Dichloro-1a,2,7,7a-tetrahydro-1*H*-cyclopropa[*b*]naphthalene-4-sulfonic acid **215**



1,1-Dichloro-1a,2,7,7a-tetrahydro-1*H*-cyclopropa[*b*]naphthalene-4-sulfonyl chloride **214** (1 g, 3.21 mmol) was added to a boiling solution of sodium hydroxide (0.4 g, 10 mmol) and sodium sulfite (4.04 g, 32.05 mmol) in water (10 mL). The reaction was heated under reflux for 10 minutes, then allowed to cool down to room temperature. The solution was diluted with water (20 mL) and acidified with aq. 32% hydrochloric acid. The aqueous layer was extracted with dichloromethane (3 x 25 mL), then the combined organic extracts were dried over  $\text{MgSO}_4$ , filtered and concentrated under reduced pressure to yield an oil. The oil was diluted in minimal amount of dichloromethane (2 mL) and petroleum spirits (100 mL) was added. The mixture was stored at  $-20^\circ\text{C}$  overnight. The precipitate was filtered and washed with petroleum spirits. The filtrate was concentrated under reduced pressure to yield sulfonic acid **215** as a brown oil (0.645 g, 30%).

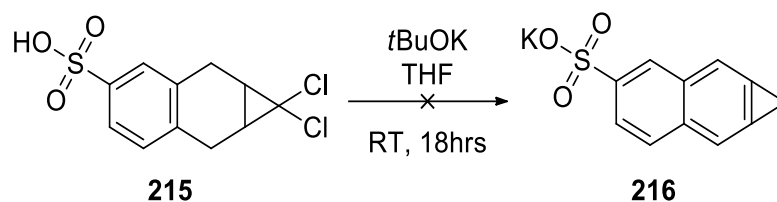
**$^1\text{H}$  NMR (400 MHz,  $\text{CDCl}_3$ )**  $\delta$  7.63 (s, 1H), 7.59 (d,  $J = 7.9$  Hz, 1H), 7.17 (d,  $J = 7.9$  Hz, 1H), 3.19 (m, 2H), 2.77 (m, 2H), 2.06 – 1.94 (m, 2H) ppm.

**$^{13}\text{C}$  NMR (101 MHz,  $\text{CDCl}_3$ )**  $\delta$  138.45 (2 x CH), 134.88 (CH), 129.05 (C), 126.32 (C), 123.84 (C), 65.78 (C), 26.91 ( $\text{CH}_2$ ), 26.89 ( $\text{CH}_2$ ), 25.00 (CH), 24.75 (CH) ppm.

**HRMS (Orbitrap) m/z:**  $[\text{M}+\text{H}]^+$   $\text{C}_{11}\text{H}_{10}\text{Cl}_2\text{O}_3\text{S}$  requires 290.9649, found 290.9648

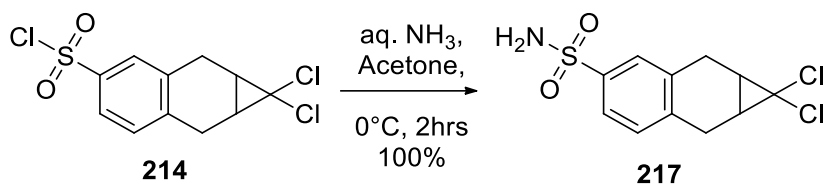
**ATR IR**  $\text{cm}^{-1}$  3500-2500 (O-H), 1683 ( $\text{SO}_3$ ), 1114 ( $\text{SO}_3$ ), 1027 ( $\text{SO}_3$ )

## Potassium 1*H*-cyclopropa[*b*]naphthalene-4-sulfonate **216** (attempted)



Potassium *tert*-butoxide (0.14 g, 1.25 mmol) was added in portions to a solution of 1,1-dichloro-1a,2,7,7a-tetrahydro-1*H*-cyclopropa[*b*]naphthalene-4-sulfonic acid **215** (0.073 g, 0.25 mmol) in anhydrous tetrahydrofuran (2 mL) under nitrogen. The mixture was stirred at room temperature for 18 hours. The reaction mixture was diluted with pH 7 buffer phosphate solution (2 mL) and then concentrated under reduced pressure to yield a red oil. The NMR spectrum of the crude oil did not contain characteristic signals of cycloproparenes.

## 1,1-Dichloro-1a,2,7,7a-tetrahydro-1*H*-cyclopropa[*b*]naphthalene-4-sulfonamide **217**



Aqueous 28% ammonia (11.2 mL) was added to a solution of 1,1-dichloro-1a,2,7,7a-tetrahydro-1*H*-cyclopropa[*b*]naphthalene-4-sulfonyl chloride **214** (0.973 g, 3.12 mmol) in acetone (8 mL) at 0 °C and stirred for 2 hours. The reaction mixture was concentrated under reduced pressure, then diluted with water (20 mL) and extracted with dichloromethane (3 x 25 mL). The combined organic extracts were dried over MgSO<sub>4</sub>, filtered and concentrated under reduced pressure to yield a brown oil. The oil was purified by flash chromatography (20% ethyl acetate in petroleum spirits) and titration (1% petroleum spirits in dichloromethane at -20 °C), yielding pure sulfonamide **217** as white crystals (1.04 g, 100%).

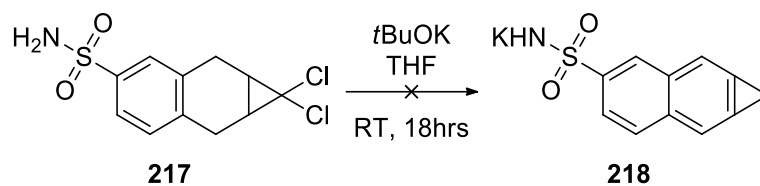
**<sup>1</sup>H NMR (400 MHz, CDCl<sub>3</sub>)** δ 7.67 (s, 1H), 7.64 (dd, *J* = 8.0, 2.0 Hz, 1H), 7.24 (d, *J* = 8.0 Hz, 1H), 4.91 (s, 2H) 3.29 (m, 2H), 2.90 (m, 2H), 2.09 (m, 2H)

**<sup>13</sup>C NMR (101 MHz, CDCl<sub>3</sub>)** δ 139.7 (C), 139.3 (C), 135.1 (C), 129.4 (CH), 126.6 (CH), 124.0 (CH), 65.4 (C), 26.8 (2xCH), 25.1 (CH<sub>2</sub>), 24.9 (CH<sub>2</sub>)

**HRMS (Orbitrap) m/z:** [M+H]<sup>+</sup> C<sub>11</sub>H<sub>11</sub>Cl<sub>2</sub>NO<sub>2</sub>S requires 291.9960, found 291.9955

**ATR IR** cm<sup>-1</sup> 3344 (N-H), 3253 (N-H) 1542 (C-H), 1312 (S=O), 1151 (S=O)

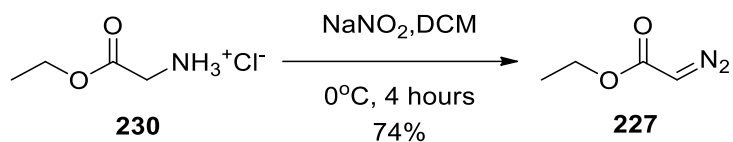
**Potassium ((1*H*-cyclopropa[*b*]naphthalen-4-yl)sulfonyl)amide **218**  
(attempted)**



Potassium *tert*-butoxide (0.14 g, 1.25 mmol) was added in portions to a solution of 1,1-dichloro-1a,2,7,7a-tetrahydro-1*H*-cyclopropa[*b*]naphthalene-4-sulfonamide **217** (0.063 g, 0.22 mmol) in anhydrous tetrahydrofuran (2 mL) under nitrogen. The mixture was stirred at room temperature for 18 hours. The reaction mixture was diluted with pH 7 buffer phosphate solution (2 mL) and then concentrated under reduced pressure. The NMR spectrum of the crude solid did not have signals characteristic for cycloproparenes.

## 7.2 Triazolopyridines

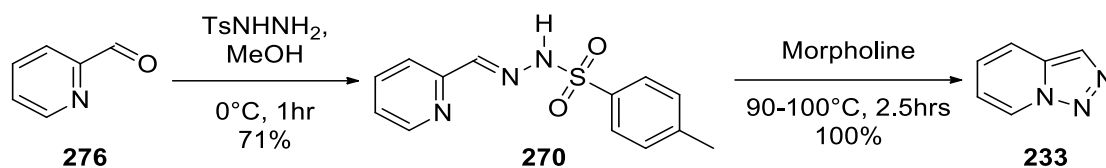
### Ethyl 2-diazoacetate **227**



Sodium nitrate (1.49 g, 17.5 mmol) was added to an ice-cold solution of glycine ethyl ester hydrochloride **230** (2.05 g, 14.7 mmol) and the reaction mixture was stirred at  $0^\circ\text{C}$  for 4 hours under nitrogen. The organic layer was separated, washed with water (50 mL) and brine (50 mL), then dried over  $\text{MgSO}_4$ , filtered and concentrated under reduced pressure to yield ethyl 2-diazoacetate **227** as a lime oil (1.25 g, 74%). The NMR spectrum matched the data of Braun et al.<sup>376</sup> and Jiang et al.<sup>377</sup>

**$^1\text{H}$  NMR (400 MHz,  $\text{CDCl}_3$ )**  $\delta$  4.72 (s, 1H), 4.22 (q,  $J = 7.1$  Hz, 2H), 1.27 (t,  $J = 7.1$  Hz, 3H) ppm.

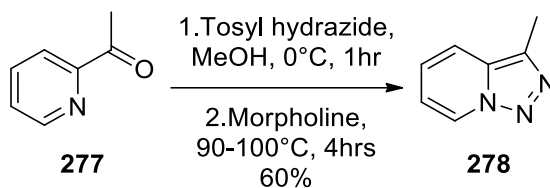
## 2-Pyridinecarboxaldehyde tosylhydrazone and [1,2,3]Triazolo[1,5-*a*]pyridine **233**



2-Pyridinecarboxaldehyde **276** (4.28 g, 39.9 mmol) and *p*-toluenesulfonyl hydrazide (8.18 g, 43.9 mmol) in methanol (15 ml) was stirred at 0 °C for 1 hour. The resulting precipitate was collected by vacuum filtration and washed with ice-cold methanol (5 x 10 mL) to yield of 2-pyridinecarboxaldehyde tosylhydrazone **270** as a mixture of *E/Z* isomers in 1:1 ratio, as a white solid (7.83 g, 71%). The solid was used directly in the next reaction. 2-Pyridinecarboxaldehyde tosylhydrazone **270** (7.83 g, 28.4 mmol) solid was dissolved in morpholine (50 mL) and stirred at 95 °C for 2.5 hours. The resulting mixture was concentrated under reduced pressure, diluted with diethyl ether (50 mL) and filtered. The filtrate was concentrated under reduced pressure to yield [1,2,3]triazolo[1,5-*a*]pyridine **233** as a yellow liquid (5.16 g, 100%). The NMR spectrum matched the data of Roy et al.<sup>285</sup>

<sup>1</sup>H NMR (400 MHz, CDCl<sub>3</sub>) δ 8.75 (dq, *J* = 7.0, 1.1 Hz, 1H), 8.06 (d, *J* = 1.1 Hz, 1H), 7.74 (dt, *J* = 9.0, 1.1 Hz, 1H), 7.25 (ddd, *J* = 9.0, 7.0, 1.1 Hz 2H), 6.98 (dd, *J* = 7.0, 1.1 Hz, 1H) ppm.

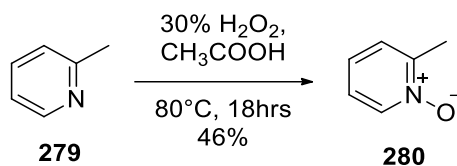
### 3-Methyl-[1,2,3]triazolo[1,5-*a*]pyridine **278**



A solution of 1-(pyridin-2-yl)ethanone **277** (4 g, 33.0 mmol) and *p*-toluenesulfonyl hydrazide (6.45 g, 34.7 mmol) in methanol (8 ml) was stirred at 0 °C for 1 hour. The resulting precipitate was collected by vacuum filtration and washed with cooled methanol (0 °C, 5 x 20 mL) to yield the intermediate (*E*)-4-methyl-*N'*-(1-(pyridin-2-yl)ethylidene)benzenesulfonohydrazide as a white solid (7.83 g, 71%) which was used directly in the next reaction. The forgoing solid was dissolved in morpholine (17 mL) and stirred at 95 °C for 2.5 hours. The reaction mixture was concentrated under reduced pressure, diluted with diethyl ether (50 mL) and filtered. The filtrate was concentrated under reduced pressure to yield a yellow oil (3.36 g, 76%). The oil was purified by flash chromatography (1:1 ethyl acetate:petroleum spirits) to yield 3-methyl-[1,2,3]triazolo[1,5-*a*]pyridine **278** as light yellow solid (2.66 g, 60%). The NMR spectrum matched the data of Lamaa et al.<sup>260</sup>

<sup>1</sup>H NMR (400 MHz, CDCl<sub>3</sub>) δ 8.65 (dt, *J* = 7.1, 1.1 Hz, 1H), 7.62 (dt, *J* = 8.9, 1.1 Hz, 1H), 7.16 (ddd, *J* = 8.9, 6.7, 1.1 Hz, 1H), 6.92 (dd, *J* = 6.7, 1.1 Hz, 1H), 2.62 (s, 3H) ppm.

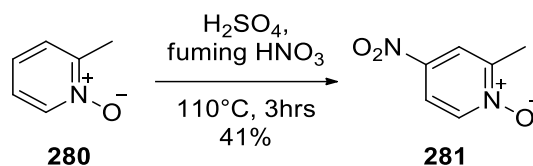
## 2-Methylpyridine 1-oxide **280**



A mixture of an aqueous 30% w/v hydrogen peroxide solution (32 mL, 0.313 mol) and 2-methylpyridine **279** (15 mL, 0.153 mol) in acetic acid (60 mL) was stirred at 80 °C for 18 hours. The reaction mixture was concentrated under reduced pressure to one third of the volume and poured into ice water (100 mL) and treated with potassium bicarbonate until pH 10 was reached. The solution was then washed with dichloromethane (3 x 30 mL) and the combined organic extracts were dried over MgSO<sub>4</sub>, filtered and concentrated under reduced pressure to yield 2-methylpyridine 1-oxide **280** as yellow oil (7.64 g, 46%). The NMR spectrum matched the data of Zaman et al.<sup>287</sup>

<sup>1</sup>H NMR (400 MHz, CDCl<sub>3</sub>) δ 8.27 (dd, *J* = 6.1, 1.6 Hz, 1H), 7.28 – 7.24 (m, 1H), 7.21 – 7.12 (m, 2H), 2.53 (s, 3H) ppm.

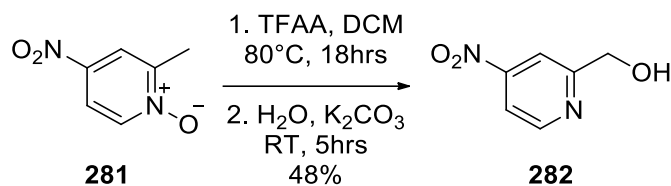
## 4-Nitro-2-methylpyridine 1-oxide **281**



2-Methylpyridine 1-oxide **280** (7.53 g, 69 mmol) was added to a solution of concentrated sulfuric acid (25 mL) and fuming nitric acid (30 mL). The reaction mixture was stirred at  $110^\circ\text{C}$  for 3 hours. The reaction mixture was then added dropwise to an ice water (200 mL), causing formation of dark brown gas. The mixture was extracted with dichloromethane (4 x 30 mL) and the combined organic extracts were washed with saturated potassium carbonate solution (150 mL). The aqueous layer was extracted with dichloromethane (2 x 30 mL) and the combined organic extracts were dried over  $\text{MgSO}_4$ , filtered and concentrated to yield 4-nitro-2-methylpyridine 1-oxide **281** as a lime solid (4.39 g, 41%). The NMR spectrum matched the data of Zaman et al.<sup>287</sup>

$^1\text{H}$  NMR (400 MHz,  $\text{CDCl}_3$ )  $\delta$  8.30 (d,  $J = 7.1$  Hz, 1H), 8.12 (d,  $J = 3.1$  Hz, 1H), 7.98 (dd,  $J = 7.1, 3.1$  Hz, 1H), 2.55 (s, 3H) ppm.

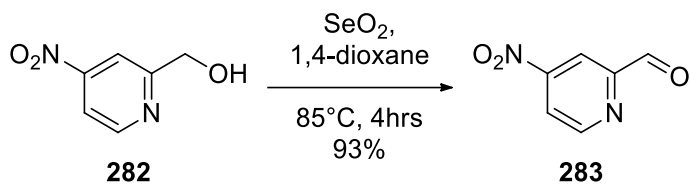
## 4-Nitro-2-methanolpyridine **282**



A solution of trifluoroacetic anhydride (8.5 mL, 58.3 mmol) in dry dichloromethane (15 mL) was added dropwise to a solution of 4-nitro-2-methylpyridine 1-oxide **281** (4.39 g, 28.5 mmol) in dry dichloromethane (50 mL) under nitrogen. The reaction mixture was stirred at room temperature for 5 hours, then concentrated under reduced pressure. The residue was dissolved in water (40 mL) and saturated aqueous potassium carbonate solution was added to the reaction mixture until pH 8 was reached and then it was further stirred for 5 hours. Potassium hydroxide was added to the reaction mixture until pH 12 was reached, then it was extracted with dichloromethane (4 x 30 mL). The combined organic extracts were washed with brine (2 x 25 mL), dried over MgSO<sub>4</sub>, filtered and concentrated under reduced pressure, yielding lime-brown solid (3.26 g). The solid was purified by flash chromatography (4:1 ethyl acetate:petroleum spirits) to yield 4-nitro-2-methanolpyridine **282** as a light green solid (2.10 g, 48%). The NMR spectrum matched the data of Zaman et al.<sup>287</sup>

<sup>1</sup>H NMR (400 MHz, CDCl<sub>3</sub>) δ 8.87 (d, *J* = 5.4 Hz, 1H), 8.10 – 8.06 (m, 1H), 7.97 – 7.92 (m, 1H), 4.94 (d, *J* = 5.4 Hz, 2H), 3.15 (t, *J* = 5.4 Hz, 1H) ppm.

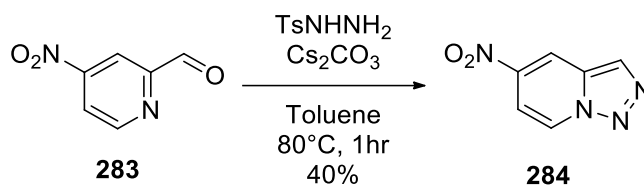
### (4-Nitro-2-pyridyl)-1-carboxaldehyde **283**



Selenium dioxide (0.36 g, 3.24 mmol) was added to solution of 4-nitro-2-methanolpyridine **282** (1.00 g, 6.5 mmol) in 1,4-dioxane (15 mL) and the reaction mixture was stirred at 85 °C for 4 hours under nitrogen. The reaction mixture was cooled to room temperature and filtered through celite. The filtrate was concentrated under reduced pressure to yield (4-nitro-2-pyridyl)-1-carboxaldehyde **283** as a red oil (0.92 g, 93%). The NMR spectrum matched the data of Zaman et al.<sup>287</sup>

**<sup>1</sup>H NMR (400 MHz, CDCl<sub>3</sub>)** δ 10.18 (s, 1H), 9.11 (dd, *J* = 5.3, 0.7 Hz, 1H), 8.64 (dd, *J* = 2.2, 0.7 Hz, 1H), 8.27 (dd, *J* = 5.3, 2.2 Hz, 1H) ppm.

## 5-Nitro-[1,2,3]triazolo[1,5-*a*]pyridine **284**



(4-Nitro-2-pyridyl)-1-carboxaldehyde **283** (0.512 g, 3.36 mmol) was diluted in toluene (20 mL) along *p*-toluenesulfonyl hydrazide (0.852 g, 4.57 mmol) and caesium carbonate (2.41 g, 7.4 mmol), then stirred at 80 °C for 1 hour. The reaction mixture was cooled to room temperature, concentrated under reduced pressure and the residue was diluted with water (25 mL) and extracted with ethyl acetate (3 x 25 mL). The combined organic extracts were dried over MgSO<sub>4</sub>, filtered and concentrated under reduced pressure to yield 5-nitro-[1,2,3]triazolo[1,5-*a*]pyridine **284** as a yellow/lime solid (0.224 g, 40%).

**<sup>1</sup>H NMR (400 MHz, CDCl<sub>3</sub>)** δ 8.85 (dt, *J* = 7.6, 1.0 Hz, 1H), 8.76 (dd, *J* = 2.3, 1.0 Hz, 1H), 8.45 (d, *J* = 1.0 Hz, 1H), 7.80 (dd, *J* = 7.6, 2.3 Hz, 1H) ppm.

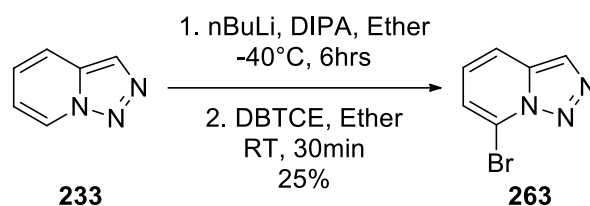
**<sup>13</sup>C NMR (101 MHz, CDCl<sub>3</sub>)** δ 144.44 (C), 132.07 (C), 131.01 (CH), 126.30 (CH), 115.6 (CH), 109.23 (CH) ppm.

**HRMS (Orbitrap) m/z:** [M+H]<sup>+</sup> C<sub>6</sub>H<sub>4</sub>N<sub>4</sub>O<sub>2</sub> requires 165.0406, found 165.0406

**ATR IR** cm<sup>-1</sup> 1513 (N-O stretch), 1343 (N-O stretch)

## Halogenation of [1,2,3]triazolo[1,5-*a*]pyridine by lithiation

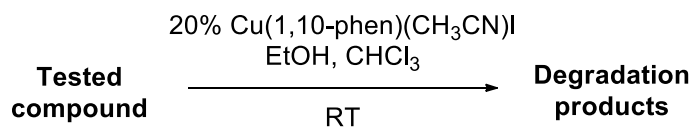
### 7-Bromo-[1,2,3]triazolo[1,5-*a*]pyridine **155**



A solution of *n*-butyllithium (1.05 mL, 1.6 M in hexanes, 1.68 mmol) was added to diisopropylamine (0.26 mL, 1.84 mmol) in solvent at -40 °C (acetonitrile and liquid nitrogen bath) under nitrogen. A solution of [1,2,3]triazolo[1,5-*a*]pyridine **233** (200 mg, 1.68 mmol) in ether (8 mL) was added to the solution and stirring continued for 6 hours. After this time, a solution of dibromotetrachloroethane (0.946 g, 5.04 mmol) in ether (8 mL) was added to the reaction mixture and the reaction mixture was allowed to warm to room temperature overnight. The reaction mixture was washed with water (3 x 20 mL). The organic layer was dried over MgSO<sub>4</sub>, filtered and concentrated under reduced pressure to yield a brown oil. The oil was purified by flash chromatography (1:9 ethyl acetate:petroleum spirits) to yield 7-bromo-[1,2,3]triazolo[1,5-*a*]pyridine **263** as a yellow solid (83.5 mg, 25%). The NMR spectrum matched the data of Abarca et al.<sup>290</sup>

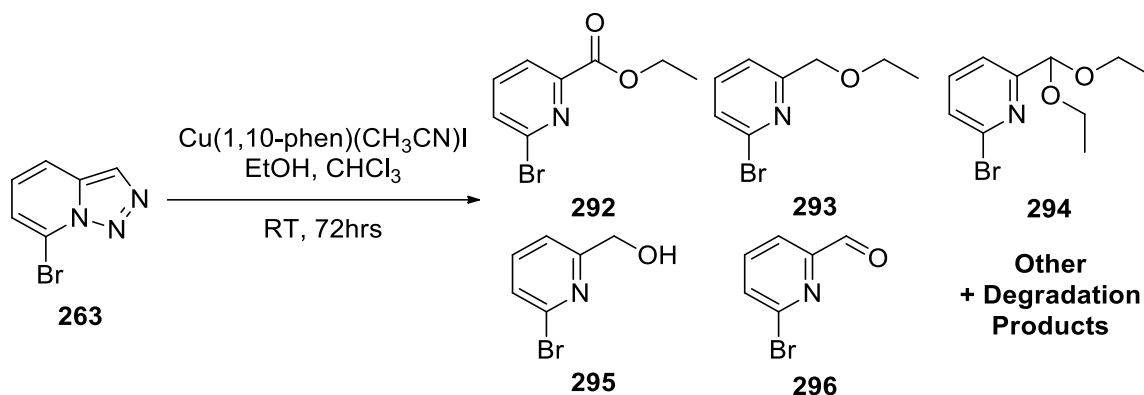
<sup>1</sup>H NMR (400 MHz, CDCl<sub>3</sub>) δ 8.21 (s, 1H), 7.75 (dd, *J* = 8.7, 1.1 Hz, 1H), 7.25 (dd, *J* = 7.1, 1.1 Hz, 1H), 7.17 (dd, *J* = 8.7, 7.1 Hz, 1H) ppm.

## General procedure for degradation catalysed by copper(I) complex



A solution of a tested compound (0.1 mmol) in chloroform (5 mL) was added to a stirred mixture of Cu(1,10-phen)(CH<sub>3</sub>CN)I (9.0 mg, 0.021 mmol) in ethanol (20 mL). The reaction mixture was stirred at room temperature until completion by TLC, then concentrated under reduced pressure. The remaining residue was diluted with dichloromethane (20 mL) and washed with water (3 x 20 mL). The organic extract was concentrated under reduced pressure and purified by flash chromatography.

**Degradation of 7-bromo-[1,2,3]triazolo[1,5-*a*]pyridine **263** catalysed by copper(I) complex**



A solution of 7-bromo-[1,2,3]triazolo[1,5-*a*]pyridine **263** (15 mg, 0.1 mmol) in chloroform (5 mL) was added to a stirred mixture of Cu(1,10-phen)(CH<sub>3</sub>CN)I (9.0 mg, 0.021 mmol) in ethanol (20 mL). The reaction mixture was stirred at room temperature for 3 days, then concentrated under reduced pressure. The remaining residue was diluted with dichloromethane (20 mL) and washed with water (3 x 20 mL). The organic layer was dried over MgSO<sub>4</sub>, filtered and concentrated under reduced pressure to yield a yellow oil (32 mg). The oil was purified by flash chromatography (1:1 ethyl acetate:petroleum spirits) to yield ethyl 2-bromopyridine-6-carboxylate **292** as a yellow solid (0.2 mg, 1%), 2-bromo-6-(ethoxymethyl)pyridine **293** as a yellow oil (0.1 mg, >1%), 2-bromo-6-(diethoxymethyl)pyridine **294** as a yellow oil (0.1 mg, >1%), (6-bromopyridin-2-yl)methanol **295** as a yellow oil (0.1 mg, >1%) and 6-bromopicolinaldehyde **296** as a yellow oil (0.1 mg, >1%). The NMR spectra matched the data of Kiran et al.,<sup>294</sup> Ulrich et al.,<sup>295</sup> Orita et al.<sup>296</sup> and Ali et al.<sup>297</sup>

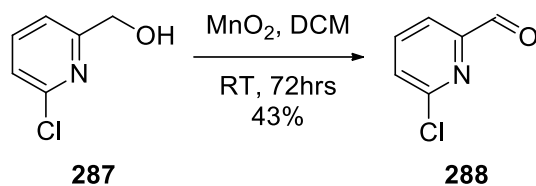
**<sup>1</sup>H NMR (400 MHz, CDCl<sub>3</sub>) ethyl ester **292**** δ 8.22 – 7.95 (dd, *J* = 6.8, 1.7 Hz, 1H), 7.97 – 7.50 (m, 2H), 4.80 – 3.93 (q, *J* = 7.1 Hz, 2H), 1.51 – 1.37 (t, *J* = 7.1 Hz, 3H)

**<sup>1</sup>H NMR (400 MHz, CDCl<sub>3</sub>) ethyl ether **293**, acetal **294**** δ 7.60 – 7.40 (1H), 7.40 – 7.20 (m, 2H), 5.1 – 4.5 (d, 2H), 3.55 – 3.20 (m, 2H), 1.4 – 1.0 (t, 3H)

**<sup>1</sup>H NMR (400 MHz, CDCl<sub>3</sub>) alcohol **295**** δ 7.56 (t, *J* = 7.7 Hz, 1H), 7.40 (d, *J* = 7.7 Hz, 1H), 7.28 (d, *J* = ? Hz, 1H), 4.75 (s, 2H), 2.94 (s, OH)

**<sup>1</sup>H NMR (400 MHz, CDCl<sub>3</sub>) aldehyde **296**** δ 10.01 (s, 1H), 7.93 (dd, *J* = 6.6, 1.9 Hz, 1H), 7.74 (m, 2H)

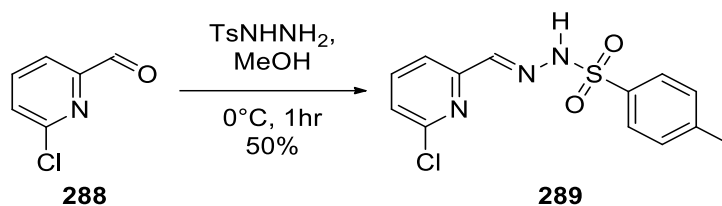
## 6-Chloro-2-pyridinecarboxaldehyde **288**



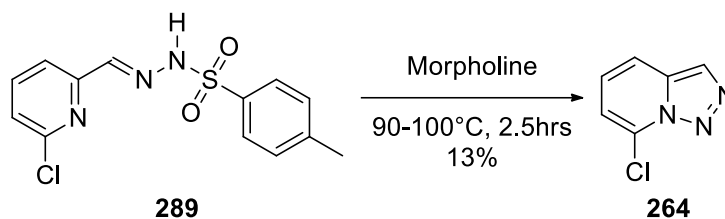
A mixture of (6-chloro-2-pyridinyl)methanol **287** (0.50 g, 3.48 mmol) and activated manganese dioxide (5.00 g, 57.5 mmol) in dry dichloromethane (50 mL) was stirred at room temperature for 3 days under nitrogen. The resulting mixture was filtered through celite and carefully concentrated under reduced pressure to yield 6-chloro-2-pyridinecarboxaldehyde **288** as a white solid (0.21 g, 43%), which was used without further purification. The NMR spectrum matched the data of Ashimori et al.<sup>293</sup>

**<sup>1</sup>H NMR (400 MHz, CDCl<sub>3</sub>)**  $\delta$  9.99 (s, 1H), 7.89 (dd,  $J = 7.5, 1.4$  Hz, 1H), 7.85 (dd,  $J = 7.5, 0.8$  Hz, 1H), 7.57 (dd,  $J = 7.5, 1.4$  Hz, 1H) ppm.

## 2-(2-Chloropyridyl)carboxaldehyde tosylhydrazone **289** and 7-Chloro-[1,2,3]triazolo[1,5-*a*]pyridine **264**



6-Chloro-2-pyridinecarboxaldehyde **288** (0.21 g, 1.39 mmol) was added to the stirred solution of *p*-toluenesulfonyl hydrazide (0.285 g, 1.53 mmol) in methanol (1.5 mL) at 0 °C and the reaction mixture was stirred at 0 °C for 1 hour. The reaction mixture was filtered through celite and washed with cold methanol (0 °C, 5 x 10 mL), to yield 2-(2-chloropyridyl)carboxaldehyde tosylhydrazone **289** as a white solid (0.227 g, 50%), used directly in the next reaction.



A solution of 2-(2-chloropyridyl)carboxaldehyde tosylhydrazone **289** (0.227 g, 0.73 mmol) in morpholine (5 mL) was stirred at 90-100 °C for 2.5 hours. The reaction mixture was concentrated under reduced pressure, the residue was diluted with diethyl ether (20 mL). The mixture was filtered through celite, and the filtrate was concentrated under reduced pressure to yield a yellow oil. The oil was purified by flash chromatography (1:1 ethyl acetate:petroleum spirits) to yield 7-chloro-[1,2,3]triazolo[1,5-*a*]pyridine **264** as a yellow solid (15 mg, 13%).

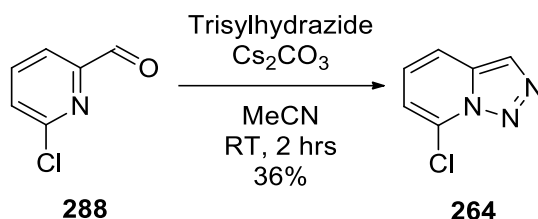
**<sup>1</sup>H NMR (400 MHz, CDCl<sub>3</sub>)** δ 8.17 (s, 1H), 7.72 (dd, *J* = 8.8, 1.1 Hz, 1H), 7.27 – 7.21 (m, 1H), 7.09 (dd, *J* = 7.1, 1.1 Hz, 1H) ppm.

**<sup>13</sup>C NMR (101 MHz, CDCl<sub>3</sub>)** δ 135.50 (C), 127.73 (C), 127.22 (CH), 125.84 (CH), 116.43 (CH), 115.24 (CH) ppm.

**HRMS (Orbitrap) m/z:** [M+H]<sup>+</sup> C<sub>6</sub>H<sub>4</sub>ClN<sub>3</sub> requires 154.0167, found 154.0166

**ATR IR** cm<sup>-1</sup> 1627 (C-H bending), 1496 (C-N stretching), 806 (C-Cl)

## 7-Chloro-[1,2,3]triazolo[1,5-*a*]pyridine **264**



2,4,6-Triisopropylbenzenesulfonyl hydrazide (0.52 g, 1.75 mmol), caesium carbonate (0.812 g, 2.49 mmol) and 6-chloro-2-pyridinecarboxaldehyde **288** (0.235 g, 1.66 mmol) in dry acetonitrile (12 mL) were stirred at room temperature for 2 hours under nitrogen. The reaction mixture was concentrated under reduced pressure and the remaining residue was dissolved in ethyl acetate (30 mL) and washed with water (2 x 30 mL). The organic layer was dried over MgSO<sub>4</sub>, filtered and concentrated under reduced pressure, to give a yellow oil (0.266 g). The oil was purified by titration (20:80 ethyl acetate:petroleum spirits) to yield 7-chloro-[1,2,3]triazolo[1,5-*a*]pyridine **264** as a yellow solid (92 mg, 36%).

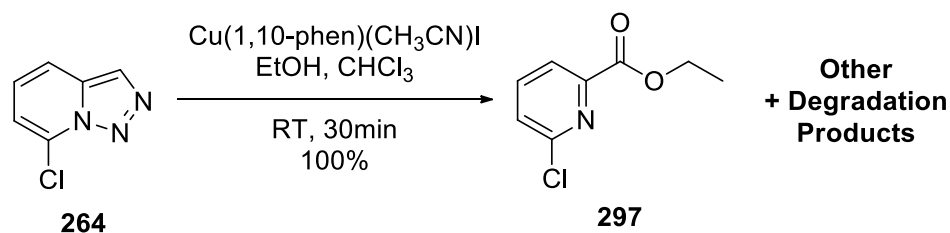
**<sup>1</sup>H NMR (400 MHz, CDCl<sub>3</sub>)** δ 8.17 (s, 1H), 7.73 (d, *J* = 8.8 Hz, 1H), 7.24 (dd, *J* = 7.1 Hz, 1H), 7.08 (d, *J* = 7.1 Hz, 1H) ppm.

**<sup>13</sup>C NMR (101 MHz, CDCl<sub>3</sub>)** δ 135.50 (C), 127.73 (C), 127.22 (CH), 125.84 (CH), 116.43 (CH), 115.24 (CH) ppm.

**HRMS (Orbitrap) m/z:** [M+H]<sup>+</sup> C<sub>6</sub>H<sub>4</sub>ClN<sub>3</sub> requires 154.0167, found 154.0166

**ATR IR** cm<sup>-1</sup> 1627 (C-H bending), 1496 (C-N stretching), 806 (C-Cl)

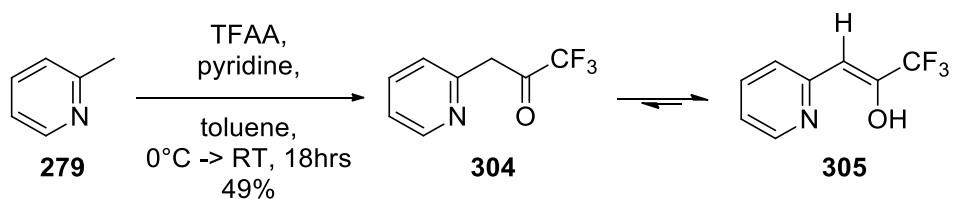
## Degradation of 7-chloro-[1,2,3]triazolo[1,5-*a*]pyridine **264** in presence of copper(I) complex in ethanol



A solution of 7-chloro-[1,2,3]triazolo[1,5-*a*]pyridine **264** (9 mg, 0.1 mmol) in chloroform (5 mL) was added to a stirred solution of Cu(1,10-phen)(CH<sub>3</sub>CN)I (9 mg, 0.021 mmol) in ethanol (20 mL). The reaction mixture was stirred at room temperature for 30 minutes, then concentrated under reduced pressure. The remaining residue was diluted with diethyl ether (20 mL) and washed with water (2 x 20 mL). The organic extract was dried over MgSO<sub>4</sub>, filtered and concentrated under reduced pressure to yield a complex mixture as a yellow oil (15 mg). The <sup>1</sup>H NMR spectrum had a complex mixture of products with a major product matching an ethyl ester **297**, which matched the data of Riflade et al.<sup>301</sup>

**<sup>1</sup>H NMR (400 MHz, CDCl<sub>3</sub>) ethyl ester** δ 8.05 (dd, *J* = 7.6, 0.9 Hz, 1H), 7.80 (t, *J* = 7.6 Hz, 1H), 7.51 (dd, *J* = 8.0, 0.9 Hz, 1H), 4.48 (q, *J* = 7.1 Hz, 2H), 1.44 (t, *J* = 7.1 Hz, 3H) ppm.

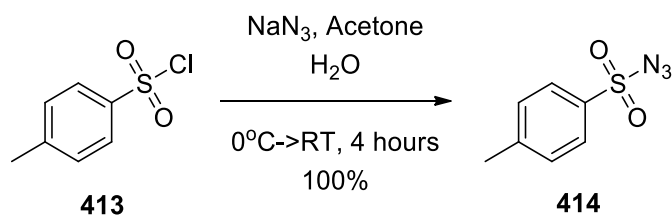
**1,1,1-Trifluoro-3-(pyridin-2-yl)propan-2-one 304 / 3,3,3-trifluoro-1-(2-pyridinyl)-1-propen-2-ol 305**



Trifluoroacetic anhydride (2.6 mL, 18 mmol) was added dropwise to a solution of 2-picoline **279** (0.588 g, 6.31 mmol) and pyridine (2.4 mL, 30 mmol) in dry toluene (15 mL) at 0 °C under nitrogen. The reaction mixture was stirred at room temperature overnight, then poured into aqueous 3 wt.% potassium carbonate solution (60 mL) and extracted with ethyl acetate (2 x 60 mL). The combined organic extracts were washed with brine (60 mL), dried over MgSO<sub>4</sub>, filtered and concentrated under reduced pressure to yield a brown oil (0.868 g). The oil was purified by flash chromatography (40:60 ethyl acetate:petroleum spirits) to yield 1,1,1-trifluoro-3-(pyridin-2-yl)propan-2-one **304** as lime-green solid (0.585 g, 49%). The NMR spectrum matched the data of Wang et al.<sup>311</sup>

**<sup>1</sup>H NMR (400 MHz, CDCl<sub>3</sub>)** δ 8.08 (d, *J* = 5.7 Hz, 1H), 7.71 (ddd, *J* = 8.7, 7.3, 1.7 Hz, 1H), 7.10 (dt, *J* = 8.7, 1.1 Hz, 1H), 7.04 (ddd, *J* = 7.3, 5.7, 1.1 Hz, 1H), 5.84 (s, 1H) ppm.

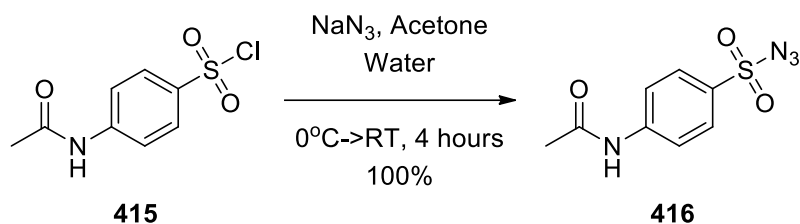
## 4-Methylbenzenesulfonyl azide **414**



Sodium azide (3.58 g, 55.1 mmol) was added to an ice-cold solution of 4-methylbenzene-1-sulfonyl chloride **413** (10.0 g, 52.5 mmol) in acetone (100 mL) and water (50 mL), then the reaction mixture was allowed to warm up to room temperature over 4 hours. The reaction mixture was concentrated under reduced pressure to remove acetone and the remaining aqueous mixture was extracted with dichloromethane (3 x 50 mL). The combined organic extracts were dried over MgSO<sub>4</sub>, filtered and concentrated under reduced pressure to yield 4-methylbenzenesulfonyl azide **414** as a white solid (9.94 g, 100%). The NMR spectrum matched the data of Waser et al.<sup>378</sup>

<sup>1</sup>H NMR (400 MHz, CDCl<sub>3</sub>) δ 7.88 – 7.81 (m, 2H), 7.45 – 7.37 (m, 2H), 2.48 (s, 3H) ppm.

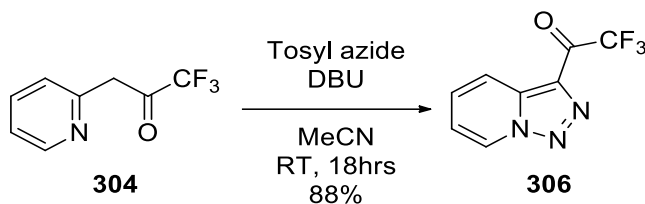
## 4-acetamidobenzenesulfonyl azide **416**



Sodium azide (2.93 g, 45.0 mmol) was added to an ice-cold solution of 4-acetamidobenzene-1-sulfonyl chloride **415** (10.0 g, 42.8 mmol) in acetone (100 mL) and water (50 mL), then the reaction mixture was allowed to warm up to room temperature over 4 hours. The reaction mixture was concentrated under reduced pressure to remove acetone and the remaining aqueous mixture was extracted with dichloromethane (3 x 50 mL). The combined organic extracts were dried over MgSO<sub>4</sub>, filtered and concentrated under reduced pressure to yield 4-methylbenzenesulfonyl azide **416** as a white solid (9.94 g, 100%). The NMR spectrum matched the data of Hu et al.<sup>379</sup>

**<sup>1</sup>H NMR (400 MHz, CDCl<sub>3</sub>)** δ 7.95 – 7.87 (m, 2H), 7.80 – 7.72 (m, 2H), 7.45 (s, 1H), 2.25 (s, 3H) ppm.

## 1-([1,2,3]Triazolo[1,5-*a*]pyridin-3-yl)-2,2,2-trifluoroethanone **306**



Tosyl azide (0.407 g, 2.06 mmol) was added in small portions to a solution of 1,1,1-trifluoro-3-(pyridin-2-yl)propan-2-one **304** (0.1 g, 0.53 mmol) and DBU (97 mg, 0.64 mmol) in dry acetonitrile (3 mL) at 0 °C under nitrogen. The reaction mixture was allowed to warm up to room temperature and was stirred overnight. The reaction mixture was diluted with ether (20 mL) and washed with water (2 x 25 mL) and brine (25 mL). The organic layer was dried over MgSO<sub>4</sub>, filtered and concentrated under reduced pressure to yield a white solid (0.41 g). The solid was dissolved in dichloromethane and left to sit at -20 °C overnight and 1-([1,2,3]triazolo[1,5-*a*]pyridin-3-yl)-2,2,2-trifluoroethanone **306** crystallised out as a white solid (0.1 g, 88%).

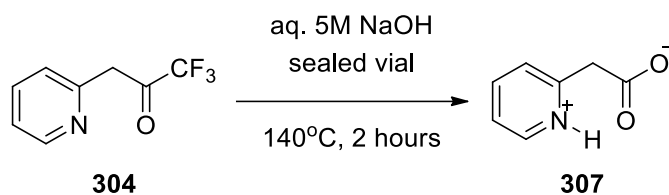
**<sup>1</sup>H NMR (400 MHz, CDCl<sub>3</sub>)** δ 8.97 (dt, *J* = 6.9, 1.1 Hz, 1H), 8.45 (dt, *J* = 8.8, 1.1 Hz, 1H), 7.79 (ddd, *J* = 8.8, 6.9, 1.1 Hz, 1H), 7.34 (dd, *J* = 6.9, 1.1 Hz, 1H) ppm.

**<sup>13</sup>C NMR (101 MHz, CDCl<sub>3</sub>)** δ 173.99 (C), 136.55 (C), 132.62 (CH), 131.85 (C), 126.79 (CH), 119.70 (CH), 118.00 (CH), 115.10 (C) ppm.

**HRMS (Orbitrap) m/z:** [M+H]<sup>+</sup> C<sub>8</sub>H<sub>4</sub>F<sub>3</sub>N<sub>3</sub>O requires 216.0378, found 216.0378

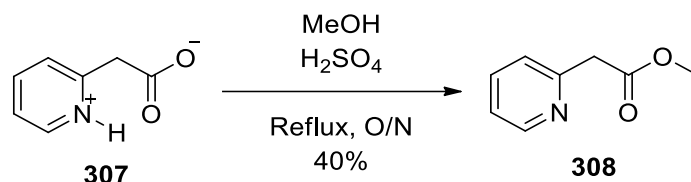
**ATR IR** cm<sup>-1</sup> 1680 (C=O stretch), 1515 (C-H aromatic), 1145 (C-O stretch)

## 2-(Pyridin-1-ium-2-yl)acetate **307**



1,1,1-Trifluoro-3-(pyridin-2-yl)propan-2-one **304** (0.24 g, 1.26 mmol) was dissolved in aqueous 5M sodium hydroxide solution (20 mL) and stirred in a sealed vial at 140 °C for 2 hours. The reaction mixture was allowed to cool down to room temperature, then was diluted with water (100 mL) and acidified with aqueous 32% v/v HCl solution. The mixture was extracted with ether (50 mL) and the aqueous layer was concentrated under reduced pressure to yield 2-(pyridin-1-ium-2-yl)acetate **307** as a salt mixture used directly in the next experiment.

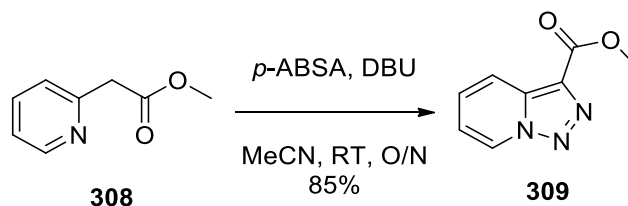
## Methyl 2-(pyridin-2-yl)acetate **308**



The forgoing 2-(pyridin-1-ium-2-yl)acetate **307** in a salt mixture was added to a solution of concentrated sulphuric acid (1 mL) in methanol (25 mL) and stirred at ~80 °C overnight. The reaction mixture was concentrated under reduced pressure, neutralised with aqueous 10 wt.% sodium bicarbonate solution (50 mL) and extracted with ethyl acetate (100 mL). The organic layer was washed with brine (100 mL), dried over MgSO<sub>4</sub>, filtered and concentrated under reduced pressure to yield methyl 2-(pyridin-2-yl)acetate **308** as white solid (0.758 g, 40% over 2 steps). The NMR spectrum matched the data of Allen et al.<sup>313</sup>

<sup>1</sup>H NMR (400 MHz, CDCl<sub>3</sub>) δ 8.48 (ddd, *J* = 4.9, 1.9, 1.0 Hz, 1H), 7.58 (dd, *J* = 7.7, 1.9 Hz, 1H), 7.22 (dt, *J* = 7.8, 1.0 Hz, 1H), 7.11 (ddd, *J* = 7.6, 4.9, 1.0 Hz, 1H), 3.79 (s, 2H), 3.65 (s, 3H) ppm.

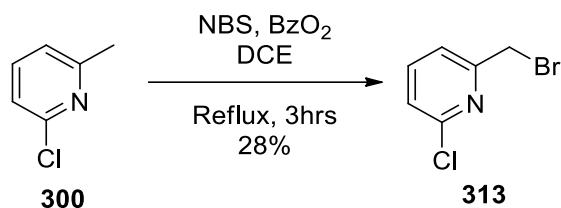
## Methyl [1,2,3]triazolo[1,5-*a*]pyridine-3-carboxylate **309**



*p*-ABSA (41 mg, 0.17 mmol) was added in small portions to a solution of methyl 2-(pyridin-2-yl)acetate **308** (25.8 mg, 0.171 mmol) and DBU (29.3 mg, 0.192 mmol) in dry acetonitrile (10 mL) at 0 °C under nitrogen. The reaction mixture was allowed to warm up to room temperature and was stirred overnight, then the reaction mixture was diluted with dichloromethane (20 mL) and washed with water (2 x 20 mL) and brine (20 mL). The organic layer was dried over MgSO<sub>4</sub>, filtered and concentrated under reduced pressure to yield methyl [1,2,3]triazolo[1,5-*a*]pyridine-3-carboxylate **309** as pale yellow solid (40.7 mg, 85%). The NMR spectrum matched the data of Chuprakov et al.<sup>257</sup>

<sup>1</sup>H NMR (400 MHz, CDCl<sub>3</sub>) δ 8.83 (dt, *J* = 6.9, 1.1 Hz, 1H), 8.27 (dt, *J* = 8.9, 1.1 Hz, 1H), 7.55 (ddd, *J* = 8.9, 6.9, 1.1 Hz, 1H), 7.16 (dd, *J* = 6.9, 1.1 Hz, 1H), 4.04 (s, 3H) ppm.

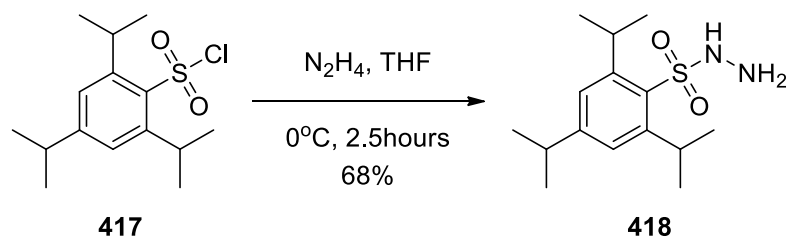
## 2-(Bromomethyl)-6-chloropyridine **313**



2-Chloro-6-methylpyridine **300** (7.12 g, 55.8 mmol), *N*-bromosuccinimide (9.91 g, 55.7 mmol) and benzoyl peroxide (1.31 g, 5.41 mmol) in dichloroethane (170 mL) were heated at reflux (~85 °C) for 3 hours under nitrogen. The reaction mixture was allowed to cool down to room temperature, then washed with aqueous 5 wt.% sodium hydroxide solution (2 x 170 mL), water (170 mL) and brine (170 mL), then dried over MgSO<sub>4</sub>, filtered and concentrated under reduced pressure to yield an orange oil (13.7 g). The oil was purified by flash chromatography (10:90 ethyl acetate:petroleum spirits) and (10:90 acetone:petroleum spirits) to yield 2-(bromomethyl)-6-chloropyridine **313** as a colourless solid (3.25 g, 28%). The NMR spectrum matched the data of Jaafar et al.<sup>315</sup>

<sup>1</sup>H NMR (400 MHz, CDCl<sub>3</sub>) δ 7.66 (t, *J* = 7.7 Hz, 1H), 7.38 (dd, *J* = 7.7, 0.9 Hz, 1H), 7.26 (dd, *J* = 7.7, 0.9 Hz, 1H), 4.50 (s, 2H) ppm.

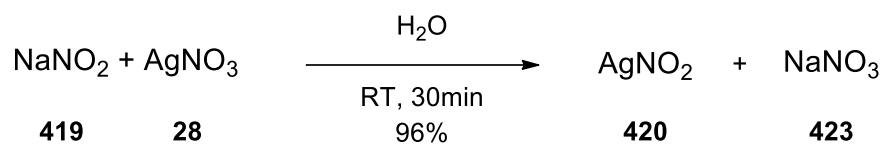
## 2,4,6-Triisopropylbenzenesulfonylhydrazide **418**



Hydrazine hydrate (5.37 g, 0.168 mol) was added dropwise to a solution of 2,4,6-triisopropylbenzene-1-sulfonyl chloride **417** (9.4 g, 31 mmol) in dry tetrahydrofuran (50 mL) at 0 °C and stirred for 2.5 hours. The reaction mixture was diluted with ice-cold ethyl acetate (100 mL) and washed with ice-cold aqueous 10 wt.% sodium chloride solution (5 x 75 mL). The organic extract was dried over MgSO<sub>4</sub>, filtered and concentrated under reduced pressure to yield a yellow solid. The residue was extracted with petroleum spirits (5 x 100 mL) and filtered to yield 2,4,6-triisopropylbenzenesulfonylhydrazide **418** as a pale yellow solid (6.30 g, 68%). The NMR spectrum matched the data of Pattabiraman et al.<sup>380</sup>

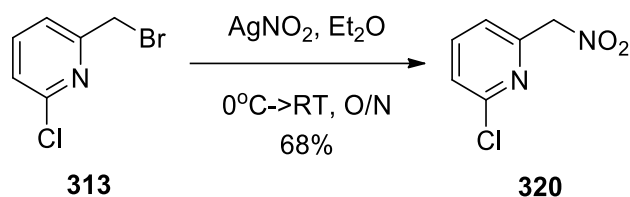
<sup>1</sup>H NMR (400 MHz, CDCl<sub>3</sub>) δ 7.20 (s, 2H), 4.15 (h, *J* = 6.9 Hz, 2H), 2.91 (p, *J* = 6.9 Hz, 1H), 1.34 – 1.28 (m, 6H), 1.29 – 1.25 (m, 12H) ppm.

## Silver nitrite **420**



Silver nitrate **419** (17.0 g, 0.1 mol) was added in portions to a solution of sodium nitrite **28** (7.60 g, 0.11 mol) in water (75 mL) in dark environment (foiled flask), then stirred at room temperature for 30 minutes. The mixture was filtered, and the residue was washed with water (3 x 50 mL) and MeOH (50 mL). The residue was dried to yield silver nitrite **420** as a lime solid (14.8 g, 96%).

## 2-Chloro-6-(nitromethyl)pyridine **320**



Silver nitrite **420** (0.41 g, 2.67 mmol) in diethyl ether (25 mL) was stirred at  $0^\circ\text{C}$  for 15 minutes in foil covered flask. 2-(Bromomethyl)-6-chloropyridine **313** (0.503 g, 2.45 mmol) was diluted in ether (5 mL) and added dropwise to the silver nitrite solution at  $0^\circ\text{C}$ . The reaction mixture was allowed to warm up to room temperature and stirred overnight. The solution was filtered through celite and extracted with ethyl acetate (50 mL). The organic solution was washed with water (50 mL), dried over  $\text{MgSO}_4$ , filtered and concentrated under reduced pressure to yield an orange oil (0.723 g). The oil was purified by flash chromatography (10:90, ethyl acetate:petroleum spirits) to yield 2-chloro-6-(nitromethyl)pyridine **320** as an orange oil (0.288 g, 68%).

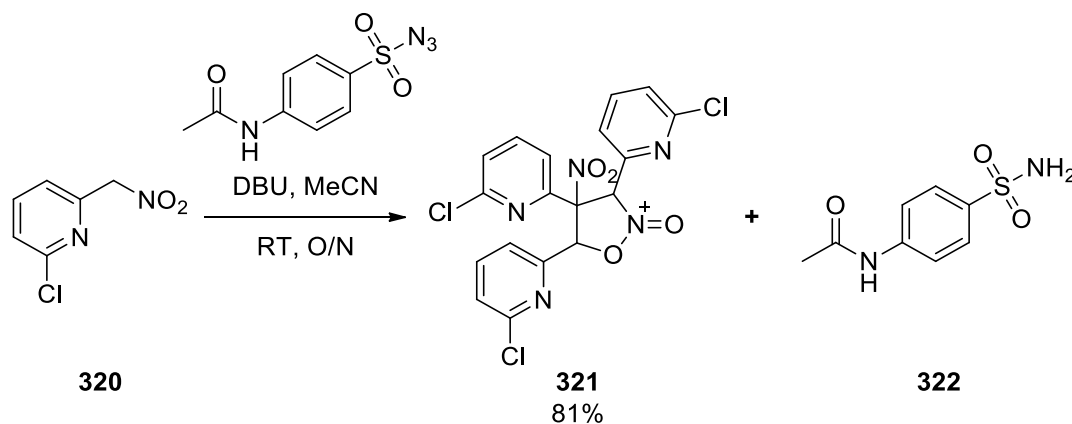
**$^1\text{H}$  NMR (400 MHz,  $\text{CDCl}_3$ )**  $\delta$  7.77 (t,  $J = 7.8$  Hz, 1H), 7.44 – 7.39 (m, 2H), 5.59 (s, 2H) ppm.

**$^{13}\text{C}$  NMR (101 MHz,  $\text{CDCl}_3$ )**  $\delta$  151.72 (C), 149.67 (C), 139.91 (CH), 125.41 (CH), 123.36 (CH), 80.02 ( $\text{CH}_2$ ) ppm.

**HRMS (Orbitrap) m/z:**  $[\text{M}+\text{H}]^+$   $\text{C}_6\text{H}_5\text{ClN}_2\text{O}_2$  requires 173.0112, found 173.0111

**ATR IR**  $\text{cm}^{-1}$  1551 (N-O asymm. stretch), 1371 (N-O symm. stretch)

**3,4,5-tris(6-chloropyridin-2-yl)-4-nitroisoxazolidin-2-olate 195**  
**(tentative)**



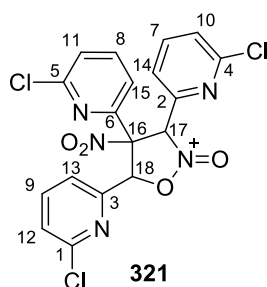
*p*-ABSA **416** (0.1735 g, 0.72 mmol) was added in small portions to a solution of 2-chloro-6-(nitromethyl)pyridine **320** (0.1235 g, 0.72 mmol) and DBU (0.133 g, 0.87 mmol) in dry acetonitrile (12 mL) under nitrogen. The reaction mixture was stirred at room temperature overnight, then concentrated under reduced pressure. The residue was dissolved in dichloromethane (20 mL) and washed with water (2 x 20 mL) and brine (20 mL). The organic layer was dried over MgSO<sub>4</sub>, filtered and concentrated under reduced pressure to yield a red oil (0.1768 g). The oil was purified by titration (petroleum spirits and ethyl acetate) to yield trimer **321** as a light yellow oil (0.0997 mg, 81%).

**<sup>1</sup>H NMR (400 MHz, CDCl<sub>3</sub>)** δ 8.44 (dd, *J* = Hz, 1H), 7.72 (t, *J* = Hz, 1H), 7.68 (t, *J* = Hz, 1H), 7.65 (t, *J* = Hz, 1H), 7.58 (dt, *J* = Hz, 1H), 7.56 (dd, *J* = Hz, 1H), 7.31 (dt, *J* = Hz, 1H), 7.23 (dd, *J* = Hz, 1H) and 7.17 (dd, *J* = Hz, 1H), 5.97 (d, *J* = Hz, 1H), 5.55 (d, *J* = Hz, 1H) ppm.

Coupling constants undetermined due to signals overlap

**<sup>13</sup>C NMR (101 MHz, CDCl<sub>3</sub>)** δ 158.46, 158.44, 151.87, 151.52, 150.69, 146.45, 139.93, 139.46, 139.23, 124.53, 125.12, 123.80, 123.22, 120.34, 119.12, 116.58, 80.60, 57.06 ppm.

**HRMS (Orbitrap) m/z:** [M+H]<sup>+</sup> not found

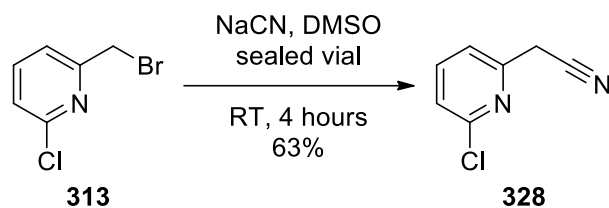


Scheme 127 Proposed structure of 3,4,5-tris(6-chloropyridin-2-yl)-4-nitrosoxazolidin-2-olate **321**

Table 12 NMR spectra analysis of the compound **321**

| C# | <sup>13</sup> C | DEPT | HSQC | <sup>1</sup> H | COSY                            | HMBC   |
|----|-----------------|------|------|----------------|---------------------------------|--|
| 1  | 158.46          | C    | -    | -              | -                               | 5.55 (18#), 7.65 (9#)                            |
| 2  | 158.44          | C    | -    | -              | -                               | 5.97 (17#), 7.72 (7#)                            |
| 3  | 151.87          | C    | -    | -              | -                               | 5.55 (18#)                                       |
| 4  | 151.52          | C    | -    | -              | -                               | None observed                                    |
| 5  | 150.69          | C    | -    | -              | -                               | 8.44 (14#), 7.68 (8#),                           |
| 6  | 146.45          | C    | -    | -              | -                               | 8.44 (14#), 7.68 (8#),<br>7.17 (11#), 5.55 (18#) |
| 7  | 139.93          | CH   | 7.72 | t              | 7.31 (s, 10#)                   | 7.31 (10#), 5.97 (17#),                          |
| 8  | 139.46          | CH   | 7.68 | t              | 8.44 (s, 14#),<br>7.17 (s, 11#) | 8.44 (14#), 5.55 (18#),<br>7.17 (11#),           |
| 9  | 139.23          | CH   | 7.65 | t              | 7.23 (s, 12#)                   | 7.23 (12#),                                      |
| 10 | 124.53          | CH   | 7.31 | dt             | 7.72 (s, 7#)                    | 7.72 (7#), 7.58 (15#),                           |
| 11 | 125.12          | CH   | 7.17 | dd             | 7.68 (s, 8#),<br>8.44 (w, 14#)  | 8.44 (14#),                                      |
| 12 | 123.80          | CH   | 7.23 | dd             | 7.65 (s, 9#)                    | 7.56 (13#),                                      |
| 13 | 123.22          | CH   | 7.56 | dd             | ?                               | 5.55 (18#), 7.23 (12#),                          |
| 14 | 120.34          | CH   | 8.44 | dd             | 7.68 (s, 8#),<br>7.17 (w, 11#)  | 7.68 (8#), 7.17 (11#),<br>5.55 (18#)             |
| 15 | 119.12          | CH   | 7.58 | dt             | ?                               | 7.31 (10#), 5.97 (17#),                          |
| 16 | 116.58          | C    | -    | -              | -                               | 8.44 (14#), 7.68 (8#),<br>5.97 (17#), 5.55 (18#) |
| 17 | 80.60           | CH   | 5.97 | d              | 5.55 (18#)                      | 7.72 (7#), 7.58 (15#),<br>7.31 (10#), 5.55 (18#) |
| 18 | 57.06           | CH   | 5.55 | d              | 5.97 (17#)                      | 7.65 (9#), 7.56 (13#),<br>7.23 (12#), 5.97 (17#) |

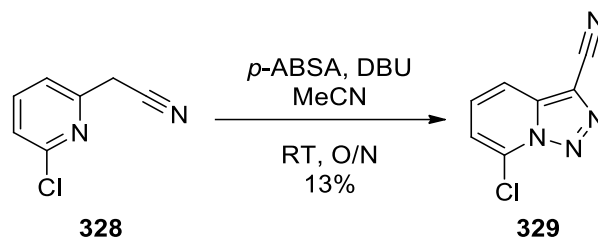
## 2-(6-Chloropyridin-2-yl)acetonitrile **328**



A pressure vessel was charged with 2-(bromomethyl)-6-chloropyridine **313** (0.5 g, 2.44 mmol) and sodium cyanide (0.3 g, 6.12 mmol) in dry dimethyl sulfoxide (5 mL) under nitrogen and stirred at room temperature for 4 hours. The reaction mixture was diluted with ethyl acetate (50 mL) and washed with water (3 x 50 mL) and saturated aqueous copper sulfate solution (50 mL). The organic layer was dried over MgSO<sub>4</sub>, filtered and concentrated under reduced pressure to yield an orange oil (0.319 g). The oil was purified by flash chromatography (5:47.5:47.5, ethyl acetate:toluene:petroleum spirits) to yield 2-(6-chloropyridin-2-yl)acetonitrile **328** as an orange solid (0.233 g, 63%). The NMR spectrum matched the data of Blagg.<sup>319</sup>

**<sup>1</sup>H NMR (400 MHz, CDCl<sub>3</sub>)**  $\delta$  7.72 (t,  $J = 7.8$  Hz, 1H), 7.42 (dd,  $J = 7.8, 0.8$  Hz, 1H), 7.33 (dd,  $J = 7.8, 0.8$  Hz, 1H), 3.93 (s, 2H) ppm.

## 7-Chloro-[1,2,3]triazolo[1,5-*a*]pyridine-3-carbonitrile **329**



*p*-ABSA **416** (0.315 g, 1.32 mmol) was added in small portions to a solution of 2-(6-chloropyridin-2-yl)acetonitrile **328** (0.2 g, 1.32 mmol) and DBU (0.235 g, 1.54 mmol) in dry acetonitrile (3 mL) under nitrogen. The reaction mixture was stirred at room temperature overnight, then concentrated under reduced pressure. The residue was dissolved in dichloromethane (20 mL) and washed with water (2 x 20 mL) and brine (20 mL). The organic layer was dried over MgSO<sub>4</sub>, filtered and concentrated under reduced pressure to yield a red oil (0.28 g). The oil was purified by titration (petroleum spirits and ethyl acetate) to yield methyl [1,2,3]triazolo[1,5-*a*]pyridine-3-carboxylate **329** as a light yellow oil (30 mg, 13%).

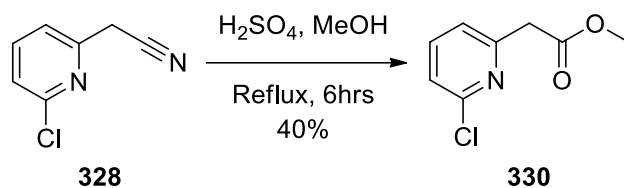
**<sup>1</sup>H NMR (400 MHz, CDCl<sub>3</sub>)** δ 7.91 (d, *J* = 8.8 Hz, 1H), 7.63 (dd, *J* = 8.8, 7.2 Hz, 1H), 7.32 (dd, *J* = 7.2, 0.8 Hz, 1H) ppm.

**<sup>13</sup>C NMR (101 MHz, CDCl<sub>3</sub>)** δ 130.65 (CH), 129.15 (CH), 119.62 (C), 117.07 (CH), 115.27 (2 x C), 111.51 (C) ppm.

**HRMS (Orbitrap) m/z:** [M+H]<sup>+</sup> C<sub>7</sub>H<sub>3</sub>ClN<sub>4</sub> requires 179.0119, found 179.0119

**ATR IR** cm<sup>-1</sup> 2240 (C≡N), 2127 (C=N), 1504 (C-C aromatic stretch), 798 (C-Cl)

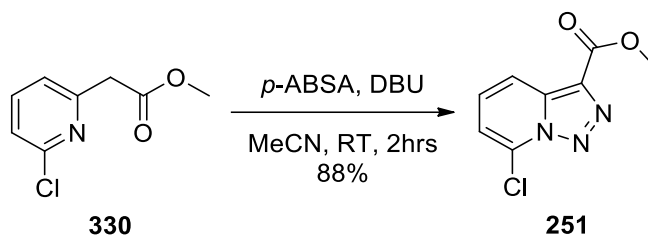
## Methyl 2-(6-chloropyridin-2-yl)acetate **330**



2-(6-Chloropyridin-2-yl)acetonitrile **328** (0.5 g, 3.28 mmol) was added to a solution of concentrated sulphuric acid (2.2 mL) in methanol (7.2 mL) and stirred at ~95 °C for 6 hours. The reaction mixture was neutralised with aqueous 10 wt.% sodium bicarbonate solution (50 mL) and extracted with ethyl acetate (100 mL). The organic layer was washed with brine (100 mL), dried over MgSO<sub>4</sub>, filtered and concentrated under reduced pressure to yield a yellow oil (0.61 g). The oil was purified by flash chromatography (10:90, ethyl acetate: petroleum spirits) to yield methyl 2-(pyridin-2-yl)acetate **330** as a white solid (0.24 g, 40%). The NMR spectrum matched the data of Chuprakov et al.<sup>257</sup>

**<sup>1</sup>H NMR (400 MHz, CDCl<sub>3</sub>)** δ 7.63 (dd, *J* = 8.0, 7.5 Hz, 1H), 7.26 – 7.22 (m, 2H), 3.84 (s, 2H), 3.72 (s, 3H) ppm.

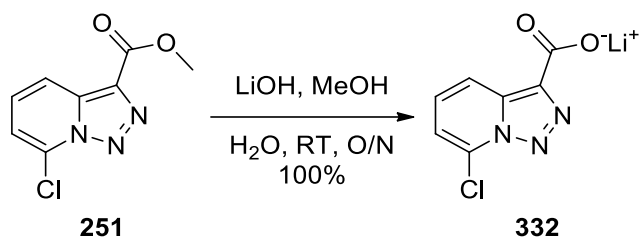
## Methyl 7-chloro-[1,2,3]triazolo[1,5-*a*]pyridine-3-carboxylate **251**



*p*-ABSA **416** (0.129 g, 0.54 mmol) was added in small portions to a solution of methyl 2-(6-chloropyridin-2-yl)acetate **330** (0.1 g, 0.54 mmol) and DBU (90 mg, 0.59 mmol) in dry acetonitrile (10 mL) at 0 °C under nitrogen. The reaction mixture was allowed to warm up to room temperature and was stirred overnight. The reaction mixture was diluted with dichloromethane (20 mL) and washed with water (2 x 20 mL) and brine (20 mL). The organic layer was dried over MgSO<sub>4</sub>, filtered and concentrated under reduced pressure to yield methyl 7-chloro-[1,2,3]triazolo[1,5-*a*]pyridine-3-carboxylate **251** as a pale yellow solid (0.10 g, 88%). The NMR spectrum matched the data of Chuprakov et al.<sup>257</sup>

<sup>1</sup>H NMR (400 MHz, CDCl<sub>3</sub>) δ 8.24 (s, 1H), 7.53 (dd, *J* = 8.7, 7.3 Hz, 1H), 7.22 (s, 1H), 4.02 (s, 3H) ppm.

## Lithium 7-chloro-[1,2,3]triazolo[1,5-*a*]pyridine-3-carboxylate **332**

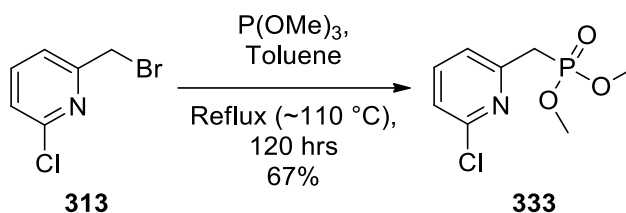


Methyl 7-chloro-[1,2,3]triazolo[1,5-*a*]pyridine-3-carboxylate **251** (50 mg, 0.24 mmol) and lithium hydroxide (5.7 mg, 0.24 mmol) were added to a solution of methanol (2 mL) and water (0.6 mL), the reaction mixture was stirred at room temperature overnight, and then concentrated under reduced pressure to yield lithium 7-chloro-[1,2,3]triazolo[1,5-*a*]pyridine-3-carboxylate **332** as a white solid (48 mg, 100%)

**<sup>1</sup>H NMR (400 MHz, D<sub>2</sub>O)** δ 8.05 (dd, *J* = 8.8, 1.1 Hz, 1H), 7.43 (dd, *J* = 8.8, 7.3 Hz, 1H), 7.24 (dd, *J* = 7.3, 1.1 Hz, 1H) ppm.

**ATR IR** cm<sup>-1</sup> 1627 (C=O stretch)

## Dimethyl (6-chloropyridin-2-yl)phosphonate **333**



2-(Bromomethyl)-6-chloropyridine **313** (1.30 g, 6.30 mmol) and trimethyl phosphite (0.74 g, 6.0 mmol) in toluene (10 mL) were heated at reflux ( $\sim 110^\circ\text{C}$ ) for 120 hours and then concentrated under reduced pressure to yield a yellow solid. The solid was purified by flash chromatography (100% ethyl acetate) to yield dimethyl (6-chloropyridin-2-yl)phosphonate **333** as yellow solid (0.99 g, 67%).

**$^1\text{H NMR}$  (400 MHz,  $\text{CDCl}_3$ )**  $\delta$  7.62 (dd,  $J = 7.7, 0.8$  Hz, 1H), 7.32 (ddd,  $J = 7.7, 2.4, 0.8$  Hz, 1H), 7.23 (ddd,  $J = 7.7, 2.4, 0.8$  Hz, 1H), 3.80 – 3.73 (m, 6H), 3.43 (s, 1H), 3.38 (s, 1H) ppm.

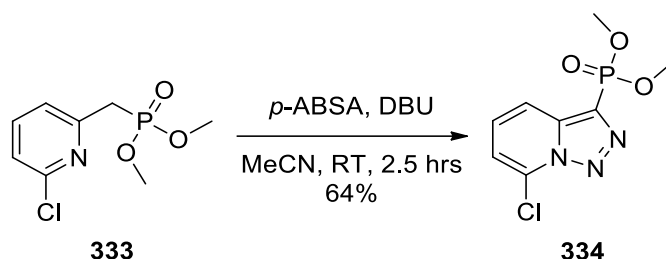
**$^{13}\text{C NMR}$  (101 MHz,  $\text{CDCl}_3$ )**  $\delta$  153.38 (C), 151.01 (C), 139.37 (CH), 122.93 (CH), 122.77 (CH), 53.14 (2 x  $\text{CH}_3$ ), 36.12 (CH), 34.77 (CH) ppm.

**HRMS (Orbitrap) m/z:**  $[\text{M}+\text{H}]^+$   $\text{C}_8\text{H}_{11}\text{ClNO}_3\text{P}$  requires 236.0238, found 236.0231

**ATR IR**  $\text{cm}^{-1}$  3469 (P-O), 1021 (P-O)

## Dimethyl (7-chloro-[1,2,3]triazolo[1,5-*a*]pyridin-3-yl)phosphonate

334



DBU (1.59 g, 10.5 mmol) was added to a solution of dimethyl (6-chloropyridin-2-yl)phosphonate **333** (2.24 g, 9.51 mmol) in dry acetonitrile (120 mL) at 0 °C under nitrogen developing a bright red colour and was stirred for 2.5 hours. *p*-ABSA (2.29 g, 9.51 mmol) was added in small portions to the reaction mixture, allowed to warm up to room temperature and was stirred overnight. The reaction mixture was diluted with dichloromethane (25 mL) and washed with water (2 x 25 mL) and brine (25 mL). The organic layer was dried over MgSO<sub>4</sub>, filtered and concentrated under reduced pressure to yield a brown solid. The solid was purified by flash chromatography (1:1 ethyl acetate:petroleum spirits) to yield dimethyl (7-chloro-[1,2,3]triazolo[1,5-*a*]pyridin-3-yl)phosphonate **334** as pale yellow solid (1.61 g, 64%).

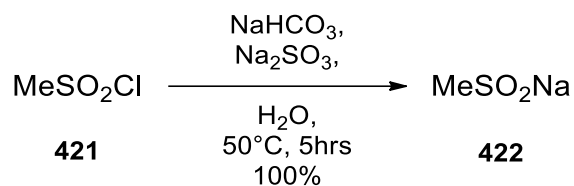
**<sup>1</sup>H NMR (400 MHz, CDCl<sub>3</sub>)** δ 8.20 (d, *J* = 8.8 Hz, 1H), 7.46 (dd, *J* = 8.8, 7.2 Hz, 1H), 7.21 (d, *J* = 7.2 Hz, 1H), 3.88 (s, 3H), 3.85 (s, 3H) ppm.

**<sup>13</sup>C NMR (101 MHz, CDCl<sub>3</sub>)** δ 140.28 (C), 139.92 (C), 129.04 (CH), 128.38 (C), 117.56 (CH), 116.36 (CH), 53.73 (CH<sub>3</sub>), 53.68 (CH<sub>3</sub>) ppm.

**HRMS (Orbitrap) m/z:** [M+H]<sup>+</sup> C<sub>8</sub>H<sub>9</sub>ClN<sub>3</sub>O<sub>3</sub>P requires 262.0143, found 262.0143

**ATR IR** cm<sup>-1</sup> 3469 (broad, P-O), 1025 (P-O)

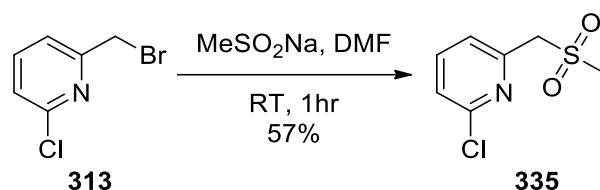
## Sodium methanesulfonate **422**



Sodium sulfite (5.00 g, 39.7 mmol), sodium bicarbonate (3.33 g, 39.7 mmol) and methylsulfonyl chloride **421** (4.54 g, 19.8 mmol) were dissolved in DI water (20 mL) and stirred for 5 hours at 50 °C. The reaction was cooled to room temperature and concentrated under reduced pressure, then dissolved in ethanol, filtered and concentrated under reduced pressure again to yield sodium methanesulfonate **422** (4.80 g, 100%). The NMR spectrum matched the data of Brink and Mattes.<sup>381</sup>

**<sup>1</sup>H NMR (400 MHz, D<sub>2</sub>O) δ 2.75 (s)**

## 2-Chloro-6-((methylsulfonyl)methyl)pyridine **335**



Sodium methanesulfinate (0.27 g, 2.64 mmol) was added to a solution of 2-(bromomethyl)-6-chloropyridine **313** (0.555 g, 2.69 mmol) in dimethylformamide (5 mL) and was stirred at room temperature for 1 hour. The reaction mixture was quenched with water (25 mL) and extracted with ethyl acetate (3 x 25 mL). The combined organic layers were dried over MgSO<sub>4</sub>, filtered and concentrated under reduced pressure to yield a yellow solid (0.4872 g). The solid was purified by flash chromatography (20:80 ethyl acetate:petroleum spirits) to yield pure 2-chloro-6-((methylsulfonyl)methyl)pyridine **335** as a light yellow solid (0.314 g, 57%).

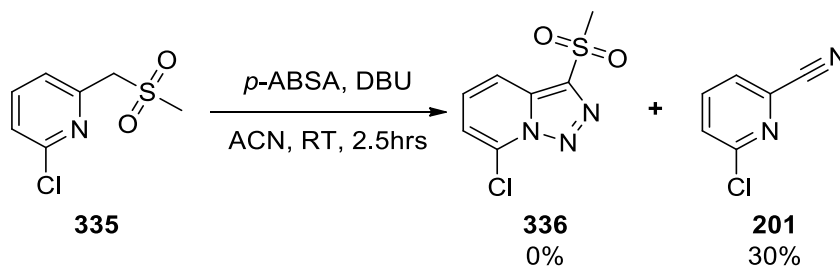
**<sup>1</sup>H NMR (400 MHz, CDCl<sub>3</sub>)** δ 7.73 (dd, *J* = 7.7 Hz, 1H), 7.63 (dd, *J* = 7.7, 0.7 Hz, 1H), 7.43 (dd, *J* = 7.7, 0.7 Hz, 1H), 4.38 (s, 2H), 2.95 (t, *J* = 0.7 Hz, 3H) ppm.

**<sup>13</sup>C NMR (101 MHz, CDCl<sub>3</sub>)** δ 151.54 (C), 150.26 (C), 140.05 (CH), 124.62 (2 x CH), 62.59 (CH<sub>2</sub>), 40.42 (CH<sub>3</sub>) ppm.

**HRMS (Orbitrap) m/z:** [M+H]<sup>+</sup> C<sub>7</sub>H<sub>8</sub>ClNO<sub>2</sub>S requires 206.0037, found 206.0034

**ATR IR** cm<sup>-1</sup> 1296 (S=O), 1115 (S=O)

**7-Chloro-3-(methylsulfonyl)-[1,2,3]triazolo[1,5-*a*]pyridine 336  
(attempted)**



DBU (0.087 g, 0.571 mmol) was added to a solution of 2-chloro-6-((methylsulfonyl)methyl)pyridine **335** (0.1 g, 0.522 mmol) in dry acetonitrile (10 mL) at 0 °C under nitrogen developing a bright red colour and was stirred for 2.5 hours. *p*-ABSA (0.125 g, 0.520 mmol) was added in small portions to the reaction mixture, allowed to warm up to room temperature and was stirred overnight. The reaction mixture was diluted with dichloromethane (25 mL) and washed with water (2 x 25 mL) and brine (25 mL). The organic layer was dried over MgSO<sub>4</sub>, filtered and concentrated under reduced pressure to yield a brown solid. The solid was purified by titration (petroleum spirits) to yield 6-chloropicolinonitrile **201** as pale yellow solid (0.038 g, 30%). The NMR spectrum matched the data of Tsukamoto et al.<sup>324</sup>

<sup>1</sup>H NMR (400 MHz, CDCl<sub>3</sub>) δ 7.82 (dd, *J* = 8.1, 7.5 Hz, 1H), 7.65 (dd, *J* = 7.5, 0.9 Hz, 1H), 7.58 (dd, *J* = 8.1, 0.9 Hz, 1H) ppm.

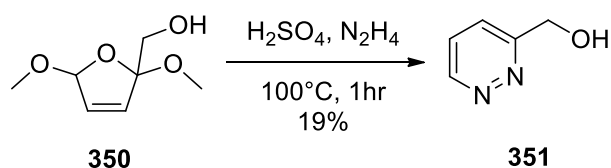
## (2,5-Dimethoxy-2,5-dihydrofuran-2-yl)methanol **350**



Furfuryl alcohol **349** (4.3 mL, 50 mmol) was added to a solution of sodium bicarbonate (7.95 g, 75 mmol) in dry methanol (50 mL) at  $-40 \text{ }^\circ\text{C}$  (acetonitrile/liquid  $\text{N}_2$  bath). Bromine (2.6 mL, 53 mmol) in dry methanol (20 mL) was added dropwise to the reaction solution over 10 minutes. The reaction mixture was allowed to warm up to room temperature and stirred for 2 hours. Saturated sodium bicarbonate solution was added until pH 8 was achieved, then the reaction mixture was filtered through celite. The filtrate was diluted with water (100 mL) and extracted with DCM (5 x 100 mL). The combined organic layers were dried over  $\text{MgSO}_4$ , filtered and concentrated under reduced pressure to yield (2,5-dimethoxy-2,5-dihydrofuran-2-yl)methanol **350** as a mixture of the two diastereoisomers in a 6:10 ratio (3.63 g, 45%). The NMR spectrum matched the data of Hammoud et al.<sup>328</sup>

**$^1\text{H}$  NMR (400 MHz,  $\text{CDCl}_3$ )**  $\delta$  6.13 (dd, 1H), 5.99 (dd, 1H), 5.75, 5.52 (t,  $J = 1.2 \text{ Hz}$ , 1H), 3.73 – 3.57 (m, 2H), 3.50 (s, 3H), 3.22 (s, 3H) ppm.

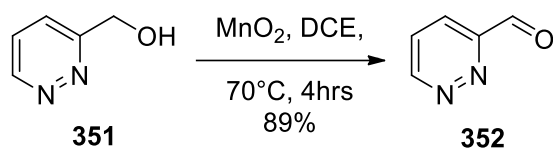
## Pyridazin-3-ylmethanol **351**



(2,5-Dimethoxy-2,5-dihydrofuran-2-yl)methanol **350** (3.63 g, 22.6 mmol) was added to a boiling concentrated sulphuric acid (16 mL) and stirred for 1 minute, then cooled rapidly in an ice bath. Hydrazine hydrate (3.66 mL, 114 mmol) was added to the cooled reaction mixture and then boiled for 20 minutes. The mixture was cooled to room temperature and neutralised with potassium carbonate (16 g, 116 mmol), then extracted with isopropanol:ethyl acetate mixture (10:90, 3 x 100 mL). The combined organic extracts were dried over MgSO<sub>4</sub>, filtered and concentrated under reduced pressure to yield a yellow oil. The oil was purified by flash chromatography (100% ethyl acetate) to yield pyridazin-3-ylmethanol **351** as a white solid (0.47 g, 19%). The NMR spectrum matched the data of Hammoud et al.<sup>328</sup>

**<sup>1</sup>H NMR (400 MHz, CDCl<sub>3</sub>)** δ 9.06 (dd, *J* = 4.9, 1.7 Hz, 1H), 7.62 (dd, *J* = 8.5, 1.7 Hz, 1H), 7.48 (dd, *J* = 8.5, 4.9 Hz, 1H), 4.97 (s, 2H) ppm.

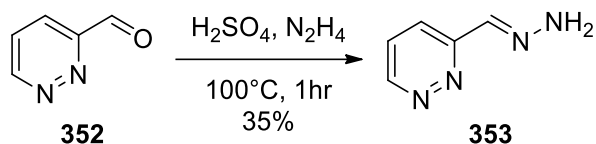
## Pyridazine-3-carbaldehyde **352**



Pyridazin-3-yl-methanol **351** (0.11 g, 1 mmol) and activated manganese dioxide (0.435 g, 5 mmol) were added to dichloroethane (5 mL) and heated at 70 °C for 4 hours. The reaction mixture was allowed to cool to room temperature, filtered through celite and concentrated under reduced pressure to yield pyridazine-3-carbaldehyde **352** (96 mg, 89%) as a colourless oil. The NMR spectrum matched the data of Tsukamoto et al.<sup>329</sup>

**<sup>1</sup>H NMR (400 MHz, CDCl<sub>3</sub>)** δ 10.36 (d, *J* = 0.9 Hz, 1H), 9.35 (dd, *J* = 5.0, 1.8 Hz, 1H), 8.03 (dd, *J* = 8.4, 1.8 Hz, 1H), 7.69 (ddd, *J* = 8.4, 5.0, 0.9 Hz, 1H) ppm.

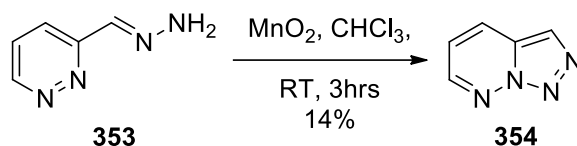
### **(E)-3-(Hydrazonomethyl)pyridazine 353**



Pyridazine-3-carbaldehyde **352** (0.23 g, 2.13 mmol) and concentrated sulphuric acid (1 drop) in hydrazine hydrate (15 mL, 468 mmol) were heated at 100 °C for 1 hour. The reaction mixture was concentrated under reduced pressure and the residue was extracted with chloroform (50 mL). The organic solution was concentrated under reduced pressure to yield (*E*)-3-(hydrazonomethyl)pyridazine **353** as a yellow oil (92 mg, 35%). The NMR spectrum matched the data of Maury et al.<sup>327</sup>

**<sup>1</sup>H NMR (400 MHz, CDCl<sub>3</sub>)** δ 9.04 (dd, *J* = 4.9, 1.7 Hz, 1H), 8.08 (s, 1H), 7.99 (dd, *J* = 8.7, 1.7 Hz, 1H), 7.44 (ddd, *J* = 8.7, 4.9, 0.7 Hz, 1H) ppm.

## [1,2,3]Triazolo[1,5-*b*]pyridazine **354**

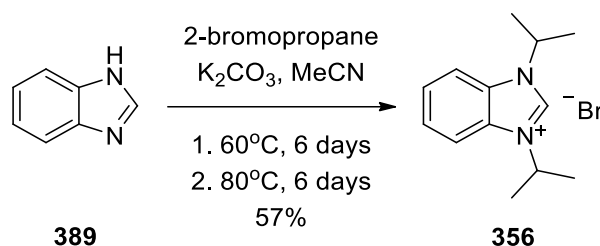


(*E*)-3-(hydrazonomethyl)pyridazine **353** (100 mg, 0.82 mmol) and activated manganese dioxide (130 mg, 1.50 mmol) in chloroform (10 mL) were stirred at room temperature for 3 hours. The reaction mixture was filtered through celite and concentrated under reduced pressure to yield [1,2,3]triazolo[1,5-*b*]pyridazine **354** as a white solid (13.7 mg, 14%). The NMR spectrum matched the data of Maury et al.<sup>327</sup>

**<sup>1</sup>H NMR (400 MHz, CDCl<sub>3</sub>)** δ 8.47 (dd, *J* = 4.3, 1.8 Hz, 1H), 8.18 (s, 1H), 8.16 (dd, *J* = 9.0, 1.8 Hz, 1H), 7.14 (dd, *J* = 9.0, 4.3 Hz, 1H) ppm.

## 7.3 DMSO

### 1,3-Diisopropylbenzimidazolium bromide **356**

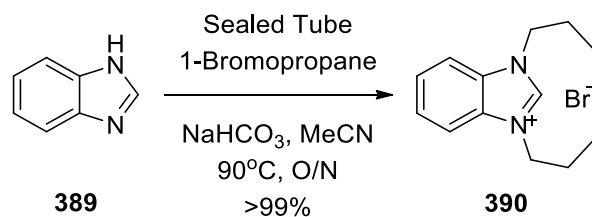


A solution of benzimidazole **389** (5.0 g, 42 mmol), potassium carbonate (6.4 g, 46 mmol) and 2-bromopropane (7.6 g, 62 mmol) in acetonitrile (20 mL) was heated at 60 °C for 6 days. It was noted large amounts of white solid residue (potassium carbonate) collected on the walls of the flask). The reaction mixture was cooled and the solvent was evaporated to form white solid; the solid was partially dissolved in ethanol (150 mL) and filtered. The combined filtrate was evaporated to form yellow oil. The oil was diluted with ethyl acetate (150 mL) and minimal amount of white solid precipitated, indicating minimal yield of product. An analysis of the solution indicated yield of the intermediate product 1-(isopropyl)-1*H*-benzo[*d*]imidazole **373**. The mixture was evaporated and placed under reaction conditions once more; dissolved in acetonitrile (20 mL) with potassium carbonate (6.4 g, 46 mmol) and 2-bromopropane (10.3 g, 84 mmol) added. The reaction mixture was heated at 80 °C for 6 days, with manual scraping of the residual solids off the walls every couple of hours during each day. The reaction mixture turned deep red over time. It was cooled and the solvent was evaporated to form red oil and white solid mixture; the mixture was diluted in ethanol (3 x 50 mL) and filtered. The combined filtrate was evaporated to form red oil. The oil was diluted with ethyl acetate (150 mL), with light yellow-green solid precipitating out. The solids were decanted and washed with ethyl acetate (5 x 50 mL) until the washings were colourless. The solids were dissolved in ethanol (50 mL) and evaporated to yield pure 1,3-Diisopropylbenzimidazolium bromide **356** as light yellow-green solid (6.81 g, 57%). The NMR spectrum matched the data of Starikova et al.<sup>366</sup>

**<sup>1</sup>H NMR (400 MHz, d<sup>6</sup> DMSO)** δ 9.80 (s, 1H), 8.18 – 8.11 (m, 2H), 7.74 – 7.66 (m, 2H), 5.06 (h, *J* = 6.7 Hz, 2H), 1.65 (d, *J* = 6.7 Hz, 12H) ppm.

**<sup>13</sup>C NMR (101 MHz, d<sup>6</sup> DMSO)** δ 139.51, 130.65, 126.49, 114.08, 50.73, 21.55 ppm.

## 1,3-Dipropyl-1*H*-benzo[*d*]imidazol-3-ium bromide **390**

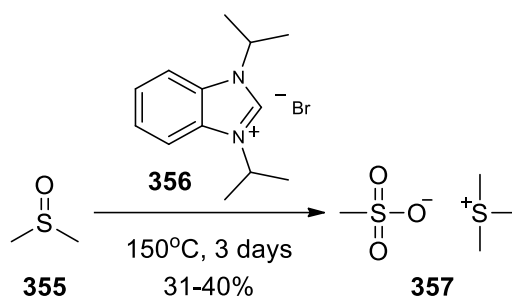


A sealed tube was charged with benzimidazole **389** (0.42 g, 3.5 mmol), sodium bicarbonate (0.61 g, 7.2 mmol) and acetonitrile (5 mL), heated at 90 °C for 1 hour and cooled to room temperature. Then 1-bromopropane (1.95 mL, 21 mmol) was added and the sealed tube was heated at 90 °C overnight. The mixture was cooled to room temperature and the solvent was concentrated under vacuum. The remaining solid residue was suspended in dichloromethane and filtered. The filtrate was concentrated under vacuum to yield the expected product **390** as white crystalline solid (1.04 g, >99%). The NMR spectrum matched the data of Gonell et al.<sup>382</sup>

**<sup>1</sup>H NMR (400 MHz, CDCl<sub>3</sub>)** δ 9.84 (s, 1H), 8.11 (dd, *J* = 3.1 Hz, 2H), 7.69 (dd, *J* = 3.1 Hz, 2H), 4.47 (t, *J* = 7.4 Hz, 4H), 1.94 (sextet, *J* = 7.4 Hz, 4H), 0.94 (t, *J* = 7.4 Hz, 6H) ppm.

**<sup>13</sup>C NMR (101 MHz, CDCl<sub>3</sub>)** δ 142.13, 131.16, 126.54, 113.73, 48.09, 22.00, 10.68 ppm.

## Trimethylsulphonium methanesulphonate **357**

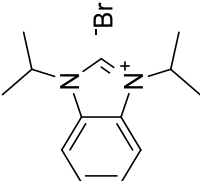
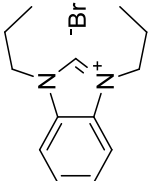
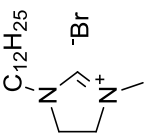


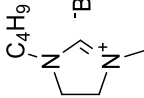
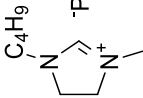
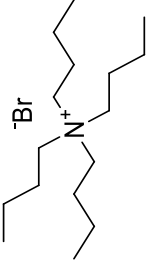
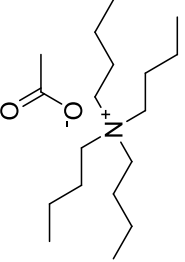
Dimethyl sulfoxide **355** (10 mL, 140.8 mmol) and diisopropylbenzimidazolium bromide **356** (0.5 g, 1.765 mmol, 1.25%) were heated in air (with double walled condenser and a CaCl<sub>2</sub> drying tube) at 150 °C for 3 days. On the second day onwards bubbling became visible in the solution and white solid started to collect on the walls of the condenser. The reaction was cooled to RT and the residue was dissolved in a minimal amount of boiling ethanol, then cooled to RT again. The reaction solution was diluted with diethyl ether (250 mL), with white solid precipitating out. The solids were filtered and washed with diethyl ether (3x25 mL) and dried in a desiccator to yield trimethylsulphonium methanesulphonate **357** as a white solid (2.5 g, 31%). The NMR spectrum matched the data of Mosset and Grée.<sup>330</sup>

<sup>1</sup>H NMR (400 MHz, d<sup>6</sup> DMSO) δ 2.86 (s, 9H), 2.41 (s, 3H) ppm.

<sup>13</sup>C NMR (101 MHz, d<sup>6</sup> DMSO) δ 39.78 (CH<sub>3</sub>), 26.13 (CH<sub>3</sub>) ppm.

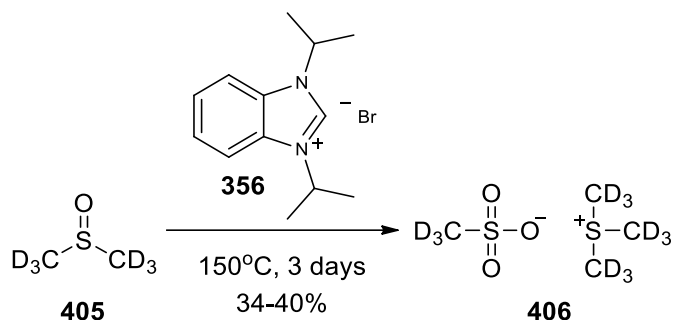
The experiment was repeated with 1/10 of the catalyst (0.05 g, 0.1765 mmol, 0.125 eq.) yielding the expected product in good yield (2.58 g, 32%).

| Catalyst used   | Catalyst amount (mol%) | Mass Recovery (g) |         |      |                          | Product yield* (%) | <sup>1</sup> H NMR signals (ppm)<br>*P = Product    | <sup>13</sup> C NMR signals# (ppm) | Notes                       |
|---|------------------------|-------------------|---------|------|--------------------------|--------------------|---|------------------------------------|-----------------------------|
|   |                        | Total             | Product | DMSO | Other (H <sub>2</sub> O) |                    |   |                                    |                             |
| None  | -                      | 2.08              | -       | 1.16 | 0.92                     | -                  | 2.54 (s, 6H, DMSO), 2.40 (s, unknown)               | 40.43 (s, DMSO-h6)                 | Unknown degradation         |
|    | 1.25                   | 2.5               | 2.5     | -    | -                        | 31                 | 2.86 (s, 9H), 2.41 (s, 3H)                          | 26.15 (s)                          |                             |
|   | 0.125                  | 2.58              | 2.58    | -    | -                        | 32                 | 2.86 (s, 9H), 2.41 (s, 3H)                          | 26.15 (s)                          |                             |
|   | 0.125                  | 3.24              | 3.24    | -    | -                        | 40                 | 2.86 (s, 9H), 2.41 (s, 3H)                          | 26.15 (s)                          |                             |
|   | 0.125 + 1 TEA          | 3.35              | 0.64    | 2.71 | -                        | 8                  | 2.85 (s, 9H), 2.54 (s, 6H, DMSO), 2.41 (s, unknown) | 40.43 (s, DMSO-h6)                 | Still bubbling when stopped |
|    | 0.125 + 0.03 BHT       | 3.52              | 0.6     | 2.92 | -                        | 7                  | 2.85 (s, 9H), 2.54 (s, 6H, DMSO), 2.41 (s, unknown) | 40.43 (s, DMSO-h6)                 | Still bubbling when stopped |
|   | 0.125                  | 2.84              | 2.84    | -    | -                        | 35                 | 2.86 (s, 9H), 2.41 (s, 3H)                          | 26.15 (s)                          |                             |
|  | 0.125                  | 3.02              | 3.02    | -    | -                        | 37                 | 2.86 (s, 9H), 2.41 (s, 3H)                          | 26.15 (s)                          |                             |
|   | 0.125                  | 2.54              | 2.54    | -    | -                        | 31                 | 2.86 (s, 9H), 2.41 (s, 3H)                          | 26.15 (s)                          |                             |

| Catalyst used   | Catalyst amount (mol%) | Mass Recovery (g) |         |      |                          | Product yield* (%) | <sup>1</sup> H NMR signals (ppm)                     | <sup>13</sup> C NMR signals (ppm) | Notes               |
|---|------------------------|-------------------|---------|------|--------------------------|--------------------|--|-----------------------------------|---------------------|
|   |                        | Total             | Product | DMSO | Other (H <sub>2</sub> O) |                    |  |                                   |                     |
|    | 0.125                  | 0.5               | 0.03    | 0.47 | -                        | <1                 | 2.85 (s, 9H), 2.54 (s, 6H), DMSO), 2.41 (s, unknown) | 40.43 (s, DMSO-h6)                | Unknown degradation |
|    | 0.125                  | 0.5               | 0.03    | 0.47 | -                        | <1                 | 2.85 (s, 9H), 2.54 (s, 6H), DMSO), 2.41 (s, unknown) | 40.43 (s, DMSO-h6)                | Unknown degradation |
|    | 0.125                  | 3.43              | 3.43    | -    | -                        | <b>42</b>          | 2.86 (s, 9H), 2.39 (s, 3H)                           | 26.13 (s), 39.76 (s)              |                     |
|  | 0.125                  | 0.5               | 0.05    | 0.45 | -                        | <1                 | 2.85 (s, 9H), 2.54 (s, 6H), DMSO), 2.51 (s, unknown) | 40.43 (s, DMSO-h6)                | Unknown degradation |
| HBr   | 0.125                  | 2.5               | 2.5     | -    | -                        | <b>30</b>          | 2.86 (s, 9H), 2.41 (s, 3H)                           | 26.15 (s)                         |                     |

#Second peak of TMSMS hidden under strong DMSO signal

## Deuterated trimethylsulphonium methanesulphonate **406**

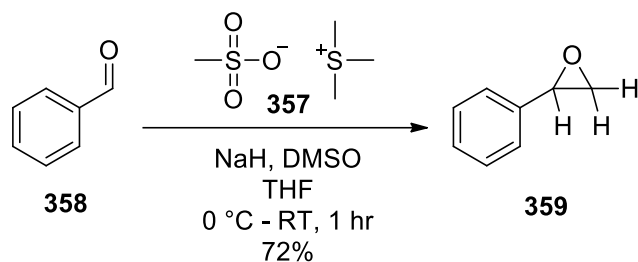


d<sub>12</sub>-Dimethyl sulfoxide **405** (10 mL, 140.8 mmol) and diisopropylbenzimidazolium bromide **356** (0.5 g, 1.765 mmol, 1.25 mol%) were heated in air (with double walled condenser and a CaCl<sub>2</sub> drying tube) at 150 °C for 3 days. On the second day onwards bubbling became visible in the solution and white solid started to collect on the walls of the condenser. The reaction was cooled to RT and the residue was dissolved in a minimal amount of boiling ethanol, then cooled to RT again. The reaction solution was diluted with diethyl ether (250 mL), with white solid precipitating out. The solids were filtered and washed with diethyl ether (3 x 25 mL) and dried in a desiccator to yield d<sub>12</sub>-trimethylsulphonium methanesulphonate **406** as a white solid (2.73 g, 34%). The experiment was repeated with 1/10 of the catalyst (0.05 g, 0.1765 mmol, 0.125%) yielding the expected product in good yield (3.2 g, 40%).

**<sup>2</sup>H NMR (400 MHz, DMSO)** δ 2.86 (s, 9H), 2.33 (s, 3H) ppm.

**<sup>13</sup>C NMR (101 MHz, D<sub>2</sub>O)** δ 37.82 (sept., CD<sub>3</sub>), 25.77 (sept., CD<sub>3</sub>) ppm.

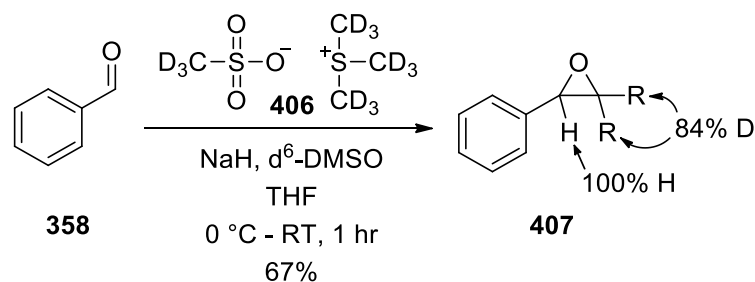
## Phenyloxirane **359**



Trimethylsulphonium methanesulphonate **357** (340 mg, 2 mmol) and NaH (260 mg, 10.8 mmol) was added to a mixture of DMSO (4 mL) and THF (2 mL). The reaction was stirred for ten minutes and then cooled on ice. Benzaldehyde **358** (0.1 g, 0.94 mmol) was added and the mixture was stirred at zero degrees for 30 minutes, warmed to room temperature and stirred for a further 30 minutes. Water (30 mL) was added, and the reaction mixture was extracted with diethyl ether (2 x 10 mL). The organic phase was dried with calcium chloride, the solvent removed under reduced pressure to yield phenyloxirane **359** as a yellow oil (0.082 g, 72%). The NMR spectrum matched the data of Chimni et al.<sup>383</sup>

<sup>1</sup>H NMR (400 MHz, d<sup>6</sup> DMSO) δ 7.41 - 7.26 (m, 5H), 3.87 (dd, *J* = 4.1, 2.5 Hz, 1H), 3.15 (dd, *J* = 5.5, 4.1 Hz, 1H), 2.81 (dd, *J* = 5.5, 2.5 Hz, 1H) ppm.

## Phenyloxirane-3,3-d<sub>2</sub> **407**



d<sub>12</sub>-Trimethylsulphonium methanesulphonate **406** (350 mg, 2 mmol) and NaH (410 mg, 17 mmol) was added to a mixture of d<sub>6</sub>-DMSO (4 mL) and THF (2 mL). The reaction was stirred for ten minutes and then cooled on ice. Benzaldehyde **358** (0.1 g, 0.94 mmol) was added and the mixture was stirred at zero degrees for 30 minutes, warmed to room temperature and stirred for a further 30 minutes. Water (30 mL) was added, and the reaction was extracted with diethyl ether (2 x 10 mL). The organic phase was dried with calcium chloride, the solvent removed under reduced pressure to yield phenyloxirane-3,3-d<sub>2</sub> **407** as a yellow oil (0.76 g, 67%).

**<sup>1</sup>H NMR (400 MHz, d<sup>6</sup> DMSO)** δ 7.40 - 7.28 (m, 5H), 3.87 (s, 1H), 3.17 – 3.12 (m, 0.05H), 2.83 – 2.78 (m, 0.05H) ppm.

**<sup>2</sup>H NMR (400 MHz, CHCl<sub>3</sub>)** δ 3.13 (s, 1H), 2.79 (s, 1H) ppm.

**<sup>13</sup>C NMR (101 MHz, CDCl<sub>3</sub>)** δ 137.66 (C), 128.53 (2 x CH), 128.20 (2 x CH), 125.53 (CH), 52.21 (CH), 50.51 (hept., CD<sub>2</sub>) ppm.

## References

1. <https://www.ers.usda.gov/topics/food-markets-prices/food-service-industry/market-segments/> (accessed 23/07/2018).
2. Statista, <https://www.statista.com/topics/1611/vegetables/> (accessed 23/07/2018).
3. Statista, <https://www.statista.com/topics/1621/fruit-production/> (accessed 23/07/2018).
4. Innovation, H., Horticulture Innovation Australian Limited Sydney, Australia: 2020.
5. Elik, A.; Yanik, D. K.; Istanbulu, Y.; Guzelsoy, N. A.; Yavuz, A.; Gogus, F., *Strategies* **2019**, 5 (3), 29-39.
6. <http://www.fao.org/save-food/resources/keyfindings/infographics/fruit/en/>.
7. Jose, L., <http://www.abc.net.au/news/rural/2017-07-11/ugly-vege-gets-a-fair-go-as-food-scientists-strive-to-cut-waste/8697192> (accessed 23/07/2018).
8. Blanke, M. M., *Journal of the Science of Food and Agriculture* **2014**, 94 (12), 2357-2361.
9. <https://www.agric.wa.gov.au/fruit/storage-fresh-fruit-and-vegetables>.
10. Thompson, A. K.; Prange, R. K.; Bancroft, R.; Puttongsiri, T., CABI: 2018.
11. Samuel, D.; Beera, V., *Journal of food science and technology* **2013**, 50 (3), 429-442.
12. Salunkhe, D.; Wu, M.; Rahman, A. R., *Critical Reviews in Food Science & Nutrition* **1974**, 5 (1), 15-54.
13. Thompson, A. K., John Wiley & Sons: 2008.
14. Rankine, J. C.; Goldsmith, G. H., Google Patents: 1913.
15. Raymond, B., Google Patents: 1964.
16. Mannaa, M.; Kim, K. D., *Mycobiology* **2018**, 46 (3), 287-295.
17. Paull, R., *Postharvest biology and technology* **1999**, 15 (3), 263-277.
18. Crocker, W.; Hitchcock, A.; Zimmerman, P., **1935**, 7 (3).
19. Galli, V.; Sanchez-Ballesta, M. T.; El-kereamy, A.; Ayub, R. A.; Jia, W., *Frontiers in Plant Science* **2021**, 12 (851).
20. [http://2013.igem.org/Team:UNITN-Trento/Extra/Fruit\\_Info](http://2013.igem.org/Team:UNITN-Trento/Extra/Fruit_Info).

21. Nelson, P. F.; Quigley, S. M., *Atmospheric Environment (1967)* **1984**, 18 (1), 79-87.
22. Nakabayashi, R.; Saito, K., *Analytical and bioanalytical chemistry* **2013**, 405 (15), 5005-5011.
23. Subba, P.; Prasad, T. S. K., *Omics: a journal of integrative biology* **2021**, 25 (12), 750-769.
24. Miller-Fleming, L.; Olin-Sandoval, V.; Campbell, K.; Ralser, M., *Journal of molecular biology* **2015**, 427 (21), 3389-3406.
25. Hemachandran, H.; Doss, C. G. P.; Siva, R., *Current Science* **2017**, 112 (10), 1990.
26. Cornell, B., <https://ib.bioninja.com.au/higher-level/topic-9-plant-biology/untitled-2/plant-hormones.html> (accessed 19/11/2021).
27. Abeles, F. B.; Heggstad, H. E., *Journal of the air pollution control association* **1973**, 23 (6), 517-521.
28. Burg, S. P.; Burg, E. A., *Plant physiology* **1962**, 37 (2), 179-89.
29. Rohrbaugh, P. W., *Plant Physiology* **1943**, 18 (1), 79-89.
30. Saltveit, M. E., *Postharvest Biology and Technology* **1999**, 15 (3), 279-292.
31. Street, I. H.; Schaller, G. E., *The Biochemist* **2016**, 38 (5), 4-7.
32. Galil, J., *Economic Botany* **1968**, 22 (2), 178-190.
33. Neljubow, D., *Bot. Centralbl. Beih.* **1901**, 10, 128-139.
34. Gane, R., *Journal of Pomology and Horticultural Science* **1935**, 13 (4), 351-358.
35. Crocker, W.; Hitchcock, A.; Zimmerman, P., *Contrib. Boyce Thompson Inst* **1935**, 7 (3).
36. Gane, R., *Nature* **1934**, 134 (3400), 1008-1008.
37. *Analyst* **1935**, 60 (715), 687-689.
38. Arshad, M.; Frankenberger, W. T., Arshad, M.; Frankenberger, W. T., Eds. Springer US: Boston, MA, 2002; pp 1-9.
39. Cremer, E.; Müller, R., *Z. Elektrochem* **1951**, 55, 217-220.
40. Kidd, F.; West, C., *Scientific Horticulture* **1936**, 4, 75-78.
41. Porritt, S., *Scientific Agriculture* **1951**, 31 (3), 99-112.
42. Burg, S. P.; Burg, E. A., *Plant Physiol* **1962**, 37 (2), 179-89.

43. Burg, S. P.; Burg, E. A., *Science* **1966**, *153* (3733), 314-5.
44. Burg, S. P. 1963.
45. Klein Geltink, R. I.; Pearce, E. L., *Elife* **2019**, *8*, e47221.
46. Martínez, Y.; Li, X.; Liu, G.; Bin, P.; Yan, W.; Más, D.; Valdivié, M.; Hu, C. A.; Ren, W.; Yin, Y., *Amino Acids* **2017**, *49* (12), 2091-2098.
47. Ravanel, S.; Gakière, B.; Job, D.; Douce, R., *Proc Natl Acad Sci U S A* **1998**, *95* (13), 7805-12.
48. Yang, S. F.; Ku, H. S.; Pratt, H. K., *Biochem Biophys Res Commun* **1966**, *24* (5), 739-43.
49. Ku, H. S.; Yang, S. F.; Pratt, H. K., *Arch Biochem Biophys* **1967**, *118* (3), 756-8.
50. Yang, S. F., *Arch Biochem Biophys* **1967**, *122* (2), 481-7.
51. Yang, S. F.; Ku, H. S.; Pratt, H. K., *J Biol Chem* **1967**, *242* (22), 5274-80.
52. Baur, A.; Yang, S. F., *Plant Physiol* **1969**, *44* (2), 189-92.
53. Yang, S. F., *Plant Physiol* **1969**, *44* (8), 1203-4.
54. Yang, S. F., *J Biol Chem* **1969**, *244* (16), 4360-5.
55. Baur, A. H.; Yang, S. F., *Plant Physiol* **1969**, *44* (9), 1347-9.
56. Baur, A. H.; Yang, S. F.; Pratt, H. K., *Plant Physiol* **1971**, *47* (5), 696-9.
57. Chou, T. W.; Yang, S. F., *Arch Biochem Biophys* **1973**, *157* (1), 73-82.
58. Lau, O. L.; Murr, D. P.; Yang, S. F., *Plant Physiol* **1974**, *54* (2), 182-5.
59. Lau, O. L.; Yang, S. F., *Plant Physiol* **1976**, *57* (1), 88-92.
60. Lau, O. L.; Yang, S. F., *Plant Physiol* **1976**, *58* (1), 114-7.
61. Adams, D. O.; Yang, S. F., *Proc Natl Acad Sci U S A* **1979**, *76* (1), 170-4.
62. Yu, Y. B.; Adams, D. O.; Yang, S. F., *Arch Biochem Biophys* **1979**, *198* (1), 280-6.
63. S F Yang, a.; Hoffman, N. E., *Annual Review of Plant Physiology* **1984**, *35* (1), 155-189.
64. Pattyn, J.; Vaughan-Hirsch, J.; Van de Poel, B., *New Phytologist* **2021**, *229* (2), 770-782.
65. Chen, Y.; Zou, T.; McCormick, S., *Plant Physiology* **2016**, *172* (1), 244-253.

66. Wang, X.; Oh, M. W.; Komatsu, S., *Biologia plantarum* **2016**, *60* (2), 269-278.
67. Van de Poel, B.; Van Der Straeten, D., *Frontiers in plant science* **2014**, *5*, 640-640.
68. Hesse, H.; Kreft, O.; Maimann, S.; Zeh, M.; Hoefgen, R., *Journal of Experimental Botany* **2004**, *55* (404), 1799-1808.
69. de Wild, H. P. J.; Balk, P. A.; Fernandes, E. C. A.; Peppelenbos, H. W., *Postharvest Biology and Technology* **2005**, *36* (3), 273-280.
70. Alicia, R. C.; Jorge, O. T., *Plant Physiology* **1984**, *76* (1), 88-91.
71. Schaller, G. E.; Binder, B. M., Springer: 2017; pp 223-235.
72. Yu, Y.-B.; Yang, S. F., *Plant physiology* **1979**, *64* (6), 1074-1077.
73. Krämer, U., *Elife* **2015**, *4*, e06100.
74. Guzmán, P.; Ecker, J. R., *Plant Cell* **1990**, *2* (6), 513-523.
75. Merchante, C.; Stepanova, A. N., *Methods Mol Biol* **2017**, *1573*, 163-209.
76. Hall, B. P.; Shakeel, S. N.; Amir, M.; Haq, N. U.; Qu, X.; Schaller, G. E., *Plant Physiology* **2012**, *159* (2), 682-695.
77. Gao, Z.; Schaller, G. E., *Plant Signaling & Behavior* **2009**, *4* (12), 1152-1153.
78. Van Norman, J. M.; Benfey, P. N., *Wiley Interdiscip Rev Syst Biol Med* **2009**, *1* (3), 372-379.
79. Woodward, A. W.; Bartel, B., *Genetics* **2018**, *208* (4), 1337-1349.
80. Hayashi, M.; Nishimura, M., *Biochimica et Biophysica Acta (BBA) - Molecular Cell Research* **2006**, *1763* (12), 1382-1391.
81. Khan, N. A., Springer: 2006.
82. Rodríguez, F. I.; Esch, J. J.; Hall, A. E.; Binder, B. M.; Schaller, G. E.; Bleecker, A. B., *Science* **1999**, *283* (5404), 996-8.
83. Schott-Verdugo, S.; Müller, L.; Classen, E.; Gohlke, H.; Groth, G., *Scientific Reports* **2019**, *9* (1), 8869.
84. Thompson, J. S.; Harlow, R. L.; Whitney, J. F., *Journal of the american chemical society* **1983**, *105* (11), 3522-3527.
85. Thompson, J. S.; Swiatek, R. M., *Inorganic Chemistry* **1985**, *24* (1), 110-113.
86. Suenaga, Y.; Wu, L. P.; Kuroda-sowa, T.; Munakata, M.; Maekawa, M., *Polyhedron* **1997**, *16* (1), 67-70.
87. Dai, X.; Warren, T. H., *Chemical Communications* **2001**, (19), 1998-1999.

88. Straub, B. F.; Eisenträger, F.; Hofmann, P., *Chemical Communications* **1999**, (24), 2507-2508.
89. Chen, J.; Eldridge, R. B.; Rosen, E. L.; Bielawski, C. W., *AIChE Journal* **2011**, 57 (3), 630-644.
90. Burg, S. P.; Burg, E. A., *Plant Physiology* **1967**, 42 (1), 144-152.
91. McDaniel, B. K.; Binder, B. M., *Journal of Biological Chemistry* **2012**, 287 (31), 26094-26103.
92. Rodriguez, F. I.; Esch, J. J.; Hall, A. E.; Binder, B. M.; Schaller, G. E.; Bleecker, A. B., *Science* **1999**, 283 (5404), 996-998.
93. Beyer Jr, E. M., *Plant physiology* **1976**, 58 (3), 268-271.
94. Halevy, A.; Kofranek, A., *Journal American Society for Horticultural Science* **1977**.
95. Veen, H.; Van de Geijn, S., *Planta* **1978**, 140 (1), 93-96.
96. Roh, K. H.; Kwak, B.-K.; Kim, J.-B.; Lee, K.-R.; Kim, H.; Kim, S.-H., *Journal of Plant Biotechnology* **2012**, 39.
97. Winstein, S.; Lucas, H. J., *Journal of the American Chemical Society* **1938**, 60 (4), 836-847.
98. Traynham, J. G.; Olechowski, J. R., *Journal of the American Chemical Society* **1959**, 81 (3), 571-574.
99. Muhs, M. A.; Weiss, F.-T., *Journal of the American Chemical Society* **1962**, 84 (24), 4697-4705.
100. Burg, S. P.; Burg, E. A., *Science* **1965**, 148 (3674), 1190-1196.
101. Sisler, E. C.; Pian, A., *Tobacco Science* **1973**, 17.
102. Sisler, E. C., *Plant Science* **2008**, 175 (1), 145-148.
103. Sisler, E. C.; Yang, S. F., *Phytochemistry* **1984**, 23 (12), 2765-2768.
104. Sisler, E. C.; Yang, S. F., *BioScience* **1984**, 34 (4), 234-238.
105. Sisler, E. C.; Goren, R.; Huberman, M., *Physiologia Plantarum* **1985**, 63 (1), 114-120.
106. Robbins, J. A.; Reid, M.; Paul, J.; Rost, T., *Journal of Plant Growth Regulation* **1985**, 4 (1), 147-157.
107. Sisler, E. C.; Blankenship, S. M.; Guest, M., *Plant Growth Regulation* **1990**, 9 (2), 157-164.
108. Sisler, E.; Serek, M., *Plant Biology* **2003**, 5 (05), 473-480.

109. Buanong, M.; Mibus, H.; Sisler, E. C.; Serek, M., *Plant growth regulation* **2005**, *47* (1), 29-38.
110. Doering, W. v. E.; DePuy, C. H., *Journal of the American Chemical Society* **1953**, *75* (23), 5955-5957.
111. Weil, T.; Cais, M., *The Journal of Organic Chemistry* **1963**, *28* (9), 2472-2472.
112. Sisler, E., Blankenship, S. 1992.
113. Sisler, E. C.; Blankenship, S. M., *Plant Growth Regulation* **1993**, *12* (1), 125-132.
114. Hock, K. J.; Koenigs, R. M., *Chemistry – A European Journal* **2018**, *24* (42), 10571-10583.
115. Hecht, S. M.; Kozarich, J. W., *Tetrahedron Letters* **1973**, *14* (16), 1397-1400.
116. Sisler, E. C.; Blankenship, S. M., *Plant Growth Regulation* **1993**, *12* (1), 155-160.
117. Sisler, E. C.; Lallu, N., *Postharvest Biology and Technology* **1994**, *4* (3), 245-254.
118. Blankenship, S. M.; Sisler, E. C., *Postharvest Biology and Technology* **1993**, *3* (2), 95-101.
119. Tian, M. S.; Gong, Y.; Bauchot, A. D., *Plant Growth Regulation* **1997**, *23* (3), 195-200.
120. Sexton, R.; Porter, A. E.; Littlejohns, S.; Thain, S. C., *Annals of Botany* **1995**, *75* (4), 337-342.
121. Sisler, E. C.; Blankenship, S. M.; Fearn, J. C.; Haynes, R., Pech, J. C.; Latché, A.; Balagué, C., Eds. Springer Netherlands: Dordrecht, 1993; pp 182-187.
122. Sisler, E. C.; Serek, M., *Botanical Bulletin of Academia Sinica* **1999**, *40* (1), 1-7.
123. Sisler, E. C.; Dupille, E.; Serek, M., *Plant Growth Regulation* **1996**, *18* (1), 79-86.
124. Putala, M.; Lemenovskii, D. A., *Russian Chemical Reviews* **1994**, *63* (3), 197.
125. Reid, M. S.; Staby, G. L., *HortScience* **2008**, *43* (1), 83-85.
126. Sisler, E. C.; Serek, M.; Roh, K.-A.; Goren, R., *Plant Growth Regulation* **2001**, *33* (2), 107-110.
127. Sisler, E. C.; Alwan, T.; Goren, R.; Serek, M.; Apelbaum, A., *Plant Growth Regulation* **2003**, *40* (3), 223-228.
128. Grichko, V., *Russian Journal of Plant Physiology* **2006**, *53* (4), 523-529.

129. M Blankenship, S.; Dole, J., 2003; Vol. 28, p 1-25.
130. Daly, J.; Kourelis, B., Google Patents: 2004.
131. Chen, X. Dissertation, Rutgers University-Graduate School-New Brunswick, 2015.
132. Sarker, M. I.; Fan, X.; Liu, L., *Scientia Horticulturae* **2015**, 188, 36-43.
133. Sarker, M. I.; Tomasula, P.; Liu, L., *Journal of Plant Studies; Vol* **2016**, 5 (1).
134. Shahrin, T.; Sarker, M. I.; Zheng, Y.; Tomasula, P.; Liu, L., *Journal of Plant Studies; Vol* **2017**, 6 (1).
135. Sarker, M. I.; Liu, L.; Shahrin, T.; Fan, X.; Tomasula, P., ACS Publications: 2020; pp 109-127.
136. Haynes, R., **2009**, 2, 1268-1298.
137. Fisher, F.; Applequist, D. E., *The Journal of Organic Chemistry* **1965**, 30 (6), 2089-2090.
138. Magid, R. M.; Clarke, T. C.; Duncan, C. D., *The Journal of Organic Chemistry* **1971**, 36 (9), 1320-1321.
139. Köster, R.; Arora, S.; Binger, P., *Justus Liebigs Annalen der Chemie* **1973**, 1973 (7), 1219-1235.
140. Daly, J.; Kourelis, B. 2004.
141. Dent, B.; Halton, B.; Smith, A., *Australian journal of chemistry* **1986**, 39 (10), 1621-1627.
142. Baird, M. S.; Hussain, H. H.; Nethercott, W., *Journal of the Chemical Society, Perkin Transactions I* **1986**, 1845-1853.
143. Al Dulayymi, A. R.; Juma'a, R.; Baird, M. S.; Gerrard, M. E.; Koza, G.; Harkins, S. D.; Roberts, E., *Tetrahedron* **1996**, 52 (10), 3409-3424.
144. Pirrung, M. C.; Bleecker, A. B.; Inoue, Y.; Rodríguez, F. I.; Sugawara, N.; Wada, T.; Zou, Y.; Binder, B. M., *Chemistry & Biology* **2008**, 15 (4), 313-321.
145. Sarker, M. I.; Tomasula, P.; Liu, L., *Journal of Plant Studies* **2016**, 5, 1.
146. Khan, S. A.; Singh, Z.; Musa, M. M.; Payne, A. D., *Scientia Horticulturae* **2016**, 213, 410-417.
147. Khan, S. A. K. U.; Singh, Z.; Musa, M. M. A.; Payne, A. D., *Scientia Horticulturae* **2016**, 213, 410-417.
148. Singh, Z.; Payne, A. D.; Khan, S. A. K. U.; Musa, M.; Miload WO2017075662, 2016.

149. Anet, R.; Anet, F., *Journal of the American Chemical Society* **1964**, 86 (3), 525-526.
150. Apeloig, Y.; Arad, D.; Halton, B.; Randall, C. J., *Journal of the American Chemical Society* **1986**, 108 (16), 4932-4937.
151. Billups, W.; Chow, W.; Leavell, K.; Lewis, E.; Margrave, J.; Sass, R.; Shieh, J.; Werness, P.; Wood, J., *Journal of the American Chemical Society* **1973**, 95 (23), 7878-7880.
152. Halton, B., *Chemical Reviews* **2003**, 103 (4), 1327-1370.
153. Apeloig, Y.; Arad, D., *Journal of the American Chemical Society* **1986**, 108 (12), 3241-3247.
154. Halton, B.; Boese, R.; Blaser, D.; Lu, Q., *Australian Journal of Chemistry* **1991**, 44 (2), 265-276.
155. Halton, B.; Kay, A. J.; Zhi-Mei, Z.; Boeseb, R.; Haumann, T., *Journal of the Chemical Society, Perkin Transactions I* **1996**, (12), 1445-1452.
156. Müller, P.; Bernardinelli, G.; Jacquier, Y., *Helvetica chimica acta* **1992**, 75 (6), 1995-2008.
157. Müller, P.; Bernardinelli, G.; Jacquier, Y.; Ricca, A., *Helvetica chimica acta* **1989**, 72 (7), 1618-1626.
158. Bläser, D.; Boese, R.; Brett, W. A.; Rademacher, P.; Schwager, H.; Stanger, A.; Vollhardt, K. P. C., *Angewandte Chemie International Edition in English* **1989**, 28 (2), 206-208.
159. Hatano, K.; Tokitoh, N.; Takagi, N.; Nagase, S., *Journal of the American Chemical Society* **2000**, 122 (19), 4829-4830.
160. Neidlein, R.; Christen, D.; Poignée, V.; Boese, R.; Bläser, D.; Gieren, A.; Ruiz - Pérez, C.; Hübner, T., *Angewandte Chemie International Edition in English* **1988**, 27 (2), 294-295.
161. Boese, R.; Bläser, D.; Billups, W. E.; Haley, M. M.; Maulitz, A. H.; Mohler, D. L.; Vollhardt, K. P. C., *Angewandte Chemie International Edition in English* **1994**, 33 (3), 313-317.
162. Payne, A. D.; Skelton, B. W.; White, A. H.; Wege, D., *ChemistrySelect* **2016**, 1 (16), 5339-5346.
163. Billups, W.; Chow, W., *Journal of the American Chemical Society* **1973**, 95 (12), 4099-4100.
164. Thummel, R. P., JAI Press: 1995.
165. Halton, B., *Chemical Reviews* **1989**, 89 (5), 1161-1185.

166. Halton, B., *Industrial & Engineering Chemistry Product Research and Development* **1980**, 19 (3), 349-364.
167. Halton, B., *Chemical Reviews* **1973**, 73 (2), 113-126.
168. Payne, A. D.; Wege, D., *Journal of the Chemical Society, Perkin Transactions I* **2001**, (14), 1579-1580.
169. Billups, W.; Blakeney, A.; Chow, W., *Chem Commun* **1971**, 1461.
170. Billups, W.; Chow, W., *Journal of the American Chemical Society* **1973**, 95 (12), 4099-4100.
171. Billups, W., *Org. Synth* **1976**, 55, 12.
172. Halton, B., *Chem Rev* **2003**, 103 (4), 1327-69.
173. Davalian, D.; Garratt, P. J., *Tetrahedron Letters* **1976**, 17 (32), 2815-2818.
174. Bee, L. K.; Garratt, P. J.; Mansuri, M. M., *Journal of the American Chemical Society* **1980**, 102 (23), 7076-7079.
175. Billups, W. E.; Lin, L.-J.; Arney, B. E.; Rodin, W. A.; Casserly, E. W., *Tetrahedron Letters* **1984**, 25 (36), 3935-3938.
176. Billups, W.; Casserly, E. W.; Arney Jr, B. E., *Journal of the American Chemical Society* **1984**, 106 (2), 440-441.
177. Müller, P.; Schaller, J.-P., *Helvetica Chimica Acta* **1990**, 73 (5), 1228-1232.
178. Davalian, D.; Garratt, P. J.; Koller, W.; Mansuri, M. M., *J. Org. Chem.* **1980**, 45 (21), 4183.
179. Billups, W. E.; A. Rodin, W.; M. Haley, M., *Tetrahedron* **1988**, 44 (5), 1305-1338.
180. Saraçolu, N.; Durucasu, I.; Balci, M., *Tetrahedron* **1995**, 51 (40), 10979-10986.
181. Bambal, R.; Fritz, H.; Rihs, G.; Tschamber, T.; Streith, J., *Angewandte Chemie International Edition in English* **1987**, 26 (7), 668-669.
182. Huben, K.; Kuberski, S.; Frankowski, A.; Gebicki, J.; Streith, J., *Journal of the Chemical Society, Chemical Communications* **1995**, (3), 315-316.
183. Müller, P.; Schaller, J.-P., *Tetrahedron Letters* **1989**, 30 (12), 1507-1510.
184. Neidlein, R.; Christen, D., *Helvetica Chimica Acta* **1986**, 69 (7), 1623-1626.
185. Korte, S. Dissertation, University of Koln, 1968.
186. Vogel, E.; Grimme, W.; Korte, S., *Tetrahedron Letters* **1965**, 6 (41), 3625-3631.

187. Okazaki, R.; Ooka, M.; Tokitoh, N.; Inamoto, N., *The Journal of Organic Chemistry* **1985**, *50* (2), 180-185.
188. Halton, B.; Jones, C. S.; Margetic, D., *Tetrahedron* **2001**, *57* (17), 3529-3536.
189. Okazaki, R.; Ooka, M.; Tokitoh, N.; Inamoto, N., *The Journal of Organic Chemistry* **1985**, *50* (2), 180-185.
190. Billups, W. E.; Chamberlain, W. T.; Asim, M. Y., *Tetrahedron Lett.* **1977**, (6), 571.
191. Billups, W.; Chow, W.; Smith, C., *Journal of the American Chemical Society* **1974**, *96* (6), 1979-1980.
192. Billups, W.; McCord, D. J.; Maughon, B. R., *Tetrahedron letters* **1994**, *35* (26), 4493-4496.
193. Musa, M. M. A. Curtin University, 2016.
194. Serek, M.; Sisler, E. C.; Tirosh, T.; Mayak, S., *HortScience* **1995**, *30* (6), 1310-1310.
195. Macnish, A. J.; Irving, D. E.; Joyce, D. C.; Vithanage, V.; Wearing, A. H., *Australian Journal of Botany* **2005**, *53* (2), 119-131.
196. Macnish, A. J.; Joyce, D. C.; Irving, D. E.; Wearing, A. H., *Postharvest Biology and Technology* **2004**, *32* (3), 321-338.
197. Macnish, A.; Hofman, P.; Joyce, D.; Simons, D.; Reid, M., *Australian Journal of Experimental Agriculture* **2000**, *40* (3), 471-481.
198. Macnish, A. J.; (Australia), R. I. R. a. D. C., 1999.
199. Macnish, A.; Irving, D.; Joyce, D.; Wearing, A.; Vithanage, V., *The Journal of Horticultural Science and Biotechnology* **2004**, *79* (2), 293-297.
200. Macnish, A. J.; Simons, D. H.; Joyce, D. C.; Faragher, J. D.; Hofman, P. J., *HortScience* **2000**, *35* (2), 254-255.
201. Abdalghani, S.; Singh, Z.; Seaton, K.; Payne, A. D., *Australian Journal of Crop Science* **2018**, *12* (12), 1875-1881.
202. Kyaw, P. N.; Singh, Z.; Tokala, V. Y., *Postharvest Biology and Technology* **2021**, *180*, 111625.
203. Kyaw, P. N. Dissertation, Curtin University, 2019.
204. Abdalghani, S. M. A. Dissertation, Curtin University, 2017.
205. Singh, Z.; Payne, A. D.; Khan, S. A. K. U.; Musa, M.; Miload WO2017075662, 2016.
206. Mattison, R. L. Dissertation, Curtin University, 2016.

207. Birche, A. J.; Murray, A. R.; Smith, H., *Journal of the Chemical Society (Resumed)* **1951**, (0), 1945-1950.
208. Cook, E. S.; Hill, A. J., *Journal of the American Chemical Society* **1940**, 62 (8), 1995-1998.
209. Menzek, A.; Altundas, A.; Gültekin, D., *Journal of Chemical Research* **2003**, 2003 (11), 752-753.
210. Wege, D., *The Journal of Organic Chemistry* **1990**, 55 (5), 1667-1670.
211. Matt, C.; Wagner, A.; Mioskowski, C., *J Org Chem* **1997**, 62 (2), 234-235.
212. Newman, M. S.; Zahm, H. V., *Journal of the American Chemical Society* **1943**, 65 (6), 1097-1101.
213. Liu, G.; Xu, B., *Tetrahedron Letters* **2018**, 59 (10), 869-872.
214. Martina, G.; Maria, A.; Tula, D.; Valentina, F.; Danilo, G.; Sandro, G.; Antonio, G.; S., H. N. J.; Stefania, M.; Rossano, N.; Franco, P.; Manuela, T.; Antonio, T.; Alberto, M. C., *ChemMedChem* **2010**, 5 (1), 65-78.
215. Divya, V.; Freire, R. O.; Reddy, M. L. P., *Dalton Transactions* **2011**, 40 (13), 3257-3268.
216. Ripin, D. H.; Evans, D. A.
217. Anderson, E. C.; Biediger, R. J.; Chen, J.; Dupre, B.; Lory, P.; Market, R. V.; Monk, K. A.; Savage, M. M.; Tennyson, R.; Young, B. M. WO2009017719A2, 05/02/2008, 2008.
218. Zoller, U., 1990; pp 185-215.
219. Liu, W.; Li, H.; Qin, H.; Zhao, W.; Zhou, C.; Jiang, S.; Yang, C., *Chemical Research in Chinese Universities* **2017**, 33 (2), 213-220.
220. Warren, D. S.; McQuillan, A. J., *The Journal of Physical Chemistry B* **2008**, 112 (34), 10535-10543.
221. O'Neill, L.; Coll, R.; Cooper, M.; Robertson, A.; Schroder, K. WO2016131098A1, 2015.
222. Koch, B. L.; Moore, T. C., *Plant physiology* **1990**, 93 (4), 1663-1664.
223. Moore, T. C., Springer: 1989; pp 228-254.
224. Kieber, J. J.; Schaller, G. E., *Plant Cell* **2019**, 31 (7), 1402-1403.
225. Shaharoon, B.; Arshad, M.; Khalid, A., *J Microbiol* **2007**, 45 (1), 15-20.
226. Arshad, M.; Frankenberger, W. T., *Applied and Environmental Microbiology* **1988**, 54 (11), 2728-2732.

227. Mahmood, M. H.; Khalid, A.; Khalid, M.; Arshad, M., *Pak. J. Bot* **2008**, *40* (2), 859-866.
228. Chang, C., *BMC Biology* **2016**, *14* (1), 7.
229. David, A. S.; Ernst, J. W.; Mikal, E. S., *Plant Physiology* **1992**, *98* (2), 769-773.
230. Dolan, L., *Journal of Experimental Botany* **1997**, *48* (2), 201-210.
231. Binder, B. M.; Patterson, S. E., *Stewart Postharvest Review* **2009**, *5* (1), 1-10.
232. Joyce, D., *Journal of the American Society for Horticultural Science* **1988**.
233. Joyce, D., *HortScience* **1989**, *24* (2).
234. Joyce, D., *Australian Journal of Experimental Agriculture* **1993**, *33* (4), 481-487.
235. Elfving, D. C.; Drake, S. R.; Reed, A. N.; Visser, D. B., *HortScience horts* **2007**, *42* (5), 1192-1199.
236. Goren, R.; Huberman, M.; Riov, J.; Goldschmidt, E. E.; Sisler, E. C.; Apelbaum, A., *Plant Growth Regulation* **2011**, *65* (2), 327.
237. Huberman, M.; Riov, J.; Goldschmidt, E. E.; Apelbaum, A.; Goren, R., *Plant Growth Regulation* **2014**, *73* (3), 249-255.
238. Wu, M.-J.; Zacarias, L.; Saltveit, M. E.; Reid, M. S., *HortScience* **1992**, *27* (2), 136-138.
239. Piergiovanni, L.; Scolaro, M.; Fava, P., *Packaging Technology and Science* **1992**, *5* (4), 189-196.
240. Siracusa, V., *International Journal of Polymer Science* **2012**, *2012*, 302029.
241. Wen, C.-K., Springer: 2014.
242. Tucker, M.; Wen, C.-K., Springer: 2015; pp 245-261.
243. Yaseen, M. Dissertation, Curtin University, 2018.
244. Malekipoor, R.; Singh, Z.; Payne, A., V International Symposium on Postharvest Pathology: From Consumer to Laboratory-Sustainable Approaches to Managing Postharvest 1325, 2019; pp 47-54.
245. Lwin, H. P.; Lee, J., *Horticulture, Environment, and Biotechnology* **2021**, *62* (1), 53-61.
246. Manigo, B. I.; Limbaga Jr, C. A., *International Journal for Agricultural Innovations and Research (IJAIR)* **2019**, *8* (1).
247. Da Silva, J. T., *J. Biol. Sci* **2003**, *3* (4), 406-442.

248. Serek, M.; Woltering, E.; Sisler, E.; Frello, S.; Sriskandarajah, S., *Biotechnology advances* **2006**, *24* (4), 368-381.
249. Tokala, V. Y.; Singh, Z.; Kyaw, P. N., *Scientia Horticulturae* **2020**, *272*, 109597.
250. Tokala, V. Y. Dissertation, Curtin University, 2019.
251. Murphy, P. V.; O'Sullivan, T. J.; Geraghty, N. W. A., *Journal of the Chemical Society, Perkin Transactions 1* **2000**, (13), 2109-2119.
252. Wong, F. M.; Wang, J.; Hengge, A. C.; Wu, W., *Organic Letters* **2007**, *9* (9), 1663-1665.
253. Reck, L. M.; Haberhauer, G.; Lüning, U., *European Journal of Organic Chemistry* **2016**, *2016* (6), 1119-1131.
254. Jiang, X.; Liu, R.; Xu, J.; Zhang, M. CN110627674, 2019.
255. Lv, X.; Yang, H.; Shi, T.; Xing, D.; Xu, X.; Hu, W., *Advanced Synthesis & Catalysis* **2019**, *361* (6), 1265-1270.
256. Egner, U.; Gerbling, K. P.; Hoyer, G. A.; Krüger, G.; Wegner, P., *Pesticide science* **1996**, *47* (2), 145-158.
257. Chuprakov, S.; Hwang, F. W.; Gevorgyan, V., *Angewandte Chemie International Edition* **2007**, *46* (25), 4757-4759.
258. Cohen, R.; Rybtchinski, B.; Gandelman, M.; Rozenberg, H.; Martin, J. M. L.; Milstein, D., *Journal of the American Chemical Society* **2003**, *125* (21), 6532-6546.
259. Vigalok, A.; Milstein, D., *Organometallics* **2000**, *19* (11), 2061-2064.
260. Lamaa, D.; Lin, H.-P.; Bzeih, T.; Retailleau, P.; Alami, M.; Hamze, A., *European Journal of Organic Chemistry* **2019**, *2019* (15), 2602-2611.
261. Shen, R.; Dong, C.; Yang, J.; Han, L.-B., *Advanced Synthesis & Catalysis* **2018**, *360* (21), 4252-4258.
262. Blanco, F.; Alkorta, I.; Elguero, J.; Cruz, V.; Abarca, B.; Ballesteros, R., *Tetrahedron* **2008**, *64* (49), 11150-11158.
263. Ballesteros Garrido, R. Dissertation, Strasbourg University, 2009.
264. Ueda, S.; Nagasawa, H., *Journal of the American Chemical Society* **2009**, *131* (42), 15080-15081.
265. Zheng, Z.; Ma, S.; Tang, L.; Zhang-Negrerie, D.; Du, Y.; Zhao, K., *The Journal of Organic Chemistry* **2014**, *79* (10), 4687-4693.
266. Song, L.; Tian, X.; Lv, Z.; Li, E.; Wu, J.; Liu, Y.; Yu, W.; Chang, J., *The Journal of Organic Chemistry* **2015**, *80* (14), 7219-7225.

267. Elliott, H.; Jaume, B., *European Journal of Organic Chemistry* **2005**, 2005 (17), 3761-3765.
268. Boyer, J. H.; Borgers, R.; Wolford, L. T., *Journal of the American Chemical Society* **1957**, 79 (3), 678-680.
269. Bower, J. D.; Ramage, G. R., *Journal of the Chemical Society (Resumed)* **1957**, (0), 4506-4510.
270. Jones, G.; Sliskovic, D. R., *Journal of the Chemical Society, Perkin Transactions 1* **1982**, (0), 967-971.
271. Jones, G.; Mouat, D. J.; Tonkinson, D. J., *Journal of the Chemical Society, Perkin Transactions 1* **1985**, (0), 2719-2723.
272. Jones, G., Academic Press: 2002; Vol. 83, pp 1-70.
273. Jones, G.; Sliskovic, D. R., Katritzky, A. R., Ed. Academic Press: 1983; Vol. 34, pp 79-143.
274. Boyer, J.; Goebel, N., *The Journal of Organic Chemistry* **1960**, 25 (2), 304-305.
275. Abarca, B.; Hayles, D. J.; Jones, G.; Sliskovic, D. R., *Chemischer Informationsdienst* **1983**, 14 (37).
276. Jones, G.; Pitman, M. A.; Lunt, E.; Lythgoe, D. J.; Abarca, B.; Ballesteros, R.; Elmasnaouy, M., *Tetrahedron* **1997**, 53 (24), 8257-8268.
277. Regitz, M., *Chemische Berichte* **1966**, 99 (9), 2918-2930.
278. Regitz, M., *Angewandte Chemie International Edition in English* **1965**, 4 (5), 431-431.
279. Jones, G.; J. Mouat, D.; A. Pitman, M.; Lunt, E.; J. Lythgoe, D., *Tetrahedron* **1995**, 51 (40), 10969-10978.
280. Balli, H.; Löw, R.; Müller, V.; Rempfler, H.; Sezen-Gezgin, A., *Helvetica Chimica Acta* **1978**, 61 (1), 97-103.
281. Monteiro, H. J., *Synthetic Communications* **1987**, 17 (8), 983-992.
282. Cai, Y.-M.; Zhang, X.; An, C.; Yang, Y.-F.; Liu, W.; Gao, W.-X.; Huang, X.-B.; Zhou, Y.-B.; Liu, M.-C.; Wu, H.-Y., *Organic Chemistry Frontiers* **2019**, 6 (9), 1481-1484.
283. Tamura, Y.; Kim, J.-H.; Miki, Y.; Hayashi, H.; Ikeda, M., *Journal of Heterocyclic Chemistry* **1975**, 12 (3), 481-483.
284. Raghavendra, M. S.; Lam, Y., *Tetrahedron Letters* **2004**, 45 (32), 6129-6132.
285. Roy, S.; Das, S. K.; Chattopadhyay, B., *Angewandte Chemie International Edition* **2018**, 57 (8), 2238-2243.

286. Liu, S.; Sawicki, J.; Driver, T. G., *Organic Letters* **2012**, *14* (14), 3744-3747.
287. Zaman, N.; Guillot, R.; Sénéchal-David, K.; Boillot, M.-L., *Tetrahedron Letters* **2008**, *49* (51), 7274-7275.
288. Yang, F.; Wang, X.; Pan, B.-B.; Su, X.-C., *Chemical Communications* **2016**, *52* (77), 11535-11538.
289. Jones, G.; Sliskovic, D., *Tetrahedron Letters* **1980**, *21*, 4529-4530.
290. Abarca, B.; Ballesteros, R.; Mojarred, F.; Jones, G.; Mouat, D. J., *Journal of the Chemical Society, Perkin Transactions 1* **1987**, (0), 1865-1868.
291. Aoyama, T.; Sonoda, N.; Yamauchi, M.; Toriyama, K.; Anzai, M.; Ando, A.; Shioiri, T., *Synlett* **1998**, *1998* (01), 35-36.
292. Liu, Z.; Raveendra Babu, K.; Wang, F.; Yang, Y.; Bi, X., *Organic Chemistry Frontiers* **2019**, *6* (1), 121-124.
293. Ashimori, A.; Ono, T.; Uchida, T.; Ohtaki, Y.; Fukaya, C.; Watanabe, M.; Yokoyama, K., *Chemical & Pharmaceutical Bulletin* **1990**, *38* (9), 2446-2458.
294. Kiran, Y. B.; Ikeda, R.; Sakai, N.; Konakahara, T., *Synthesis* **2010**, *2010* (02), 276-282.
295. Ulrich, S.; Buhler, E.; Lehn, J.-M., *New Journal of Chemistry* **2009**, *33* (2), 271-292.
296. Orita, A.; Taniguchi, H.; Otera, J., *Chemistry – An Asian Journal* **2006**, *1* (3), 430-437.
297. Ali, T. F. S.; Taira, N.; Iwamaru, K.; Koga, R.; Kamo, M.; Radwan, M. O.; Tateishi, H.; Kurosaki, H.; Abdel-Aziz, M.; Abuo-Rahma, G. E.-D. A. A.; Beshr, E. A. M.; Otsuka, M.; Fujita, M., *Bioorganic & Medicinal Chemistry Letters* **2020**, *30* (7), 127002.
298. Morilla, M. E.; Molina, M. J.; Díaz-Requejo, M. M.; Belderraín, T. R.; Nicasio, M. C.; Trofimenko, S.; Pérez, P. J., *Organometallics* **2003**, *22* (14), 2914-2918.
299. Noels, A.; Demonceau, A.; Petiniot, N.; Hubert, A. J.; Teyssié, P., *Tetrahedron* **1982**, *38* (17), 2733-2739.
300. Daniels, R.; Rush, C. C.; Bauer, L., *Journal of chemical education* **1960**, *37* (4), 205.
301. Riflade, B.; Lachkar, D.; Oble, J.; Li, J.; Thorimbert, S.; Hasenknopf, B.; Lacôte, E., *Organic Letters* **2014**, *16* (15), 3860-3863.
302. Lejeune, R.; Thunus, L.; Lapiere, C. L., *J. Pharm. Belg.* **1980**, *35* (1), 5-11.
303. Kametani, T.; Nemoto, H.; Takeda, H.; Takano, S., *Tetrahedron* **1970**, *26* (24), 5753.

304. Meisenheimer, J., *Berichte der deutschen chemischen Gesellschaft (A and B Series)* **1926**, 59 (8), 1848-1853.
305. Penjarla, T. R.; Kundarapu, M.; Baquer, S. M.; Bhattacharya, A., *ChemistrySelect* **2018**, 3 (19), 5386-5389.
306. Muthyala, R.; Rastogi, N.; Shin, W. S.; Peterson, M. L.; Sham, Y. Y., *Bioorganic & Medicinal Chemistry Letters* **2014**, 24 (11), 2535-2538.
307. Hideo, S.; Masato, Y.; Hidehiko, H.; Kazuyoshi, A.; Michio, K., *Bulletin of the Chemical Society of Japan* **1986**, 59 (1), 215-219.
308. Ford, N. F.; Browne, L. J.; Campbell, T.; Gemenden, C.; Goldstein, R.; Gude, C.; Wasley, J. W. F., *Journal of Medicinal Chemistry* **1985**, 28 (2), 164-170.
309. Kametani, T.; Nemoto, H.; Takeda, H.; Takano, S., *Chem Ind* **1970**, 41, 1323-4.
310. Kawase, M.; Teshima, M.; Saito, S.; Tani, S., *Heterocycles* **1998**, 48 (10), 2103-2109.
311. Wang, D.; Ding, K., *Chemical Communications* **2009**, (14), 1891-1893.
312. Park, C. M.; Kim, S. Y.; Park, W. K.; Park, N. S.; Seong, C. M., *Bioorg Med Chem Lett* **2008**, 18 (14), 3844-3847.
313. Allen, A. D.; Fedorov, A. V.; Tidwell, T. T.; Vukovic, S., *Journal of the American Chemical Society* **2004**, 126 (48), 15777-15783.
314. Ferjancic, Z.; Quiclet-Sire, B.; Zard, S. Z., *Synthesis* **2008**, 2008 (18), 2996-3008.
315. Jaafar, H.; Vileno, B.; Thibon, A.; Mandon, D., *Dalton Transactions* **2011**, 40 (1), 92-106.
316. Ando, K.; Shimazu, Y.; Seki, N.; Yamataka, H., *The Journal of Organic Chemistry* **2011**, 76 (10), 3937-3945.
317. Kanemasa, S.; Yoshimiya, T.; Wada, E., *Tetrahedron Lett.* **1998**, 39 (48), 8869-8872.
318. Altman, M.; Christopher, M.; Grimm, J. B.; Haidle, A.; Konrad, K.; Lim, J.; Maccoss, R. N.; Machacek, M.; Osimboni, E.; Otte, R. D.; Siu, T.; Spencer, K.; Taoka, B.; Tempest, P.; Wilson, K.; Woo, H. C.; Young, J.; Zabierek, A. WO2008156726, 2008.
319. Blagg, J. 2015.
320. Seiji Yoshimura, R. S., Tomoaki Kawano, Daisuke Sasuga, Mitsuru Hosaka, Hiroki Fukudome, Kazuo Kurosawa, Hirofumi Ishii, Takanori Koike 2006.

321. Dayal, B.; Salen, G.; Toome, B.; Tint, G. S.; Shefer, S.; Padia, J., *Steroids* **1990**, 55 (5), 233-237.
322. Hinchliffe, P.; Tanner, C. A.; Krismanich, A. P.; Labbé, G.; Goodfellow, V. J.; Marrone, L.; Desoky, A. Y.; Calvopiña, K.; Whittle, E. E.; Zeng, F.; Avison, M. B.; Bols, N. C.; Siemann, S.; Spencer, J.; Dmitrienko, G. I., *Biochemistry* **2018**, 57 (12), 1880-1892.
323. Nuria A. Tamayo, J. G. A., Abhisek Banerjee, Jian Jeffrey Chen, Michael J. Frohn, Matthew Richard KALLER, Thomas T. Nguyen, Nobuko Nishimura, Qiufen May Xue 2021.
324. Tsukamoto, I.; Koshio, H.; Kuramochi, T.; Saitoh, C.; Yanai-Inamura, H.; Kitada-Nozawa, C.; Yamamoto, E.; Yatsu, T.; Shimada, Y.; Sakamoto, S.; Tsukamoto, S.-i., *Bioorg. Med. Chem.* **2009**, 17 (8), 3130-3141.
325. Jarvis, B. B.; Nicholas, P. E., *The Journal of Organic Chemistry* **1980**, 45 (11), 2265-2268.
326. Jarvis, B. B.; Nicholas, P. E.; Midiwo, J. O., *Journal of the American Chemical Society* **1981**, 103 (13), 3878-3882.
327. Maury, G.; Meziane, D.; Sraïri, D.; Paugan, J.-P.; Paugam, R., *Bulletin des Sociétés Chimiques Belges* **1982**, 91 (2), 153-161.
328. Hammoud, A.; Nshimyumuremyi, J.-B.; Bourotte, J.; Lucaccioni, F.; Robeyns, K.; Dîrtu, M. M.; Garcia, Y.; Singleton, M. L., *European Journal of Inorganic Chemistry* **2018**, 2018 (27), 3253-3263.
329. Tsukamoto, I.; Koshio, H.; Kuramochi, T.; Saitoh, C.; Yanai-Inamura, H.; Kitada-Nozawa, C.; Yamamoto, E.; Yatsu, T.; Shimada, Y.; Sakamoto, S.; Tsukamoto, S.-i., *Bioorganic & Medicinal Chemistry* **2009**, 17 (8), 3130-3141.
330. Mosset, P.; Grée, R., *Synthetic Communications* **1985**, 15 (8), 749-757.
331. Head, D. L.; McCarty, C. G., *Tetrahedron Letters* **1973**, 14 (16), 1405-1408.
332. Fierz, H., Central Safety Research Laboratory, CIBA-GEIGY AG, Basle, Switzerland: 1994.
333. Deguchi, Y.; Kono, M.; Koizumi, Y.; Izato, Y.-i.; Miyake, A., *Organic Process Research & Development* **2020**, 24 (9), 1614-1620.
334. Yang, Q.; Sheng, M.; Li, X.; Tucker, C.; Vásquez Céspedes, S.; Webb, N. J.; Whiteker, G. T.; Yu, J., *Organic Process Research & Development* **2020**, 24 (6), 916-939.
335. Urben, P. G.; Pitt, M. J.; Young, J. A., *Journal of Chemical Education* **2007**, 84 (5), 768-769.
336. Brogli, F.; Grimm, P.; Meyer, M.; Zubler, H., Proc 3rd Int Symp Loss Prev Safety Promot Proces Ind, 1980; pp 665-683.

337. Hall, J., *Loss Prevention Bulletin* **1993**, 114 (12), 9-14.
338. Traynelis, V. J.; Hergenrother, W. L., *The Journal of Organic Chemistry* **1964**, 29 (1), 221-222.
339. Travers, G. Dissertation, Curtin University, 2015.
340. Sealy, C.; Brown, D. H., Curtin University: 2011.
341. Banci, F., *Ann. Chim. (Rome)* **1967**, 57 (5), 549.
342. Fronczek, F. R.; Johnson, R. J.; Strongin, R. M., *Acta Crystallogr., Sect. E: Struct. Rep. Online* **2001**, 57 (5), o447.
343. Rosenberger, M.; Jackson, W.; Saucy, G., *Helvetica Chimica Acta* **1980**, 63 (6), 1665-1674.
344. Corey, E. J.; Chaykovsky, M., *Journal of the American Chemical Society* **1962**, 84 (19), 3782-3783.
345. Franzen, V.; Driesen, H.-E., *Chemische Berichte* **1963**, 96 (7), 1881-1890.
346. Coxon, J. M.; Dansted, E.; Hartshorn, M. P.; Richards, K. E., *Tetrahedron* **1968**, 24 (3), 1193-1197.
347. Pulido, F. J.; Barbero, A.; Castreño, P., *The Journal of Organic Chemistry* **2011**, 76 (14), 5850-5855.
348. Bermand, C.; Comel, A.; Kirsch, G., *ARKIVOC* **2000**, 1 (2), 128-132.
349. Botella, G. M.; Harrison, B. L.; Robichaud, A. J.; Salituro, F. G.; Beresis, R. T. WO2015180679, 2015.
350. Huang, Y. D.; Zhang, X. J.; Wang, Z. X.; Chen, F. E., *Chin. Chem. Lett.* **2003**, 14 (1), 29-31.
351. Mahuteau-Betzer, F.; Ghosez, L., *Tetrahedron* **2002**, 58 (35), 6991-7000.
352. Nagano, T.; Einaru, S.; Shitamichi, K.; Asano, K.; Matsubara, S., *Eur. J. Org. Chem.* **2020**, 2020 (46), 7131-7133.
353. Wang, Y.; Chen, M.; Chen, P.; Hu, A., *Jingxi Huagong Zhongjianti* **2003**, 33 (2), 16-17.
354. Zhong, Y.-W.; Tian, P.; Lin, G.-Q., *Tetrahedron: Asymmetry* **2004**, 15 (5), 771-776.
355. Zierke, T.; Gebhardt, J.; Schaefer, P.; Vogelbacher, U. J.; Rack, M.; Lohmann, J. K. WO2014108286, 2014.
356. Hodgson, D. M.; Fleming, M. J.; Stanway, S. J., *Organic Letters* **2005**, 7 (15), 3295-3298.

357. Okazaki, R.; Negishi, Y.; Inamoto, N., *The Journal of Organic Chemistry* **1984**, *49* (20), 3819-3824.
358. Alcaraz, L.; Harnett, J. J.; Mioskowski, C.; Martel, J. P.; Le Gall, T.; Shin, D.-S.; Falck, J. R., *Tetrahedron Letters* **1994**, *35* (30), 5453-5456.
359. Wang, Y.; Zhang, Z.; Deng, L.; Lao, T.; Su, Z.; Yu, Y.; Cao, H., *Org. Lett.* **2021**, *23* (18), 7171-7176.
360. Verkade, J. G.; Mohan, T.; Wroblewski, A. E. US5698737, 1997.
361. Wang, B.; Qin, L.; Mu, T.; Xue, Z.; Gao, G., *Chemical Reviews* **2017**, *117* (10), 7113-7131.
362. Buteau, K. C., *J. High Tech. L.* **2009**, *10*, 22.
363. Timmins, G. S., *Expert opinion on therapeutic patents* **2017**, *27* (12), 1353-1361.
364. Martinez, A. Dissertation, Assumption University, 2021.
365. Starikova, O.; Dolgushin, G.; Larina, L.; Ushakov, P.; Komarova, T.; Lopyrev, V., *Russian journal of organic chemistry* **2003**, *39* (10), 1467-1470.
366. Starikova, O. V.; Dolgushin, G. V.; Larina, L. I.; Ushakov, P. E.; Komarova, T. N.; Lopyrev, V. A., *Russ. J. Org. Chem.* **2003**, *39* (10), 1467-1470.
367. Clarke, C. J.; Puttick, S.; Sanderson, T. J.; Taylor, A. W.; Bourne, R. A.; Lovelock, K. R. J.; Licence, P., *Physical Chemistry Chemical Physics* **2018**, *20* (24), 16786-16800.
368. Freire, M. G.; Neves, C. M.; Marrucho, I. M.; Coutinho, J. A.; Fernandes, A. M., *J Phys Chem A* **2010**, *114* (11), 3744-9.
369. Vygodskii, Y. S.; Sapozhnikov, D. A.; Shaplov, A. S.; Lozinskaya, E. I.; Ignat'Ev, N. V.; Schulte, M.; Vlasov, P. S.; Malyshkina, I. A., *Polymer journal* **2011**, *43* (2), 126-135.
370. Huang, S.; Wang, H.; Liu, Y.; Sun, B.; Tian, H.; Liang, S., *J. Sulfur Chem.* **2021**, *42* (6), 604-613.
371. Cheng, S.; Wei, W.; Zhang, X.; Yu, H.; Huang, M.; Kazemnejadi, M., *Green Chemistry* **2020**, *22* (6), 2069-2076.
372. Huang, S.; Wang, H.; Liu, Y.; Sun, B.; Tian, H.; Liang, S., *Journal of Sulfur Chemistry* **2021**, 1-10.
373. Wang, H.; Xi, Z.; Huang, S.; Ding, R.; Gao, Y.; Liu, Y.; Sun, B.; Tian, H.; Liang, S., *The Journal of Organic Chemistry* **2021**, *86* (7), 4932-4943.
374. Romero-Hernández, L. L.; Merino-Montiel, P.; Meza-Reyes, S.; Vega-Baez, J. L.; López, Ó.; Padrón, J. M.; Montiel-Smith, S., *European Journal of Medicinal Chemistry* **2018**, *143*, 21-32.

375. Pétrier, C.; Suslick, K., *Ultrasonics Sonochemistry* **2000**, 7 (2), 53-61.
376. Braun, I.; Rudroff, F.; Mihovilovic, M.; Bach, T., *Synthesis-stuttgart* **2007**, 2007, 3896-3906.
377. Jiang, L.; Davison, A.; Tennant, G.; Ramage, R., *Tetrahedron* **1998**, 54 (47), 14233-14254.
378. Waser, J.; Gaspar, B.; Nambu, H.; Carreira, E. M., *Journal of the American Chemical Society* **2006**, 128 (35), 11693-11712.
379. Hu, X.; Sun, J.; Wang, H.-G.; Manetsch, R., *Journal of the American Chemical Society* **2008**, 130 (42), 13820-13821.
380. Pattabiraman, V. R.; Stymiest, J. L.; Derksen, D. J.; Martin, N. I.; Vederas, J. C., *Organic Letters* **2007**, 9 (4), 699-702.
381. Brink, K.; Mattes, R., *Chemische Berichte* **1987**, 120 (3), 351-354.
382. Gonell, S.; Peris, E.; Poyatos, M., *Eur. J. Inorg. Chem.* **2019**, 2019 (33), 3776-3781.
383. Chimni, S. S.; Bala, N.; Dixit, V. A.; Bharatam, P. V., *Tetrahedron* **2010**, 66 (16), 3042-3049.

Every reasonable effort has been made to acknowledge the owners of copyright material. I would be pleased to hear from any copyright owner who has been omitted or incorrectly acknowledged.

**Appendix A**  
**Permission Statements**

## JOHN WILEY AND SONS LICENSE TERMS AND CONDITIONS

Jun 15, 2022

---

---

This Agreement between Curtin University (School of Molecular & Life Sciences) -- Jan Sozynski ("You") and John Wiley and Sons ("John Wiley and Sons") consists of your license details and the terms and conditions provided by John Wiley and Sons and Copyright Clearance Center.

License Number 5330231153997

License date Jun 15, 2022

Licensed Content  
Publisher John Wiley and Sons

Licensed Content  
Publication ChemistrySelect

Licensed Content Title Synthesis, Chemistry and Structure of Some 1,1-Dimethylcyclopropazulenes

Licensed Content Author Dieter Wege, Allan H. White, Brian W. Skelton, et al

Licensed Content Date Oct 11, 2016

Licensed Content  
Volume 1

Licensed Content Issue 16

Licensed Content Pages 8

Type of use Dissertation/Thesis

Requestor type University/Academic

Format Print and electronic

|                            |  |
|----------------------------|--|
| Portion                    | Figure/table   |
| Number of figures/tables   | 1  |
| Will you be translating?   | No   |
| Title                      | Synthesis of Novel Ethylene Antagonists  |
| Institution name           | Curtin University (School of Molecular & Life Sciences)                                  |
| Expected presentation date | Nov 2022   |
| Portions                   | Figure 3 on page 5341  |
|                            | Curtin University (School of Molecular & Life Sciences)<br>[REDACTED]                    |
| Requestor Location         | [REDACTED]<br>Australia<br>Attn: Curtin University (School of Molecular & Life Sciences) |
| Publisher Tax ID           | EU826007151  |
| Total                      | 0.00 AUD   |
| Terms and Conditions       |  |

### TERMS AND CONDITIONS

This copyrighted material is owned by or exclusively licensed to John Wiley & Sons, Inc. or one of its group companies (each a "Wiley Company") or handled on behalf of a society with which a Wiley Company has exclusive publishing rights in relation to a particular work (collectively "WILEY"). By clicking "accept" in connection with completing this licensing transaction, you agree that the following terms and conditions apply to this transaction (along with the billing and payment terms and conditions established by the Copyright Clearance Center Inc., ("CCC's Billing and Payment terms and conditions"), at the time that you opened your RightsLink account (these are available at any time at <http://myaccount.copyright.com>).

#### Terms and Conditions

- The materials you have requested permission to reproduce or reuse (the "Wiley Materials") are protected by copyright.

- You are hereby granted a personal, non-exclusive, non-sub licensable (on a stand-alone basis), non-transferable, worldwide, limited license to reproduce the Wiley Materials for the purpose specified in the licensing process. This license, **and any CONTENT (PDF or image file) purchased as part of your order**, is for a one-time use only and limited to any maximum distribution number specified in the license. The first instance of republication or reuse granted by this license must be completed within two years of the date of the grant of this license (although copies prepared before the end date may be distributed thereafter). The Wiley Materials shall not be used in any other manner or for any other purpose, beyond what is granted in the license. Permission is granted subject to an appropriate acknowledgement given to the author, title of the material/book/journal and the publisher. You shall also duplicate the copyright notice that appears in the Wiley publication in your use of the Wiley Material. Permission is also granted on the understanding that nowhere in the text is a previously published source acknowledged for all or part of this Wiley Material. Any third party content is expressly excluded from this permission.
- With respect to the Wiley Materials, all rights are reserved. Except as expressly granted by the terms of the license, no part of the Wiley Materials may be copied, modified, adapted (except for minor reformatting required by the new Publication), translated, reproduced, transferred or distributed, in any form or by any means, and no derivative works may be made based on the Wiley Materials without the prior permission of the respective copyright owner. **For STM Signatory Publishers clearing permission under the terms of the [STM Permissions Guidelines](#) only, the terms of the license are extended to include subsequent editions and for editions in other languages, provided such editions are for the work as a whole in situ and does not involve the separate exploitation of the permitted figures or extracts,** You may not alter, remove or suppress in any manner any copyright, trademark or other notices displayed by the Wiley Materials. You may not license, rent, sell, loan, lease, pledge, offer as security, transfer or assign the Wiley Materials on a stand-alone basis, or any of the rights granted to you hereunder to any other person.
- The Wiley Materials and all of the intellectual property rights therein shall at all times remain the exclusive property of John Wiley & Sons Inc, the Wiley Companies, or their respective licensors, and your interest therein is only that of having possession of and the right to reproduce the Wiley Materials pursuant to Section 2 herein during the continuance of this Agreement. You agree that you own no right, title or interest in or to the Wiley Materials or any of the intellectual property rights therein. You shall have no rights hereunder other than the license as provided for above in Section 2. No right, license or interest to any trademark, trade name, service mark or other branding ("Marks") of WILEY or its licensors is granted hereunder, and you agree that you shall not assert any such right, license or interest with respect thereto
- NEITHER WILEY NOR ITS LICENSORS MAKES ANY WARRANTY OR REPRESENTATION OF ANY KIND TO YOU OR ANY THIRD PARTY, EXPRESS, IMPLIED OR STATUTORY, WITH RESPECT TO THE MATERIALS OR THE ACCURACY OF ANY INFORMATION CONTAINED IN THE MATERIALS, INCLUDING, WITHOUT LIMITATION, ANY IMPLIED WARRANTY OF MERCHANTABILITY, ACCURACY, SATISFACTORY QUALITY, FITNESS FOR A PARTICULAR PURPOSE, USABILITY, INTEGRATION OR NON-INFRINGEMENT AND ALL SUCH WARRANTIES ARE HEREBY EXCLUDED BY WILEY AND ITS LICENSORS AND WAIVED BY YOU.
- WILEY shall have the right to terminate this Agreement immediately upon breach of this Agreement by you.

- You shall indemnify, defend and hold harmless WILEY, its Licensors and their respective directors, officers, agents and employees, from and against any actual or threatened claims, demands, causes of action or proceedings arising from any breach of this Agreement by you.
- IN NO EVENT SHALL WILEY OR ITS LICENSORS BE LIABLE TO YOU OR ANY OTHER PARTY OR ANY OTHER PERSON OR ENTITY FOR ANY SPECIAL, CONSEQUENTIAL, INCIDENTAL, INDIRECT, EXEMPLARY OR PUNITIVE DAMAGES, HOWEVER CAUSED, ARISING OUT OF OR IN CONNECTION WITH THE DOWNLOADING, PROVISIONING, VIEWING OR USE OF THE MATERIALS REGARDLESS OF THE FORM OF ACTION, WHETHER FOR BREACH OF CONTRACT, BREACH OF WARRANTY, TORT, NEGLIGENCE, INFRINGEMENT OR OTHERWISE (INCLUDING, WITHOUT LIMITATION, DAMAGES BASED ON LOSS OF PROFITS, DATA, FILES, USE, BUSINESS OPPORTUNITY OR CLAIMS OF THIRD PARTIES), AND WHETHER OR NOT THE PARTY HAS BEEN ADVISED OF THE POSSIBILITY OF SUCH DAMAGES. THIS LIMITATION SHALL APPLY NOTWITHSTANDING ANY FAILURE OF ESSENTIAL PURPOSE OF ANY LIMITED REMEDY PROVIDED HEREIN.
- Should any provision of this Agreement be held by a court of competent jurisdiction to be illegal, invalid, or unenforceable, that provision shall be deemed amended to achieve as nearly as possible the same economic effect as the original provision, and the legality, validity and enforceability of the remaining provisions of this Agreement shall not be affected or impaired thereby.
- The failure of either party to enforce any term or condition of this Agreement shall not constitute a waiver of either party's right to enforce each and every term and condition of this Agreement. No breach under this agreement shall be deemed waived or excused by either party unless such waiver or consent is in writing signed by the party granting such waiver or consent. The waiver by or consent of a party to a breach of any provision of this Agreement shall not operate or be construed as a waiver of or consent to any other or subsequent breach by such other party.
- This Agreement may not be assigned (including by operation of law or otherwise) by you without WILEY's prior written consent.
- Any fee required for this permission shall be non-refundable after thirty (30) days from receipt by the CCC.
- These terms and conditions together with CCC's Billing and Payment terms and conditions (which are incorporated herein) form the entire agreement between you and WILEY concerning this licensing transaction and (in the absence of fraud) supersedes all prior agreements and representations of the parties, oral or written. This Agreement may not be amended except in writing signed by both parties. This Agreement shall be binding upon and inure to the benefit of the parties' successors, legal representatives, and authorized assigns.
- In the event of any conflict between your obligations established by these terms and conditions and those established by CCC's Billing and Payment terms and conditions, these terms and conditions shall prevail.
- WILEY expressly reserves all rights not specifically granted in the combination of (i) the license details provided by you and accepted in the course of this licensing transaction, (ii) these terms and conditions and (iii) CCC's Billing and Payment terms and conditions.

- This Agreement will be void if the Type of Use, Format, Circulation, or Requestor Type was misrepresented during the licensing process.
- This Agreement shall be governed by and construed in accordance with the laws of the State of New York, USA, without regards to such state's conflict of law rules. Any legal action, suit or proceeding arising out of or relating to these Terms and Conditions or the breach thereof shall be instituted in a court of competent jurisdiction in New York County in the State of New York in the United States of America and each party hereby consents and submits to the personal jurisdiction of such court, waives any objection to venue in such court and consents to service of process by registered or certified mail, return receipt requested, at the last known address of such party.

## WILEY OPEN ACCESS TERMS AND CONDITIONS

Wiley Publishes Open Access Articles in fully Open Access Journals and in Subscription journals offering Online Open. Although most of the fully Open Access journals publish open access articles under the terms of the Creative Commons Attribution (CC BY) License only, the subscription journals and a few of the Open Access Journals offer a choice of Creative Commons Licenses. The license type is clearly identified on the article.

### The Creative Commons Attribution License

The [Creative Commons Attribution License \(CC-BY\)](#) allows users to copy, distribute and transmit an article, adapt the article and make commercial use of the article. The CC-BY license permits commercial and non-

### Creative Commons Attribution Non-Commercial License

The [Creative Commons Attribution Non-Commercial \(CC-BY-NC\) License](#) permits use, distribution and reproduction in any medium, provided the original work is properly cited and is not used for commercial purposes.(see below)

### Creative Commons Attribution-Non-Commercial-NoDerivs License

The [Creative Commons Attribution Non-Commercial-NoDerivs License](#) (CC-BY-NC-ND) permits use, distribution and reproduction in any medium, provided the original work is properly cited, is not used for commercial purposes and no modifications or adaptations are made. (see below)

### Use by commercial "for-profit" organizations

Use of Wiley Open Access articles for commercial, promotional, or marketing purposes requires further explicit permission from Wiley and will be subject to a fee.

Further details can be found on Wiley Online Library  
<http://olabout.wiley.com/WileyCDA/Section/id-410895.html>

### Other Terms and Conditions:

**v1.10 Last updated September 2015**

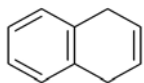
Questions? [customercare@copyright.com](mailto:customercare@copyright.com) or +1-855-239-3415 (toll free in the US) or

**+1-978-646-2777.**

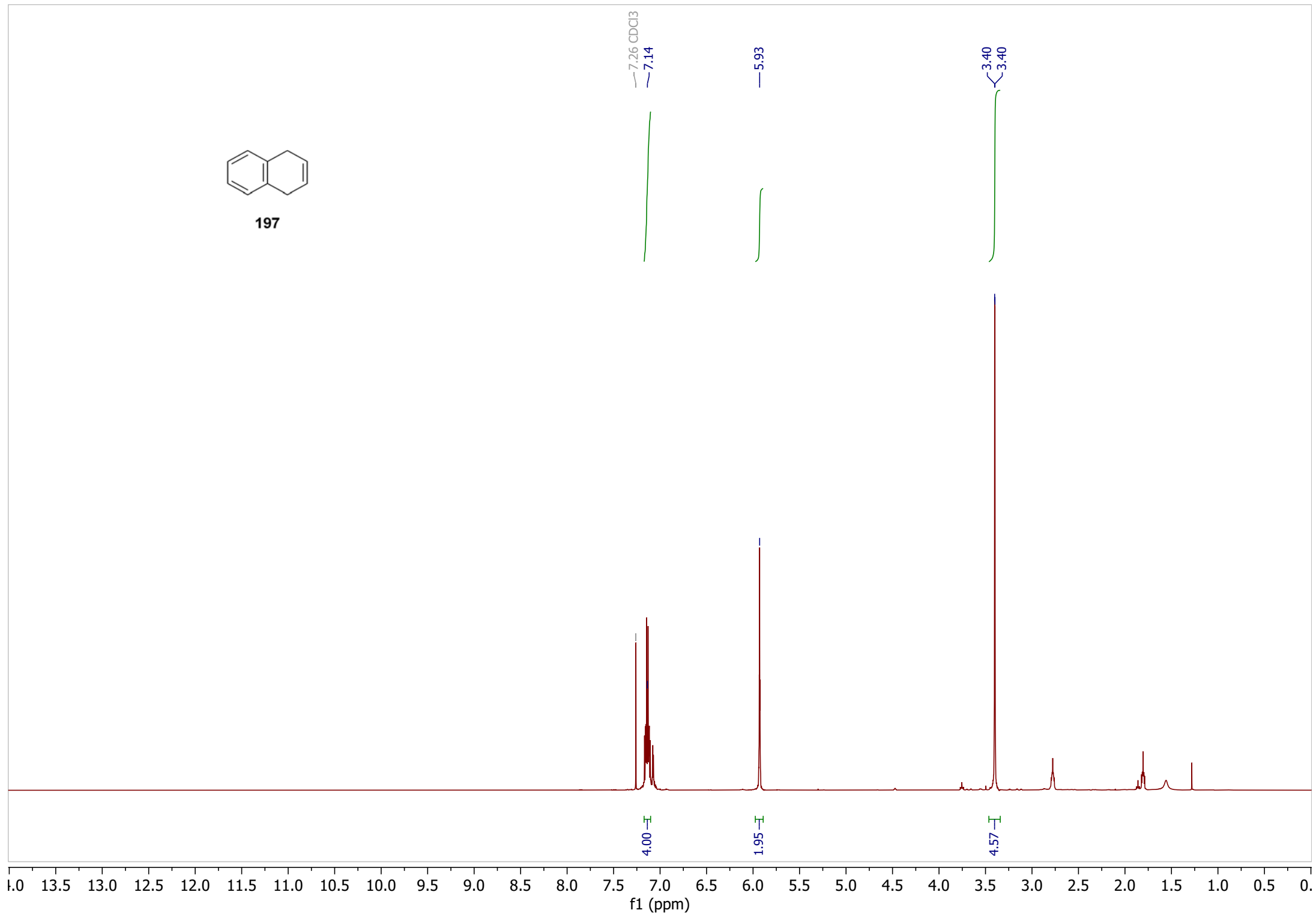
---

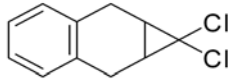
---

**Appendix B**  
**NMR Spectra of selected compounds**

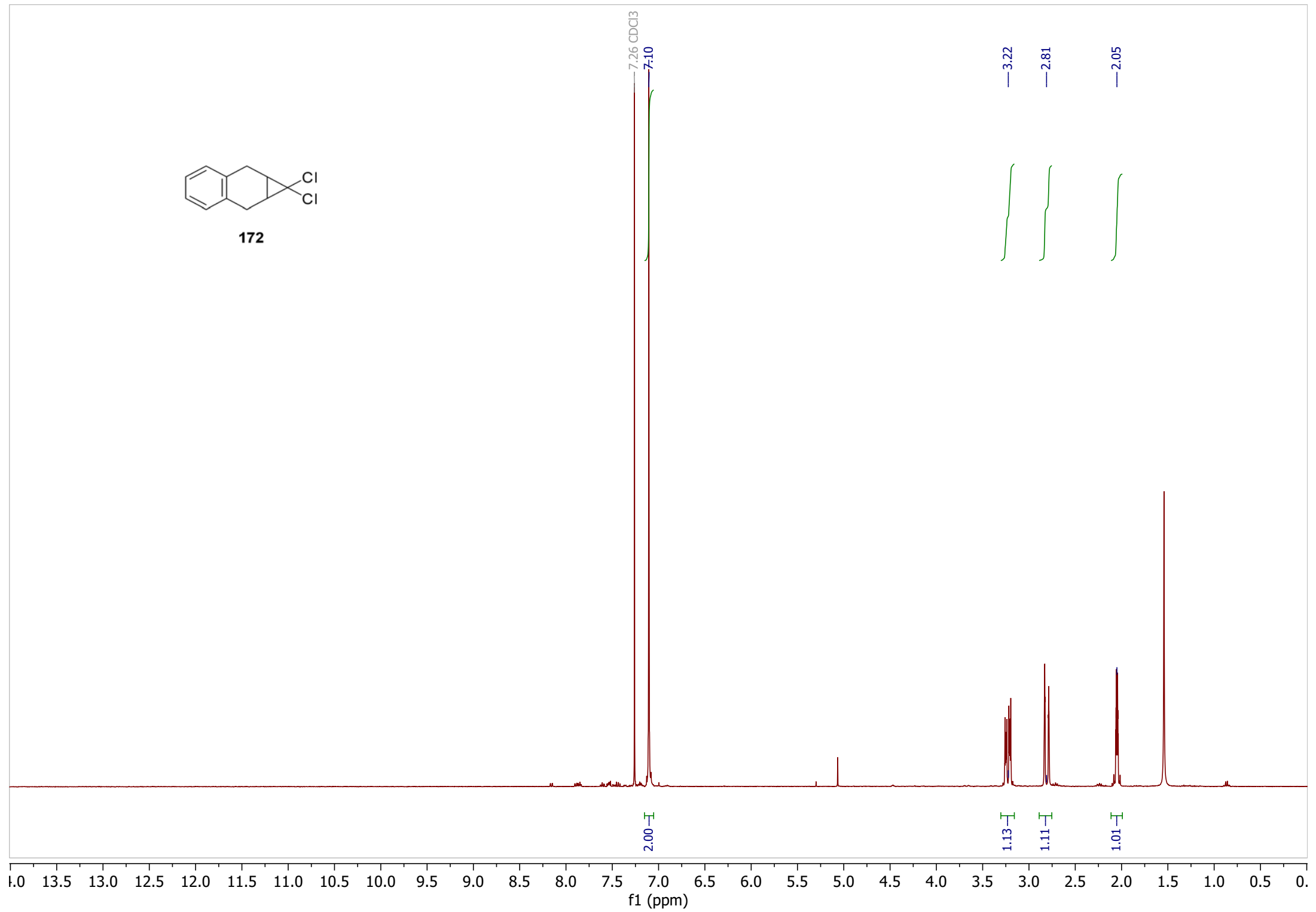


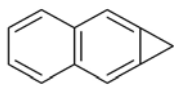
197



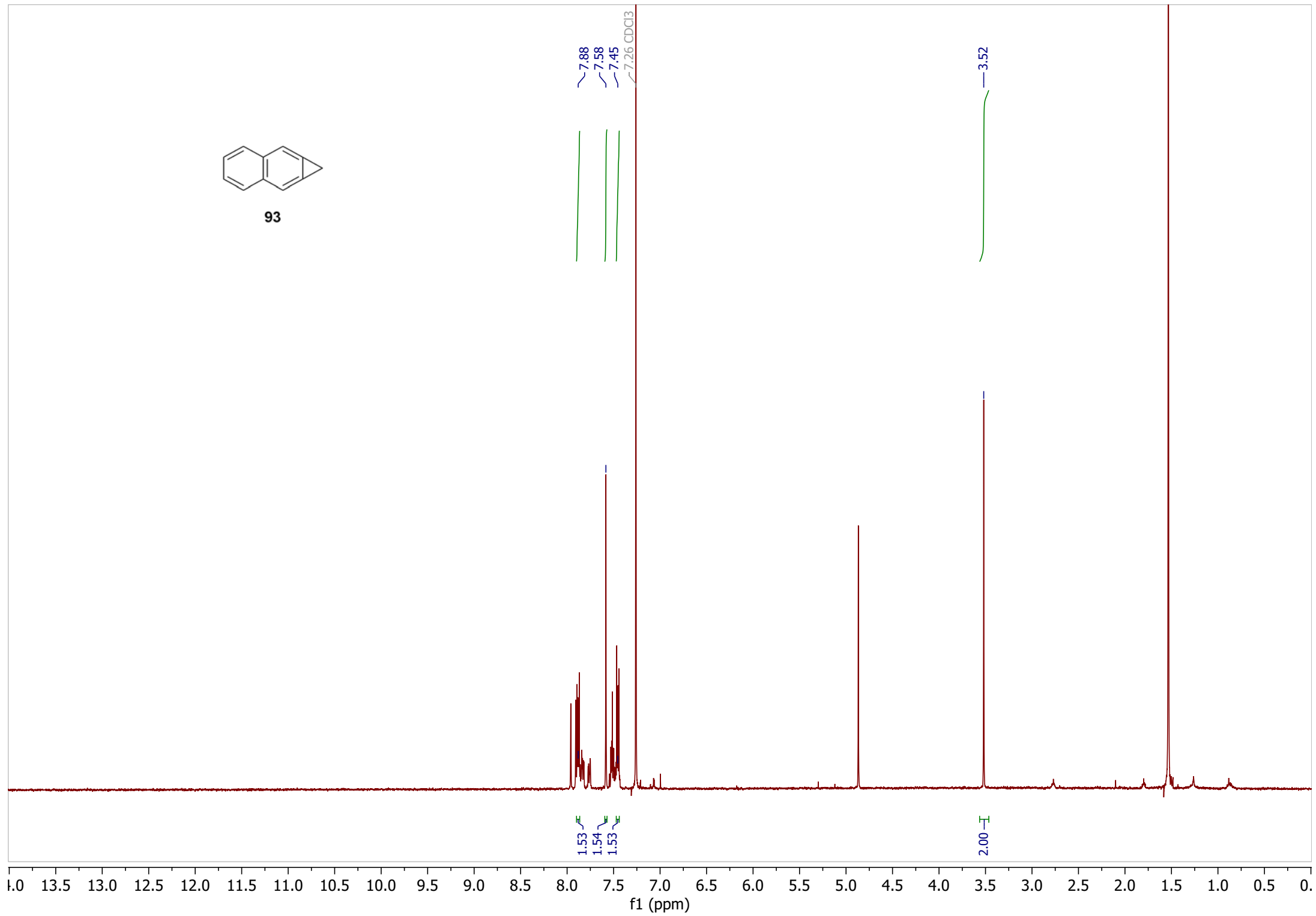


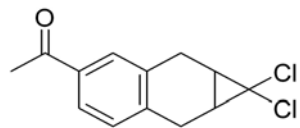
172



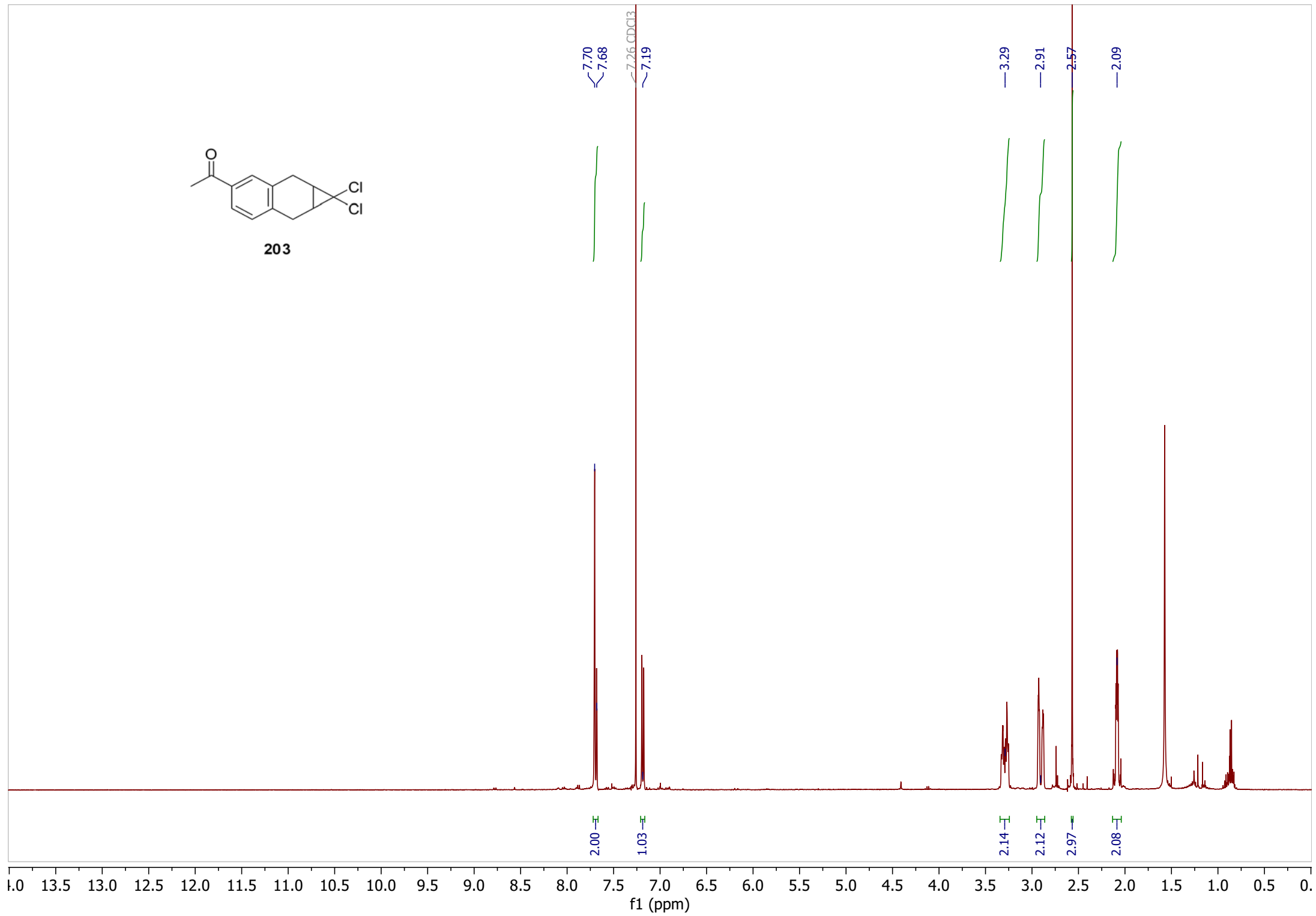


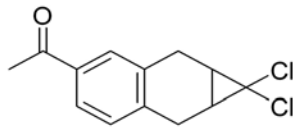
93





203





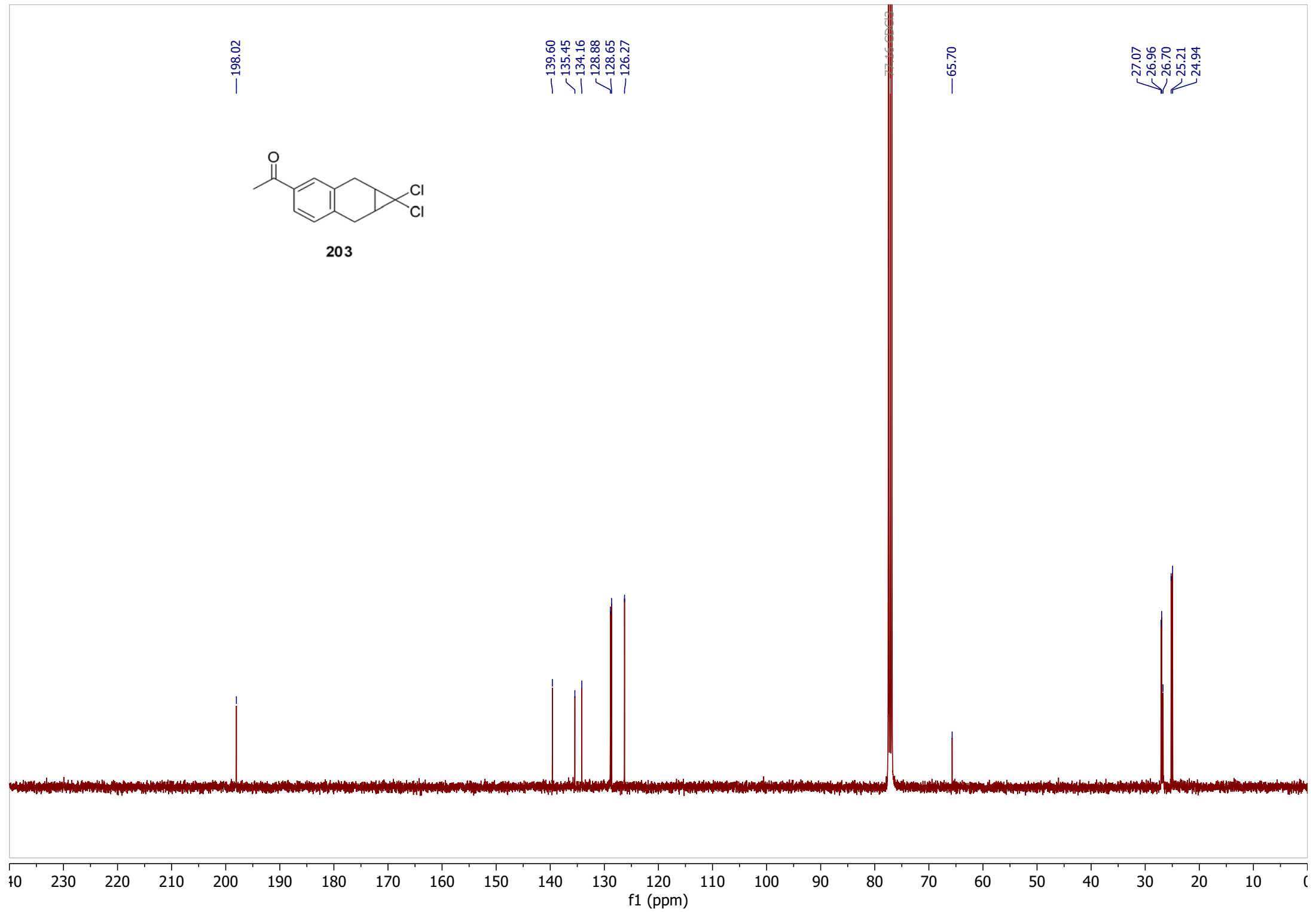
203

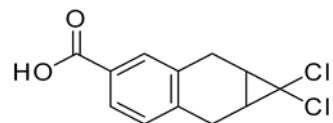
—198.02

—139.60  
—135.45  
—134.16  
—128.88  
—128.65  
—126.27

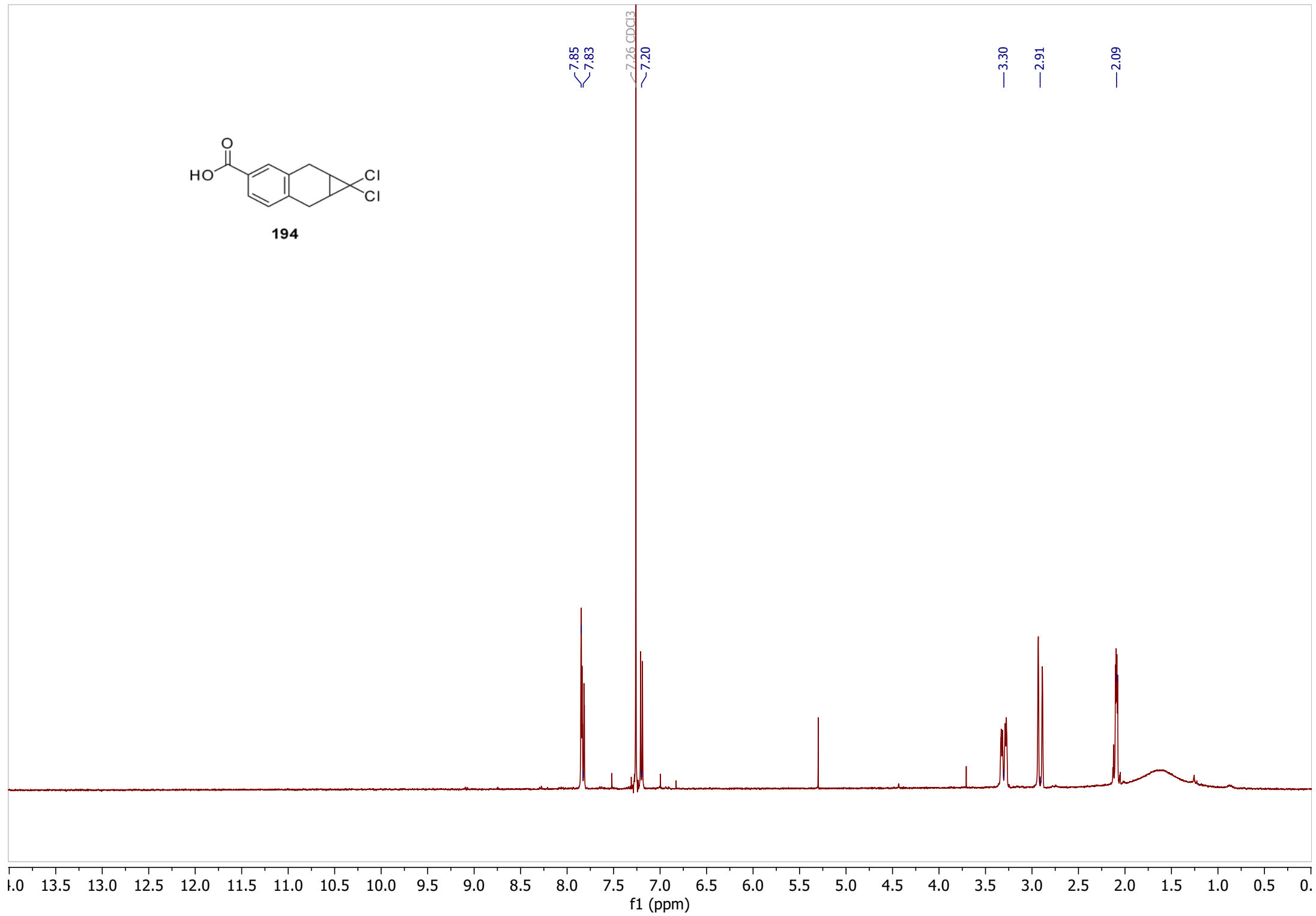
—65.70

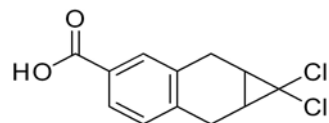
27.07  
26.96  
26.70  
25.21  
24.94



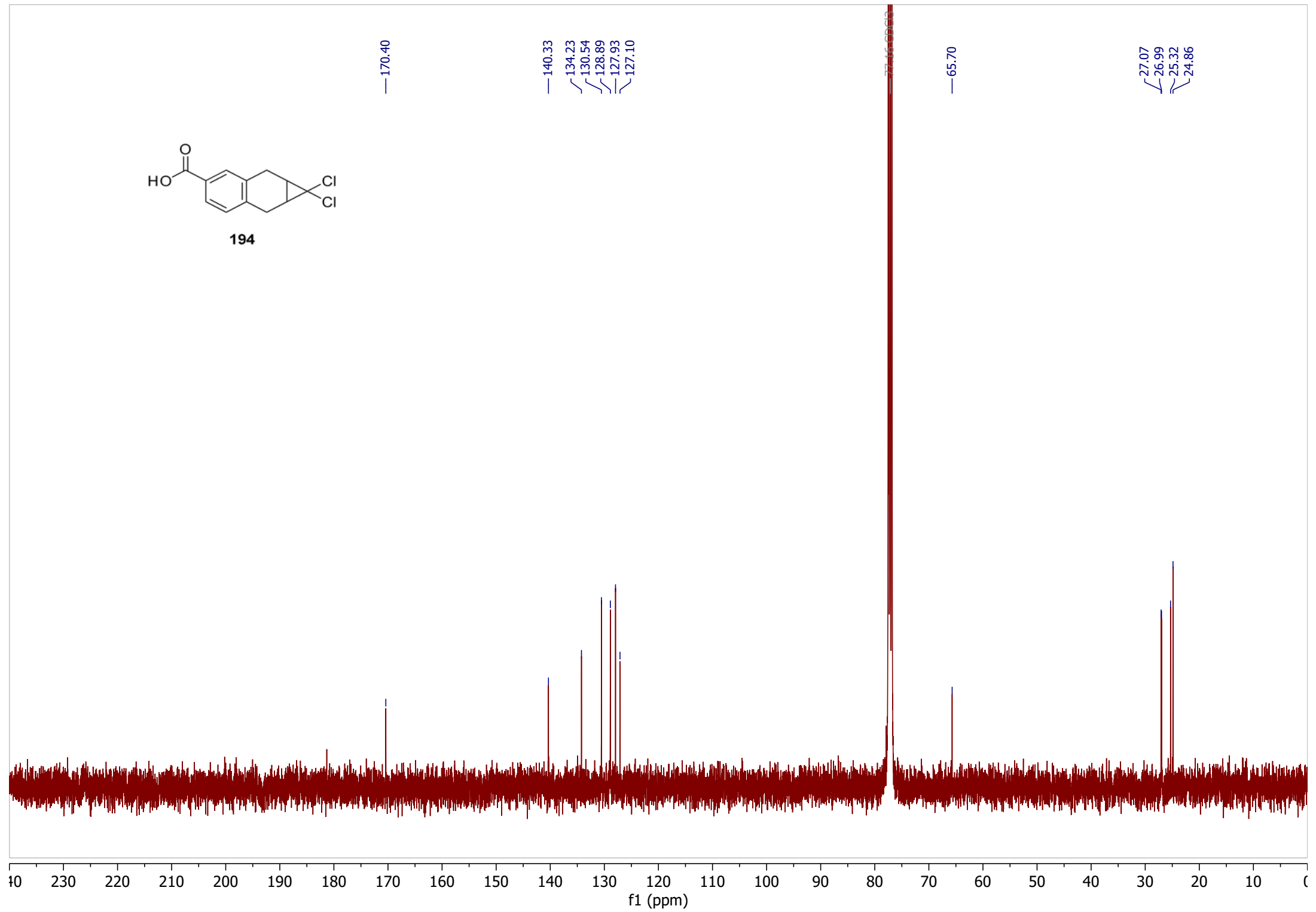


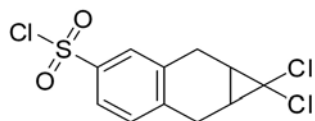
**194**



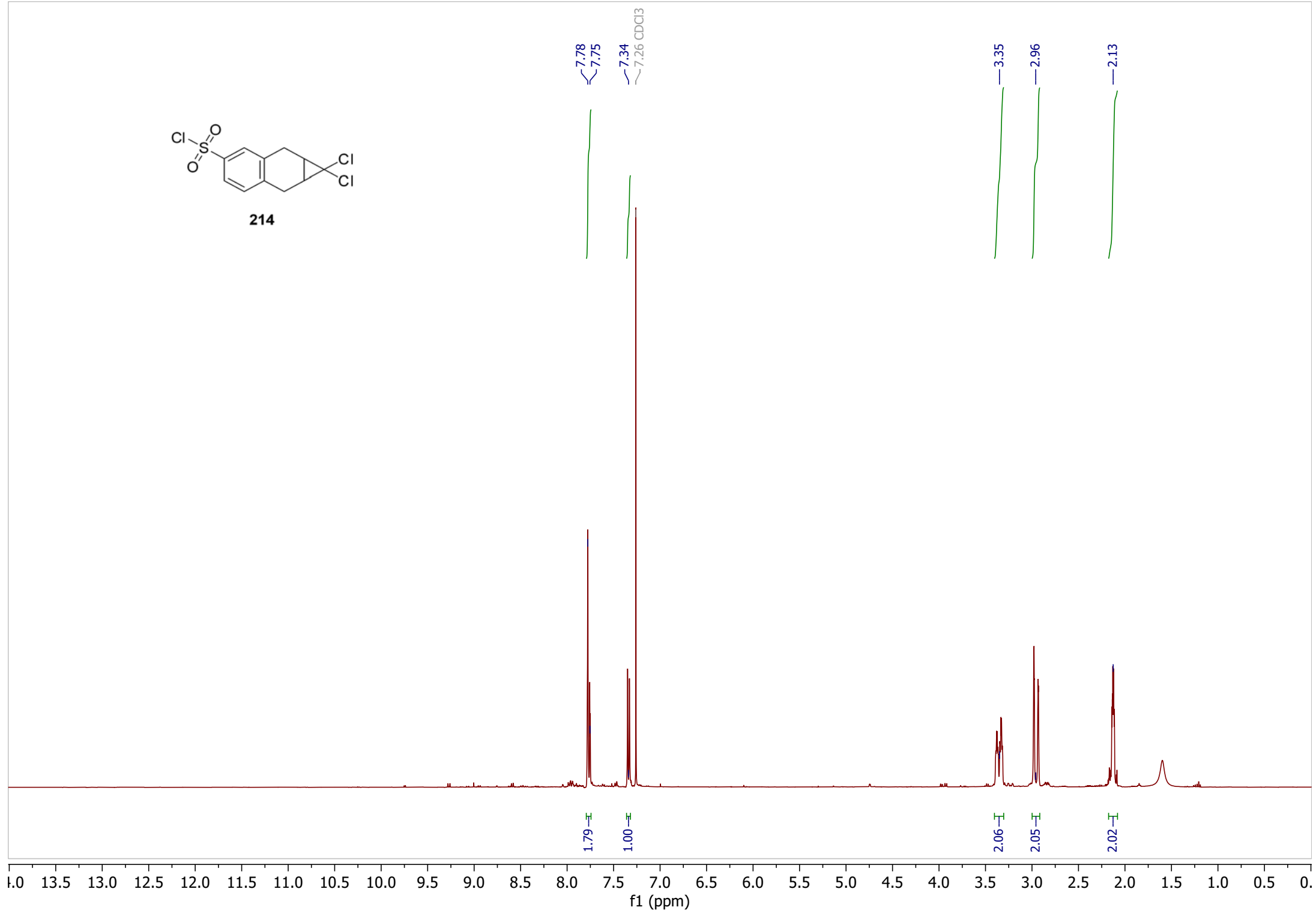


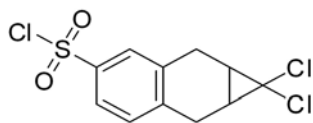
**194**



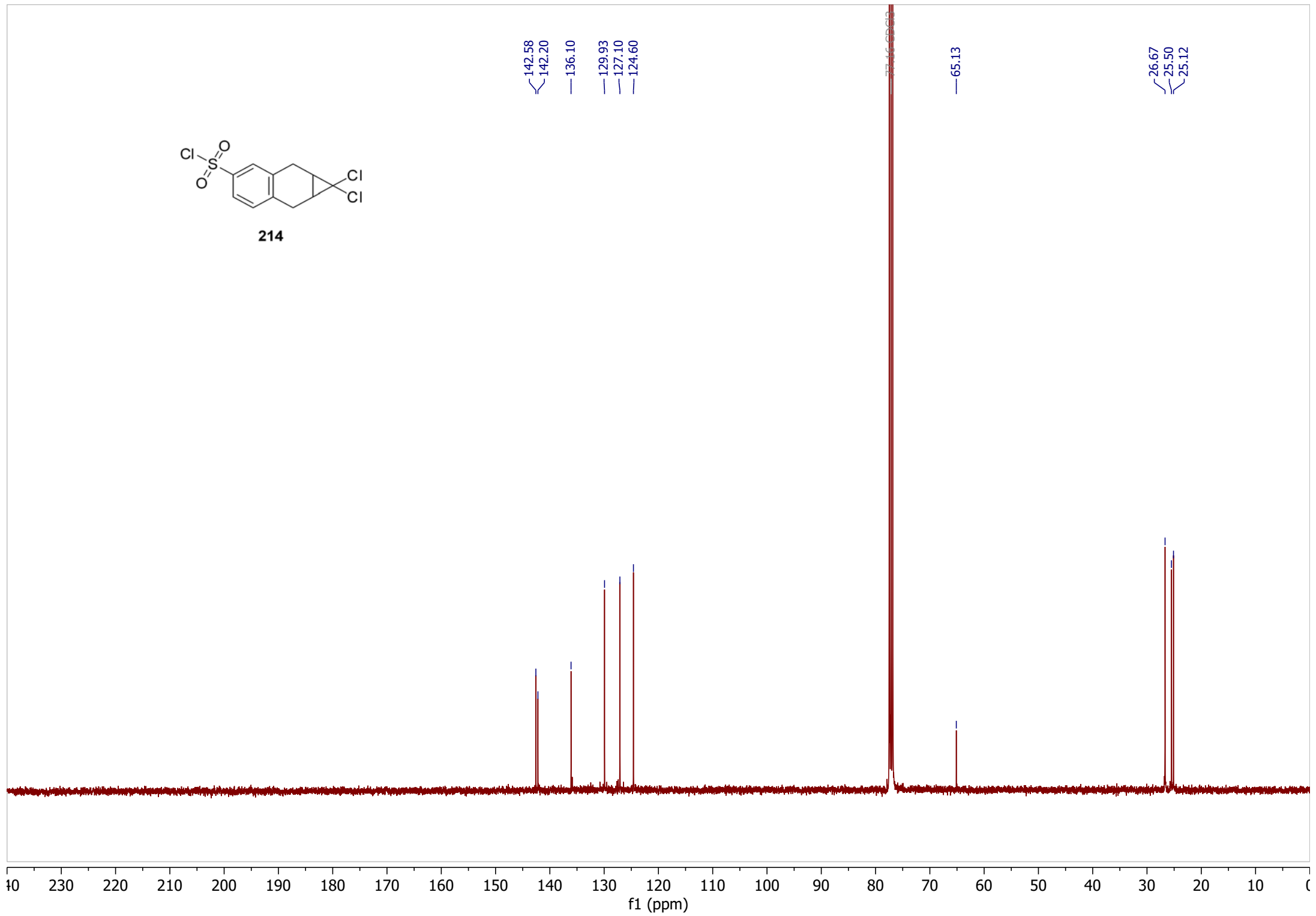


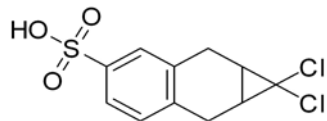
214



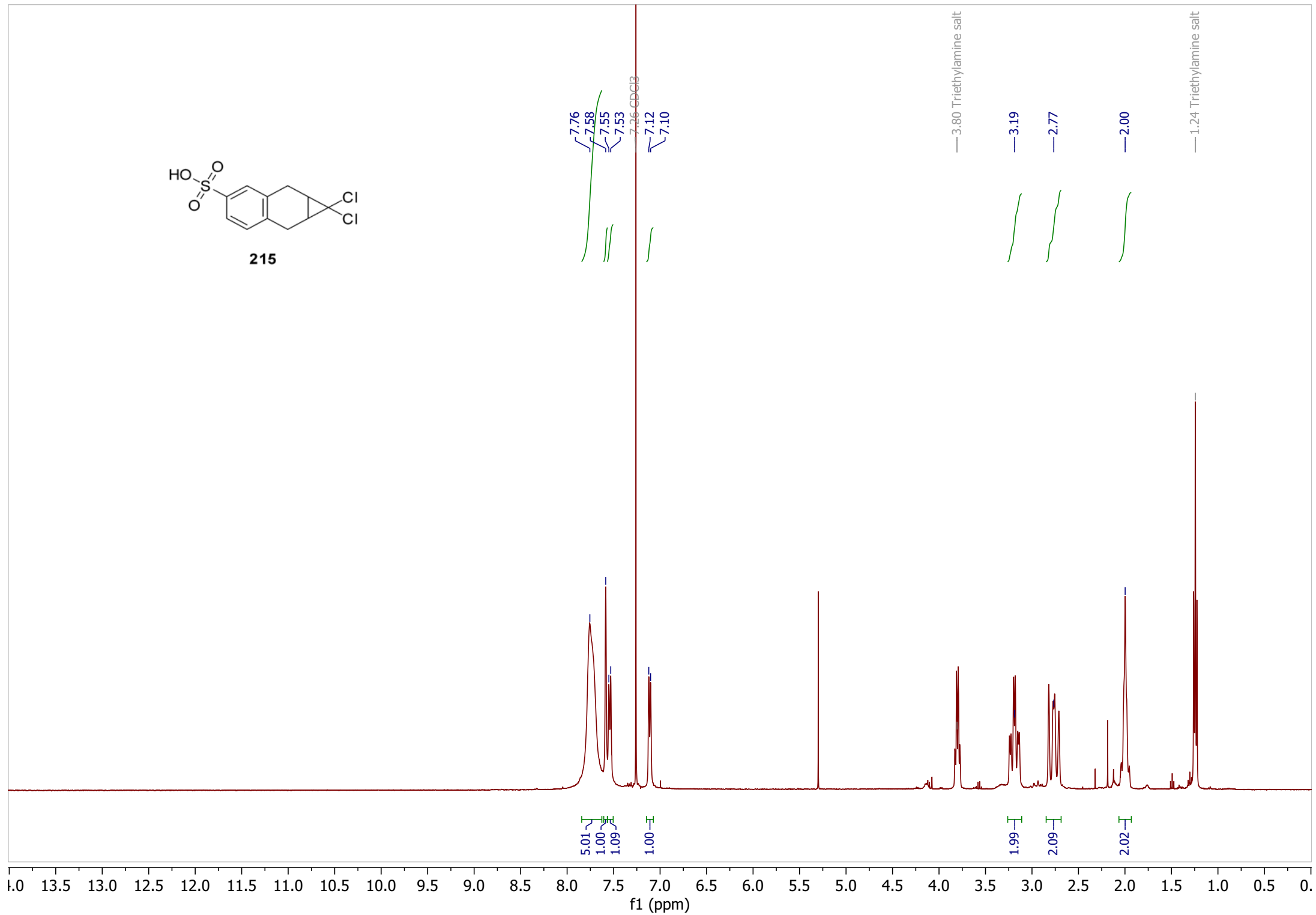


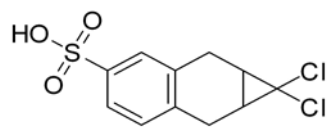
214





215





215

—138.45

—134.88

—129.05

—126.32

—123.84

—65.78

—59.29

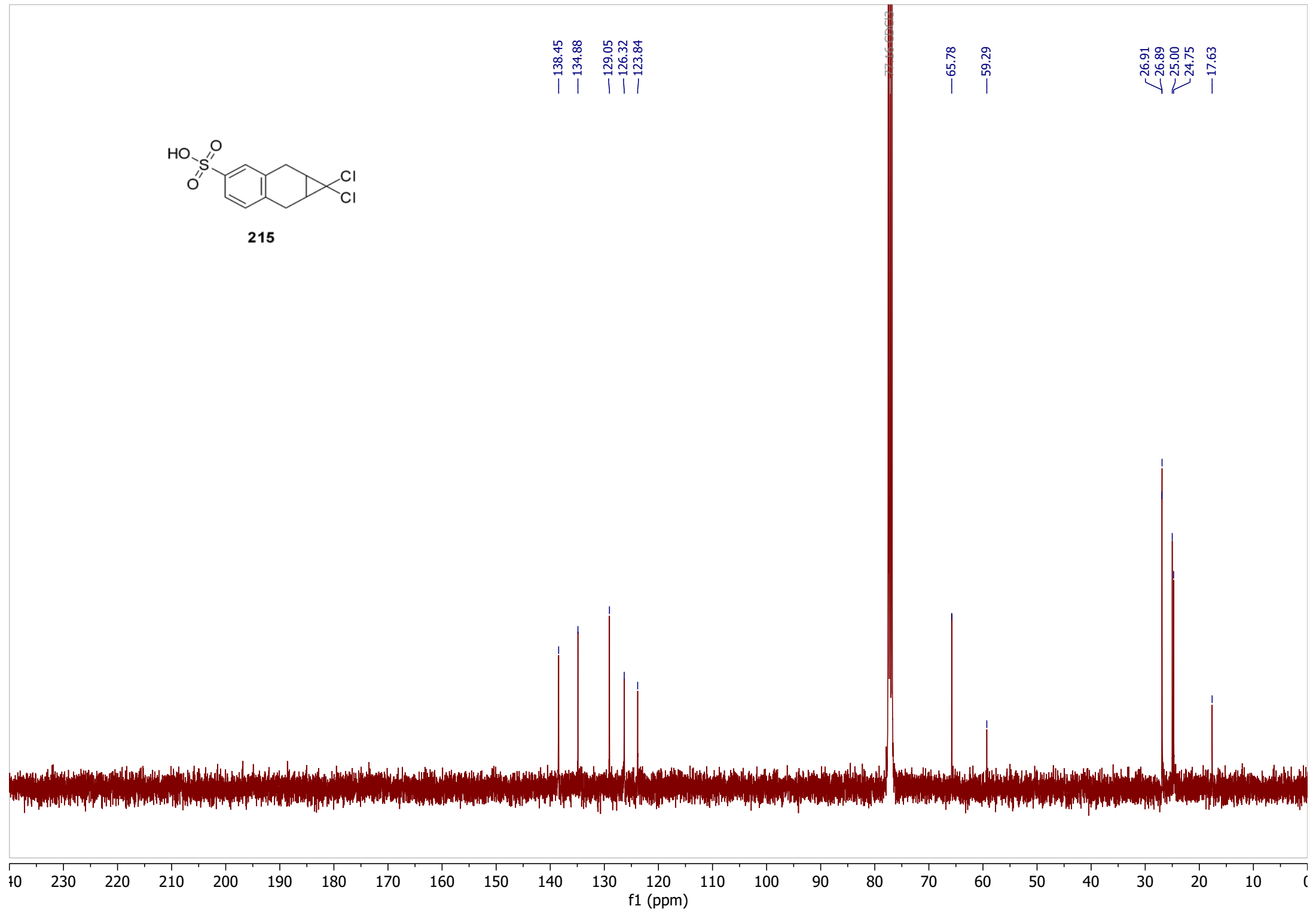
—26.91

—26.89

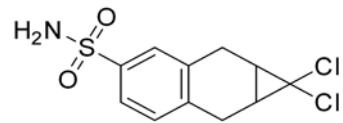
—25.00

—24.75

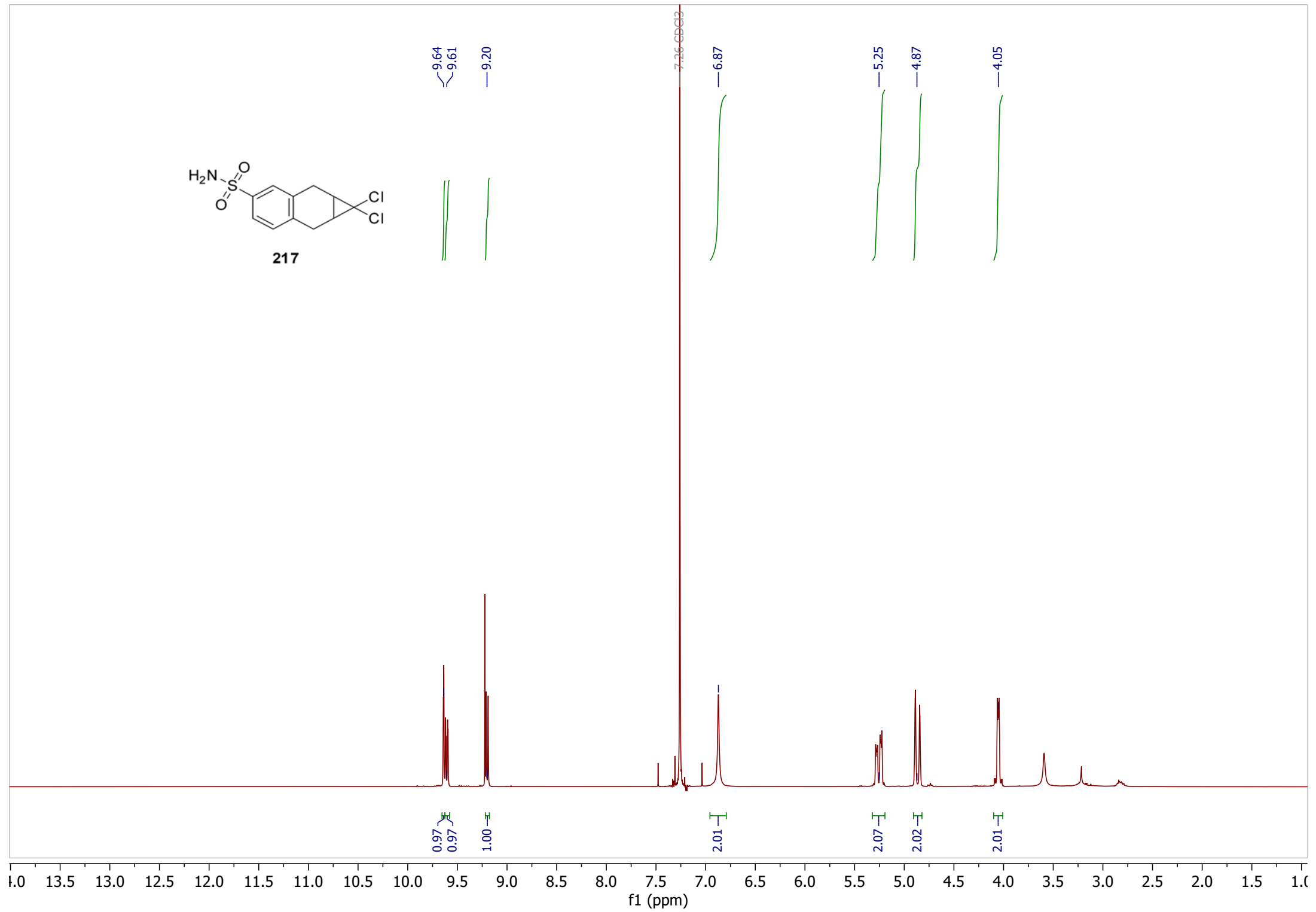
—17.63

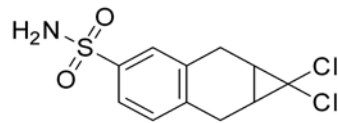


f1 (ppm)



217





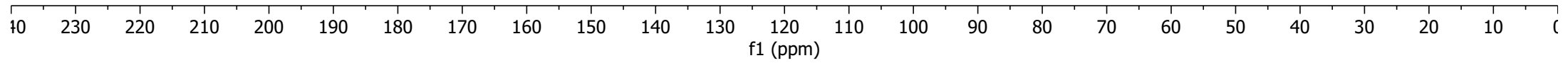
217

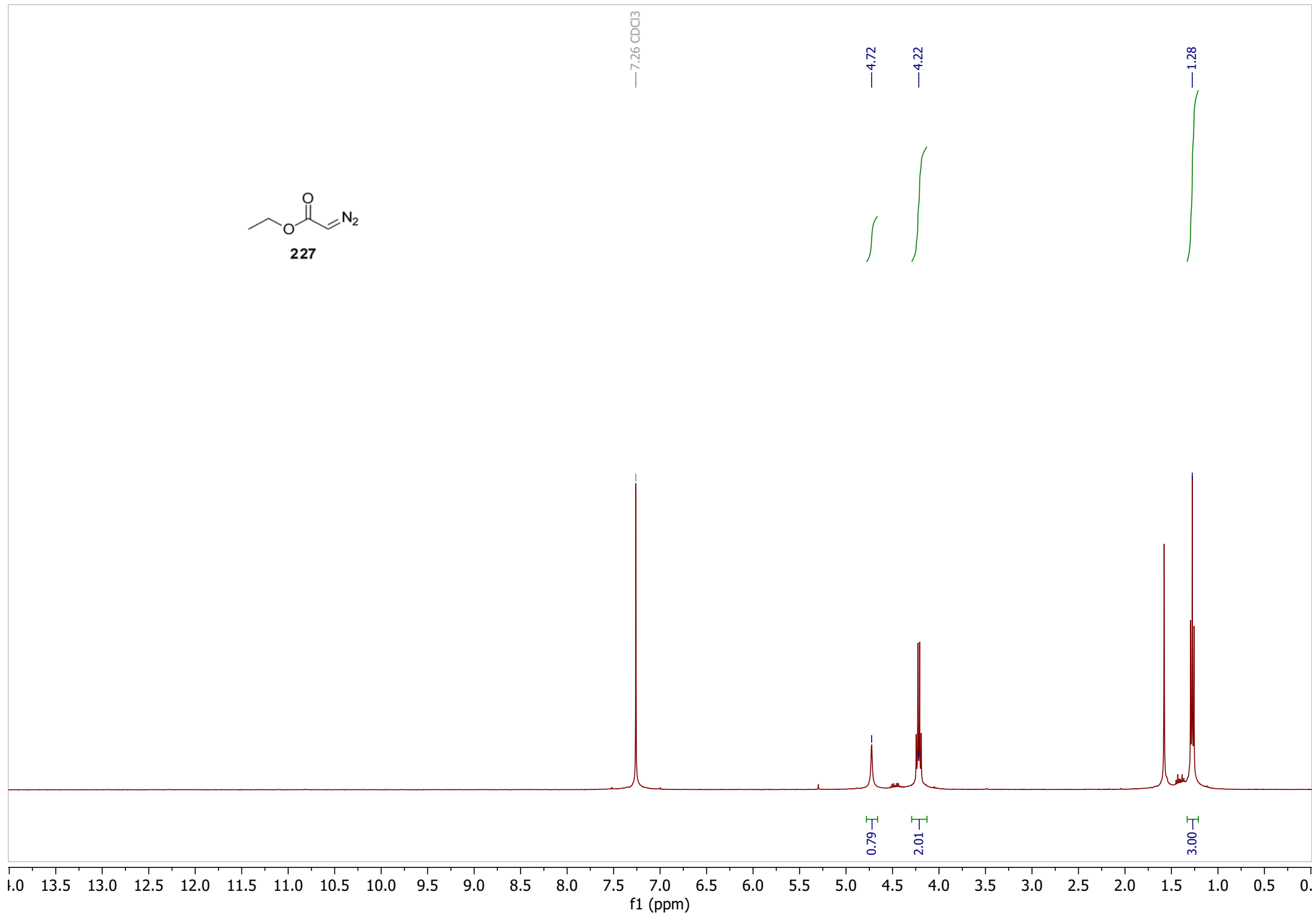
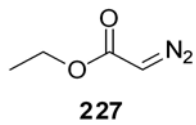
139.72  
139.31  
135.14  
129.39  
126.59  
124.02

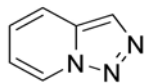
77.16 CDCl<sub>3</sub>

65.43

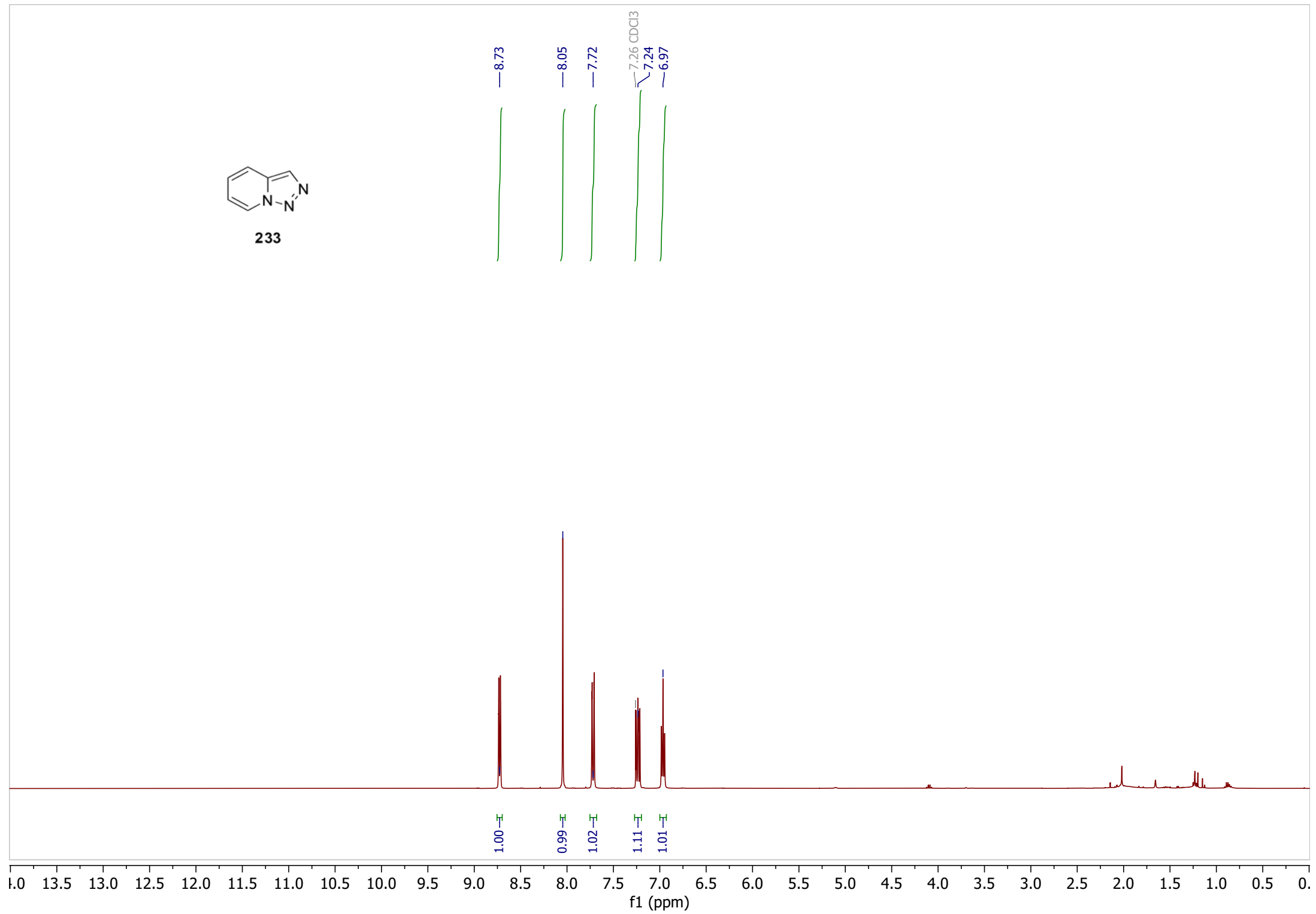
26.79  
26.77  
25.07  
24.91

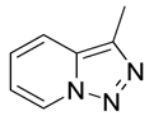




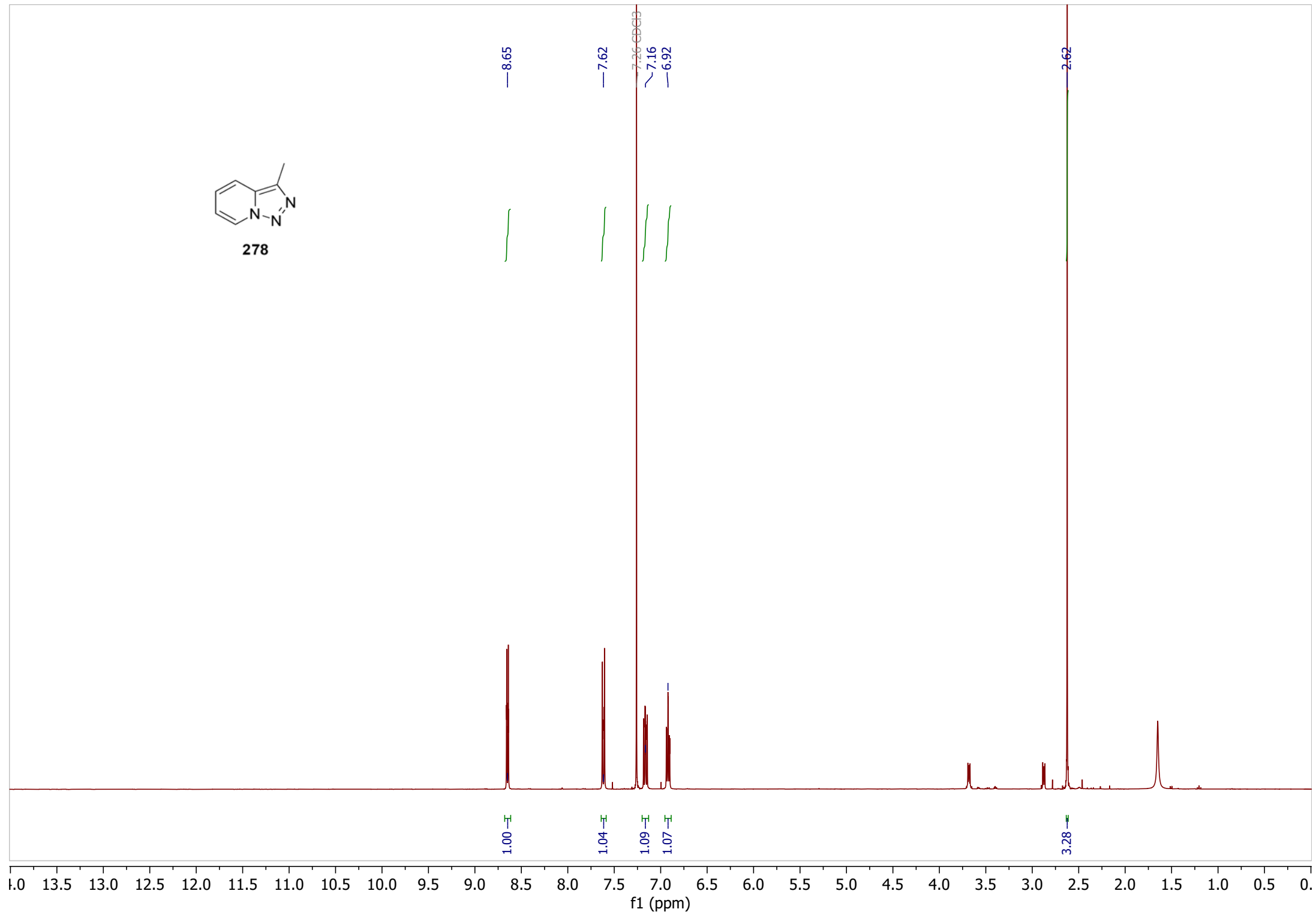


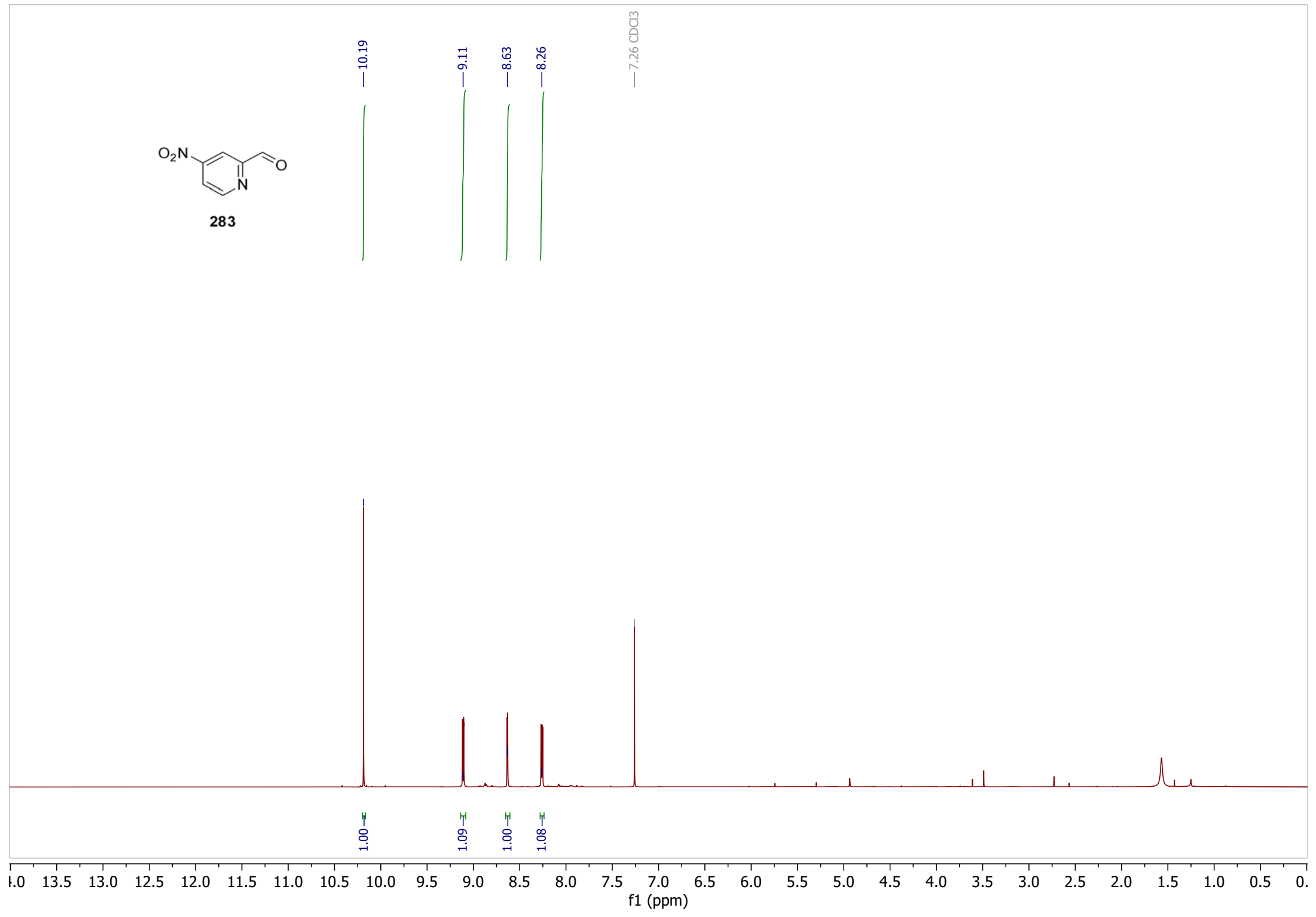
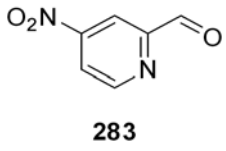
233

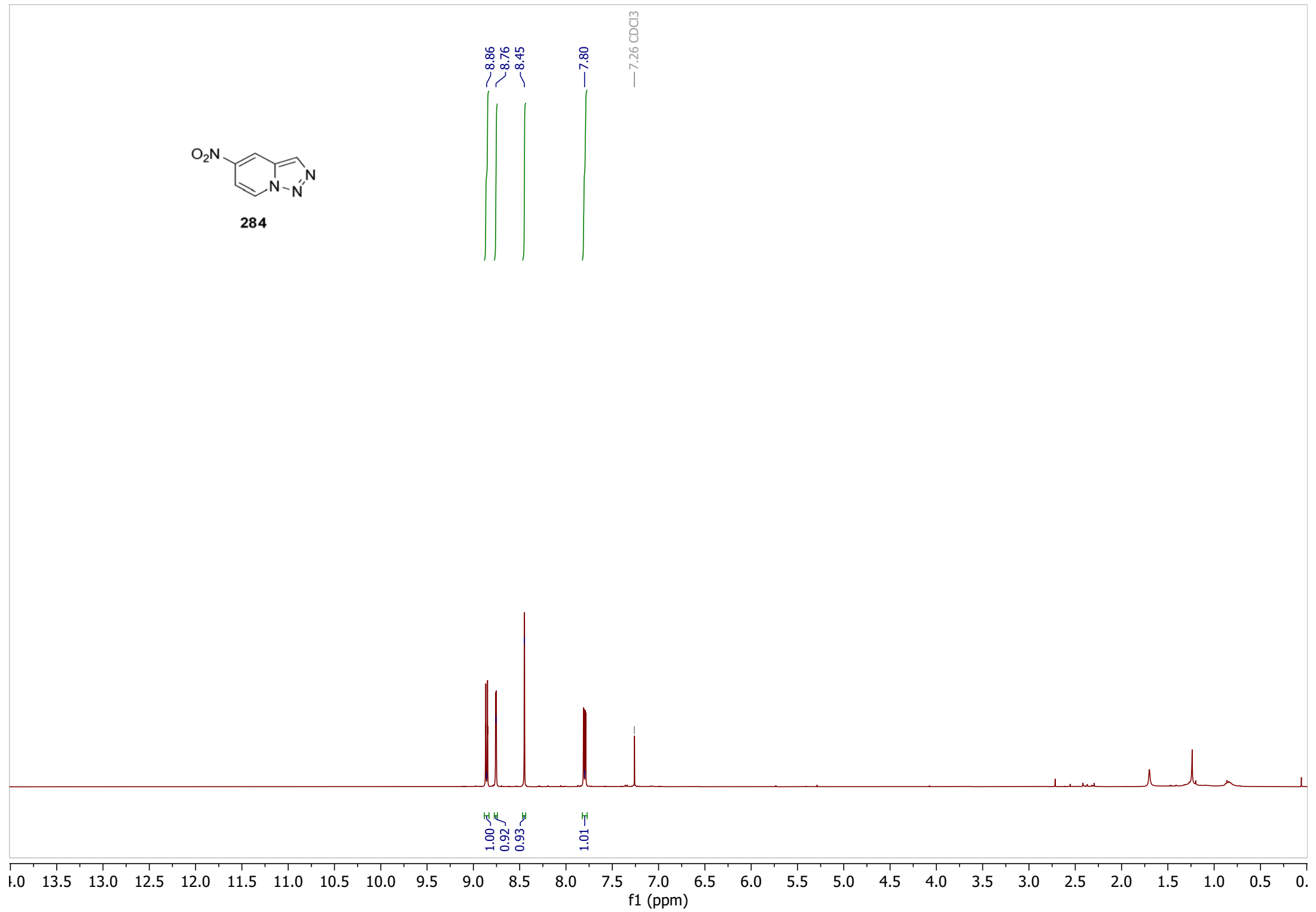
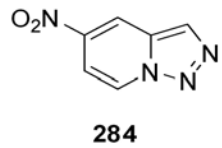


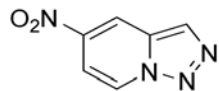


278

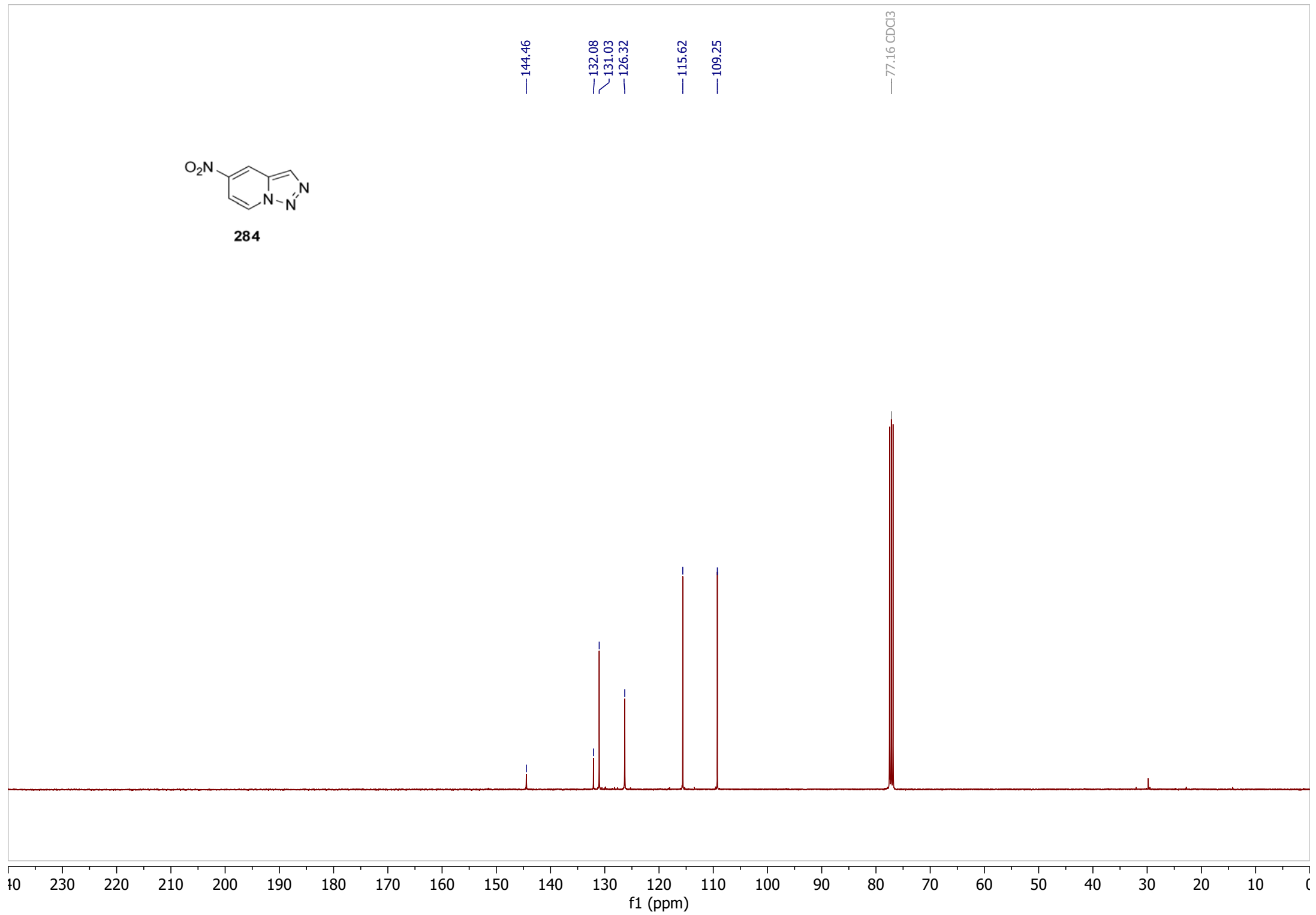


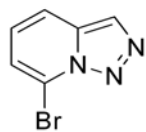




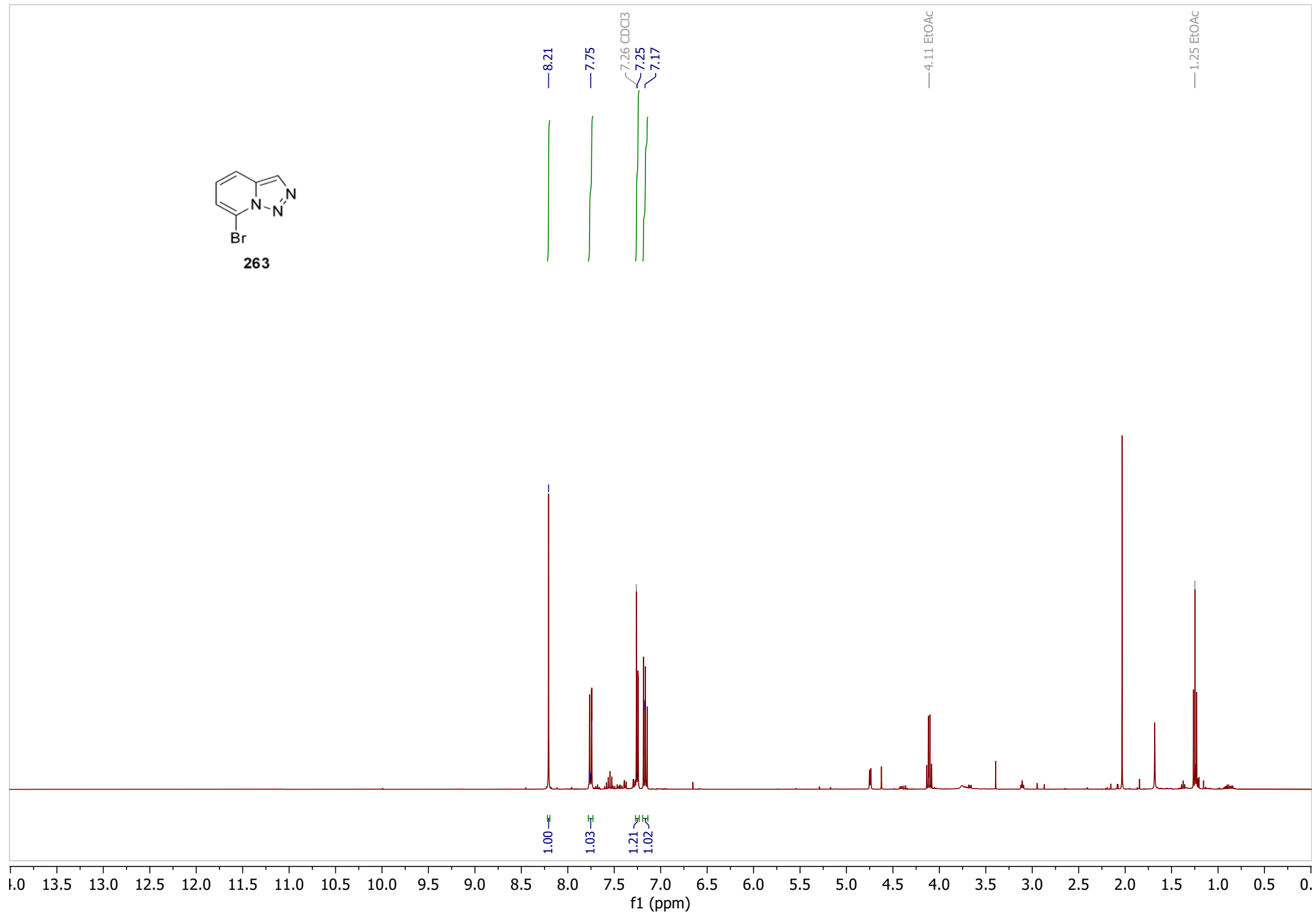


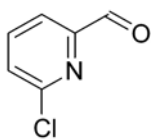
284





263





288

9.99

7.88

7.85

7.57

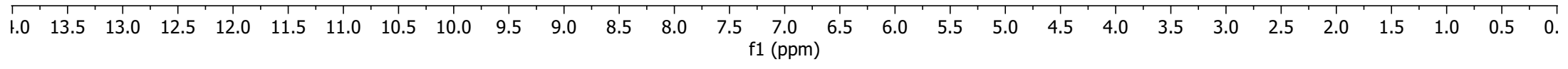
7.26 CDCl3

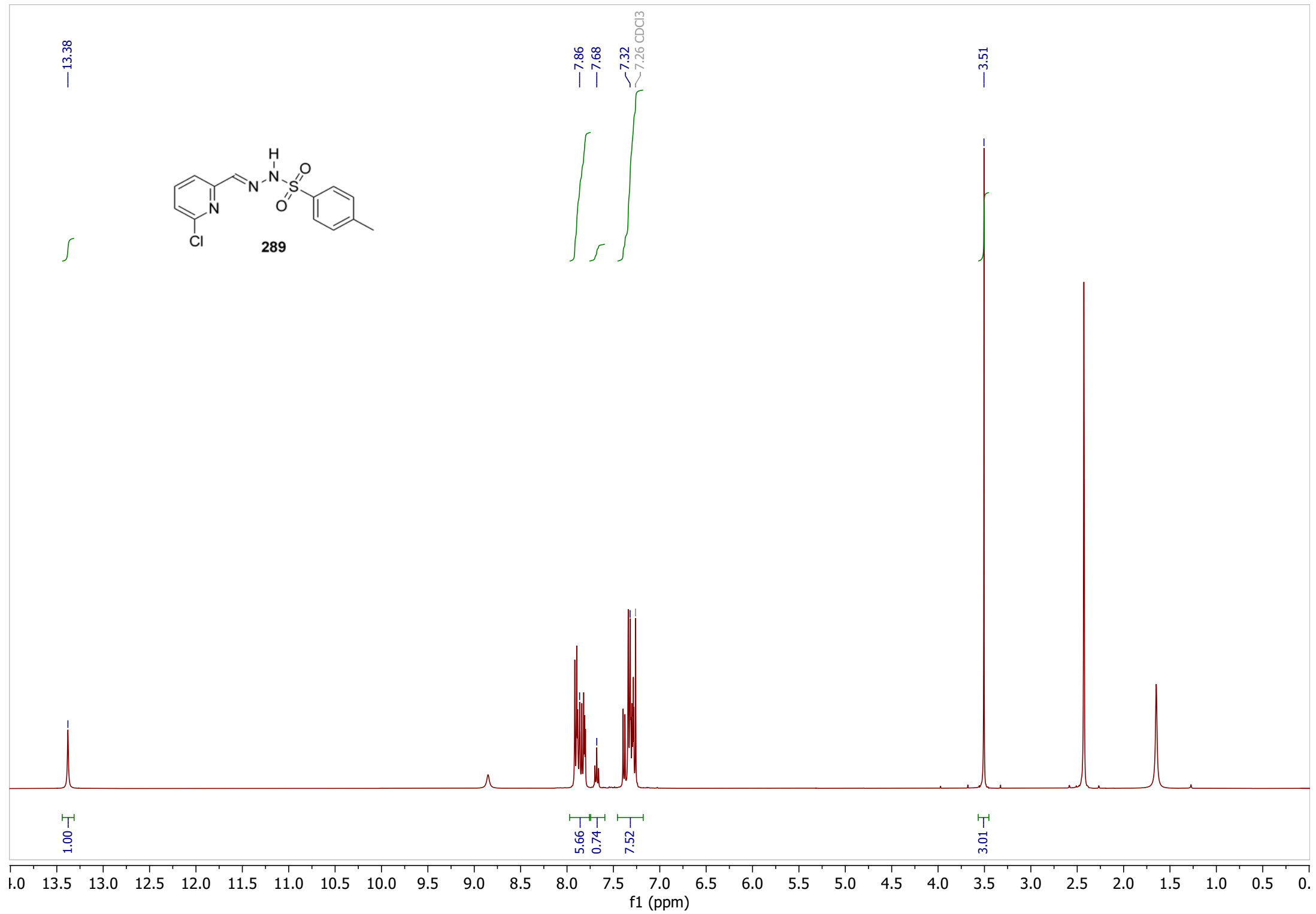
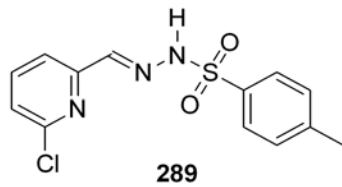
0.91

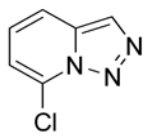
1.00

1.04

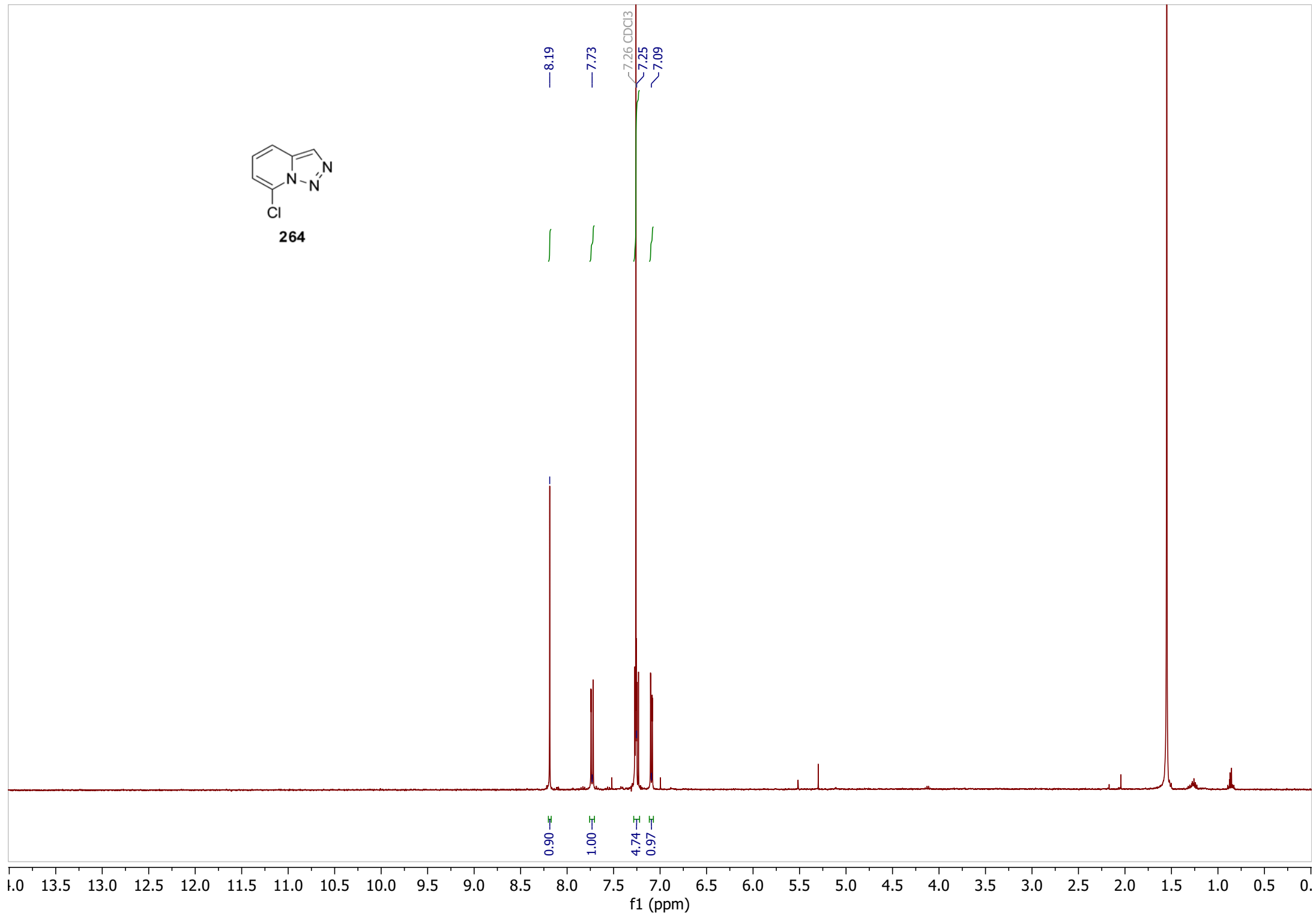
1.00

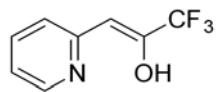




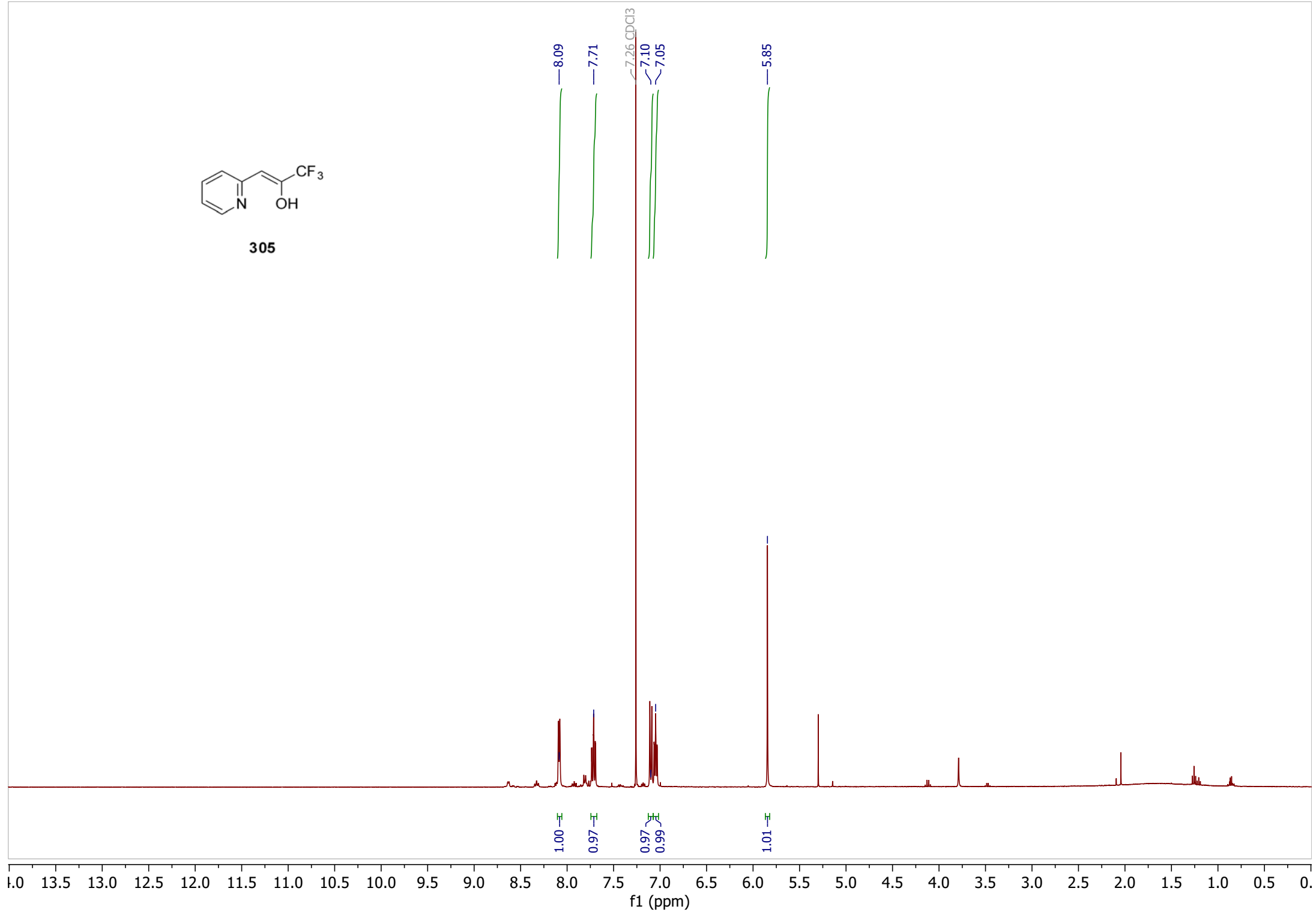


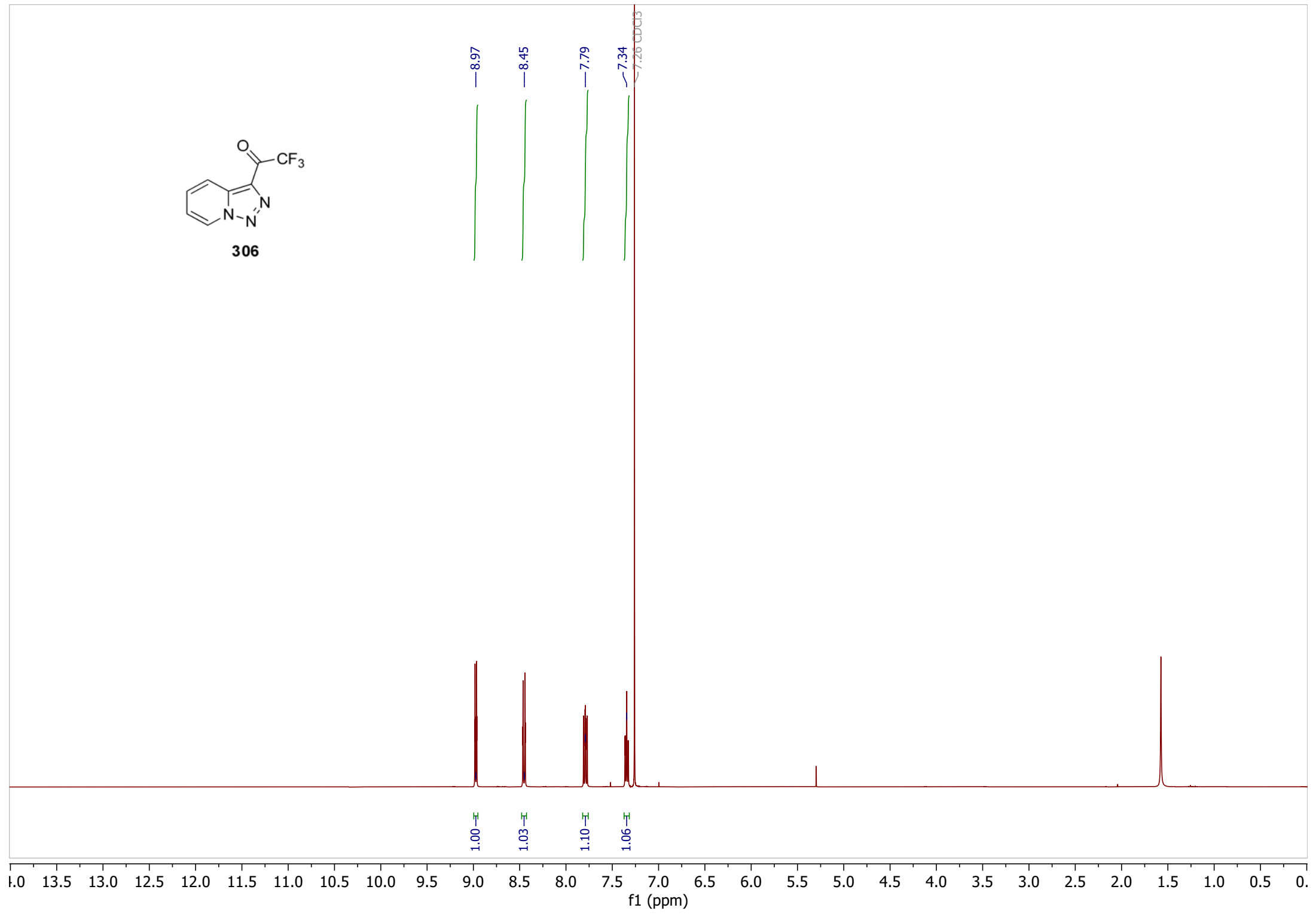
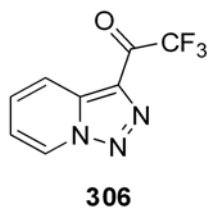
264

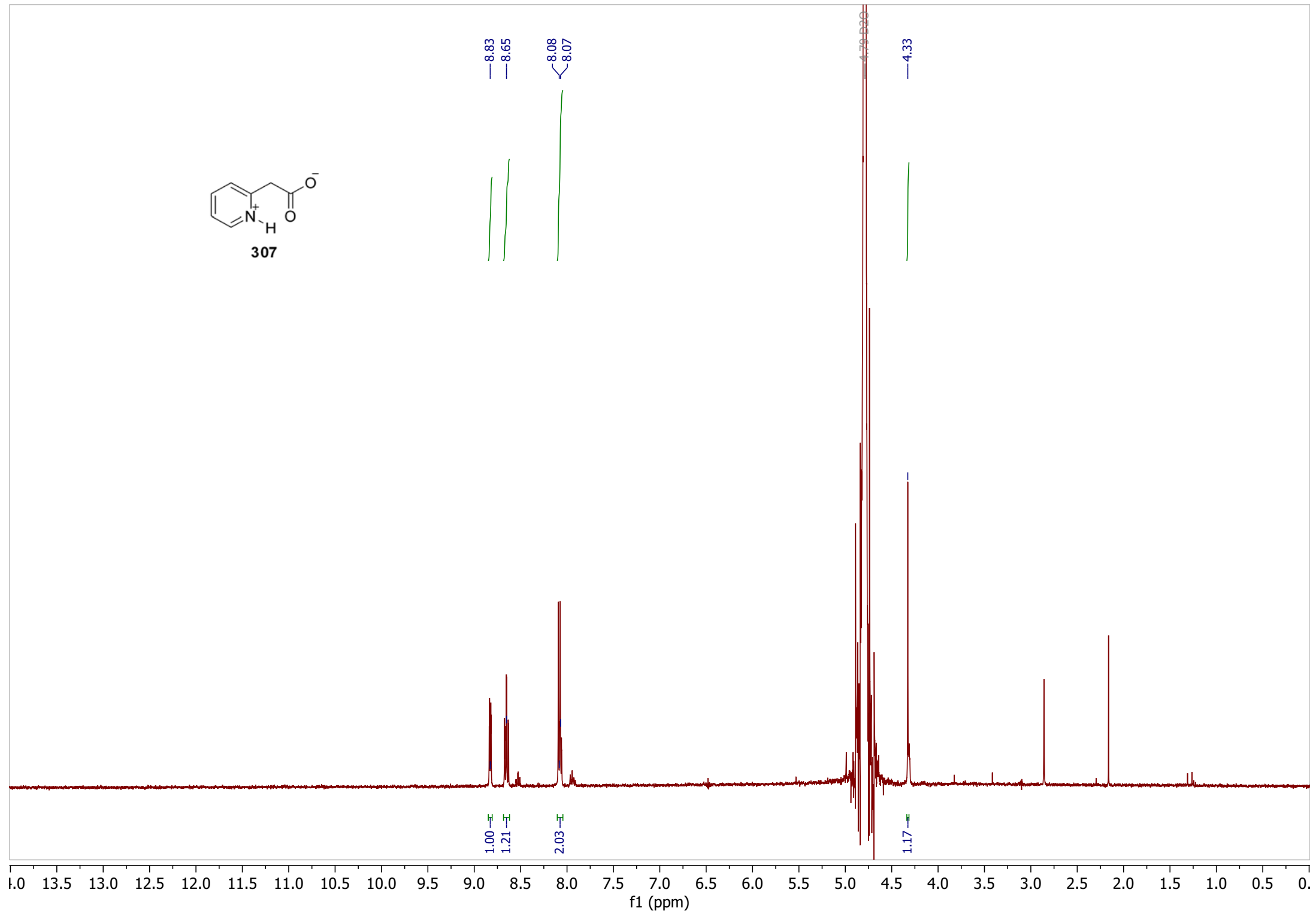
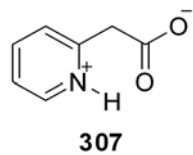


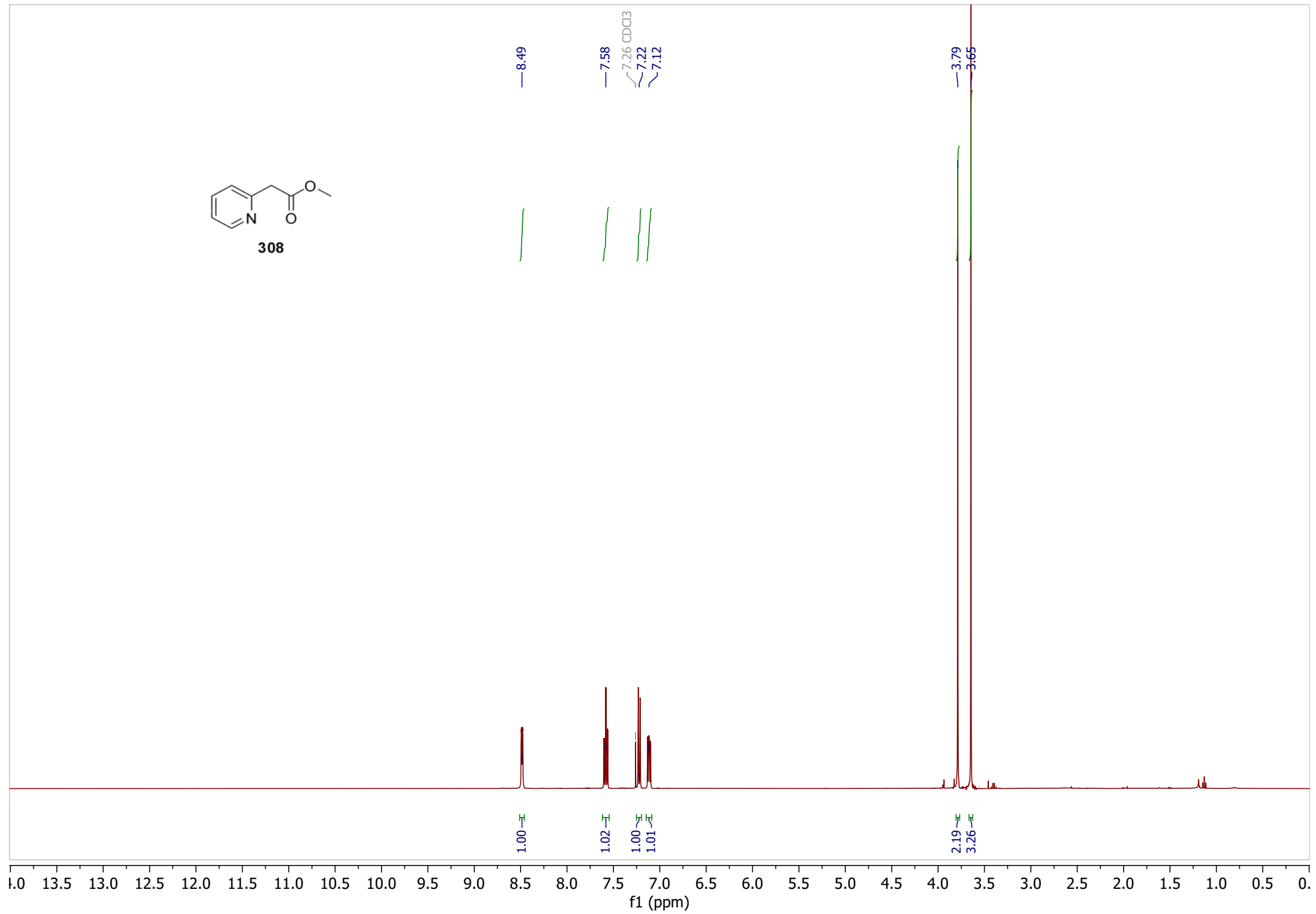
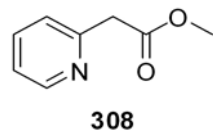


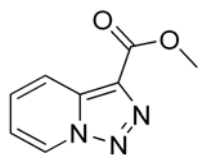
305



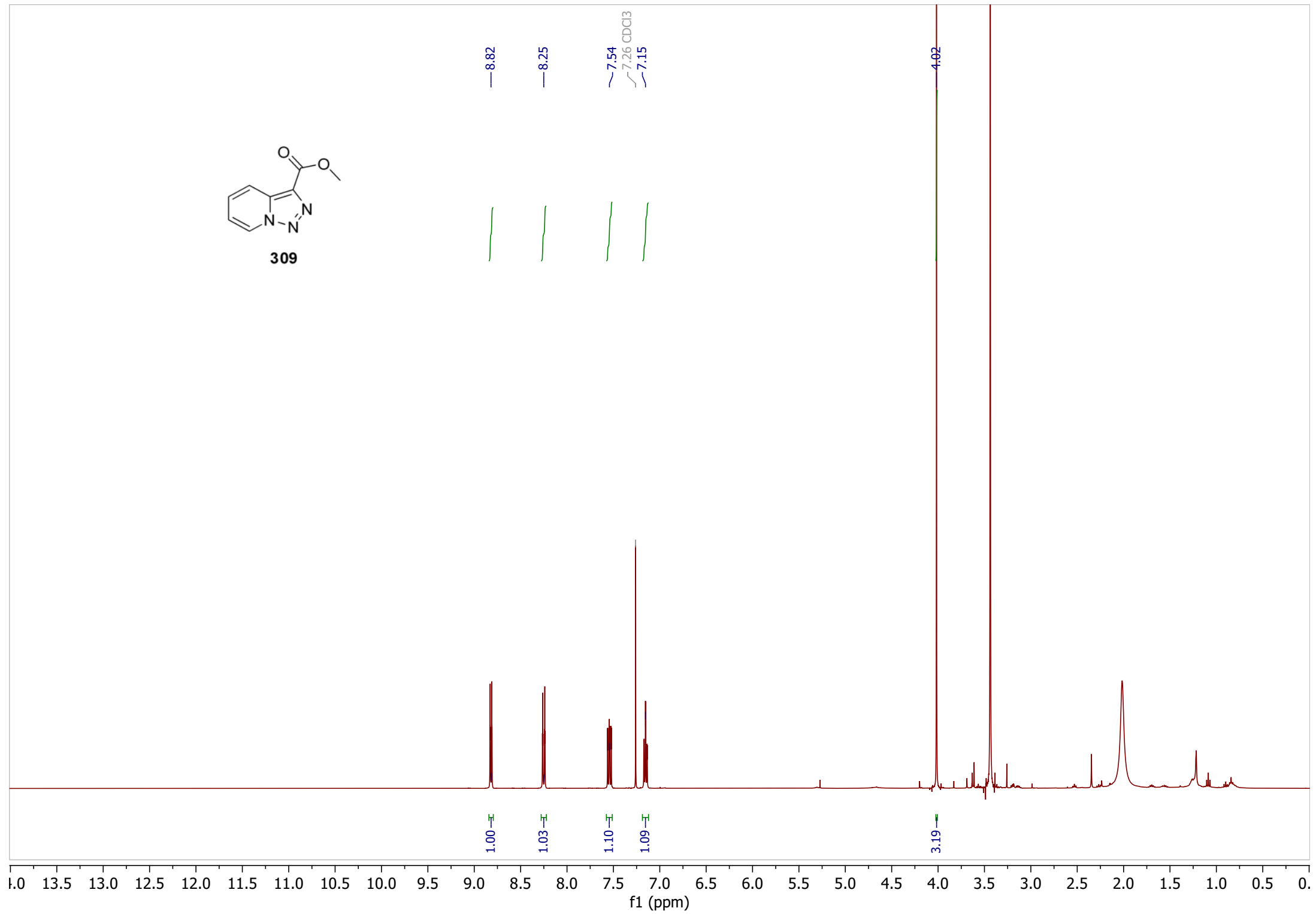


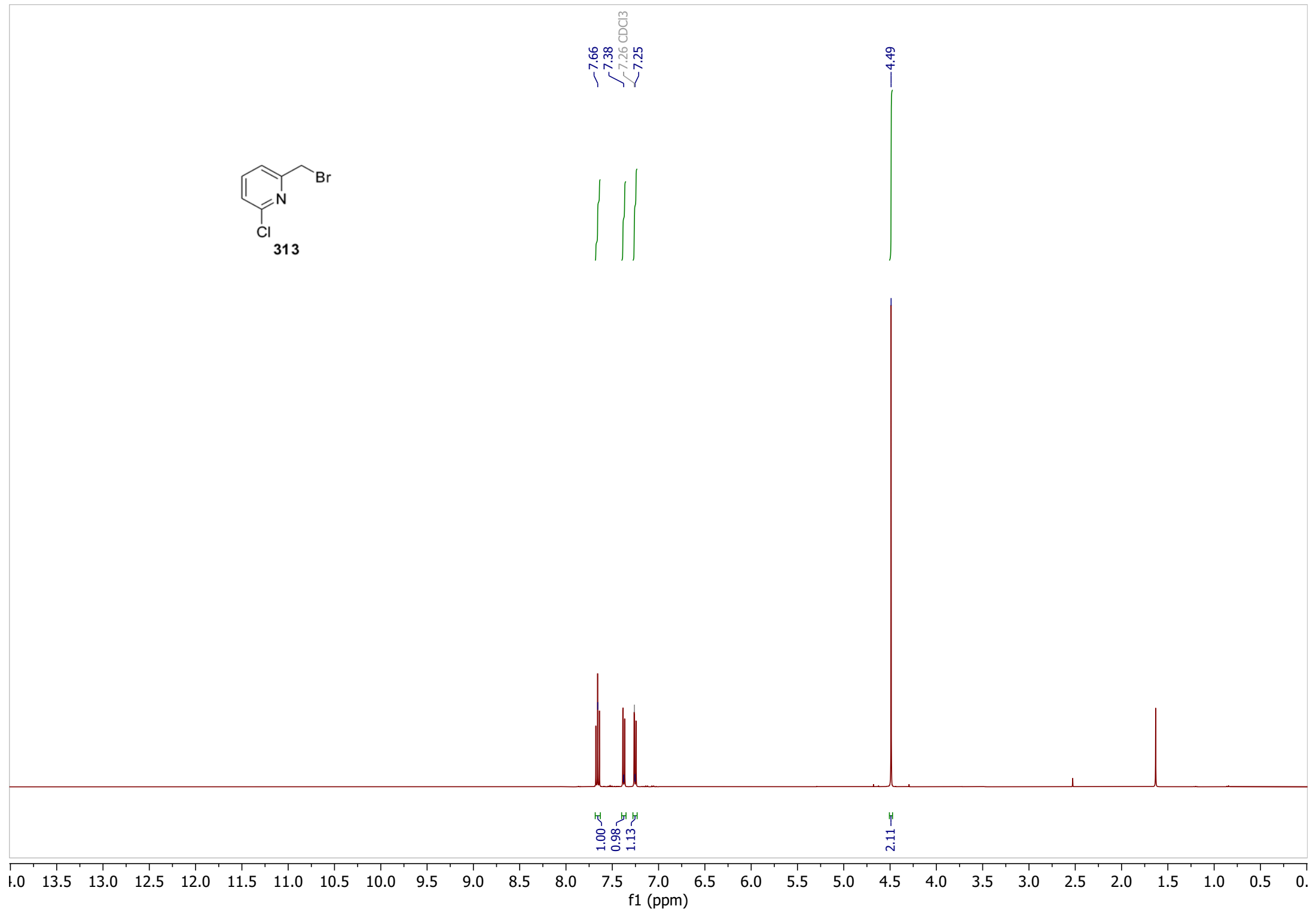
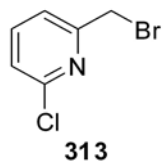


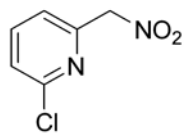




309

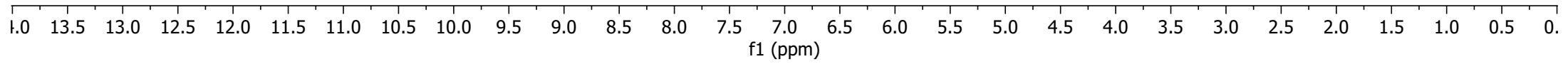


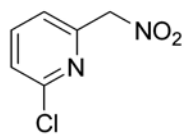




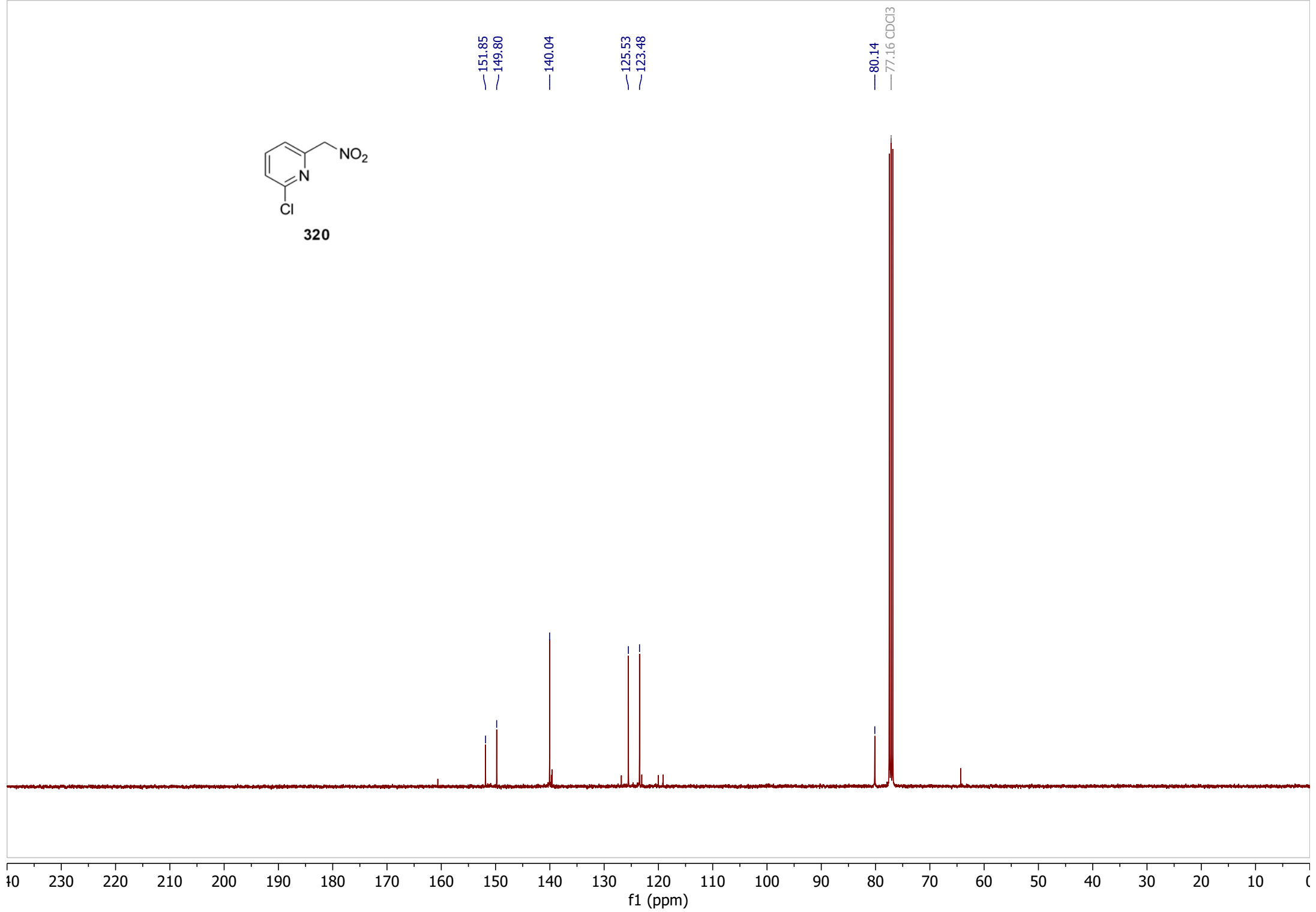
320

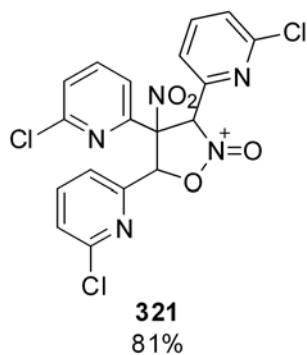
7.77  
7.43  
7.41  
7.26 CDCl3  
5.59



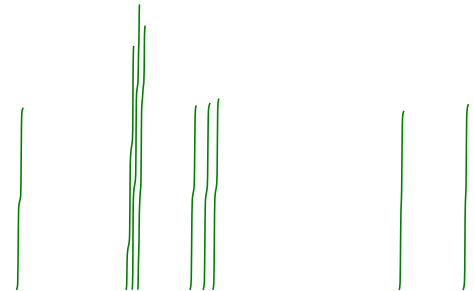


320

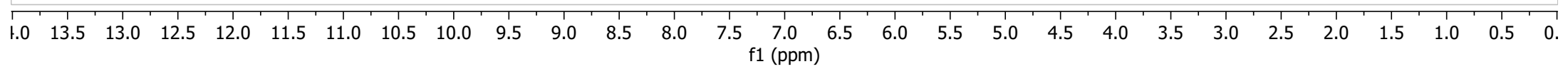


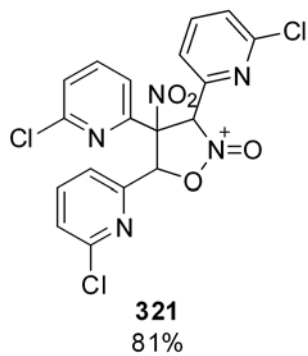


8.43  
7.72  
7.68  
7.65  
7.58  
7.56  
7.31  
7.26 CDCl3  
7.23  
7.17  
5.97  
5.55



1.00  
1.34  
1.57  
1.45  
1.01  
1.03  
1.05  
0.98  
1.02

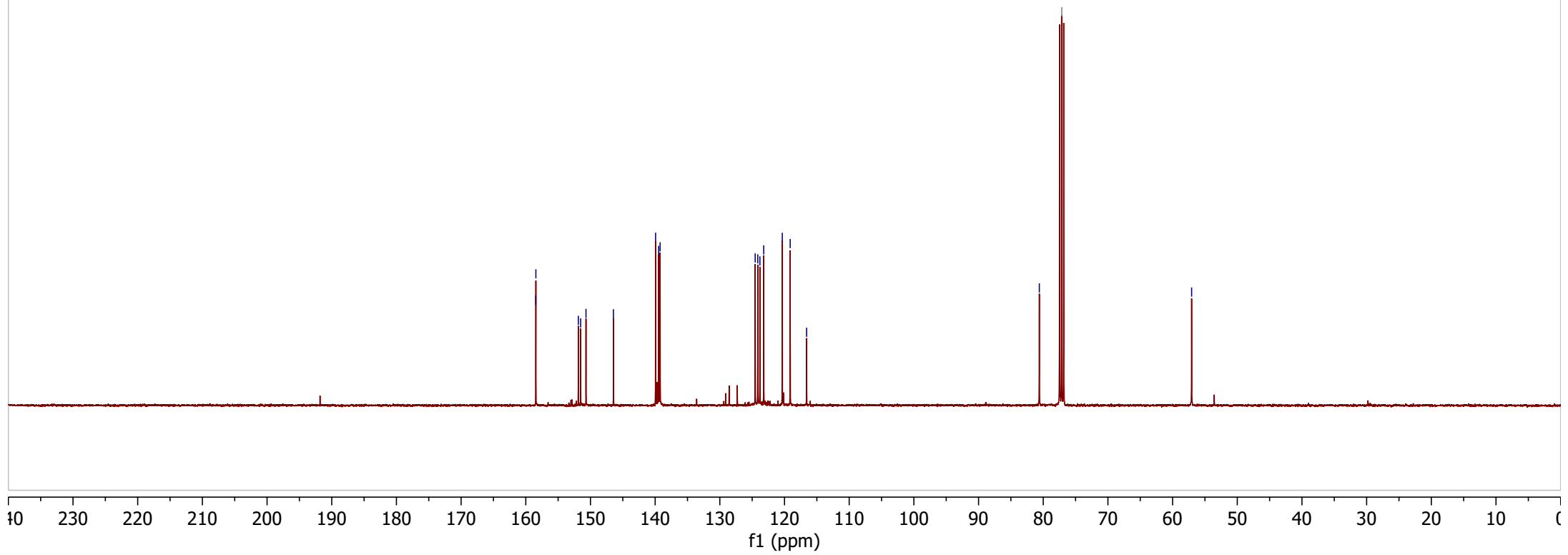


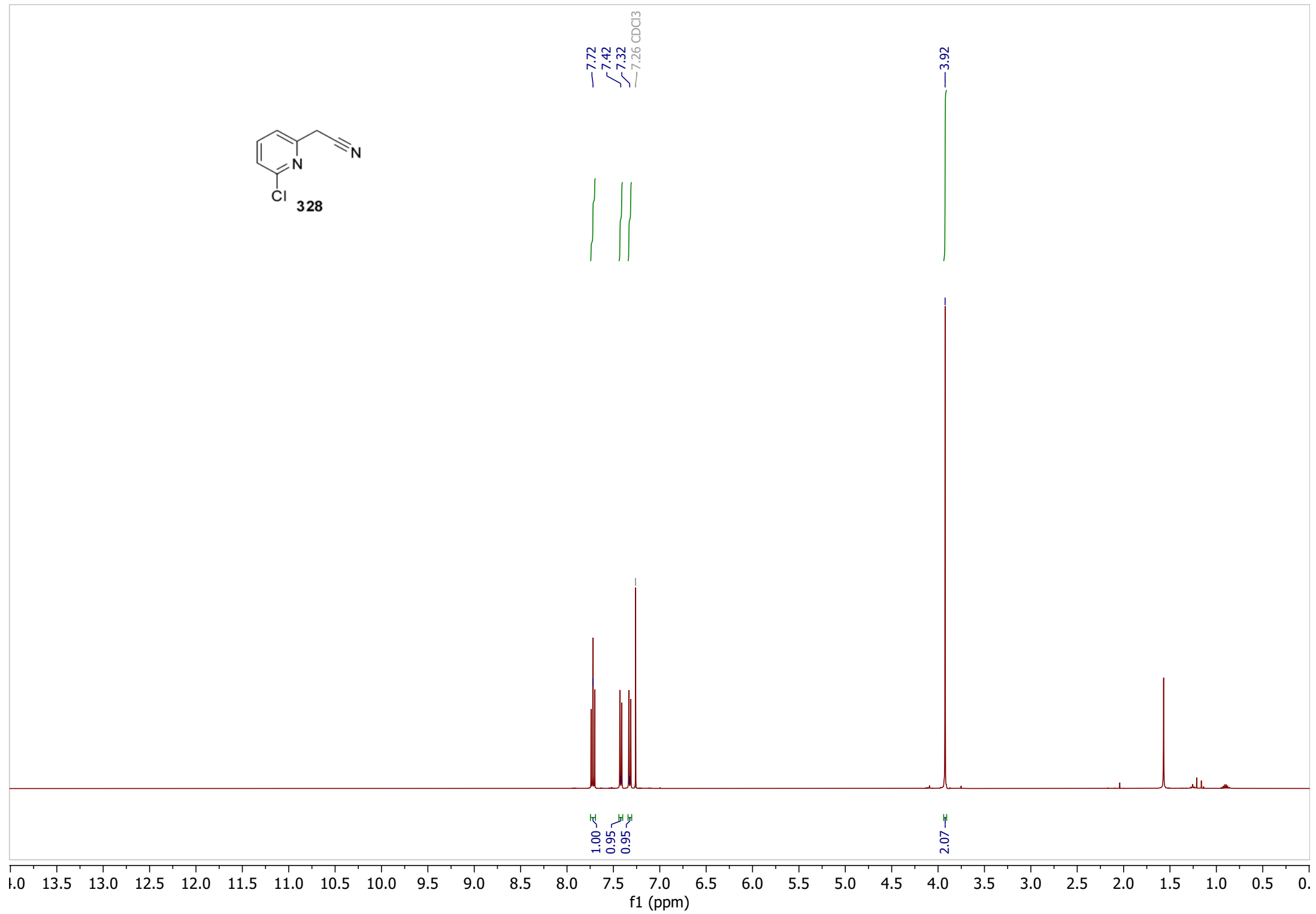
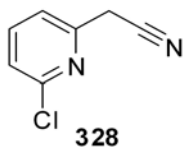


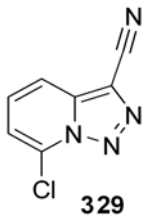
158.46  
158.44  
151.87  
151.52  
150.69  
146.45  
139.93  
139.46  
139.23  
124.53  
124.13  
123.80  
123.22  
120.35  
119.12  
116.59

80.60  
77.16 CDCl3

57.06





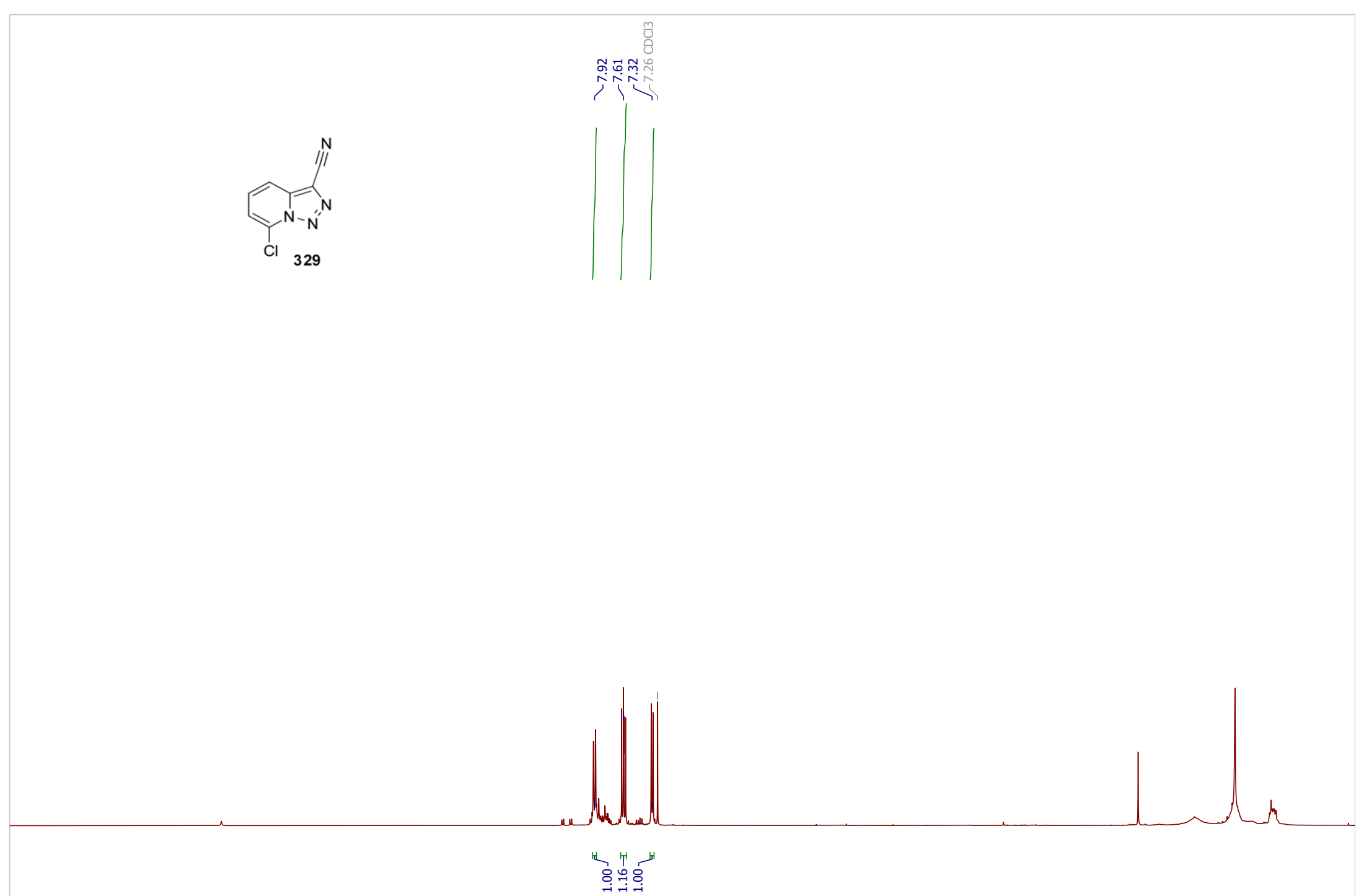


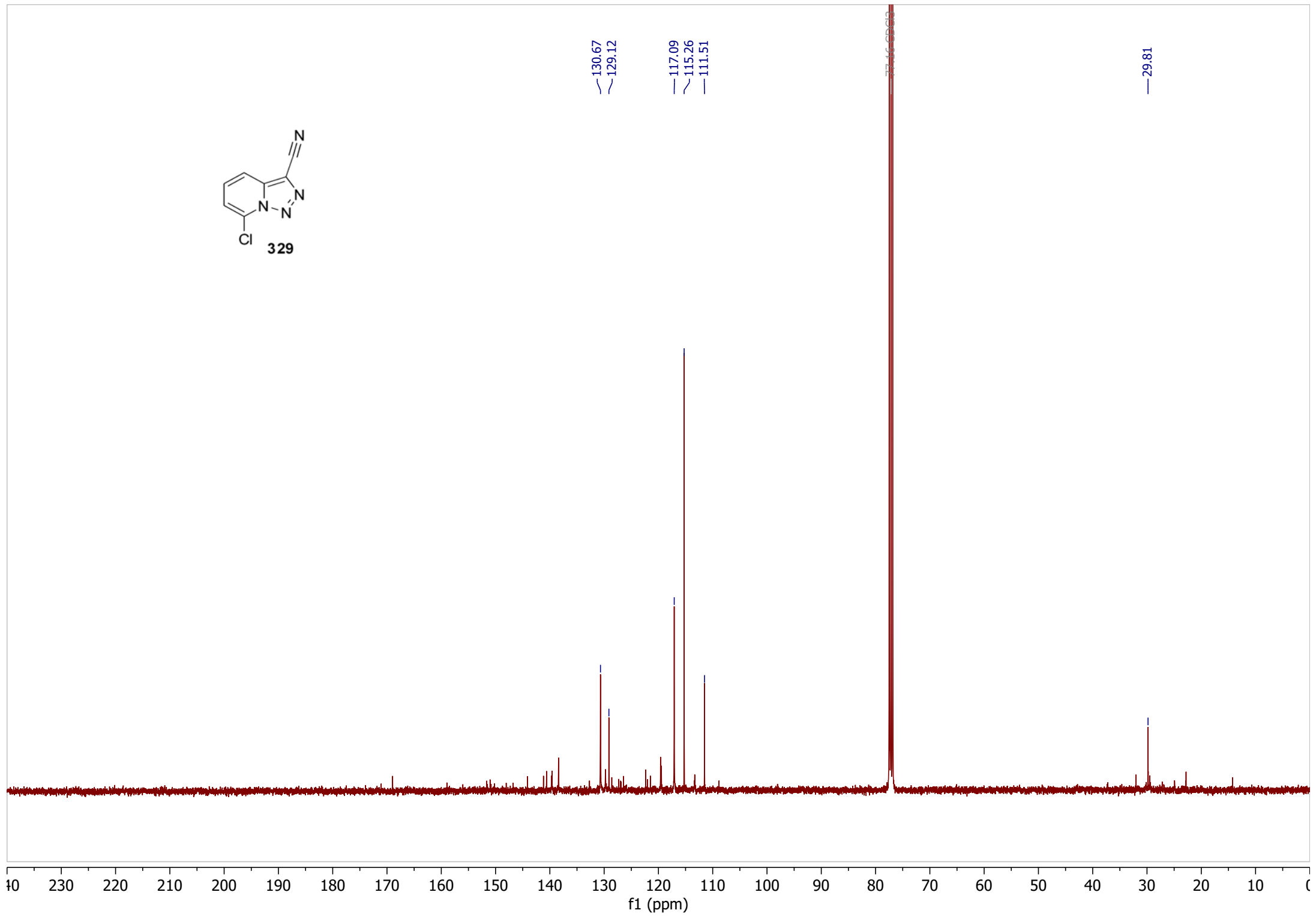
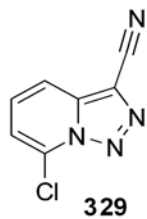
7.92  
7.61  
7.32  
7.26 CDCl3

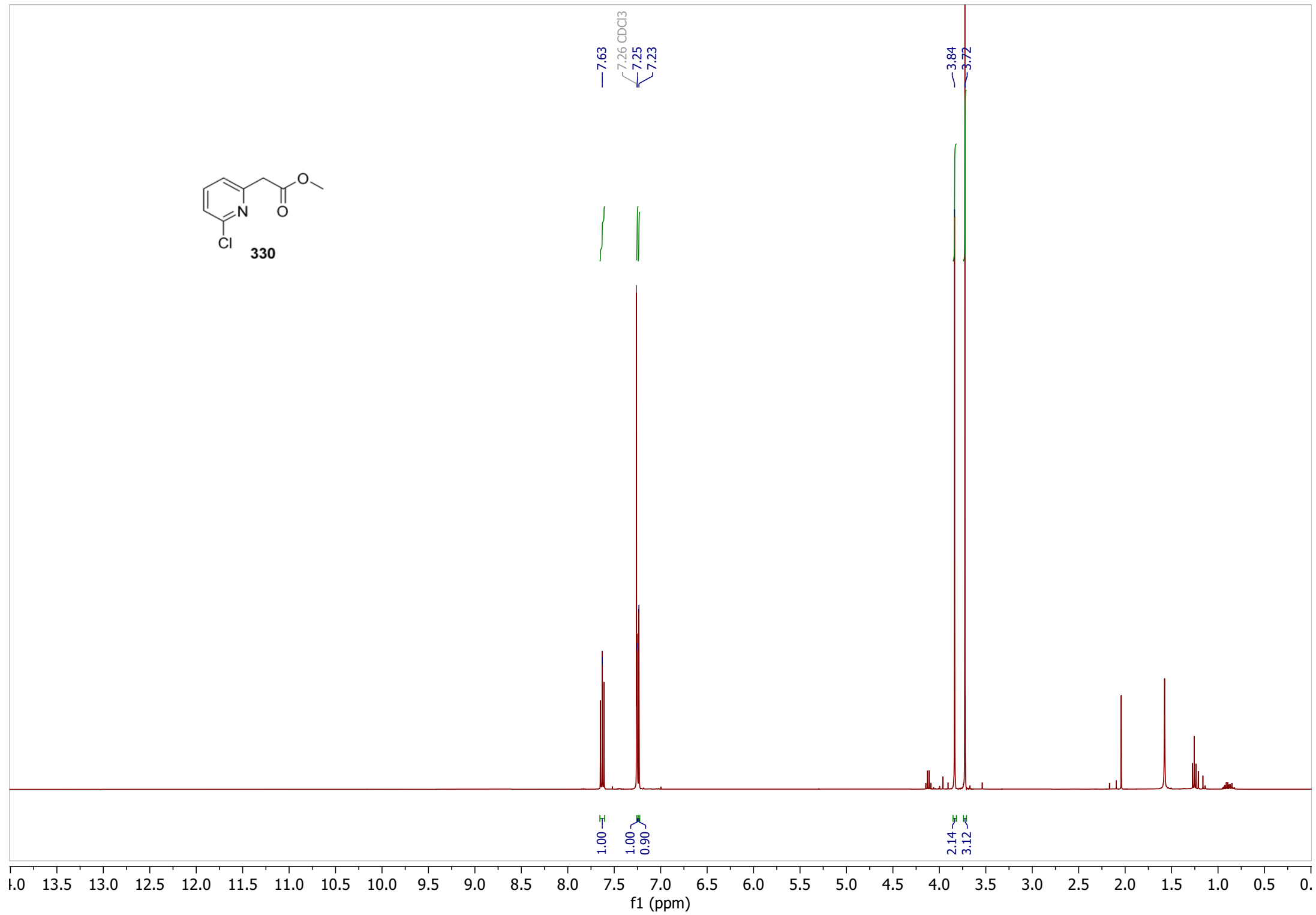
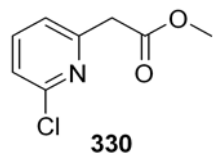
1.0 13.5 13.0 12.5 12.0 11.5 11.0 10.5 10.0 9.5 9.0 8.5 8.0 7.5 7.0 6.5 6.0 5.5 5.0 4.5 4.0 3.5 3.0 2.5 2.0 1.5 1.0 0.5 0.0

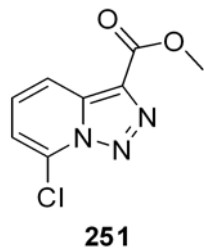
f1 (ppm)

1.00  
1.16  
1.00

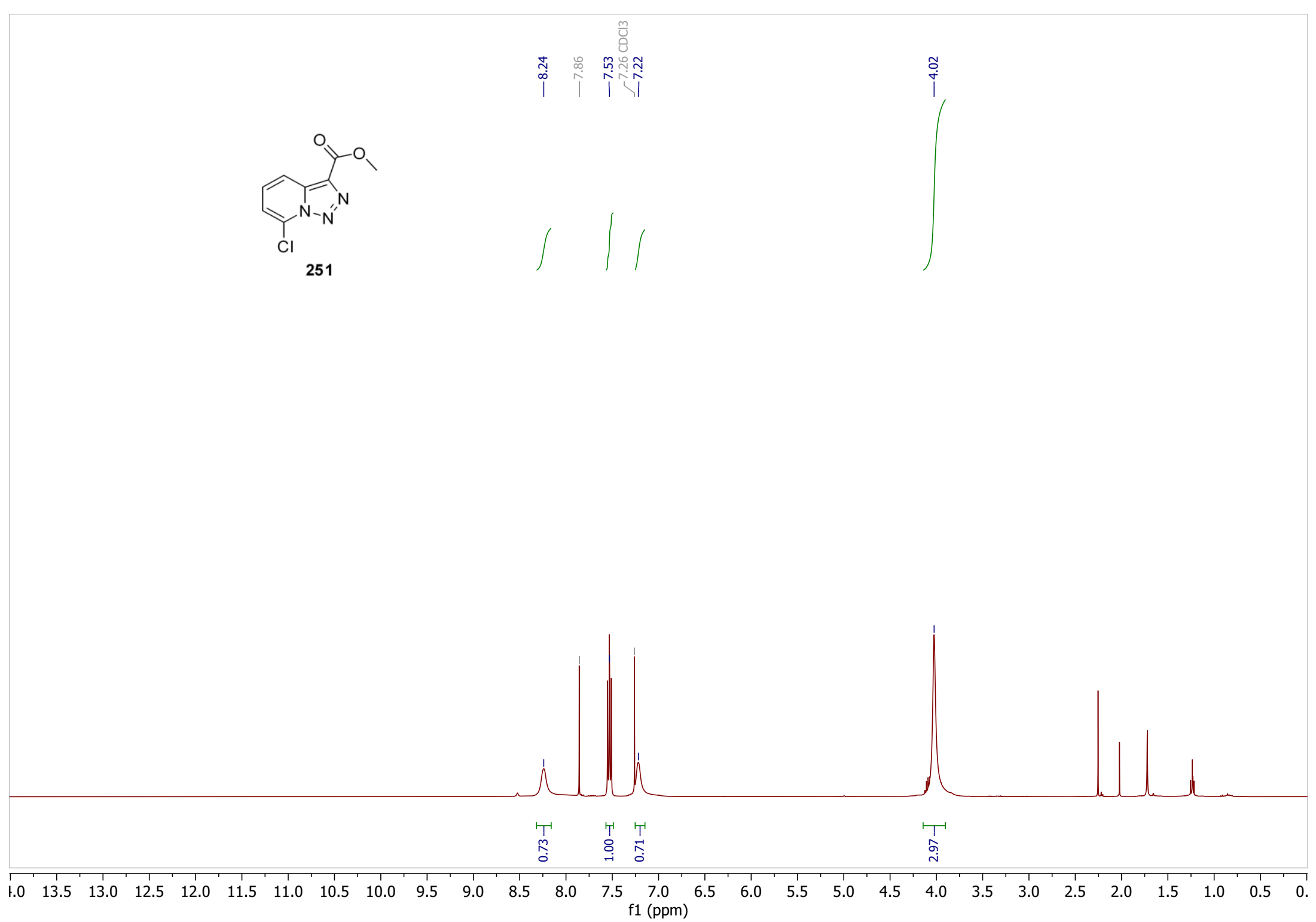




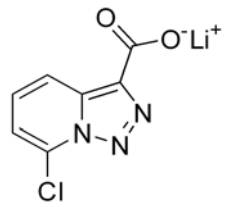




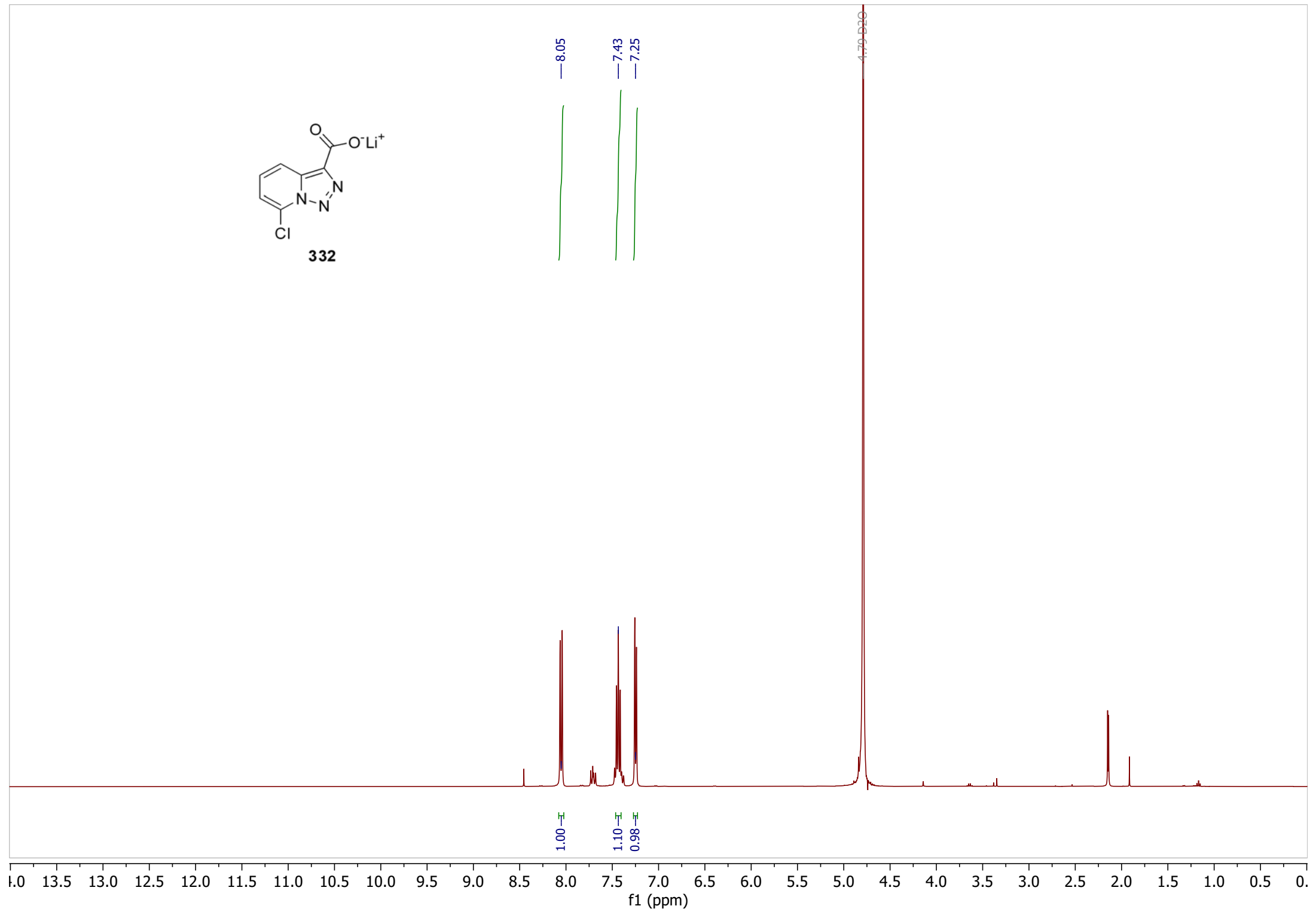
8.24  
7.86  
7.53  
7.26 CDCl3  
7.22  
4.02

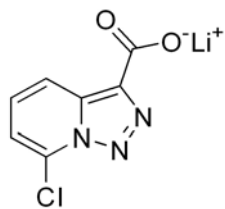


0.73  
1.00  
0.71  
2.97

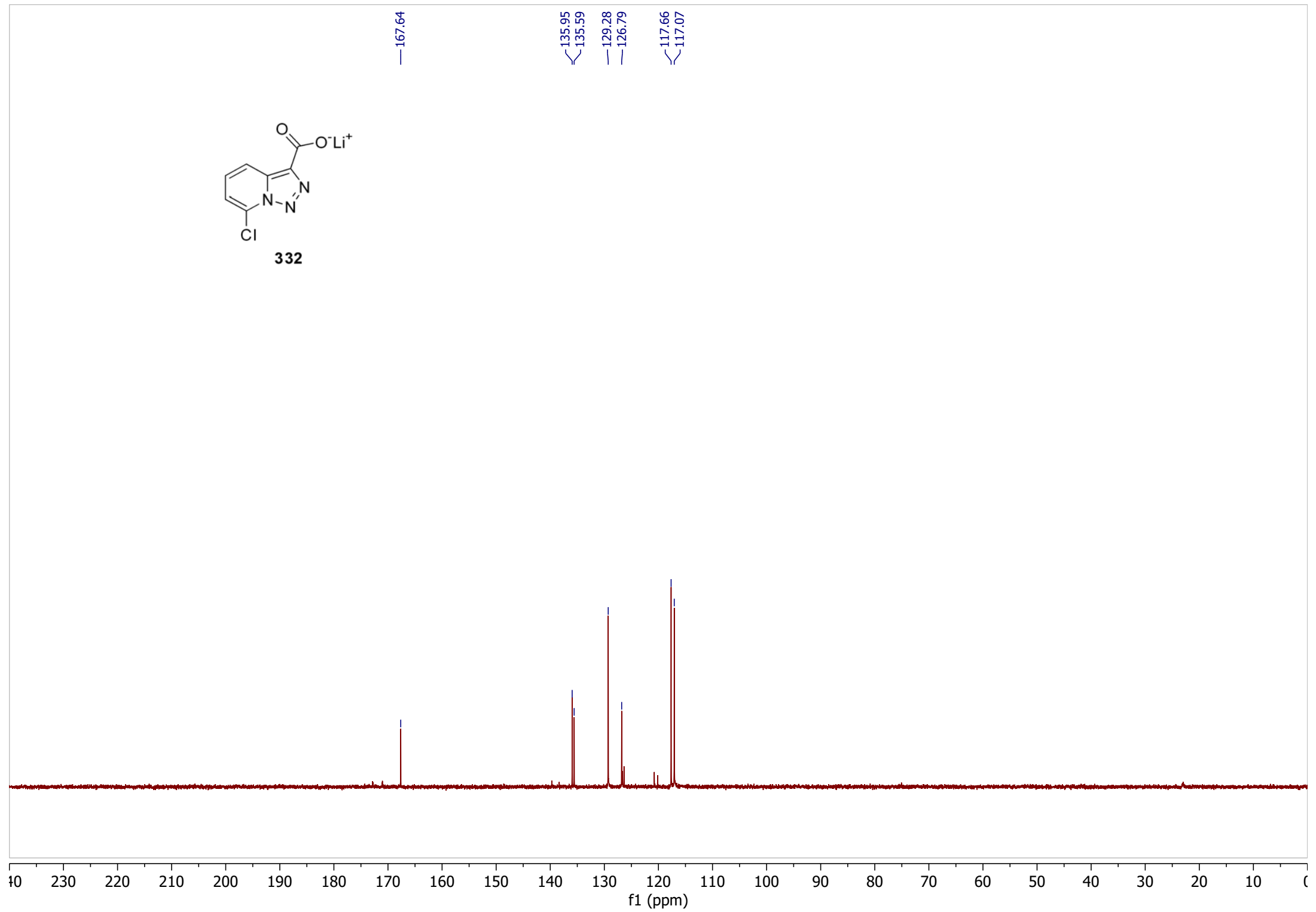


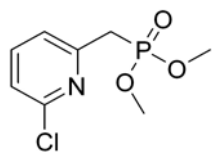
332



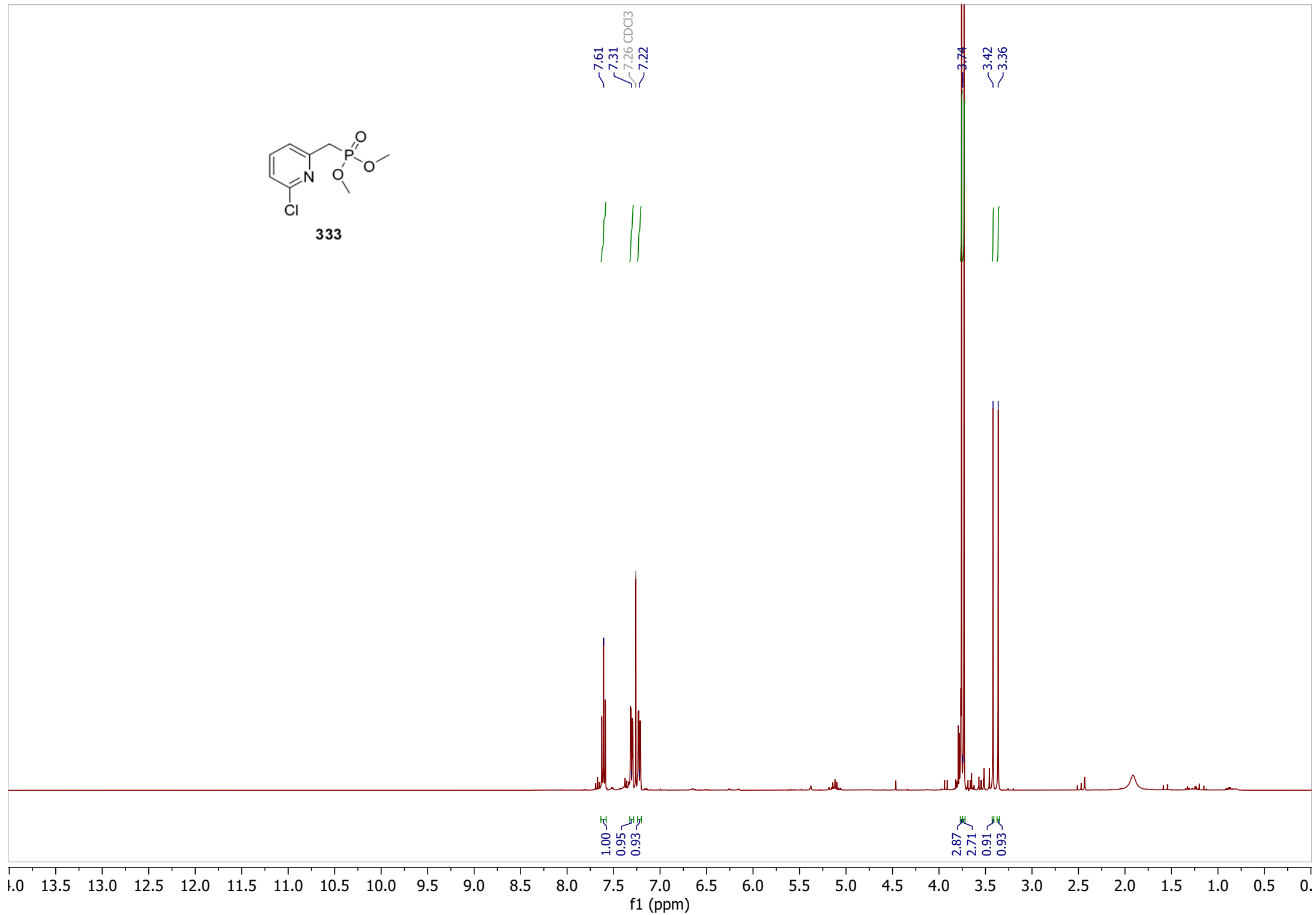


332

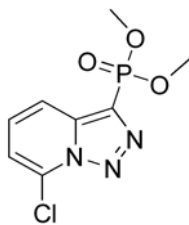




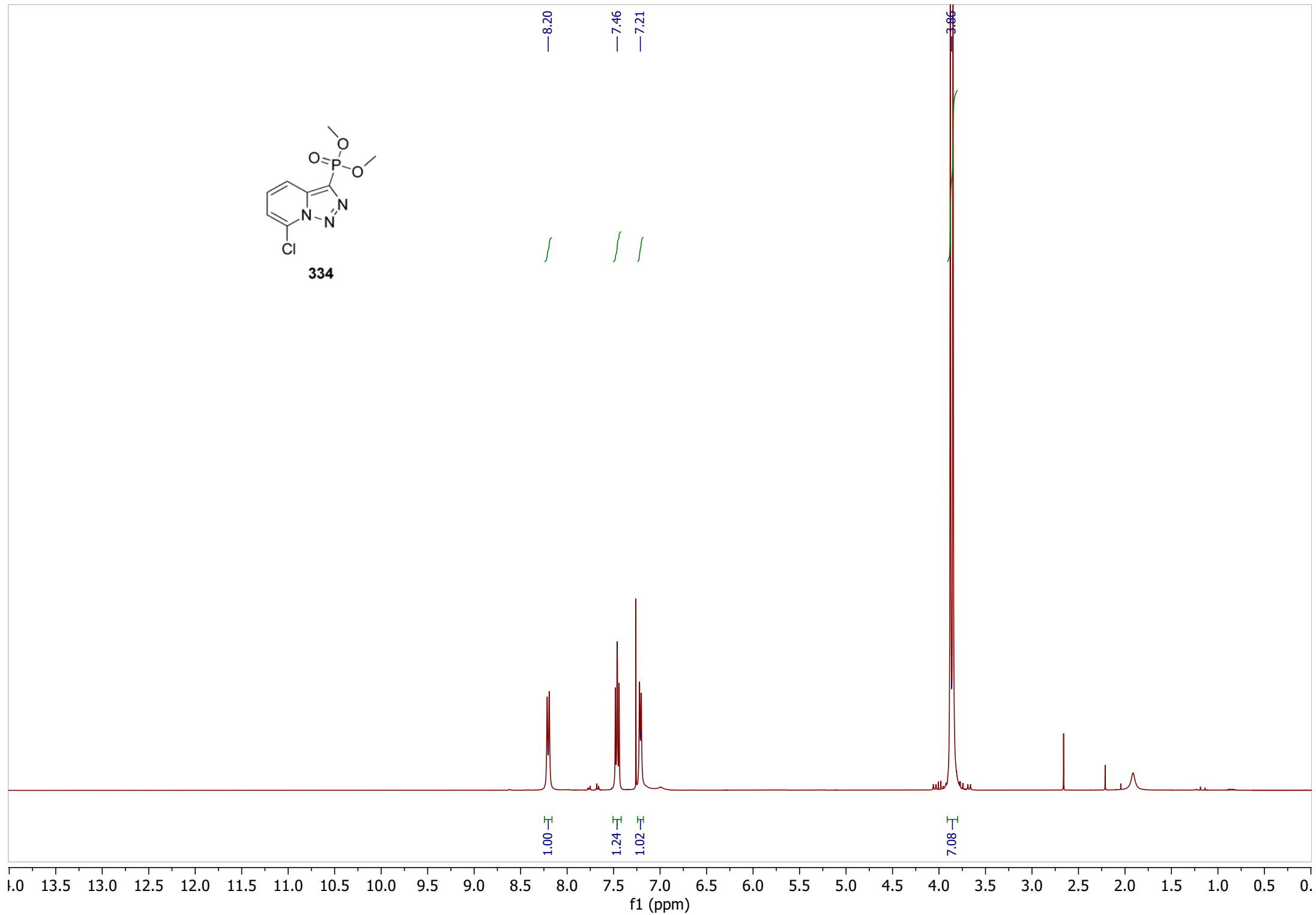
333

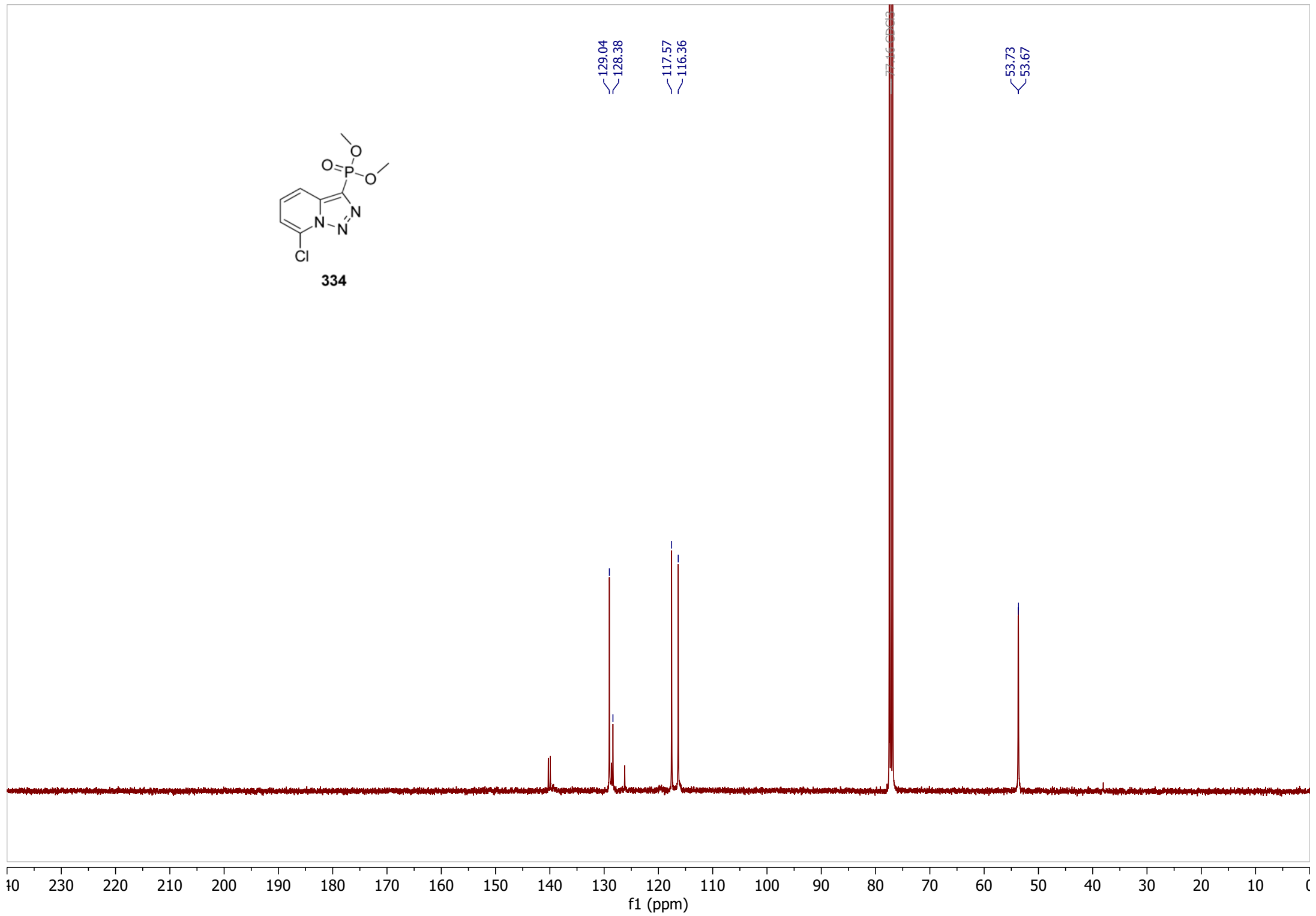
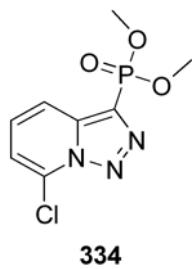


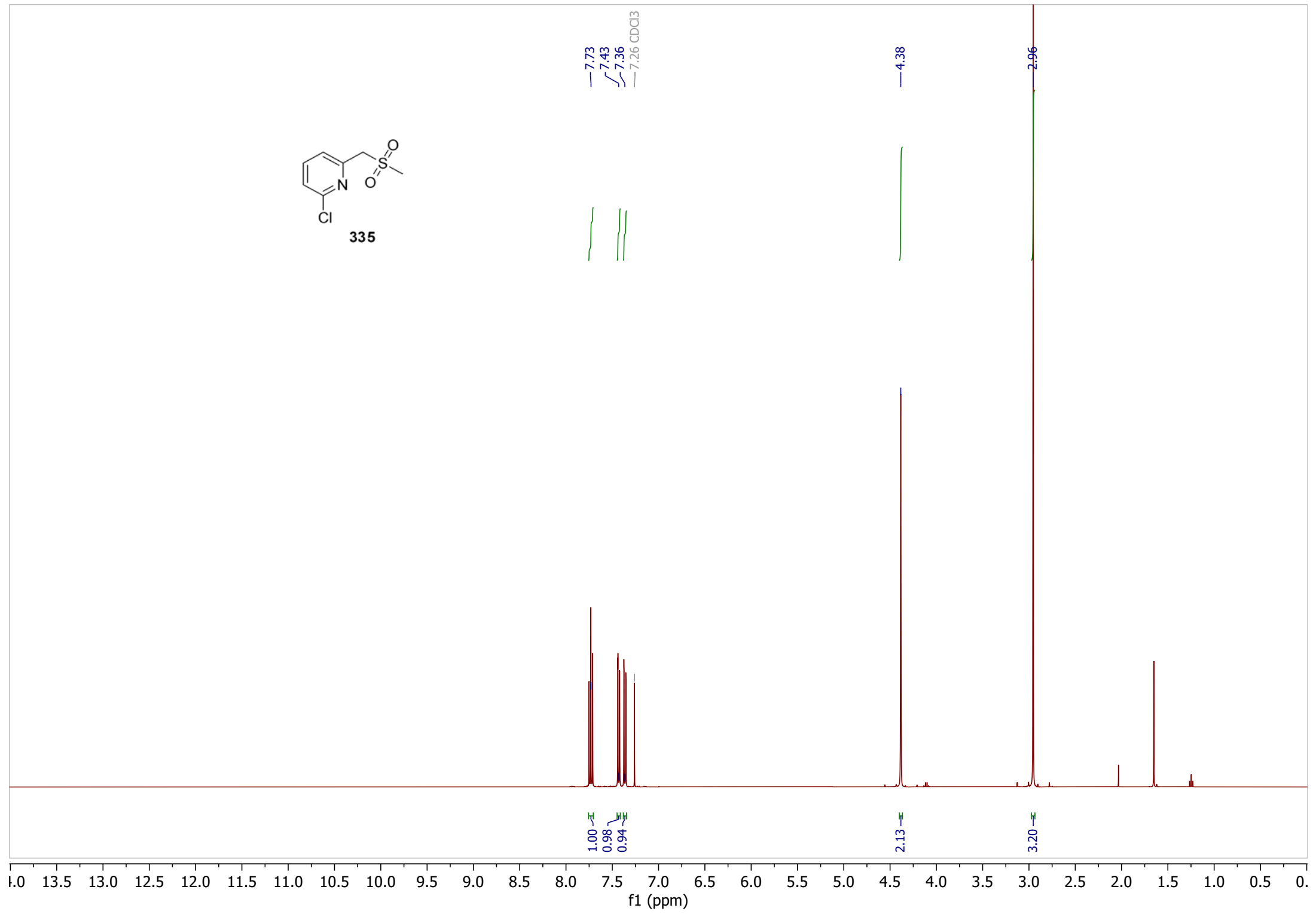
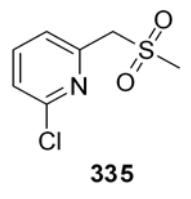


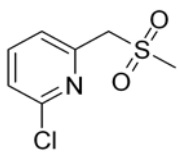


334

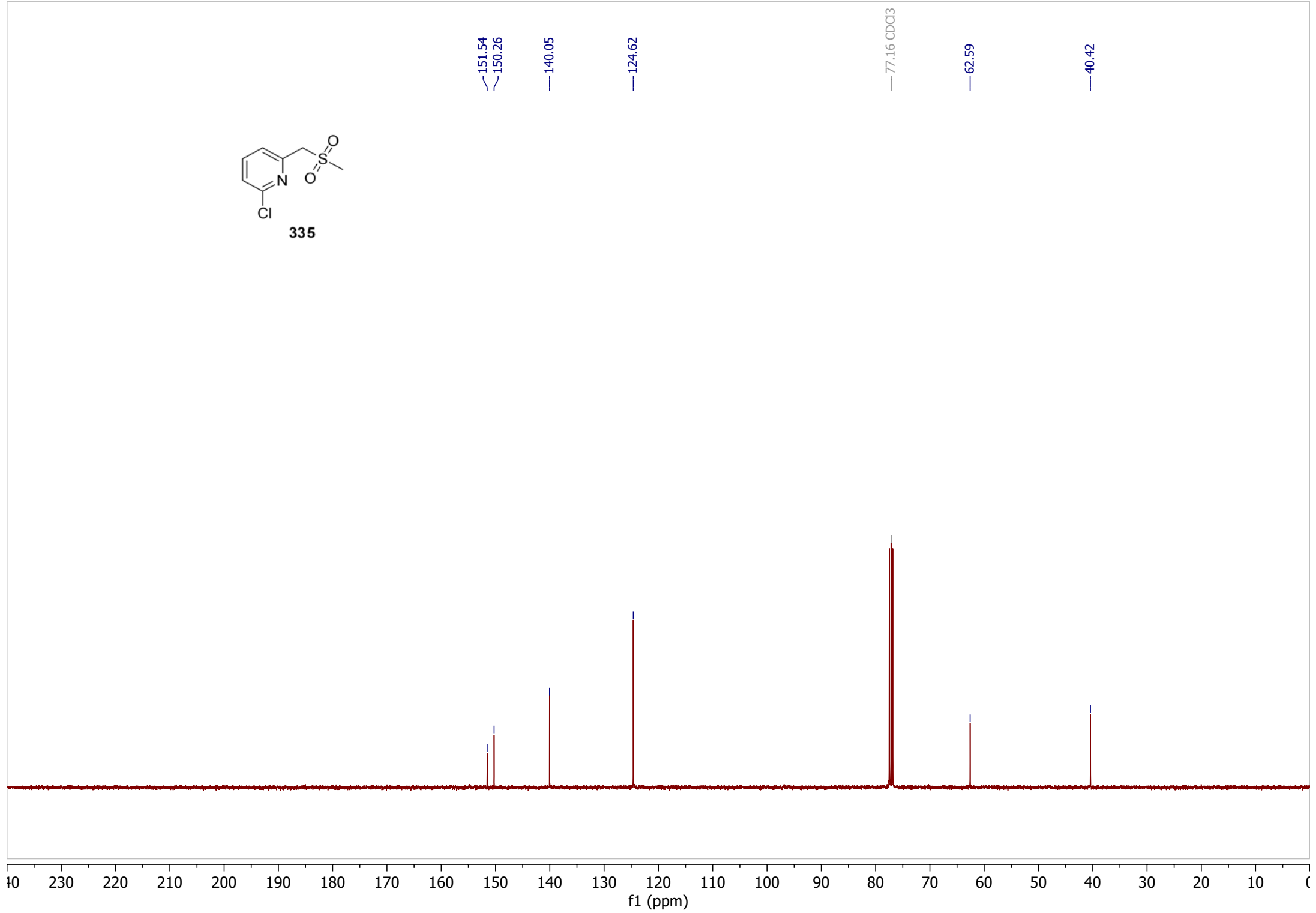


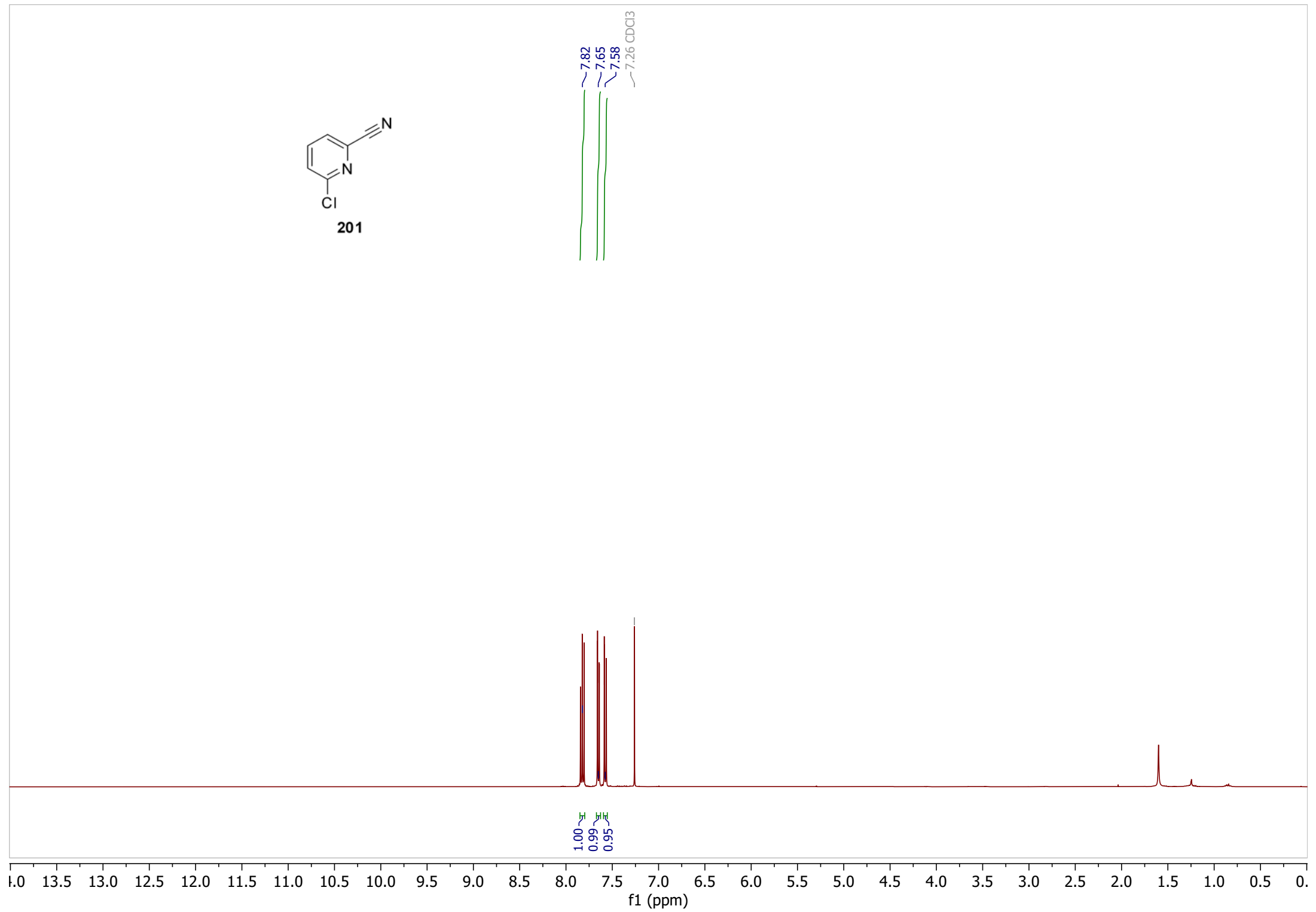
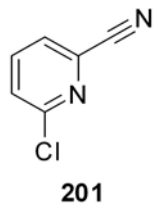


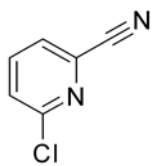




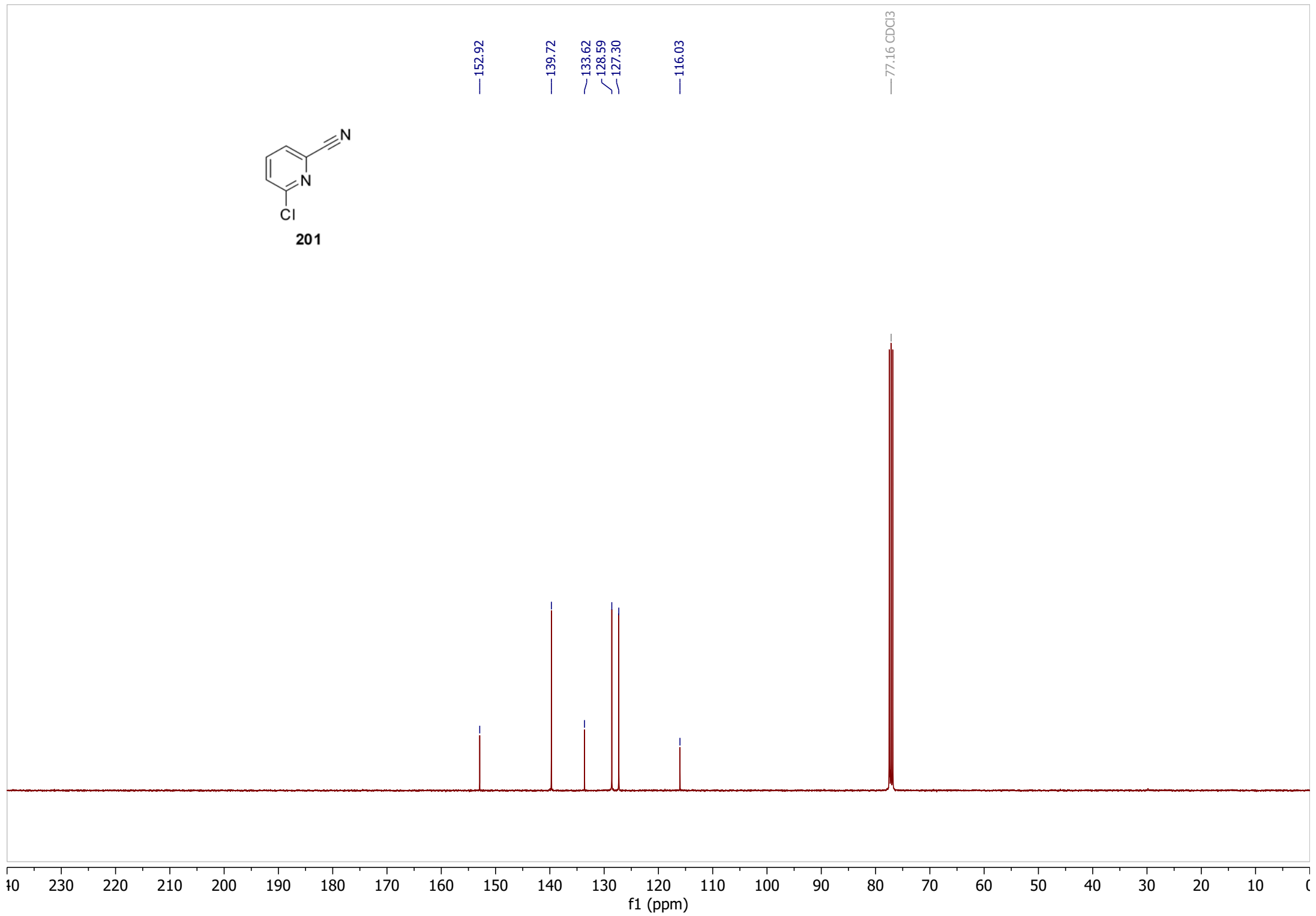
335

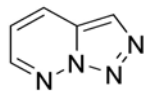




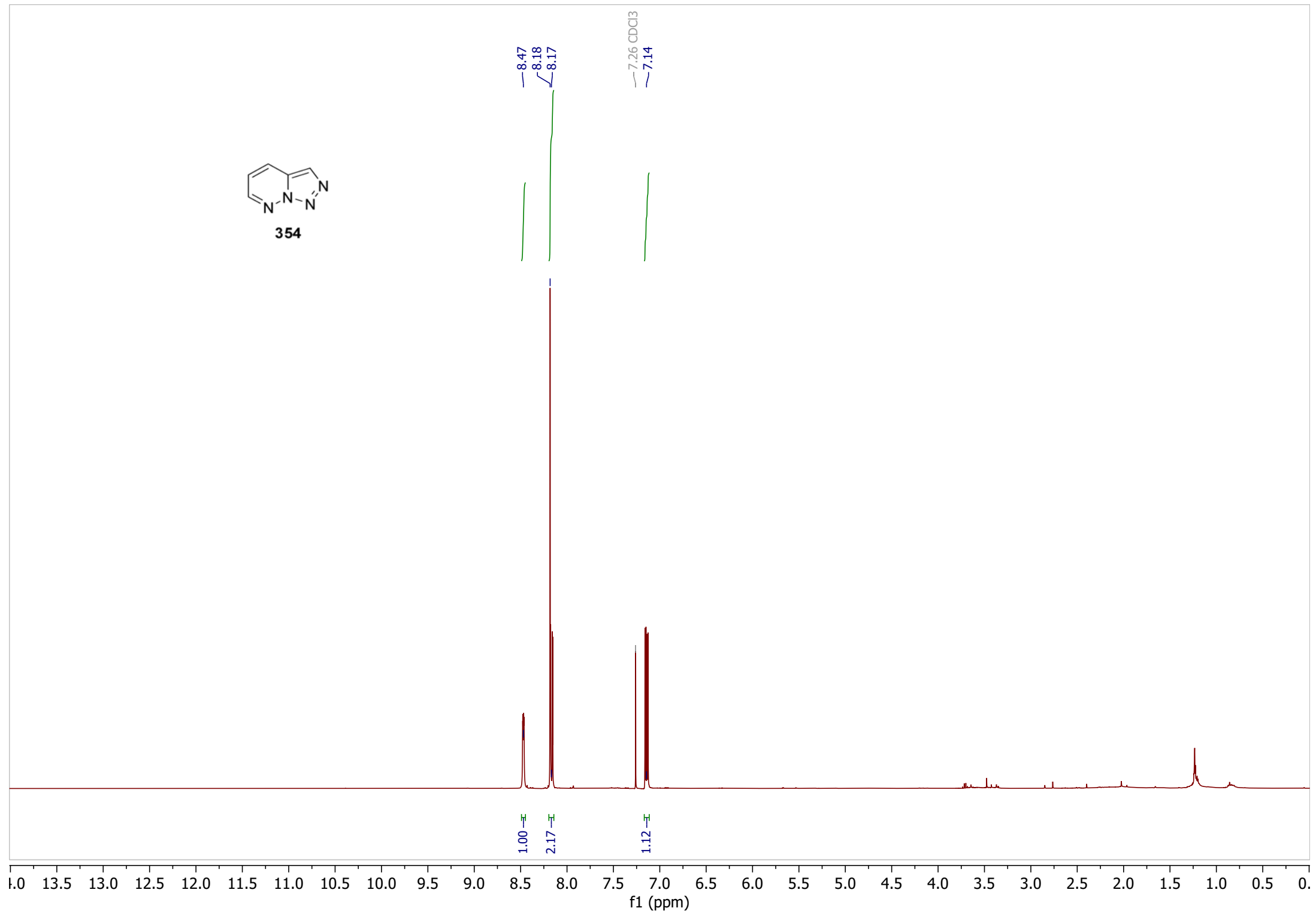


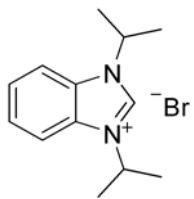
201



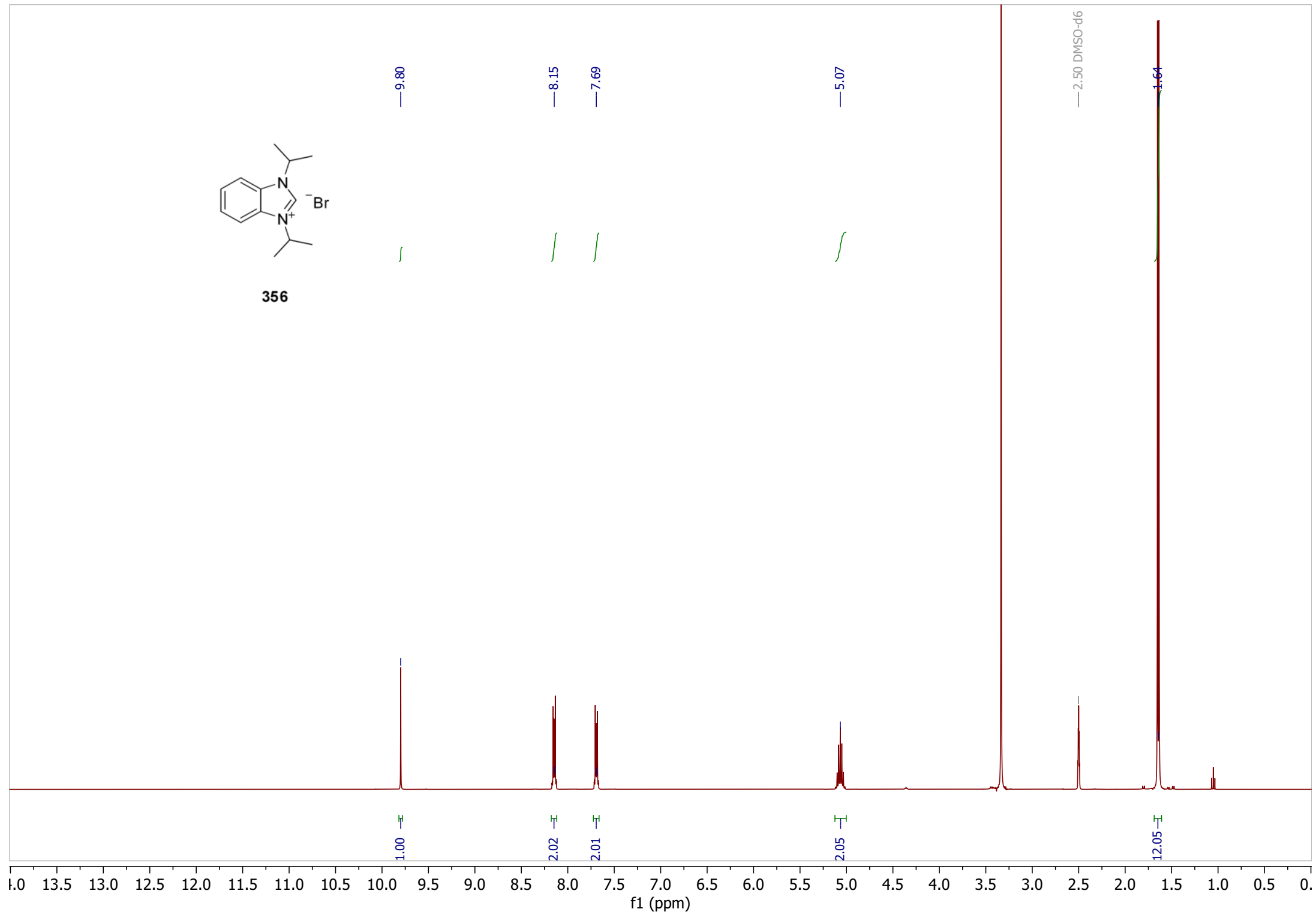


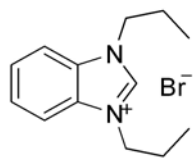
354



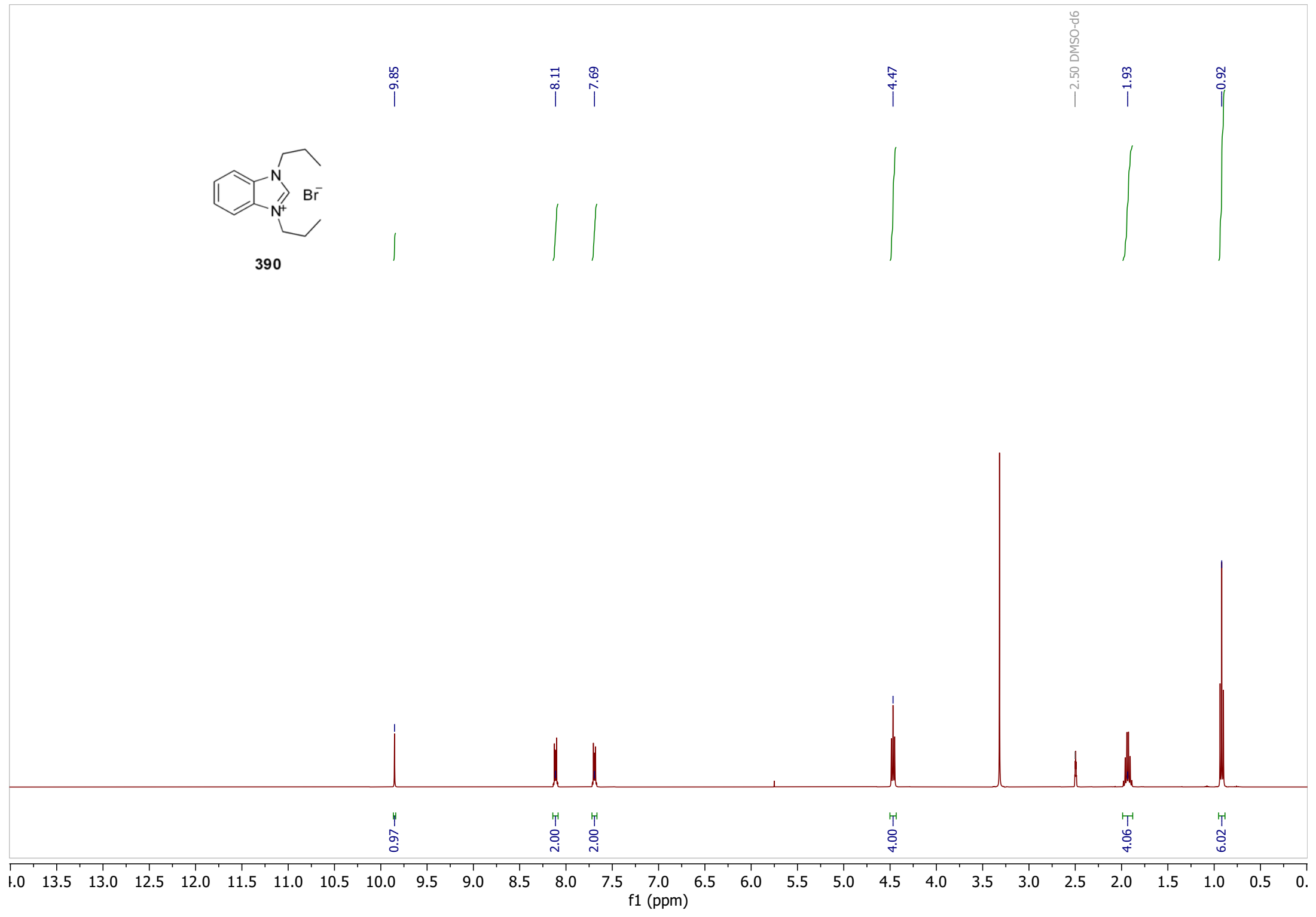


356

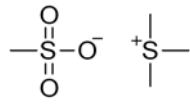




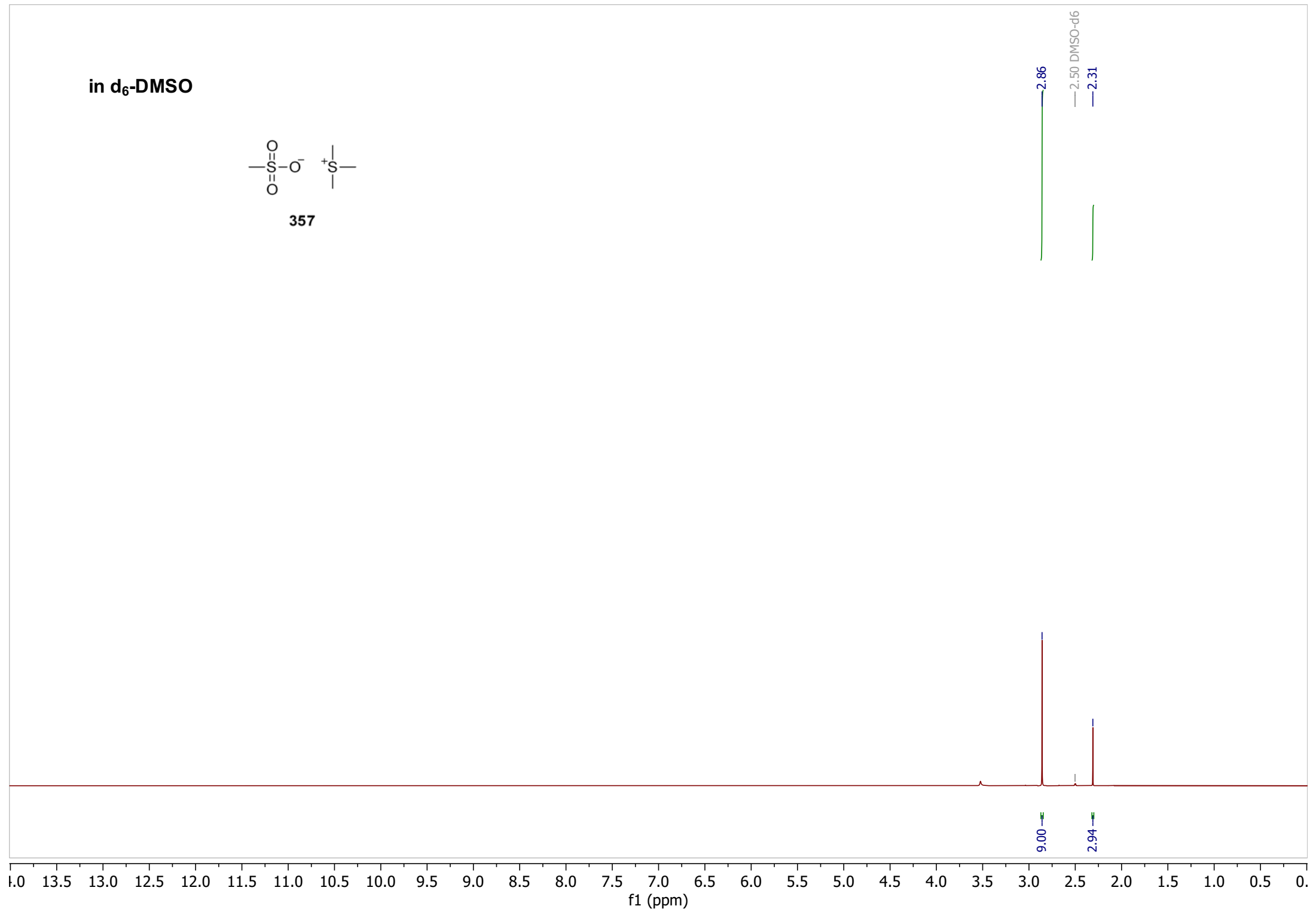
390



in d<sub>6</sub>-DMSO



357



2.86

— 2.50 DMSO-d6

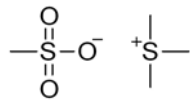
— 2.31

9.00

2.94

f1 (ppm)

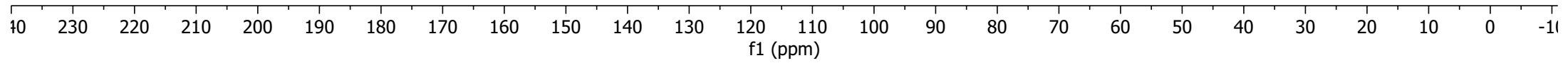
in d<sub>6</sub>-DMSO



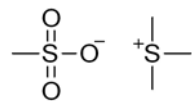
357

39.78  
39.52 DMSO-d6

26.13

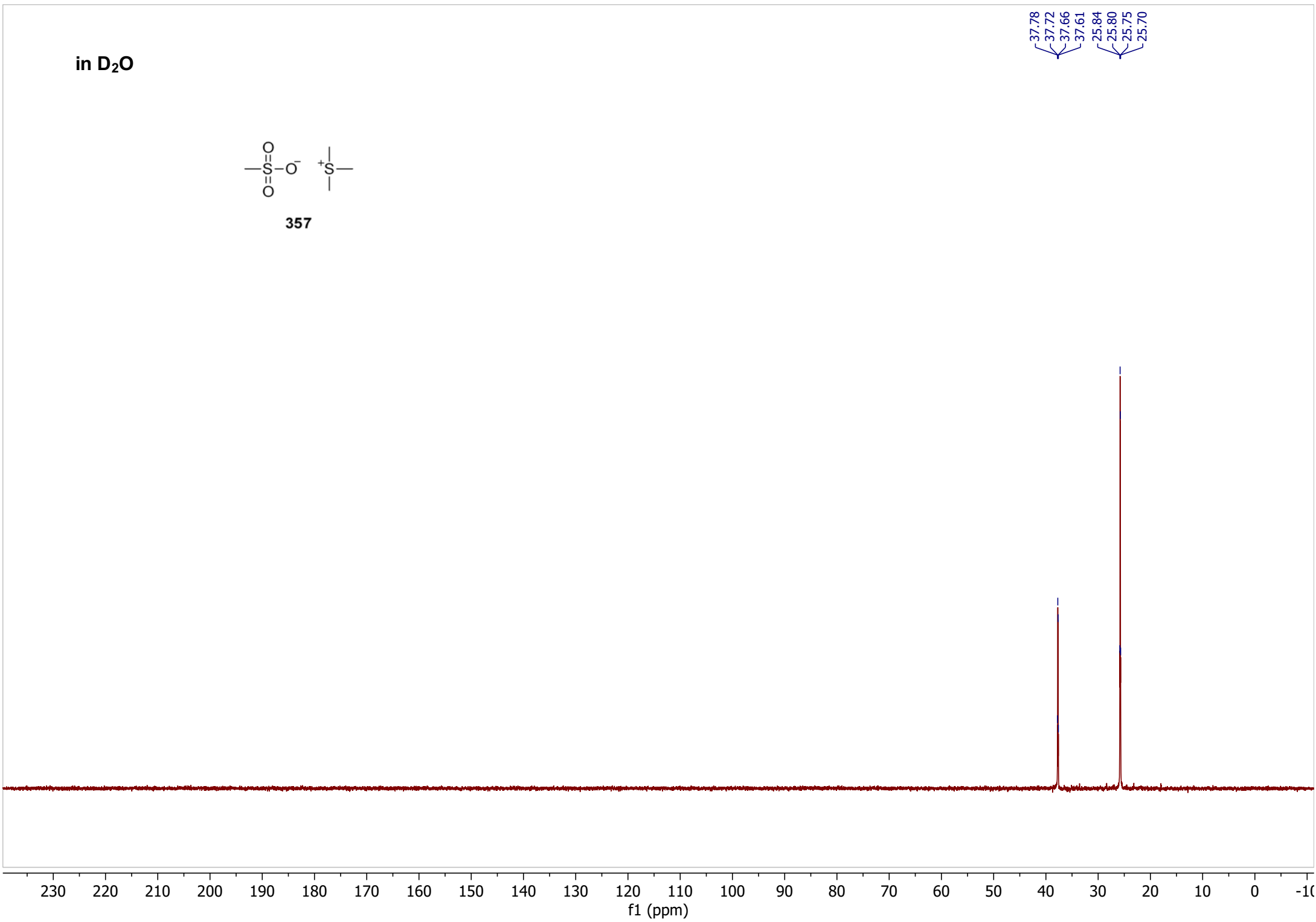


in D<sub>2</sub>O

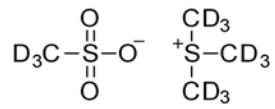


357

37.78  
37.72  
37.66  
37.61  
25.84  
25.80  
25.75  
25.70

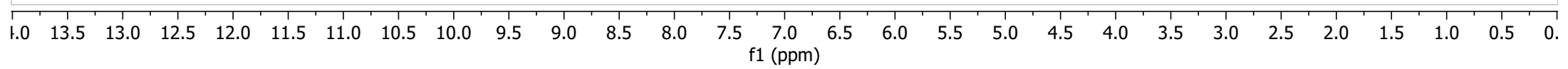


in d<sub>6</sub>-DMSO

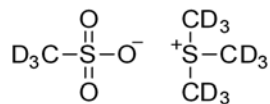


406

— 2.50 DMSO-d6



in D<sub>2</sub>O



406

— 2.86

— 2.33

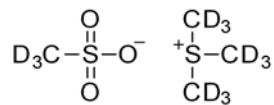
9.00

3.38

f1 (ppm)

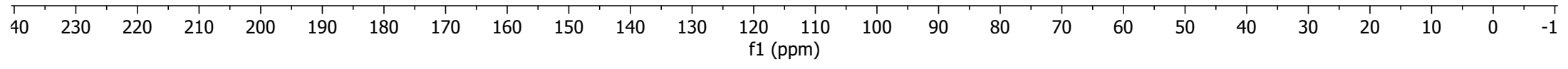


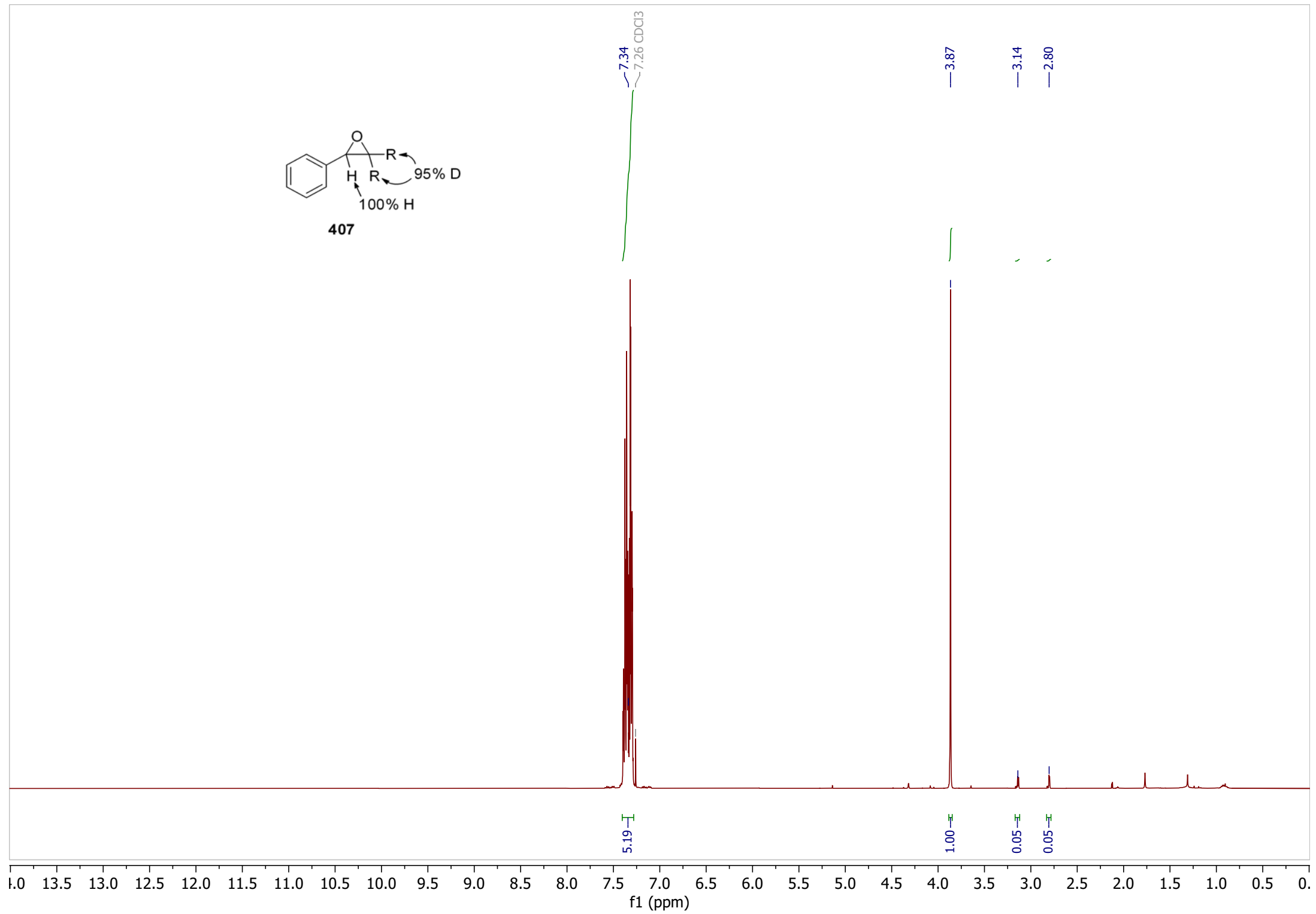
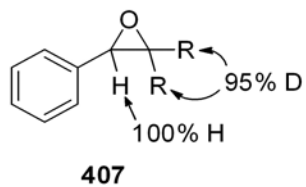
in D<sub>2</sub>O



406

38.24  
38.03  
37.83  
37.62  
37.41  
26.21  
25.99  
25.77  
25.55  
25.33





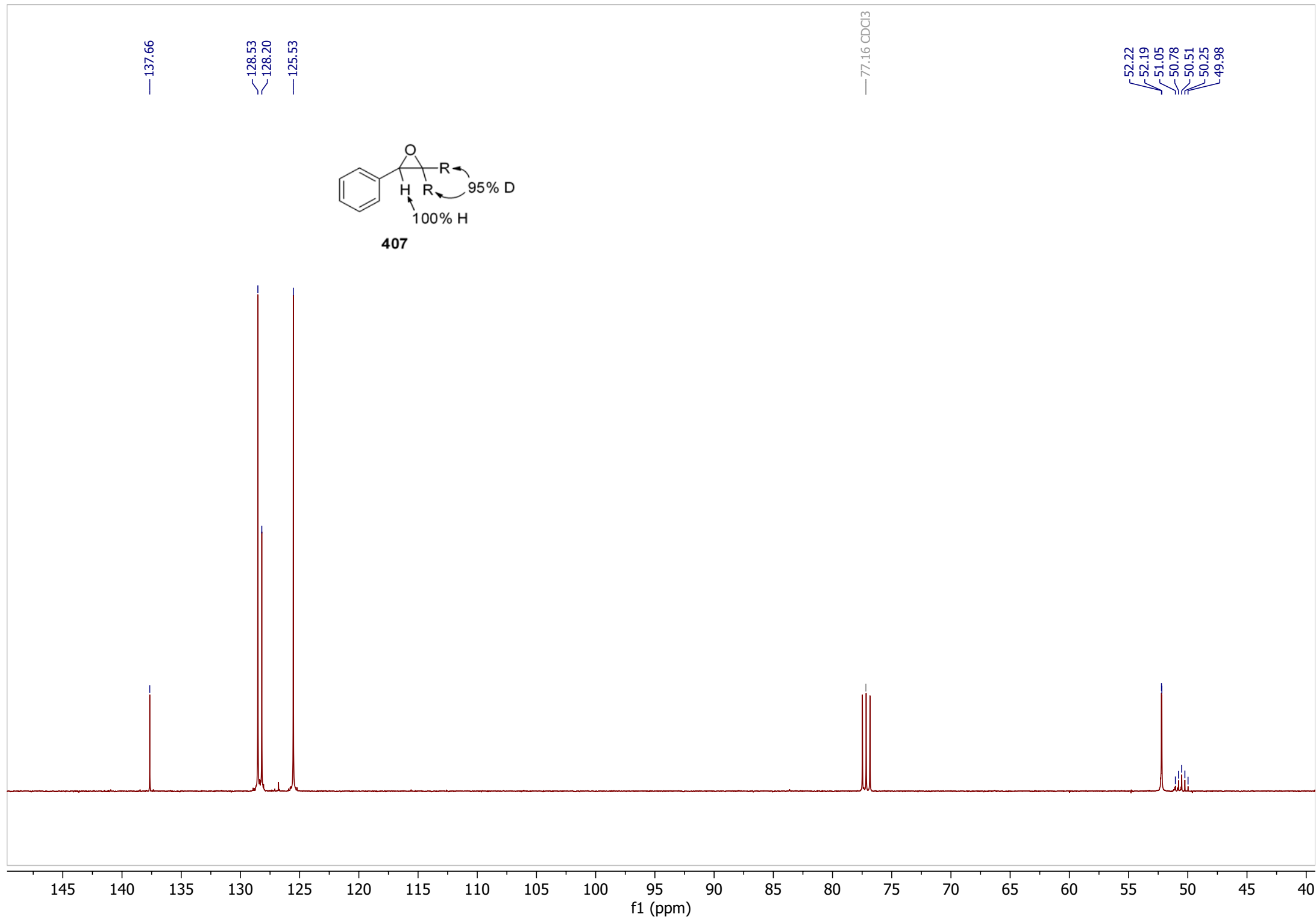
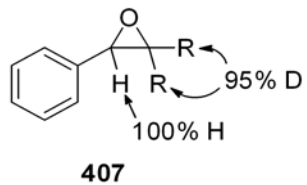
—137.66

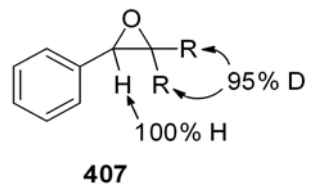
128.53  
128.20

—125.53

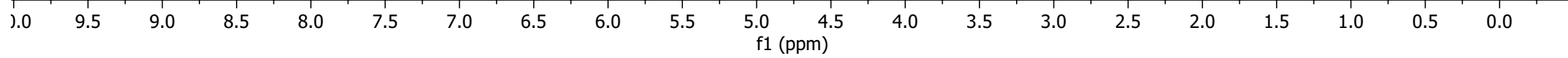
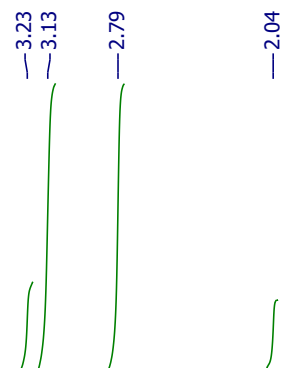
—77.16 CDCl<sub>3</sub>

52.22  
52.19  
51.05  
50.78  
50.51  
50.25  
49.98





— 7.26 CDCl<sub>3</sub>

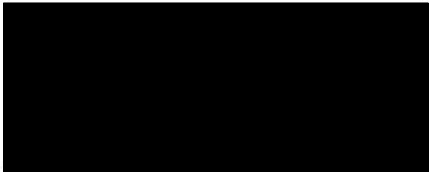


To whom it may concern

I, **Jan Sozynski**, contributed conceptualization, investigation, methodology, visualization, writing-original draft, writing-review & editing to the following paper:

Jan Sozynski and Alan D. Payne

Triazolopyridines as potential antagonists of ethylene action. Draft publication.



I as a Co-Author, endorse that this level of contribution by the candidate indicated above is appropriate.



**Alan D. Payne**